RAC 1333
(SSD-1027)
17 June 1963

SYNCHRONOUS METEOROLOGICAL SATELLITE (SMS) STUDY.

Volume 3:

Meteorological Sensors

RAC 1333

Prepared for

NATIONAL AERONAUTICS AND SPACE ADMINISTRATION
Goddard Space Flight Center
Greenbelt, Maryland

under

(NASA Contract No. NAS5-3189)

REPUBLIC AVIATION CORPORATION
Farmingdale, L.I., N.Y.

FOREWORD

This final report on Contract NAS 5-3189 is presented by Republic Aviation Corporation to the Goddard Space Flight Center of the National Aeronautics and Space Administration and consists of the seven volumes listed below. The period of the contract work was February through May, 1963.

The sub-titles of the seven volumes of this report are:

1 Summary and Conclusions

2 Configurations and Systems

3 Meteorological Sensors

4 Attitude and Station Control

5 Communications, Power Supply, and Thermal Control

6 System Synthesis and Evaluation

7 Classified Supplement on Sensors and Control

Except for Volume 7, all of these are unclassified. Volume 7 contains only that information on specific subsystems which had to be separated from the other material because of its present security classification. Some of these items may later be cleared for use in unclassified systems.

Volumes 3, 4, and 5 present detailed surveys and analyses of subsystems and related technical problems as indicated by their titles.

In Volume 2, several combinations of subsystems are reviewed as complete spacecraft systems, including required structure and integration. These combinations were selected primarily as examples of systems feasible within different mass limits, and are associated with the boosters to be available.

Volume 6 outlines methods and procedures for synthesizing and evaluating system combinations which are in addition to those presented in Volume 2.

Volume 1 presents an overall summary and the principal conclusions of the study.

ACKNOWLEDGEMENTS

The authors of this volume gratefully acknowledge the cooperation of the companies listed below for supplying information for the study reported herein.

- RCA, Tube Division, Lancaster, Pennsylvania
- RCA, Astro-Electronic Division, Princeton, New Jersey
- Westinghouse Air Arm Division, Baltimore, Maryland
- Westinghouse Tube Division, Elmira, New York
- General Electric Company, Syracuse, New York
- General Electric Company, Utica, New York
- Optomechanism Inc., Plainview, New York
- System Associates Inc., Halesite, New York
- Goerz, American Optical, Inwood, New York
- Perkin Elmer, Norwalk, Connecticut
- Hazeltine Corporation, Little Neck, New York
- Admiral Corporation, Chicago, Illinois
- Itek, Lexington, Massachusetts
- Chicago Aerial Industries, Inc., Barrington, Illinois
- Raytronics, Sparks, Maryland
- EMR, Sarasota, Florida
- General Electro Dynamics, Garland, Texas

TABLE OF CONTENTS

TABLE OF CONTENTS (Continued)

TABLE OF CONTENTS (Continued)

TABLE OF CONTENTS (Continued)

LIST OF ILLUSTRATIONS

LIST OF ILLUSTRATIONS (Continued)

LIST OF ILLUSTRATIONS (Continued)

LIST OF ILLUSTRATIONS (Continued)

SECTION 1 - INTRODUCTION AND SUMMARY

The Synchronous Meteorological Satellite (SMS) will provide the means for continuous observation of the manifestations of the Earth's weather from a fixed vantage point. The need for such a surveillance satellite has long been recognized. The data that a synchronous weather satellite will be capable of providing will not only fill the voids left by low altitude weather satellites and ground stations, but will in addition provide meteorologists with a powerful new tool for the location, identification, tracking, and analysis of weather phenomena.

As outlined in the NASA work statement, the primary function of the meteorological sensors is to provide 24-hour surveillance of the Earth's cloud cover, and measurements of the Earth's heat budget, during a satellite lifetime objective of one year. Accomplishment of 24-hour surveillance requires an investigation of the problems associated with narrow-field imaging over extreme variations in illumination, ranging from the darkest night with no Moon, to high noon. Wide-field sensors must be capable of operating under conditions where the Earth view encompasses sunrise or sunset on one edge and a moonless night on the other. Additionally, detailed information is required on the variation of solar and terrestrial radiation intensity within the field of view of the spacecraft as a function of the time of day.

Subsidiary studies which affect the meteorological sensors must include a state of the art survey of applicable sensor tubes together with an understanding of operational advantages and limitations. Further, the meteorological sensors are the critical payload of the satellite, and sensor resolution represents the basic parameter against which all other trade-offs are made. Comparative data must be developed to show the interrelationship between meteorological sensor parameters, and the interfaces between the sensor system and other spacecraft systems.

The meteorological sensor study contained in this volume of the SMS Final Report sets forth the essential considerations and requirements for the cloud cover and heat budget sensory systems in compliance with the NASA work statement and satellite objectives. The succeeding sections of this volume are briefly described in the following paragraphs.

Section 2 "Energy Considerations," develops a model from which estimates can be made of the radiation incident on the meteorological sensors for both cloud cover imaging and heat budget measurement. The section is divided into two parts. The first treats the problem of estimating and predicting radiation incident on the sensor. The various constituents of the visible spectrum relating to cloud imaging illumination are identified and subsequently analyzed. A series of graphs and tables are employed to establish illumination levels at the sensor as a function of time of day and the object's geographical position. For the heat budget measurements, similar data is developed in the second part of the section, enabling estimates of solar and terrestrial infrared radiation incident on the sensors to be made.

Section 3, "Cloud Cover Sensors-Visible Spectral Region," considers cloud imaging sensor requirements and then proceeds to a comprehensive survey and analysis. Comparative data on various photosurfaces, photoemissive tubes, and photoconductive tubes, as well as hybrid and special types, are included. Theoretical performance characteristics of idealized tubes are discussed and performance data

on sensor tube types pertinent to the SMS program are presented. Optical considerations are included, covering the relationships between lenses, focal length, area coverage and ground resolution, and the relationships between these factors and sensor capabilities. Special techniques for improvement of dynamic range, operational reliability, and system optimization are discussed in a separate subsection. Finally, systems are synthesized as representative of possible actual configurations for minimum, and medium capability satellites, based on the working tables, charts and graphs prepared.

Section 4, "Heat Budget Measurement," describes sensor parameters and potential equipment designed to perform this function in the various satellite configurations. The techniques of V.E. Suomi are discussed; with some modifications, these methods are utilized for low and medium resolution measurements. Where high angular resolution coupled with reasonable thermal sensitivity is required, the use of optical, rather than geometrical systems is dictated. Such a system, suitable for use in satellites which provides stabilization in three axes is described. With modification, this system could also be used in a spin-stabilized vehicle.

Section 5, "Cloud Cover Sensors - Infrared," considers the use of infrared techniques for performing the same general cloud cover mission described previously. The section discusses some of the characteristics and requirements of point detectors and infrared image tubes that are pertinent to their application in cloud cover imaging systems. An analysis of a typical mechanically scanned system utilizing a quantum detector is also presented. Due to security restrictions, some data on infrared sensor performance had to be included in Volume 7, which is classified, of this report.

Section 6, "Problem Areas," acknowledges the need for recognizing real and potential problem areas which could impede the successful implementation of the meteorological sensor system. As a result of various studies conducted during the course of the program, a number of specific problem areas have been identified; these are discussed in this section, with recommendations for feasible solutions, where possible.

SECTION 2 - ENERGY CONSIDERATIONS

A. SOLAR RADIATION CONSIDERATIONS

The SMS will be capable of providing day and night cloud cover information and data on the Earth's heat budget. The radiations involved in these observations are:

(1) Reflected solar radiation from the Earth's surface

(2) Reflected solar radiation from the atmosphere (clouds)

(3) Solar radiation scattered by the atmosphere toward space

(4) Reflected moonlight and starlight (during nighttime observations)

(5) Thermal radiation from the Earth

(6) Thermal radiation from the atmosphere

(7) Airglow (nightglow, twilight glow, etc.)

Up to the present time, considerably more work has been done on solar and terrestrial radiation than on airglow and nighttime illumination. It is the intent of this report to develop a model from which estimates may be made of the radiation incident on the SMS as a function of the following parameters:

(1) Surface from which the radiation emanates (geographical position, altitude, reflective characteristics, temperature, etc.).

(2) Surface-Sun relationship (solar altitude). This may be related to the time of day, by considering geographic position and season.

1. Solar Radiation

Normally, solar radiation returned to space by reflection from the atmosphere, the Earth, and by atmospheric scattering mechanisms is grouped under a general heading of albedo radiation. The often quoted figure of about 0.35 for the Earth's reflectivity (albedo) includes these effects and means that approximately 35% of the incident solar radiation is returned to space. The magnitude of this radiation is dependent upon the incident solar radiation (insolation) and the albedo values of Earth and atmosphere. For purposes of the present analysis, exact values for insolation and albedo will be used together with a given set of surface-Sun parameters to obtain the radiation incident on the SMS.

2. Solar Constant

The solar constant refers to the rate at which solar radiation is received on a unit area surface normal to the Sun's direction, outside the Earth's atmosphere, at the Earth's mean distance from the Sun. Since 1940, various values have been published for the solar constant. These values tend to differ due to corrections for the ultraviolet and infrared spectral regions which are measured with difficulty, and changes in the absolute calibration factors of the instruments used in the measurements. Table 2-1 presents a selection of published solar constant values.

TABLE 2-1
SELECTED CHRONOLOGICAL SOLAR CONSTANT VALUES
(Howard, 1961)

Author	Date	Solar Constant Value	
		cal/cm^2min	$watts/m^2$
Moon	1940	1.896	1322
Allen	1950	1.97 ± 0.01	1374
Smithsonian	1952	1.946	1357
Johnson	1954	2.00 ± 0.04	1396
Stair	1956	2.05	1430

3. Optical Air Mass

Optical air mass (m) is the ratio of the path length of radiation through the atmosphere at any given angle to the path length toward the zenith. If the angle referred to is measured from the zenith, the air mass will be approximately equal to the secant for angles up to 62°. Table 2-2 presents values of the air mass as a function of the solar altitude above the horizon, rather than the distance from zenith, since solar altitude has been used in the calculations.

TABLE 2-2
OPTICAL AIR MASS FOR VARIOUS SOLAR ALTITUDES
(Howard, 1961)

Solar Altitude degrees	0	1	2	3	4	5	6	7	8	9
0	-	26.96	19.79	15.36	12.44	10.39	8.90	7.77	6.88	6.18
10	5.60	5.12	4.72	4.37	4.07	3.82	3.59	3.39	3.21	3.05
20	2.90	2.77	2.65	2.55	2.45	2.36	2.27	2.19	2.12	2.06
30	2.00	1.94	1.88	1.83	1.78	1.74	1.70	1.66	1.62	1.59
40	1.55	1.52	1.49	1.46	1.44	1.41	1.39	1.37	1.34	1.32
50	1.30	1.28	1.27	1.25	1.23	1.22	1.20	1.19	1.18	1.17
60	1.15	1.14	1.13	1.12	1.11	1.10	1.09	1.09	1.08	1.07
70	1.06	-	-	-	-	1.04	-	-	-	-
80	1.02	-	-	-	-	1.01	-	-	-	-
90	1.00	-	-	-	-	-	-	-	-	-

(For a solar attitude of 44°, the optical air mass = 1.44.)

4. Solar Irradiance

P. Moon (1940) derived a spectral distribution curve and, using the solar constant shown in Table 2-1, arrived as spectral irradiance values corresponding to air mass = 0. He then calculated the atmospheric attenuation and obtained irradiance values for several spectral bandwidths and air mass values. Table 2-3 presents this data corrected by a factor of 1.026 to account for the increase in the determined values of the solar constant (1.95 /1.90). The tabulated values also apply to a solar constant of 2.00 cal/cm^2 min. since the added 0.05 cal/cm^2 min. is the the wavelength regions below 0.29 micron and above 2.4 microns.

Moon's calculated data have been compared with observational data from Miami, Florida, and the ratio of calculated to observed data was found to vary between 83 and 103%, indicating good experimental correlation.

5. Atmospheric Attenuation

Attenuation in the atmosphere includes both absorption and scattering mechanisms which are functions of altitude, absorption and scattering media, and wavelength of the incident radiation. For the present application, a reasonable way of approaching the problem is to consider attenuation in a homogeneous atmosphere, combining all the above mechanisms into a single exponential attenuation formula:

$$E = E_0 \, e^{-ax}$$

where E = radiation intensity after passage through the attenuating medium
E_0 = radiation intensity entering attenuating medium
a = attenuation factor of medium (1/length)
x = distance radiation travels in medium (length)

TABLE 2-3
SOLAR IRRADIATION NORMAL TO SUN'S RAYS AT SEA LEVEL
(Corrected from Moon, 1940)

Irradiation (watts/meter^2)

Bandwidth Microns	M = 0	M = 1 θ = 90	M = 2 θ = 30	M = 3 θ = 19.5	M = 4 θ = 14.3	M = 5 θ = 11.2
0.29-0.40	97.1	41.1	20.3	10.3	5.5	2.8
0.40-0.70	554.0	430.6	336.3	265.3	211.2	168.0
0.70-1.1	374.9	317.2	274.5	239.5	210.4	186.2
1.1-1.5	166.7	97.8	72.2	58.5	49.4	41.8
1.5-1.9	74.7	52.1	46.3	42.1	39.0	36.1
1.9 - ∞	89.1	13.1	9.4	7.7	6.7	6.0
TOTAL	1356.5	951.9	759.0	623.4	522.2	440.9

θ = solar altitude (degrees)
M = air mass

The Earth's atmosphere is definitely inhomogeneous, but a model homogeneous atmosphere can be synthesized by using the "atmospheric reduced equivalent thickness;" that is, the depth of the atmosphere reduced to an equivalent depth at 0° C and 1013 millibars (NTP). Table 2-4 and Figure 2-1 present data on the atmospheric reduced equivalent thickness (NTP), and H_r is calculated from the 1959 ARDC Model Atmosphere. Again, H_r represents the thickness of a homogeneous atmosphere at NTP conditions existing above any altitude.

TABLE 2-4
ATMOSPHERIC REDUCED EQUIVALENT THICKNESS (NTP), H_r
(Howard, 1961)

Altitude Z (km)	H_r (km)	Altitude Z (km)	H_r (km)
0	7.995	10	2.098
1	7.094	11	1.797
2	6.277	12	1.537
3	5.538	13	1.314
4	4.872	14	1.123
5	4.272	15	0.9603
6	3.733	16	0.8210
7	3.251	17	0.7021
8	2.820	18	0.6003
9	2.437	19	0.5134
		20	0.4391

The basic data is now available with which to develop a model and arrive at the solution of the first part of the problem, which is the determination of the insolation on a horizontal surface as a function of altitude, solar altitude, and radiation spectral bandwidth. The model consists of the Earth surrounded by a homogeneous atmosphere (thickness 7.995 km) with attenuation factors dependent upon spectral bandwidth. These factors may be calculated from the exponential attenuation formula using a value of x = 7.995 km and values of E and E_0 taken from Table 2-3 where E and E_0 correspond to m = 1 and m = 0 data, respectively. Once the attenuation factors have been determined they can be applied to any portion of the homogeneous atmosphere, and in this way, irradiation normal to the Sun's rays at a solar altitude of 90° may be calculated as a function of altitude. Using the atmospheric reduced equivalent thickness H_r results in a straight line plot on semilog graph paper. Table 2-5 presents the pertinent data, including two end points for the curves; altitude Z = 0 and 20 km corresponding to H_r = 7.995 and 0.4391 km, respectively.

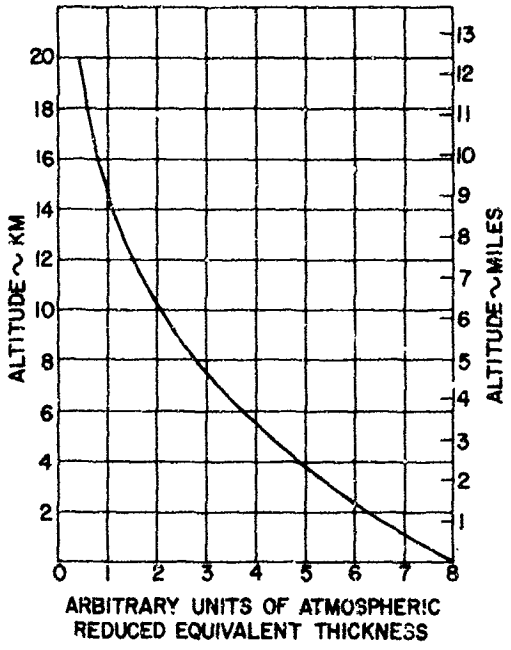

Figure 2-1. Atmospheric Reduced Equivalent Thickness (km) as a Function of Altitude (Data from Howard, 1961)

TABLE 2-5
DETERMINATION OF ATTENUATION FACTOR
AND LIMITING IRRADIATION VALUES

Bandwidth Microns	E_0 Watts/M^2	E_1 Watts/M^2	A KM^{-1}	E_2 Watts/M^2
0.29 to 0.40	97.1	41.1	0.1075	92.6
0.40 to 0.70	554.0	430.6	0.0316	546.0
0.70 to 1.1	374.9	317.2	0.0209	372.0
1.1 to 1.5	166.7	97.8	0.0666	161.0
1.5 to 1.9	74.7	52.1	0.0450	73.2
1.9 to ∞	89.1	13.1	0.240	80.1

E_0 corresponds to solar constant values (from Table 2-3)
E_1 corresponds to Z = 0 km, H_r = 7.995 km (from Table 2-3)
E_2 corresponds to Z = 20 km, H_r = 0.4391 km
A attenuation factor

Above figures apply to irradiation for solar altitude of 90°

Figure 2-2 presents curves giving irradiation values as functions of the atmospheric reduced equivalent thickness. Provision for varying solar altitude must now be included. This can be accomplished by use of the data from Table 2-3 if it is realized that the geometry of the problem is such that for any height and solar altitude, the ratio of the path length along the solar altitude line to the path length corresponding to a solar altitude of 90° is a constant. Since a homogeneous atmosphere model is being used, the ratio of the solar radiation incident on a surface for a solar altitude of 90° is also constant, regardless of the altitude of the surface. That is,

$$\frac{E\ (Z = O,\ \theta = \theta)}{E\ (Z = O,\ \theta = 90)} = \frac{E\ (Z = Z,\ \theta = \theta)}{E\ (Z = Z,\ \theta = 90)} = \text{Constant}$$

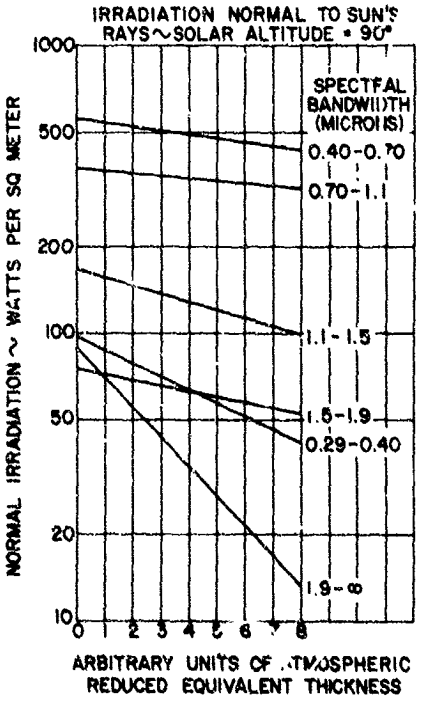

Figure 2-2. Irradiation Normal to Sun's Rays (Solar Altitude = 90°)

The data of Table 2-3 permits calculation of this constant for different solar altitudes (90°, 30°, 19.5°, 14.3°, and 11.2°). A sin θ term must also be included since the calculations must yield irradiation on a horizontal surface rather than on a surface normal to the Sun's rays. For example, consider the case of 0.29 to 0.40 micron bandwidth and air mass of 3 (solar altitude = 19.5°). The constant will be $\frac{10.3}{41.1}$ (sin 19.5) = 0.0835. This means that the irradiation on a horizontal surface for a solar altitude of 19.5° will be 8.35% of the irradiation on the surface for a solar altitude of 90°. Furthermore, this percentage will hold for any surface altitude.

Table 2-6 gives calculated values for the constants mentioned above, and Figure 2-3 presents curves for the constants as functions of solar altitude. However, it has already been shown that the 90° solar altitude irradiation varies with height (as plotted in Figure 2-2). Therefore, given a surface at a certain altitude and solar altitude, the 90° irradiation can be obtained from Figure 2-2 and the depletion constant from Figure 2-3. The product of the two terms will give the solar irradiation for any bandwidth of interest.

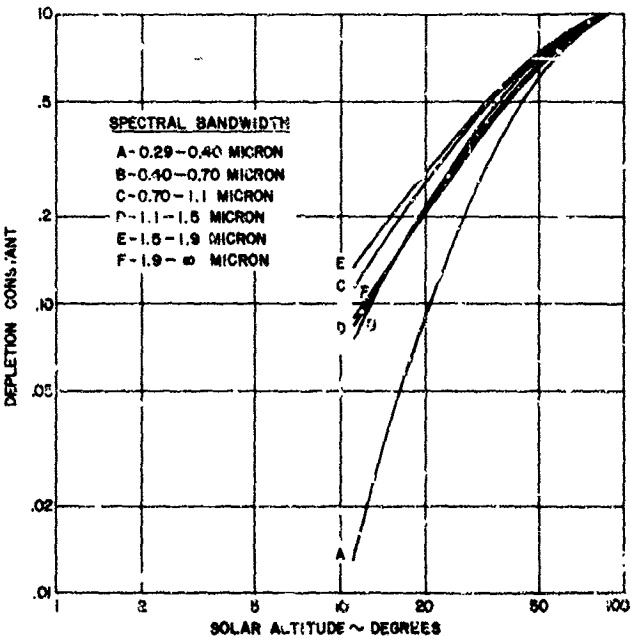

Figure 2-3. Depletion of Radiation With Solar Altitude

TABLE 2-6
DEPLETION CONSTANTS FOR IRRADIATION ON HORIZONTAL SURFACES

Bandwidth Microns	Solar Altitude (Degrees) 90	30	19.5	14.3	11.2
0.29 to 0.40	1	0.246	0.0835	0.0330	0.0132
0.40 to 0.70	1	0.389	0.205	0.121	0.0756
0.70 to 1.1	1	0.432	0.252	0.1635	0.114
1.1 to 1.5	1	0.369	0.200	0.125	0.083
1.5 to 1.9	1	0.444	0.270	0.1845	0.134
1.9 to ∞	1	0.358	0.196	0.126	0.0889

6. Albedo

Having determined the irradiation on a surface, the next step is to determine the amount of this incoming radiation that will be reflected back through the atmosphere to the SMS. Data on the albedo values of various surfaces are presented first. Subsequently, the problem of estimating the portion of this reflected radiation that is monitored by the SMS is considered.

The albedos of natural surfaces may be considered under three classifications: surface features, water surfaces, and clouds. Figure 2-4 presents a fairly complete collection of data for surface features. It can be seen that the albedo has a wide range of values. The highest values apply for snow or ice. For all surfaces except fresh fallen snow the albedo increases with wavelength of irradiation. In general, the lowest albedos are found over water; however, the values do depend on solar altitude. The data points used to plot the water curve are from Fritz, 1951. The major contribution to the Earth's albedo (0.35) comes from the tops of clouds. Therefore, for the SMS application, clouds constitute the most important surfaces to be observed. This is true because the albedo of most clouds is higher than any surface other than snow or ice and water for solar altitudes less than 5 to 10°, and because of their altitude, clouds receive more incident irradiation than surfaces at sea level. Surface and aircraft observations have shown that clouds are generally encountered over a range of altitude varying from sea level to 18 km (about 60,000 ft.). Table 2-7 presents some data on various cloud types, the heights at which they occur, and albedo ranges. To further classify clouds, that part of the atmosphere in which they usually occur has been divided into three étages (stages); high, middle, and low. These étages overlap and vary with latitude with the approximate altitude limits shown in Table 2-8.

It is now possible to consider any surface and obtain the irradiation (E) on it and its albedo (A). The total radiation reflected from a surface will be (A x E). Consider now the determination of the portion of (A x E) that is received by the SMS.

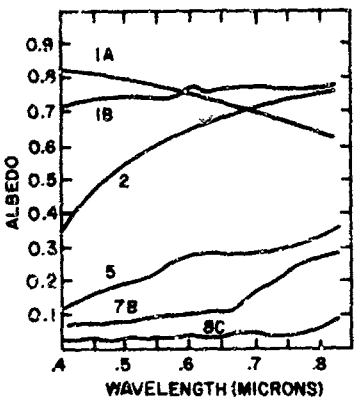

CLASS B – BARE AREAS AND SOIL

1A – FRESH FALLEN SNOW

1B – SNOW COVERED WITH FILM OF ICE

2 – LIMESTONE, CLAY AND SIMILAR BRIGHT OBJECTS

5 – SANDS, BARE AREAS IN THE DESERT, AND SOME MOUNTAIN OUTCROPS

7B – PODZOL, CLAY, LOAM AND OTHER SOILS, PAVED ROADS AND SOME BUILDINGS

8C – BLACK EARTH, SAND LOAM AND EARTH ROADS

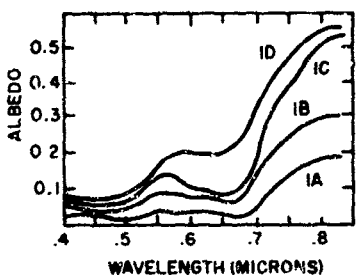

CLASS C – VEGETATION

1A – CONIFEROUS FORESTS IN WINTER

1B – CONIFEROUS FORESTS IN SUMMER, DRY MEADOWS, AND GRASS IN GENERAL, EXCLUDING LUSH GRASS

1C – DECIDUOUS FORESTS IN SUMMER AND ALL LUSH GRASS

1D – FORESTS IN AUTUMN AND RIPE FIELD CROPS

Figure 2-4a. Albedos of Various Surfaces (Condron, 1961)

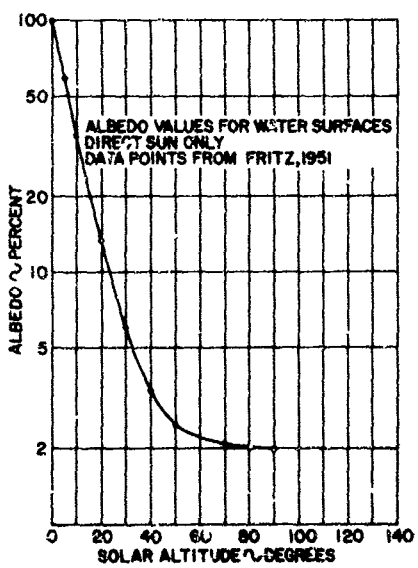

Figure 2-4b. Albedo Values for Water Surfaces - Direct Sun Only

TABLE 2-7

CLOUD ALBEDO INFORMATION

Cloud Genera	Height		Albedo
	Miles	Km	(Percent)
Stratus	0.08-1.2	0.13-1.93	56-65
Strato cumulus	0.19-2.8	0.31-4.5	56-81*
Nimbostratus	0.04-3.4	0.064-5.48	70-73
Altocumulus	0.5-3.74	0.81-6.02	
Altostratus	0.95-3.74	1.53-6.02	48-52
Cirrostratus	3.74-8.54	6.02-13.7	44-50*
Cirrocumulus	3.74-8.54	6.02-13.7	
Cirrus	3.74-8.54	6.02-13.7	16-23
Cumulus	0.3-8.54	0.48-13.7	70
Cumulonimbus	0.12-8.54	0.19-13.7	70
Very dense clouds of extensive area and depth			78*
Dense clouds, nearly opaque			44*
Dense clouds, quite opaque			55-62*
Thin clouds			36-40*

* This data from Fritz, 1951. All other data supplied by NASA.

TABLE 2-8

CLOUD OCCURRENCE INFORMATION
(Byers, 1959)

'Etage	Polar Regions	Temperature Regions	Tropical Regions	Type Clouds Usually Found in 'Etage
High	3-8 Km	5-13 Km	6-18 Km	Cirrus Cirrocumulus Cirrostratus
Middle	2-4 Km	2-7 Km	2-8 Km	Altocumulus
Low	0-2 Km	0-2 Km	0-2 Km	Stratus Stratocumulus

Altostratus is usually found in the middle 'etage, but often extends higher. Nimbostratus, cumulus and cumolonimbus extend through several levels.

7. Detector Irradiation

First, the atmospheric attenuation factor for irradiation traveling from a surface to the SMS is considered. By reasoning similar to that used for determining the solar irradiation on a surface, the irradiation reflected from the surface and emerging from the atmosphere can be determined. Table 2-5 presents the data necessary to plot curves of a depletion constant (portion of brightness radiation emerging out of the atmosphere normal to a surface as a function of the height of the surface and spectral bandwidth). This is based on the concept that the portion of radiation emerging out of the atmosphere from the surface is the same as the portion of the solar constant irradiation reaching the surface. For example, for the spectrum of 0.29 to 0.40 micron this depletion constant would be $\frac{41.1}{97.1} = 0.423$ for a surface at $H_r = 7.995$ km (sea level), and $\frac{92.6}{97.1} = 0.954$ for a surface at $H_r = 0.4391$ km (20 km altitude). Table 2-9 and Figure 2-5 present values of this depletion constant as calculated from data of Table 2-5.

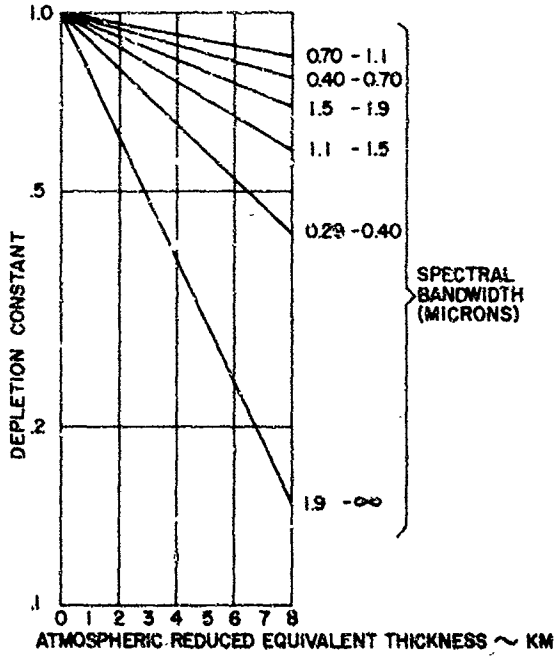

Figure 2-5. Depletion Constant for Brightness Radiation Emerging Out of Atmosphere Normal to a Surface as Function of Surface Altitude.

TABLE 2-9
DEPLETION CONSTANT FOR BRIGHTNESS
RADIATION EMERGING OUT OF ATMOSPHERE NORMAL TO A SURFACE

Bandwidth Microns	H_r (km) 0.4391	7.995
0.29-0.40	0.954	0.423
0.40-0.70	0.986	0.777
0.70-1.1	0.991	0.845
1.1-1.5	0.968	0.586
1.5-1.9	0.979	0.697
1.9-∞	0.899	0.147

The altitude angle of the SMS with respect to the surface must also be introduced as a parameter. To avoid excessive computations, the easiest way to accomplishing this is to consider the data of Table 2-3 and relate the solar altitude angle to the SMS altitude angle. In this way, a depletion constant may be obtained which operates on the radiation emerging out of the atmosphere normal to the surface; not on the solar constant radiation. This normal radiation has been established by the depletion constants of Table 2-9 and Figure 2-5. For example, referring to Table 2-3, the depletion constant for the spectral region of 0.29 to 0.40 micron with an SMS altitude angle of 30° will be $\frac{20.3}{41.1} = 0.494$. Table 2-10 and Figure 2-6 present values for this constant.

TABLE 2-10
DEPLETION CONSTANT FOR BRIGHTNESS RADIATION
EMERGING OUT OF ATMOSPHERE AS FUNCTION OF SMS ALTITUDE ANGLE
(Operates on the Radiation Emerging Normal to Surface)

Bandwidth Microns	90	30	19.5	14.3	11.2
0.29-0.40	1.0	0.494	0.250	0.134	0.068
0.40-0.70	1.0	0.780	0.615	0.489	0.389
0.70-1.1	1.0	0.865	0.755	0.663	0.587
1.1-1.5	1.0	0.738	0.598	0.505	0.427
1.5-1.9	1.0	0.887	0.807	0.747	0.692
1.9-∞	1.0	0.717	0.588	0.511	0.458

Beyond this point, it is desirable to limit discussion and illustrative examples to the visible spectral region (0.40 to 0.70 micron). Moreover, in keeping with present visible region convention, the system of units must be changed from watts to lumens. The following conversions may be used when treating the data:

- 1 watt = 680 lumens at 0.555 micron
- 1 watt = 244 lumens over 0.40 to 0.70 micron bandwidth
- 1 watt per sq. meter = 22.7 lumens per sq. ft. over 0.40 to 0.70 micron bandwidth
- 1 meter candle = 1 lumen per sq. meter = 1 lux
- 1 foot-candle = 1 lumen per sq. ft.
- 1 foot-candle = 10.76 lumens per sq. meter

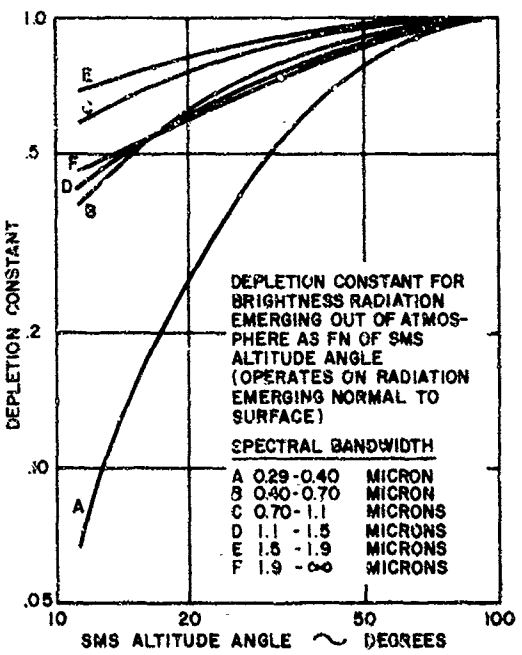

Figure 2-6. Depletion Constant for Brightness Radiation Emerging Out of Atmosphere as Function of SMS Altitude Angle

The Earth's atmosphere may be treated as a perfect diffuser, i.e., one that appears equally bright when viewed from any direction. This definition does not include atmospheric attenuation effects which must also be taken into account. The geometry of the problem is shown in Figure 2-7.

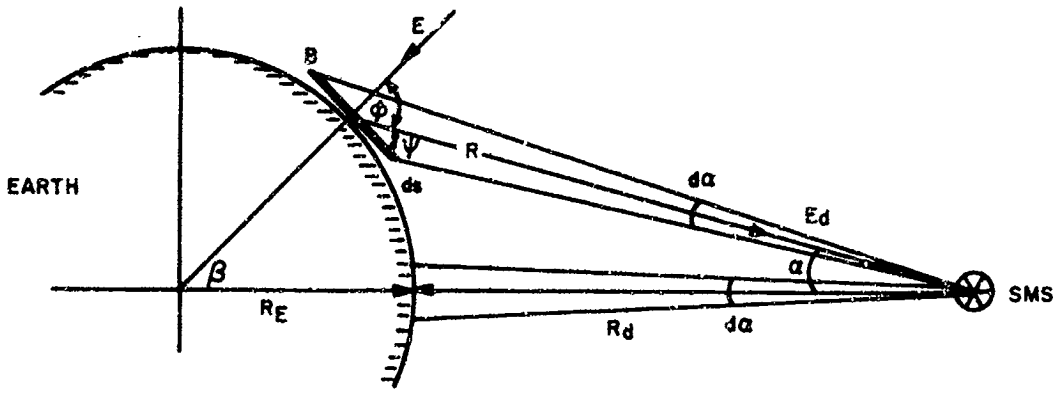

Figure 2-7. Geometry of Irradiation Problem

where

E_d	=	irradiation on detector (lumens per unit area)
B_L	=	brightness of surface (lumens per unit area)
ds	=	incremental areas (length^2)
R	=	distance from surface to detector (length)
R_d	=	altitude of detector (22,240 miles)
R_E	=	radius of the Earth (3960 miles)
ϕ	=	angle between R and the normal to the surface
Ψ	=	90 - ϕ = altitude angle of SMS with respect to the surface
α	=	angle between R and the normal to the detector
$d\alpha$	=	view angle

Table 2-11 presents data calculated from the above geometry which is useful in the analysis. The calculations for R, α, ϕ, and Ψ applicable to surfaces at sea level are assumed to be valid for surfaces at the altitudes of interest (0 to 11 miles). The determining factors then become the latitude and longitude over which the surfaces exist. Figure 2-8 presents a fairly complete set of surface-SMS relationships based on a set of lines of constant SMS altitude angles. These lines can also be interpreted as lines of constant distance at sea level from nadir and constant distance from SMS. The data are presented as functions of geographical (latitude-longitude) locations.

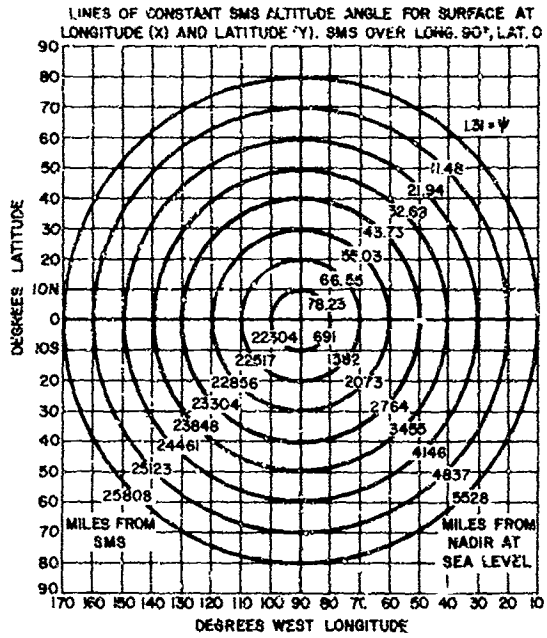

Figure 2-8. Lines of Constant SMS Altitude Angle for Surface at Longitude (x) and Latitude (y). SMS Over Longitude 90° W, Latitude 0

Using the Geometry described above, the equation for the irradiation on a detector due to a perfect diffuser reflecting surface is:

$$E_d = \int \frac{B_L \, ds \cos \phi \cos \alpha}{\pi R^2}$$

In the present case, B_L is an arbitrarily varying parameter and therefore only discrete reflecting areas will be considered. Also, note that $0 \leq \alpha < 9°$ or $1 \geq \cos \alpha > 0.988$. If $\cos \alpha$ is assumed to be a constant equal 1, the equation becomes

$$E_d = \frac{B_L S \cos \phi}{\pi R^2}$$

TABLE 2-11
SURFACE-SMS GEOMETRICAL PARAMETERS

β Degrees	α Degrees	R Miles	$\phi = \beta + \alpha$ Degrees	$\psi = 90 - \phi$ Degrees
0	0	22240	0	90
10	1.77	22304	11.77	78.23
20	3.45	22517	23.45	66.55
30	4.97	22856	34.97	55.03
40	6.27	23304	46.27	43.73
50	7.31	23848	57.31	32.69
60	8.06	24461	68.06	21.94
70	8.52	25123	78.52	11.48
80	8.69	25808	88.69	1.31

Above data calculated from

$$\tan \alpha = \frac{3960 \sin \beta}{26200 - 3960 \cos \beta} = \frac{\sin \beta}{6.61616 - \cos \beta}$$

$$R = \frac{3960 \sin \beta}{\sin \alpha}$$

Introducing the various attenuation constants yields

$$E_d = \frac{B_L S \cos \Psi}{\pi R^2} \quad K_1 K_2 K_3$$

where K_1 = depletion constant due to solar altitude with respect to the surface (Figure 2-3)

K_2, K_3 = depletion constant due to atmospheric attenuation from surface to SMS (K_2 depends upon altitude of surface and K_3 depends upon SMS altitude angle) (Figure 2-5, -6)

A depletion constant due to view angle and geometry of field of view is included in the $\frac{S \cos \Psi}{R^2}$ term.

The irradiation on the sensitive surface of the detector may be obtained from:

$$E_i = E_d \frac{\pi D^2/4}{S_i} t$$

where E_i = irradiation on sensitive surface (lumens per unit area)

E_d = irradiation on SMS aperture (lumens per unit area)

D = diameter of SMS aperture (in.)

S_i = image area on sensitive surface q. in.)

t = lens transmission factor

Use may now be made of the following relation:

$$\frac{S \cos \phi}{R^2} = \frac{S_i}{F^2}$$

or $$S_i = \frac{F^2 S \cos \phi}{R^2}$$

where $S \cos \phi$ = area of surface projected at right angle to the viewing direction R (sq. miles)

R = distance from S to SMS (miles)

F = focal length of optical system (in.)

Substituting the expression for E_D and S_i into the equation for E_i yields:

$$E_i = \frac{B_L S \cos \phi \left(\pi D^2/4\right)}{\pi R^2} \quad \frac{R^2}{F^2 S \cos \phi} K_1 K_2 K_3 t$$

$$E_i = \frac{B_L D^2}{4F^2} K_1 K_2 K_3 t$$

In addition, the following relation applies:

$$\text{f/number of optics} = \frac{F}{D}$$

The expression for E_i then becomes:

$$E_i = \frac{B_L K_1 K_2 K_3 t}{4(f/no)^2} = \frac{E_b K_1 A K_2 K_3 t}{4(f/no)^2}$$

where $B_L = E_b A$

E_b = irradiation in lumens, or watts, per unit area on surface normal to Sun's rays for solar altitude = 90° (depends upon altitude of surface) (Figure 2-2)

A = albedo of surface

If the visible spectral region is considered, and irradiation values are given in watts per sq. meter, the following conversion will be useful:

1 watt per sq. meter = 22.7 lumens per sq ft. (foot-candle) (0.40 to 0.70 micron)

If the aperture lens is corrected for coma and spherical aberration, it is impossible to have an aperture greater than twice the focal length. Thus, the lens cannot have an f/number smaller than f/0.5. Considering the above expression for E_i, it can be seen that this limiting characteristic of the lens results in a value of unity in the denominator.

An optical depletion constant K_o may now be defined:

$$K_o = \frac{t}{4(f/no)^2}$$

then: $$E_i = E_b K_1 A K_2 K_3 K_o$$

Figure 2-9 is a plot of the optical depletion constant as a function of the f/number of the optics with the lens transmission as a parameter.

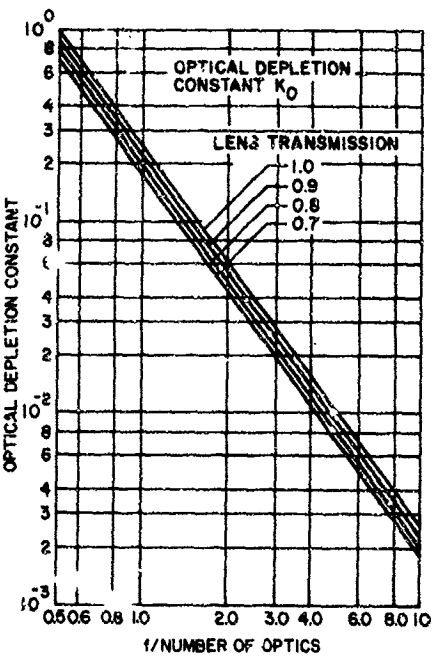

Figure 2-9. Optical Depletion Constant as a Function of the f/number of the Optics With the Lens Transmission as a Parameter

8. Night Illumination

The problems of night illumination and night observation are important ones for the SMS, since approximately 90% of the time there will be night areas in the field of view. To follow the progress of meteorological events on Earth, night observation capability becomes a necessity. For the present, the assumption will be made that the difference between the nighttime and daytime terrestrial long wave radiation situations is negligible and this radiation will be ignored.

Night illumination on Earth is a composite of many contributing factors. By far, the most important of these is moonlight. In addition, there are nightglow, starlight, galactic light, and zodiacal light. These are usually grouped under the heading "light of the night sky" and become important for moonless conditions. Figure 2-10 presents a compilation of some estimates of night ground illumination in the visible spectral region as a function of longitude degrees from the solar nadir. (The curves are from a Hazeltine Corp. Report, dated 1963. The one-value estimates are from GE/LMED and a Smithsonian report, dated 1939.) The curves labeled "Full Moon," "Quarter (Half-full) Moon" and "New (No) Moon" apply to the illumination along the equator when the Sun and Moon are both on the Equatorial plane. The general agreement in values seems to indicate that a similar situation exists for the other curves. In all cases, agreement well within an order of magnitude is obtained between the various data. Consider now the various contributions in order.

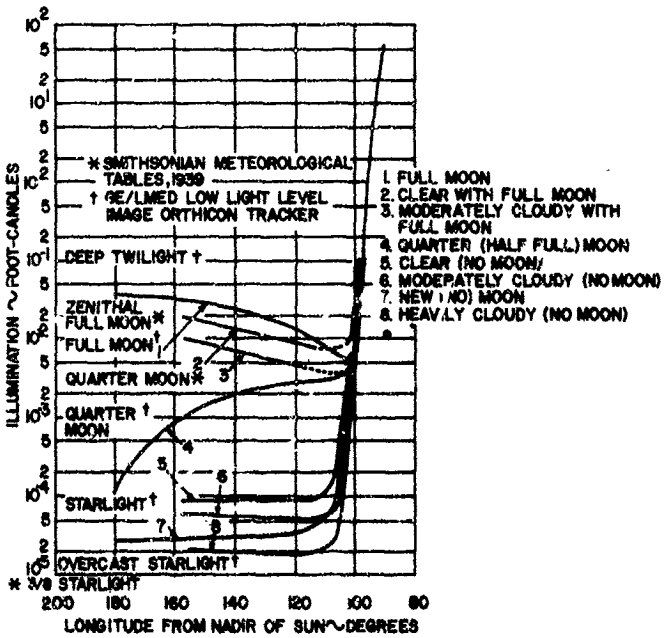

Figure 2-10. Estimates of Night Ground Illumination - Visible Spectral Region

a. Moonlight

The Moon is the predominant source of night-sky illumination on Earth. The ratios of quarter Moon and full Moon illumination to no Moon illunination are roughly 100:1 and 1000:1 respectively. This illunination varies over the Earth, as a function of cloud cover and terrestrial position. (See Figure 2-10)

In reality, the Moon is a solar radiation reflector with a wavelength-dependent reflectance (albedo). It reflects over the entire solar spectrum, but the albedo decreases toward the violet and then drops sharply in the ultraviolet, as shown in Figure 2-11.

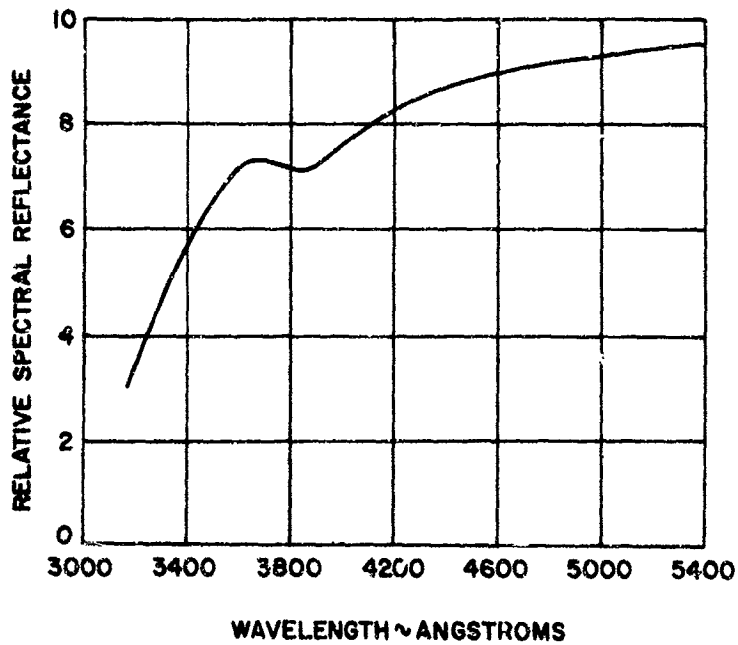

Figure 2-11. Relative Spectral Reflectance of the Moon (Katzoff, 1962)

Recent studies indicate that the rising trend toward longer wavelengths continues into the infrared. Since both the solar radiation spectrum and the Moon's albedo are maximum in the visible region (0.40 to 0.70 micron), it is convenient to consider Moon illumination to be predominantly visible radiation. Table 2-12 presents the variation of lunar brightness with phase angle, referring to the total light received from the Moon. Values are given for both the waxing and waning halves

of the lunation. The Moon may not be treated as a Lambert reflector; the brightness of the full Moon (corresponding to a Lambert sphere of 18.6% albedo or a Lambert disc of 12.4% albedo) is too great in proportion to the brightness in the partial phases. (Integration of Moonlight over all directions gives a value of 7.3% albedo, according to Katzoff.)

b. Nightglow

For conditions of no Moon, the predominant source of illumination is nightglow. The term nightglow is used to designate nocturnal radiation emitted by the Earth's upper atmosphere, other than that due to aurora. It consists of emission in the visible, ultraviolet, and near infrared spectra.

TABLE 2-12
RELATIVE TOTAL BRIGHTNESS OF THE MOON
(Katzoff, 1962)

Phase Angle (degrees)	Waxing	Waning	Phase Angle (degrees)	Waxing	Waning
0	1.0	1.0	80	0.121	0.105
10	0.810	0.750	90	0.085	0.078
20	0.616	0.572	100	0.057	0.058
30	0.482	0.445	110	0.039	0.041
40	0.356	0.342	120	0.025	0.027
50	0.281	0.264	130	0.016	0.017
60	0.220	0.204	140	0.0096	0.0096
70	0.167	0.148			

At night, the source has not been confirmed, but a possibility is the storage of chemical energy in the recombination of atomic species into molecules. Prominent components of nightglow emission are atomic oxygen lines at 5577 angstroms and 6300 angstroms, a sodium line at 5893 angstroms, a molecular oxygen band in the near ultraviolet, and a hydroxyl radical band in the near infrared. Table 2-13 presents some characteristics of the nightglow components. The rayleigh is a unit of intensity of emission which is equal to 10^6 photons emission per second in a square cm column extending up through the atmosphere.

An analytical treatment of the nightglow illumination on clouds has been performed and is contained in a Hazeltine Corp. Report (1963). The detailed derivations will not be repeated here but the results of an illustrative example from the report are presented. Basically, representative values of nightglow brightness and resultant brightness on the ground toward zenith are assumed. The illumination on a representative cloud due to this brightness is obtained along with the ratio of cloud illumination to nightglow brightness. These values are all wavelength-dependent. The parameters used for the example are:

(1) Cloud layer - top at 10 km, albedo of 0.5

(2) Optical system - f/1.5, lens transmission of 0.9, S-20 photocathode

(3) A representative wavelength-dependent atmospheric absorption coefficient

(4) The other night-light sources mentioned previously are assumed to provide additional cloud illumination equal to 1/2 that provided by the nightglow

TABLE 2-13
NIGHTGLOW CHARACTERISTICS
(Bates, 1960)

Nightglow line or Band System	Zenith Photon intensity (rayleighs) Maximum	Minimum	Mean	Measured Temperature (degrees K)	Deduced Altitude (km)
5577	518	62	259	190	95
6300	259	42	146	≤700	<200
5893	488	25	149		85 to 95
Meinel, OH			6.7×10^6	260	65 (or ~110)
				200	75 or 95
Atmospheric, O_2			2000	150	82
				200	75 or 95
Herzberg, O_2			150	≤200	75 to 95
5300 contiuum					85 to 110

Integration over the visible spectral region resulted in the following photocathode illuminations:

(1) 1.7×10^{-5} foot-candle due to nightglow alone

(2) 1.2×10^{-5} foot-candle due to Lambertian reflecting clouds

(3) 0.6×10^{-5} foot-candle due to uniform reflecting clouds

Contrast ratios are then calculated for the two cases:

(1) Lambertian reflecting clouds

$$\text{Contrast} = \frac{(1.7+1.2)\times10^{-5} - 1.7\times10^{-5}}{(1.7+1.2)\times10^{-5}} \times 100 = 41.4\%$$

(2) Uniform reflecting clouds

$$\text{Contrast} = \frac{(1.7+0.6)\times10^{-5} - 1.7\times10^{-5}}{(1.7+0.6)\times10^{-5}} \times 100 = 26.1\%$$

The correct result is postulated to lie somewhere between the two cases (clouds are neither Lambertian nor uniform reflectors). Each case of interest (particular cloud cover, ground considerations, etc.) would involve essentially the same procedure as outlined here and detailed in the Hazeltine report. The remaining components of the "light of the night sky" may be dismissed as being less important illumination contributors than the nightglow, and/or not documented sufficiently to obtain any definitive data.

9. Examples of Method

To illustrate the model and methods just outlined, examples are presented for the determination of sensitive surface irradiation as the equator is scanned from 0° longitude to 180° W longitude, and determination of contrast ratios resulting from such data. The contrast ratio is defined as $\frac{\text{Max Irradiation - Min Irradiation}}{\text{Max Irradiation}} \times 100\%$. The examples presented are applicable to the visible spectral region (0.40 to 0.70 micron).

Two Sun positions will be assumed:

(1) Solar position over the equator at 0° longitude (6a.m. at nadir)

(2) Solar position over the equator at 90° W longitude (SMS nadir) (high noon at nadir)

Two atmospheric conditions will be assumed:

(1) Completely cloudless conditions where the solar radiation is incident on the ground

(2) Completely clouded conditions with uniform cumulonimbus cloud cover (albedo = 0.7) at 14 km

Two Moon positions will be assumed:

(1) Full Moon; Moon over the equator at 180° W longitude

(2) Quarter Moon; Moon over the equator at 90° W longitude (SMS nadir)

These will apply only to the case of the solar position over the equator at 0° longitude since for the other case, (Sun over SMS nadir) there is no night area in the SMS field of view, and Moon irradiation becomes negligible. For the assumed examples, an f/0.5 optical system with a lens transmission of unity is also assumed ($K_o = 1$).

Along the equator, the Earth's surface consists of water (Atlantic Ocean) from 0 to 50° W longitude, land (northern section of South America) from 50 to 80° W longitude, and water (Pacific Ocean) from 80 to 180° W longitude. The albedo of the water surfaces will be determined by the solar altitude (daylight case) or by the lunar altitude angle (nighttime case). The land albedo was assumed to be 0.1, corresponding to an average albedo for deciduous forests in summer over the wavelength region of interest (0.40 to 0.70 micron).

The basic equation for daylight conditions is

$$E_i = 22.7\ E_b K_1 A\ K_2 K_3 K_o \text{ foot-candles}$$

where E_b is expressed in watts per meter^2 and the other components are as previously explained.

Table 2-14 and 2-15 present data on the sensitive surface irradiation and contrast ratios during daytime conditions for the two assumed solar positions.

TABLE 2-14
SENSITIVE SURFACE IRRADIATION FROM EQUATOR FOR SUN OVER NADIR
(0° LATITUDE, 90° W LONGITUDE)

W Long. Degrees	Solar Altitude Degrees	K_1	SMS Altitude Degrees	K_3	Ground Level Surface	Albedo A	E_i (ft-c)	Clouds (A=0.7) E_i (ft-c)	Contrast Percent
0	0	~0.015	-	-	Water	-	-	-	-
10	10	~0.06	1.3	-	Water	0.348	-	-	-
20	20	0.215	11.5	0.40	Water	0.134	87.4	703	87.6
30	30	0.39	21.9	0.67	Water	0.06	119	2140	94.4
40	40	0.56	32.7	0.80	Water	0.034	116	3660	96.8
50	50	0.70	43.7	0.88	Water	0.025	117	5030	97.7
					Land	0.1	467		90.7
60	60	0.805	55.0	0.94	Land	0.1	574	6180	90.7
70	70	0.89	66.6	0.97	Land	0.1	655	7050	90.7
80	80	0.95	78.2	0.98	Land	0.1	706	7600	90.7
					Water	0.0205	145		98.1
90	90	1.0	84.1	0.99	Water	0.020	150	8080	98.1

Visible spectral bandwidth (0.40 to 0.70 micron)
f/0.5 optics, lens transmission = 1.0; $K_o = 1$

E_b = 430 watts per sq meter (ground level)

= 523 watts per sq meter (14 km cumulonimbus clouds)

K_2 = 0.777 (ground level)

= 0.965 (clouds)

$E_i = 22.7\ E_b\ K_1\ A\ K_2\ K_3\ K_o$ foot-candles

$$\text{Contrast} = \frac{E_i\ (\text{clouds}) - E_i\ (\text{ground})}{E_i\ (\text{clouds})} \times 100\%$$

TABLE 2-15
SENSITIVE SURFACE IRRADIATION FROM EQUATOR FOR SUN OVER
0° LATITUDE, 0° LONGITUDE

W Long. Degrees	Solar Altitude Degrees	K_1	SMS Altitude Degrees	K_3	Ground Level Surface	Albedo A	E_i (ft-c)	Clouds (A=0.7) E_i (ft-c)	Contrast Percent
0	90	1.0	-	-	Water	0.02	-	-	-
10	80	0.95	1.3	-	Water	0.0205	-	-	-
20	70	0.89	11.5	0.40	Water	0.021	56.7	2910	98.0
30	60	0.805	21.3	0.67	Water	0.022	90.0	4400	98.0
40	50	0.70	32.7	0.80	Water	0.025	106	4570	97.7
50	40	0.56	43.7	0.88	Water	0.034	127	4020	90.8
					Land	0.1	374		90.7
60	30	0.39	55.0	0.94	Land	0.1	278	3000	90.7
70	20	0.215	66.6	0.97	Land	0.1	158	1700	90.7
80	10	~0.06	78.2	0.98	Land	0.1	44.6	480	90.6
					Water	0.348	155		67.7
85	5	~0.015	84.1	0.99	Water	0.584	65.6	121	45.5

Visible spectral bandwidth: (0.40 to 0.70 micron)
f/0.5 optics, lens transmission = 1.0; $K_o = 1$

E_b = 430 watts per sq meter (ground level)
= 533 watts per sq meter (14 km cumulonimbus clouds)

K_2 = 0.977 (ground level)
= 0.965 (clouds)

$E_i = 22.7\ E_b\ K_1\ A\ K_2\ K_3\ K_o$ foot-candles

$$\text{Contrast} = \frac{E_i\ (\text{clouds}) - E_i\ (\text{ground})}{E_i\ (\text{clouds})} \times 100\%$$

The basic equation for nighttime conditions is

$$E_i = E_m K_1 A K_2 K_3 K_o$$

where $E_m K_1$ in foot-candles, which represents the Moon irradiation on a horizontal surface, may be taken directly from Figure 2-10. Values for Moon irradiation as a function of altitude are not available. However, only the visible spectral region and reflected solar radiation are being considered. Therefore, the ratio of cloud irradiation to ground irradiation, obtainable from Table 2-14, will also apply to this case. This ratio is:

$$\frac{E_m K_1 \text{ (clouds)}}{E_m K_1 \text{ (ground)}} = \frac{533}{430} = 1.24$$

Tables 2-16 and 2-17 present data on the sensitive surface irradiation and contrast ratios during nighttime conditions for the two assumed lunar positions. Since it appears that the illumination values of Figure 2-10 represent solar twilight irradiation (extending into refraction effects) from 90 to 100°W longitude (there is no difference in illumination for different Moon conditions), the E_i values for this region cannot be reliably calculated.

Figure 2-12 presents a continuous plot of sensitive surface irradiation for the case of Sun position over the equator and 0° longitude (Table 2-15) and the two assumed lunar positions (Tables 2-16, 2-17). The twilight and refraction zone data, (shown dotted on the figure) are interpolations obtained by assuming that the irradiation gradient between the day and night zones on Earth is a smooth one. It is felt that this assumption does not introduce significant errors.

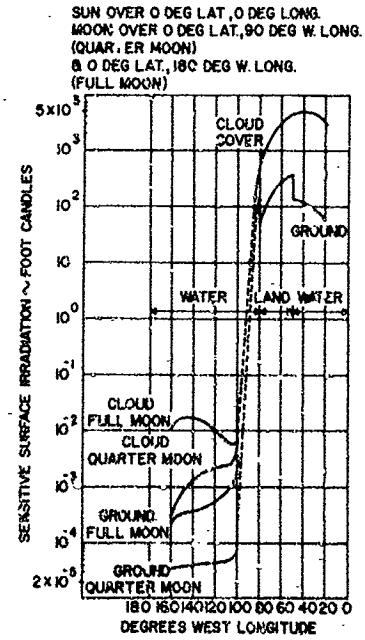

Figure 2-12. Sensitive Surface Irradiation - Sun Over the Equator

TABLE 2-16
SENSITIVE SURFACE IRRADIATION FROM EQUATOR FOR
SUN OVER 0° LATITUDE, 0° LONGITUDE AND
MOON OVER 0° LATITUDE, 180° W LONGITUDE (FULL MOON)

W Long. Degrees	Lunar Altitude Degrees	SMS Altitude Degrees	K_3	Ground Level				Clouds (A = 0.7)		
				$E_m K_1$ (ft - c)	Surface	Albedo A	E_i (ft - c)	$E_m K_1$ (ft - c)	E_i (ft - c)	Contrast Percent
90	0	90.0	1.00	50.0	Water	-	-	62.0	-	-
95	5	84.1	0.99	1.3	Water	-	-	1.61	-	-
100	10	78.2	0.98	9.0×10^{-3}	Water	0.348	2.38×10^{-3}	1.11×10^{-2}	7.35×10^{-3}	67.6
110	20	66.6	0.97	8.0×10^{-3}	Water	0.134	8.08×10^{-4}	9.91×10^{-3}	6.50×10^{-3}	87.5
120	30	55.0	0.94	1.3×10^{-2}	Water	0.060	5.70×10^{-4}	1.61×10^{-2}	1.02×10^{-2}	94.1
130	40	43.7	0.88	1.8×10^{-2}	Water	0.034	4.09×10^{-4}	2.23×10^{-2}	1.32×10^{-2}	96.9
140	50	32.7	0.80	2.4×10^{-2}	Water	0.025	3.73×10^{-4}	2.98×10^{-2}	1.61×10^{-2}	97.5
150	60	21.9	0.67	2.8×10^{-2}	Water	0.022	3.20×10^{-4}	3.47×10^{-2}	1.57×10^{-2}	98.6
160	70	11.5	0.40	3.1×10^{-2}	Water	0.021	2.02×10^{-4}	3.84×10^{-2}	1.04×10^{-2}	98.6
170	80	1.3	-	3.4×10^{-2}	Water	0.0205	-	4.21×10^{-2}	-	-
180	90	-	-	3.5×10^{-2}	Water	0.020	-	4.34×10^{-2}	-	-

Visible spectral bandwidth (0.40 to 0.70 micron)
f/0.5 optics, lens transmission = 1.0; K_o = 1

K_2 = 0.777 (ground level)
= 0.965 (clouds) (14 km cumulonimbus clouds)

$E_i = E_m K_1 A K_2 K_3 K_o$ foot-candles

$E_m K_1$ (clouds) = 1.24 $E_m K_1$ (ground) foot-candles

$$\text{Contrast} = \frac{E_i \text{ (clouds)} - E_i \text{ (ground)}}{E_i \text{ (clouds)}} \times 100\%$$

TABLE 2-17
SENSITIVE SURFACE IRRADIATION FROM EQUATOR FOR
SUN OVER 0° LATITUDE, 0° LONGITUDE AND
MOON OVER 0° LATITUDE, 90° W LONGITUDE (QUARTER MOON)

W Long. Degrees	Lunar Altitude Degrees	SMS Altitude Degrees	K_3	Ground Level $E_m K_1$ (ft - c)	Surface	Albedo A	Ground Level E_i (ft - c)	Clouds (A = 0.7) $E_m K_1$ (ft - c)	Clouds (A = 0.7) E_i (ft - c)	Contrast Percent
90	90	90.0	1.00	50	Water	-	-	62	-	-
95	85	84.1	0.99	1.3	Water	-	-	1.61	-	-
100	80	78.2	0.98	8.0×10^{-3}	Water	0.0205	1.25×10^{-4}	9.91×10^{-3}	6.56×10^{-3}	97.9
110	70	66.6	0.97	2.9×10^{-3}	Water	0.021	4.60×10^{-5}	3.60×10^{-3}	2.36×10^{-3}	97.9
120	60	55.0	0.94	2.7×10^{-3}	Water	0.022	4.35×10^{-5}	3.34×10^{-3}	2.12×10^{-3}	98.0
130	50	43.7	0.88	2.4×10^{-3}	Water	0.025	4.10×10^{-5}	2.98×10^{-3}	1.77×10^{-3}	97.7
140	40	32.7	0.80	1.9×10^{-3}	Water	0.034	4.01×10^{-5}	2.36×10^{-3}	1.28×10^{-3}	96.9
150	30	21.9	0.67	1.3×10^{-3}	Water	0.060	4.05×10^{-5}	1.61×10^{-3}	7.30×10^{-4}	94.4
160	20	11.5	0.40	8.2×10^{-4}	Water	0.134	3.42×10^{-5}	1.02×10^{-3}	2.76×10^{-4}	87.6
170	10	1.3	-	4.0×10^{-4}	Water	0.348	-	4.95×10^{-4}	-	-
180	0	-	-	1.1×10^{-4}	Water	1.0	-	1.36×10^{-4}	-	-

Visible spectral bandwidth (0.40 to 0.70 micron)
f/0.5 optics, lens transmission = 1.0; $K_o = 1$

$K_1 = 0.777$ (ground level)
$= 0.965$ (clouds) (14 km cumulonimbus clouds)

$E_i = E_m K_1 A K_2 K_3 K_o$ foot-candles

$E_m K_1$ (clouds) $= 1.24\ E_m K_1$ (ground) foot-candles

$$\text{Contrast} = \frac{E_1 \text{ (clouds)} - E_i \text{ (ground)}}{E_i \text{ (clouds)}} \times 100\%$$

The contrast ratios have not been plotted but, for the assumed conditions, can be seen to vary between 45.5 and 98.1% with the majority of values being greater than 90%.

While the examples discussed are for particular conditions, they serve the purpose of illustrating the technique. The contrast ratios are specific in that they reflect scene contrast between two limiting surfaces; the ground, and relatively high altitude, high albedo clouds. It is expected that the contrast between surfaces closer to each other in altitude and albedo values can be much smaller.

B. HEAT BUDGET

The heat budget of the Earth and its atmosphere may be considered as three problem areas:

(1) Reflection and absorption characteristics of solar radiation with respect to Earth and the atmosphere

(2) Radiation of energy from Earth and the atmosphere to space

(3) Radiant energy exchange mechanisms between Earth and the atmosphere

The solar radiation problem has been treated in some detail in the previous paragraphs. This consists of ultraviolet, visible, and infrared radiation having wavelengths between 0.29 and 4.0 microns. Terrestrial radiation consists of infrared energy, nearly all of which occurs at wavelengths beyond 4.0 microns, radiated by the Earth-atmosphere system.

The first area of interest to be considered will be the selective absorption characteristics of the atmosphere. In general, the most effective absorbing component of the atmosphere is water vapor (H_2O). Although it normally comprises less than 3% of the atmospheric gases, it accounts for nearly all of the gaseous absorption of the terrestrial radiation. The only other noticeable contributions to this absorption are made by carbon dioxide (CO_2) and ozone (O_3), with the absorption by CO_2 being at least an order of magnitude greater than that of O_3. Figures 2-13 and 2-14 show the principal features of the absorption bands and windows of the atmosphere. Since terrestrial radiation is being considered, a lower wavelength limit of 3 microns is established. For a black body at 350°K, 0.06% of the radiant energy is contained in wavelengths below 3 microns; for lower black body temperatures, this percentage figure decreases. The term "window" denotes a spectral region of relatively high transmittance lying between two regions of low transmittance. In Figure 2-13, the absorption bands of H_2O, CO_2, and O_3 are denoted. Figure 2-14 is an atmospheric transmission spectrum determined by water vapor alone, since the other two constituents do not have absorption bands above 18 microns. Above approximately 23 microns, no data are available, but it is assumed that complete absorption is obtained by H_2O up to the upper wavelength limit of interest, 40 microns.

The amount of absorption is, of course, dependent upon the concentration of the absorbing medium. In this regard, it is customary to use the following terminology:

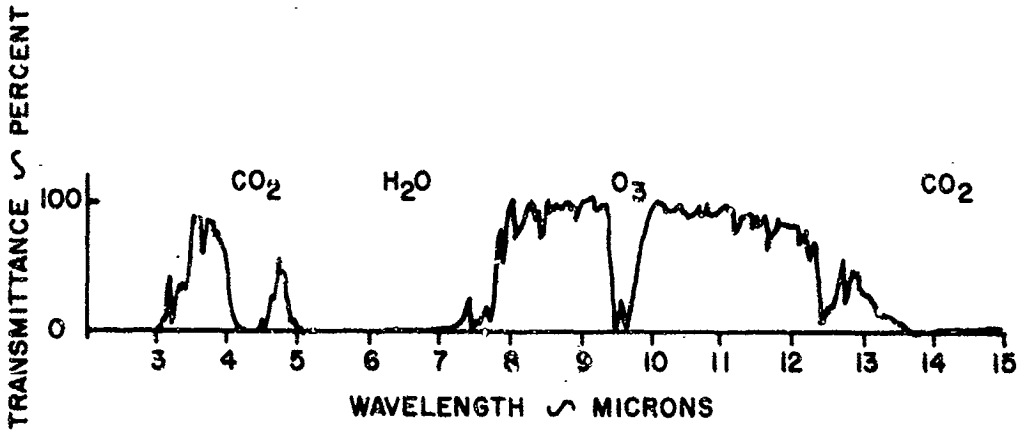

Figure 2-13. Windows and Absorption Regions of the Atmosphere (Howard, 1961)

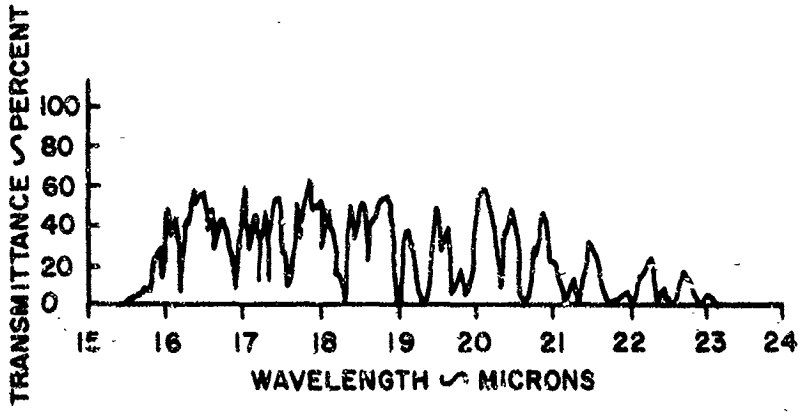

Figure 2-14. Atmospheric Transmission Spectrum Due to Water Vapor (Holter, 1962)

- Water vapor concentration in the atmosphere is expressed in precipitable centimeters (pr-cm) of water. This measure of concentration is the thickness of the layer of liquid water that would be formed if all the water vapor traversed by a beam were condensed in a container of cross sectional area equal to that of the beam. The precipitable water in an air column through the whole atmosphere varies from approximately 0.01 cm in extreme winter arctic conditions, to 10 cm in the rainy season of the tropics.

- Carbon dioxide concentration may be expressed in atmocentimeters (atmo-cm). This is the path length in centimeters which would contain the same number of molecules for a gas at NTP (0°C, 1013 millibars) as a column of arbitrary path length, pressure and temperature. Since the atmospheric abundance of CO_2 is about 0.03% by volume, the absorber concentration of CO_2 at ground level is about 30 atmo-cm per km of path length. Figures 2-15 and 2-16 give the transmittance as a function of absorber concentration in the absorption path for two of the absorption bands of interest; the 6.3 micron (5 to 8 microns) band of H_2O and the 15 micron (12 to 18 microns) band of CO_2. The transmittance values were measured under reduced pressure to simulate conditions at high altitudes. The total pressures with nitrogen were 125, 500, and 760 mm Hg, which correspond to altitudes of 42,000 feet, 11,000 feet, and ground level, respectively.

Using the data just presented, an estimate can be made for the percentage of thermal radiation transmitted through the atmosphere for a given Earth black body temperature. Consider the spectral band between 7 and 40 microns and assume H_2O and CO_2 absorber concentrations of 0.22 pr-cm and 30 atmo-cm respectively. The transmittance for the 18 to 21 micron and 21 to 40 micron H_2O bands has been estimated from Figure 2-14 to be 30% and 0 respectively. For a complete treatment, black body temperatures from 100 to 400°K are considered. This greatly exceeds the expected range of Earth temperatures (200-300°K). Table 2-18 presents the pertinent data and Figure 2-17 is a plot of the results.

It can be seen that the percentage radiation transmitted through the atmosphere increases rather rapidly with black body temperature until a broad peak region is reached between 300 and 400°K with a maximum of 41% at 345°K.

Figure 2-18 shows a spectral radiance curve illustrating the above statements. The upper black body curve represents radiation from the Earth's surface when the surface temperature is a representative 288°K. In the atmospheric window regions, this radiation escapes to space. In the absorption bands, the escaping radiation comes from the stratosphere, where a representative temperature is 218°K (lower black body curve). In intermediate spectral regions, the radiation to space falls between the two black body curves. The resultant radiation spectrum to space is illustrated by the solid curve.

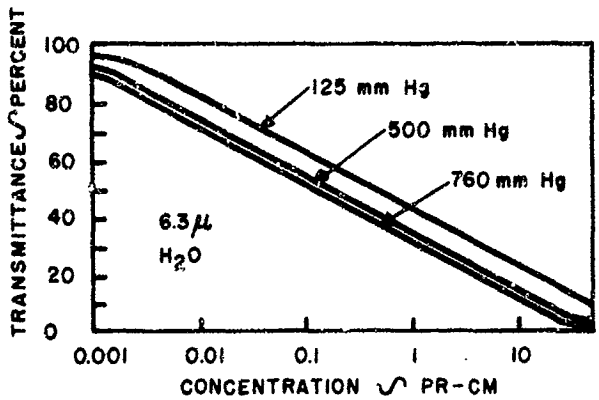

Figure 2-15. Transmittance as a Function of H_2O Concentration - 6.3 Micron Absorption Band (Howard, 1961)

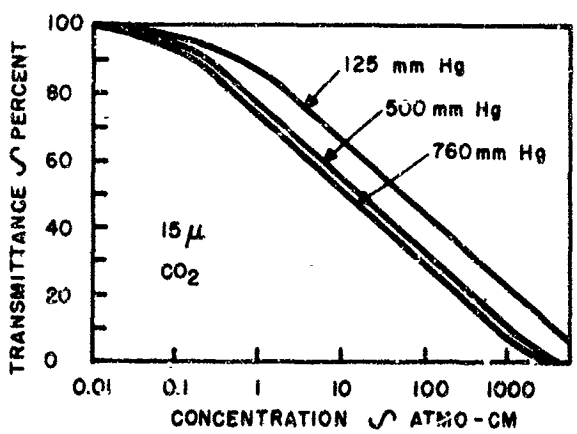

Figure 2-16. Transmittance as a Function of CO_2 Concentration - 15 Micron Absorption Band (Howard, 1961)

TABLE 2-18
ABSORPTION BANDS AND PERCENT OF ATMOSPHERIC TRANSMISSION

Band Microns	Absorber	Trans-mittance (percent)	Black Body Temperature (°K)											
			100		150		200		250		300		350		400	
			*	**	*	**	*	**	*	**	*	**	*	**	*	**
7-8	H_2O	15			0.2	0.1	1.2	0.5	3.5	1.6	6	2.7	7	3.2	10	4.5
8-9.5	-	100			0.8	0.8	3.5	3.5	7	7.0	10	10.0	12	12.0	12	12.0
9.5-10	O_3	0			0.5	-	1.5	-	3	-	3	-	4	-	4	-
10-12	-	100	0.2	0.2	2.5	2.5	8	8.0	11	11.0	13	13.0	14	14.0	12	12.0
12-18	CO_2	40	3.8	1.5	17	6.8	26	10.4	29	11.6	28	11.2	24	9.6	21	8.4
18-21	H_2O	30	5	1.5	11	3.3	11	3.3	10	3.0	8	2.4	6	1.8	5	1.5
21-40	H_2O	0	40	-	43	-	34	-	25	-	13	-	13.5	-	10.5	-
	TOTALS		49.0	3.2	75.0	13.5	85.2	25.7	88.5	34.2	86	39.3	80.5	40.6	74.5	38.4

* - percent of total black body energy contained within band (taken from G.E. Radiation Calculator)

** - percent of total black body energy transmitted through atmosphere

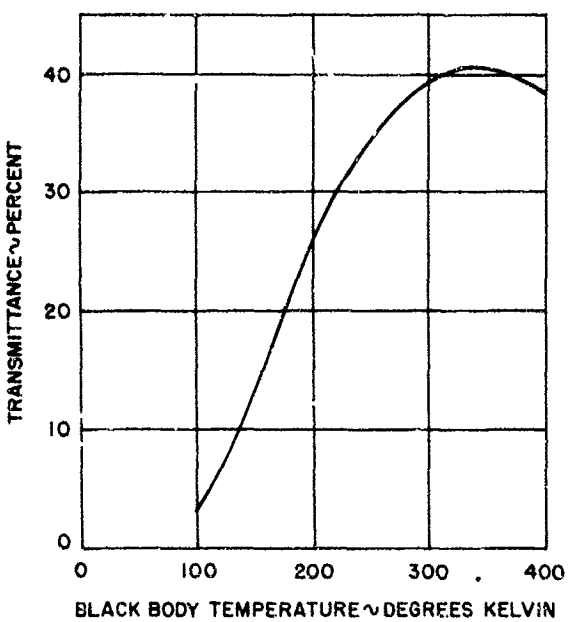

Figure 2-17. Percent of Atmospheric Transmittance as Function of Terrestrial Black Body Temperature

It has been shown that by a series of assumptions and approximations, the atmospheric transmission of the terrestrial radiation may be estimated. No effort has been made to include the attenuation effects of particulate matter in the atmosphere. This would include dust, smoke, haze, industrial effluents, organic matter, and other such materials. In addition, and most important, the effect of absorption by liquid water, as is found in clouds and fog, has been neglected. Measurements indicate that the liquid has approximately the same absorption bands as the vapor but with absorption coefficients nearly ten times as great (Byers, 1959). Around 10 microns, in the middle of the water vapor window and at a point at which the absorption is least for liquid water, a water film 0.1 mm thick will transmit only 1/100 of the incident unreflected radiation. For average clouds, the length of a path through a cloud that would contain 0.1 mm of liquid water per unit cross section would be about 160 ft.

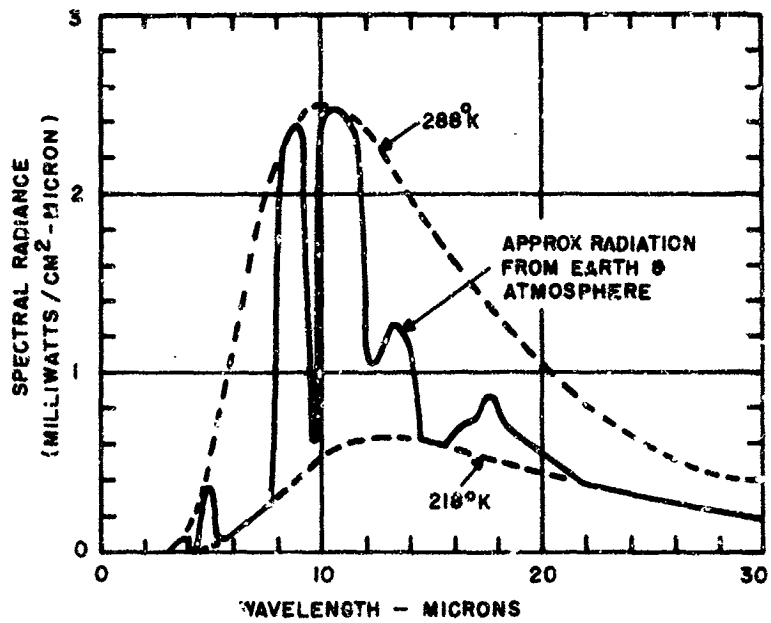

Figure 2-18. Typical Terrestrial Radiation Spectrum (Johnson, 1961)

In subsection A it was shown that cloud cover is perhaps the dominant feature in the solar radiation problem. From the above statements, it is clear that clouds also play a dominant part in terrestrial radiation considerations. Because of their great absorption capabilities, clouds may be considered as black body radiators since they absorb and re-emit radiation in all of the infrared wavelengths, including the water vapor windows. Normally, temperature decreases with altitude. The cloud layer absorbs radiation from below and re-emits radiation both below and above. As far as radiation to space (and the SMS) is concerned, the result is the creation of a radiation surface as effective as the ground but at a considerably lower temperature (often below 200°K).

In conclusion, some data on the expected levels of terrestrial radiation may be presented. The magnitudes are known to vary as a function of latitude. Table 2-18 presents values for the total outgoing radiation obtained from a meteorological study performed by Baur and Philipps in 1934. (The table is from Johnson, 1961.) The values have been averaged over a period of a day or longer but the hourly variation between daytime and nighttime values can be ignored as not being excessive.

TABLE 2-19
TOTAL LONG-WAVE RADIATION FROM THE EARTH AND ATMOSPHERE
(Johnson, 1961)

Latitude degrees	Radiated Energy (watts per sq. cm)			
	Jan.	21 March	July	23 Sept.
0 - 10	0.0203	0.0212	0.0209	0.0206
10 - 20	0.0206	0.0210	0.0210	0.0211
20 - 30	0.0203	0.0204	0.0213	0.0213
30 - 40	0.0193	0.0194	0.0216	0.0218
40 - 50	0.0175	0.0175	0.0202	0.0201
50 - 60	0.0164	0.0164	0.0195	0.0185
60 - 90	0.0156	0.0152	0.0189	0.0177

More recent estimates have been made by various investigators which indicate:

- 27.9 mw/cm^2 at 0° latitude to 18.1 mw/cm^2 at 90° latitude for clear sky conditions. (Variation diminishes as skies become overcast, according to Camack, 1962.)
- 20.9 mw/cm^2 at 0° latitude to 16.7 mw/cm^2 at 90° latitude. (No sky condition mentioned, in Cherney, 1945.)
- Recent preliminary results of data obtained by the Tiros III meteorological satellite range from 19.1 mw/cm^2 over the East Central United States under heavy cloud conditions to 33.9 mw/cm^2 over the desert in clear skies. (Nordberg, 1962).

It becomes obvious that terrestrial radiation is entirely dependent upon atmospheric transparency, which varies greatly depending principally upon the presence or absence of water vapor, carbon dioxide, and clouds. It is likely that definitive satellite data will be required before anything more than a crude estimate of the Earth's thermal radiation environment can be given.

SECTION 3 - CLOUD COVER SENSORS - VISIBLE SPECTRAL REGION

A. GENERAL

The primary function of the SMS, as defined in the NASA work statement, will be to obtain low and high resolution pictures of the Earth's cloud cover under all conditions of incident lighting; thus, 24-hour coverage is required. Factors limiting the ability of the camera system to meet this requirement include sensor availability, sensor resolution and dynamic range, and vehicle payload and power requirements. The necessity for 24-hour capability restricts the sensor selection to low light level, TV-type imaging systems, such as Image Orthicons, Intensifier Orthicons, Image Isocons, and, possibly, high sensitivity Vidicons. Infrared systems offer another possibility. Sensors suitable for use in the visible spectral region are considered in the present section; infrared cloud cover sensors are discussed separately in Section 5, "Cloud Cover Sensors - Infrared."

Section 2 has already considered, in great detail, the energy levels which will be available at the focal plane of the sensor optical system. Thus, data are provided on the illumination and contrast levels for various cloud types and terrain features, as functions of solar angle, cloud altitude, and geographical position. Stellar, lunar galactic, and airglow contributions are also considered. With these data as a starting point, it is possible to estimate the performance of a number of visual sensors for the SMS application. Such an estimate is the purpose of this section.

In the following paragraphs, detailed requirements for the cloud cover sensor will be established. Such factors as resolution, contrast, dynamic range, and signal to noise performance of the sensor tubes and systems will be established as functions of ground resolution, time of observation, optics, stabilization, data rates, etc. Earth coverage and satellite-Earth geometry will also be considered. Once the necessary requirements are established, a comprehensive survey of existing sensors is presented, in which devices such as Vidicons, SEC Vidicons, Ebicons, Isocons, Orthicons, intensifier tubes, image dissectors, and others are considered in some detail. In each instance, the sensors are identified by manufacturer (and model number, if possible) and data is presented on size, weight, power consumption, resolution, dynamic range, and sensitivity. Comparisons are presented of miniaturized versus full size Image Orthicons, and electrostatic versus magnetic Orthicons and Vidicons. Information is also presented on the effects of integration and scan time variation on sensor resolution and signal to noise performance.

A theoretical analysis is given of the performance of an ideal imaging device in terms of statistical phenomena. The effect of contrast, as well as theoretical signal to noise ratios and limiting resolution performance are presented. In both the analysis and the summation of actual tube data, only multiple scan operation at normal commercial TV rates is considered, since neither significant analysis nor definitive performance information was available on single scan sensor operation. Where single scan systems must be considered, as in the SMS application, extreme care must be taken in utilizing the information presented, so that incorrect conclusions are not drawn. This matter is discussed in more detail in Section 6, "Problem Areas."

Optical system design is then discussed. The relative merits of refractive and reflective systems are considered, and optical problems peculiar to the cloud cover sensing function are presented with regard to size, weight, resolution, image motion, lens flare, filtering, thermal control, and numerous other factors. Differences between various possible optical systems are considered, and the characteristics which render some of them suitable for the present application and preclude the use of others, are discussed.

Special techniques particularly suited to the SMS application are then considered. They include filter wheels, photocathode pulsing, and automatic iris control for controlling brightness level variation over eight or nine orders of magnitude; semi-automatic control of operating parameters to improve dynamic range capability; and automatic control of beam current, video AGC, and bandwidth rolloff to improve low light level performance and optimize resolution. The use of adjustable masking to occult sunlit portions of the Earth's disc and improve sensor performance when viewing the night portion of the Earth is discussed, as are Sun protection devices and certain other potentially useful techniques.

Based on data presented in these sections, an analysis is performed to determine the sizes and develop the characteristics of systems for inclusion in the 100 and 500 pound vehicles. The characteristics of these systems, including mechanical, electrical, and optical parameters, and expected performance, are summarized. In addition, the interfaces between the sensor system and other vehicle systems are considered.

B. REQUIREMENTS

The NASA work statement for the study of cloud cover sensors defines the constraints and objectives to be as follows.

A study of sensors will be made, to establish a basis which will enable the examination and assessment of sensor abilities and trade-offs. Sensor resolution, and subsequently the resolution of the SMS is the basic parameter. All other spacecraft trade-offs are, in one manner or another, measured against their effects upon sensor resolution. To accomplish the one-year satellite orbital lifetime required by NASA, the design of the sensory system must reflect the highest technological advancements, together with simplicity and reliability.

The sensors will provide wide area, full Earth disc, coverage of the Earth's meteorological cloud complex, as well as a narrow area coverage. The objective will be to provide meteorological resolution of 10 miles or better at the nadir for the full Earth coverage, and significantly better resolution for the narrow field coverage.

The study and survey of sensors will include at least those listed in the following categories (which are within the time limits of this study program):

(1) Various types of Vidicons (electrostatic, magnetic, etc.)

(2) Various types of Image Orthicons, (electrostatic, magnetic, etc.)

(3) Dieletric tape cameras

(4) Special types of Imaging Sensors

The use of a single sensor to provide both day and night cloud cover surveillance will be investigated. The problems associated with the sensor's abilities to provide satisfactory meteorological information when the full Earth disc encompasses daytime conditions on one edge of the Earth and nighttime conditions on the other will be examined.

During the study and survey of sensors the interrelation of inherent sensor parameters, as well as the characteristics of ancillary instrumentation, will be examined to provide additional comparative data. To do this, data will be developed in at least the following areas:

(1) Format size

(2) Limiting resolution in TV lines and in TV lines per inch

(3) Maximum signal to noise ratio

(4) Type of shutter required

(5) Dynamic range

(6) Sensitivity for maximum resolution in foot-candle seconds

(7) Image storage time relative to the time for resolution drop off to 2/3 maximum resolution

(8) Optical characteristics required for a given ground resolution and illumination

(9) Ground coverage in statute miles

(10) Allowable stabilization rates of satellite for ground smear of one-half TV line.

The objective of this study will be to fulfill the NASA requirements and to develop the necessary comparative data that will make possible an intelligent evaluation of sensor and ancillary parameters for optimum performance.

C. SENSOR SURVEY

While photographic film might prove to be a suitable recording medium, the space environment, one-year orbital lifetime, and near real time data transmission requirements preclude the use of such a system for this application. To transmit data to the ground, film would have to be processed in orbit and scanned to produce a video-like signal for transmission to Earth. System limiting resolution would then be that of the scanning device, and the inherently higher capability of the film would not be properly utilized. Equipment complexity, chemical limitations, and size, weight, and power requirements, must rule out such a technique immediately.

Electronic imaging systems are attractive for a number of reasons. Coupled with appropriate optics, these sensors are capable of meeting virtually any meteorological resolution requirement. With appropriate mechanical or electrical compensation, such sensors can accept a wide range of scene illumination conditions. The video-type sensor processes information in a form ideally suited for real time and near real time data transmission. Finally, such sensors have been used in space applications, and are being improved and upgraded in performance to meet the stringent requirements of programs such as the SMS.

The basic element in a video camera is the sensor tube itself. While drive and synchronization circuitry, deflection and focusing yoke homogeneity, and recording medium sensitivity and resolution are sometimes the limiting factors in the performance of a video camera chain, there is no fundamental reason why any or all of these cannot be improved by the application of sound engineering principles to the point where such limitations are removed. When efforts are made to eliminate such factors, the sensor tube itself invariably provides the ultimate limit to system performance. Consequently, any serious study of system capability must begin with a thorough analysis of tube performance.

In this section, a wide variety of video-type sensor tubes are considered. In each instance, a brief discussion of tube construction and operation is given, so that fundamental performance limitations may be more clearly understood. Operating characteristics of various tube types, based on theoretical calculations as well as actual measurements, are presented. Characteristics such as resolution, sensitivity, dynamic range, and signal to noise performance are compared for various models of a tube type, as a preliminary to the system analysis (subsection F), where the performance of various types of tubes is then compared to select and synthesize specific systems.

The following discussion does not restrict itself to the more common video sensor tubes, such as the Vidicon and Image Orthicon, but includes several others, such as the Ebicon, CPS-Emitron, Image Dissector, Isocon, and Image Intensifier Orthicon. In addition, attention is given to sensors which combine the characteristics of two or more storage media.

1. Photosensitive Surfaces

Television imaging sensors invariably depend upon a photosensitive surface for the primary generation of an electrical signal. In general, such surfaces are either photoemissive or photoconductive, depending upon the physical process involved, and the sensor tube itself is frequently classified in terms of

this primary process. Thus, for example, the Image Orthicon is considered photoemissive, while the Vidicon is primarily photoconductive. Devices which incorporate two or more distinct processes are considered, for the purposes of this study, to be combined sensors. The Ebicon is such a sensor, since its primary electron production is by photoemission, while charge storage is accomplished by conductivity induced in the target under electron bombardment.

As a process, photoemission is a manifestation of the photoelectric effect, in which the energy of an incoming photon (light quantum), which is directly proportional to the radiation frequency, is transferred to electrons in the photoemissive surface, giving these electrons sufficient energy to escape from the surface. The energy which binds an electron to a particular solid is proportional to the work function of the material. This binding energy is the minimum energy which must be supplied to the most energetic electrons in the solid to remove them from the solid. Most practical photoemitters have work functions lying between 1 and 2 electron volts. The sensitivity of the photoemissive process is generally expressed in quantum efficiency, as a function of wavelength; i.e., at a particular wavelength, a quantum efficiency of 100% indicates that each incoming quantum raises one electron past the material work function. For incident radiation of a particular wavelength, photoelectric current is proportional to radiation intensity.

Information on the absolute spectral response characteristics of photoemissive surfaces is widely available, and typical curves which are frequently cited in the literature are presented in Figure 3-1.

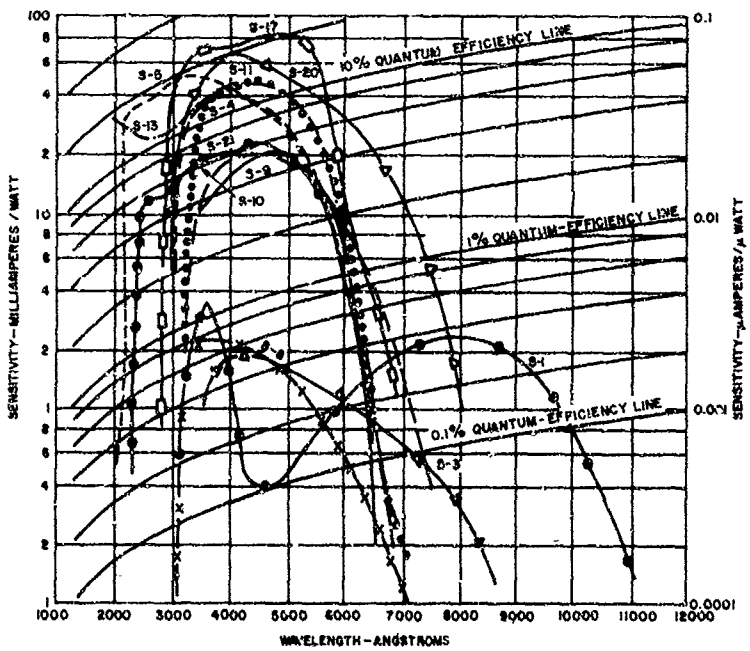

Figure 3-1. Spectral Response Characteristics

The S-20 photosurface, which is a sodium-potassium-cesium-antimony (Na-K-Cs-Sb) material deposited on a translucent substrate, possesses a broad, high efficiency sensitivity, with about 20% quantum efficiency at its peak spectral response of 4200 angstroms, 1% quantum efficiency at 7500 angstroms (in the very near infrared), and a greater sensitivity in the 5750 to 7800 angstrom range than any other currently available photoemissive surface. The S-17 photosurface, which is a cesium-antimony (Cs-Sb) material deposited on a reflecting substrate, actually possesses a higher sensitivity than the S-20 photosurface up to about 5800 angstroms, with a quantum efficiency approaching 25% at 3500 angstroms (Figure 3-2). However, its sensitivity falls off so rapidly toward the upper end of the spectrum (the S-20 photosurface being more than an order of magnitude better in sensitivity at 7000 angstroms), that the S-20 photosurface is a more desirable material to employ in those applications where substantial near infrared energy content is available. Such is the case here, where cloud-reflected solar and similar spectrally-distributed energies are utilized for viewing, since 23% of the solar energy content lies in the 5800 to 8000 angstrom wavelength band, while only 9% of the solar energy content lies in the 3000 to 4000 angstrom region. Indeed, the S-20 photosurface appears to have an undesirably high response in the 3000 to 4000 angstrom region, since a considerable contribution from atmospheric scattering appears in this region in the form of foreground noise. Optical filtering may be required to reduce this unwanted light.

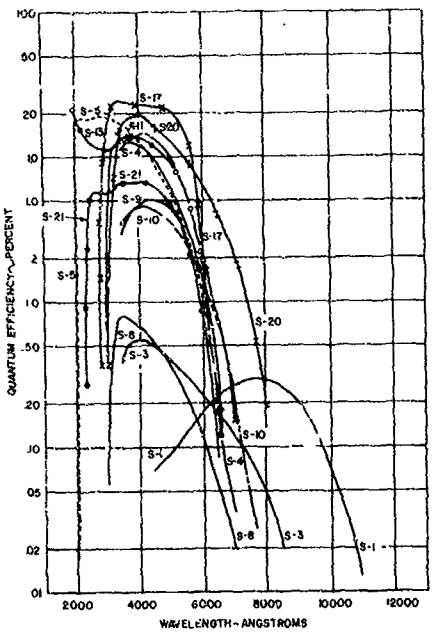

Figure 3-2. Relative Quantum Efficiency of Various Photocathodes

Photoconductivity is the increase in electrical conductivity which occurs when photons excite electrons to the conduction band or create holes in the valence band of a semiconductor. This process may be accomplished with a thin semiconducting film, whose resistance per unit volume varies with the intensity of incident illumination. Photoconductive surfaces possess broader spectral characteristics than photoemitters, but their low light level sensitivity is limited primarily by dark current; i.e., current drawn in the semiconductor under conditions of no incident illumination. It will be seen later that dark current limitations prevent most photoconductive sensors, for example, the Vidicon, from achieving the required level of performance of the SMS cloud cover sensor under night illumination conditions.

Consider now the construction and operation of various sensor tubes falling into each of these categories. Photoemissive surface devices are discussed first.

2. Photoemissive Devices

Sensors falling within the category of the photoemissive devices include Dissectors, Iconoscopes, Orthicons, CPS-Emitrons, Image Orthicons, Intensifier tubes, and Image Isocons. Combination devices which may include photoemissive imaging sections, e.g., the Ebicon, have been arbitrarily placed in subsection C.4 below.

a. The Image Dissector

The Image Dissector provides an excellent example of the counting process which underlies all picture pickup devices. The scene to be transmitted is focused on a conducting photoemissive surface (Figure 3-3).

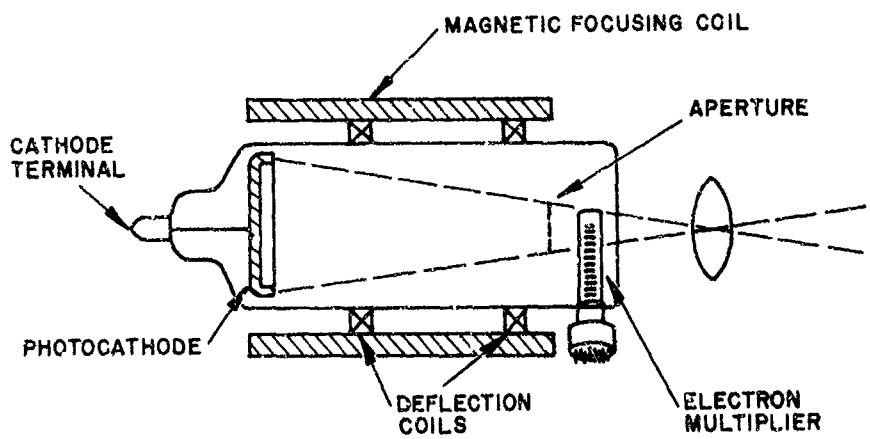

Figure 3-3. The Image Dissector

Emitted electrons are then brought to a focus at unit magnification at the other end of the tube by a magnetic focusing coil. Here, the tube is closed except for a small aperture whose size defines the dimensions of the final picture resolution element. The entire picture is scanned across by the deflection coil so that the aperture sees each portion of it once during every frame time. Electrons passing through the aperture are counted by an electron multiplier whose gain can be made arbitrarily high. At any instant, only those electrons originating in a particular picture element pass through the aperture and are counted by the multiplier. The total number of electrons passing through the aperture in the time it takes to scan a picture element is a measure of the signal output of the device; the square root of this number is the signal to noise ratio referred to that picture element.

The Image Dissector suffers from poor sensitivity, and is used only in those applications where high illumination levels are available, as in the transmission of films or slides. Its low sensitivity is due to the fact that only a small fraction of the electrons emitted by the photocathode at any one time are permitted to enter the electron multiplier. For example, if a picture resolution of 1000 x 1000 lines is required, the light level on the scene would have to be one million times greater than if all emitted electrons could be counted. Obviously, integration of all the light falling on the photosurface is needed if high sensitivity is to be achieved. Actual performance data for the Image Dissector is included in subsection C.6. Subsection C.5 contains comparative performance curves.

Advantages of the Image Dissector are its high resolution capability (greater than 3000 lines), wide dynamic range (3 to 6 orders of magnitude), linear light transfer characteristic, and absence of a thermionic cathode. With due regard to these advantages, the low sensitivity of this device makes its suitability for the SMS doubtful. Section 3 (Problem Areas) contains a further discussion of this sensor.

b. The Iconoscope

This device is included primarily for the sake of historical completeness, and for the valuable insight which it provides on subsequent developments in photoemissive devices. Charge storage is accomplished by what is effectively an elemental array of capacitors. The photoemissive surface is formed on a thin insulating sheet having a conducting coating (called the signal plate) on the reverse side. Tube construction is illustrated in Figure 3-4. When electrons are emitted from the photosensitive target, the surface charges positively at each point in proportion to the light intensity at that point. The charge accumulated at each point is then converted to a video signal by a scanning of the surface with an electron beam. As each charge element is neutralized by the beam, a current is induced in the signal plate proportional to the total charge. The basic image-storage-scan sequence described here is common to most video sensor tubes in use today.

The Iconoscope's inefficiency arises largely from the high velocity scanning beam striking the target with sufficient energy to yield a secondary emission ratio greater than unity. The target is driven positive (a result which is not undesirable) but the secondary electrons produced by the scanning beam fall back on the target in unscanned regions, thereby partially erasing the picture stored there. In addition, more secondary electrons land near the center of the target

than elsewhere, producing shading in the picture. Efficiency of signal generation in the Iconoscope is only 5% of what might be realized if all primary photoelectrons could contribute to the video signal. The weak collection field used to gather photoelectrons in the tube also prevents attainment of fully saturated emission, and further contributes to the low efficiency of the device.

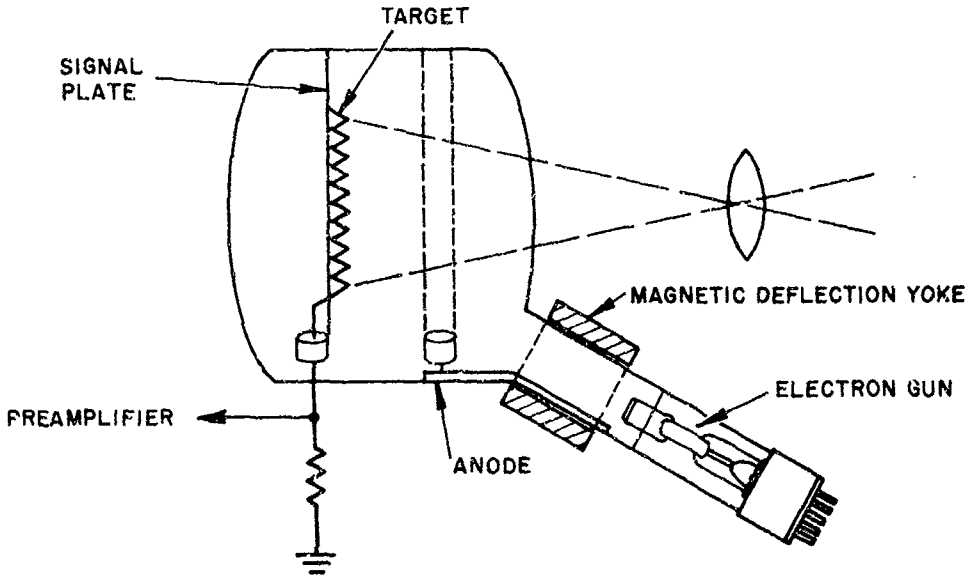

Figure 3-4. The Iconoscope

c. The Image Iconoscope

The Image Iconoscope differs from the Iconoscope in that it combines an imaging section with a high velocity scanning beam. The electron image is generated by a conducting photocathode (Figure 3-5). Sensitivity is improved 5 to 10 times over the Iconoscope because the conducting photocathode is more sensitive than the insulating target surface, and also because the electron image is amplified by secondary emission at the target. Otherwise, operation is substantially the same as in the Iconoscope. Performance characteristics compare with those of the Orthicon, which is described next.

The Iconoscope was displaced over 20 years ago by more sensitive tubes for commercial broadcasting, and is no longer manufactured in this country. The Image Iconoscope is still used in Europe, but it is also being displaced.

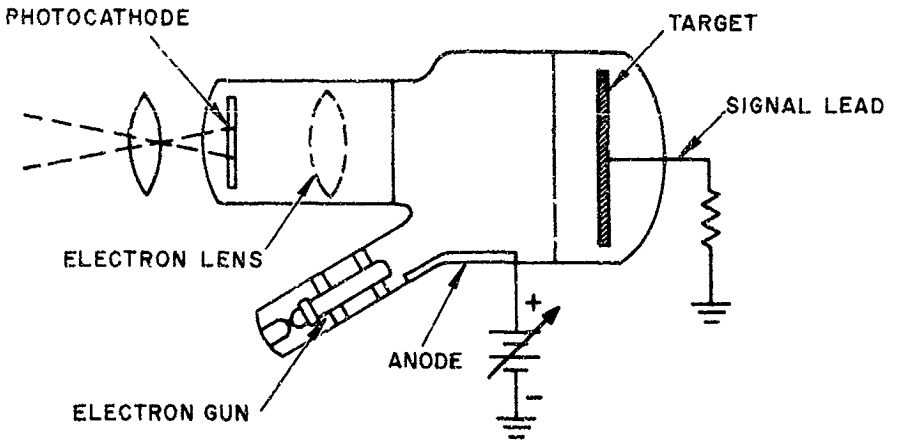

Figure 3-5. The Image Iconoscope

The relatively poor performance of both these tubes, compared with other tubes currently available and in production in this country, coupled with their massive size and relatively fragile construction, render them unacceptable for satellite application. No further consideration is given to either of these tubes in the remainder of the report, with the exception of some comparative performance curves in subsection C.5.

d. The Orthicon

The Orthicon represents a substantial improvement in performance over the basic Iconoscope design. Spurious shading and incomplete ulitization of storage in the Iconoscope both result from the impact of the high velocity scanning beam: the low velocity beam used in the Orthicon eliminates these defects. With this low velocity beam, electrons may be deposited only where a positive picture charge exists, in an amount equal to the positive charge; there is little or no interchange of electrons between different parts of the target. In addition, a strong field may now be set up to efficiently collect electrons from the photoemissive target.

While the advantages of a low velocity scanning beam are apparent, such beams are difficult to control in practice. The beam may easily be defocused or deflected by stray charges in the tube, and even by the picture charge on the target itself. In addition, the beam must be deflected so as to approach the target normally. The Orthicon accomplishes this by using a uniform magnetic focusing field extending the full length of the tube. In early Orthicons (Figure 3-6) slow speed vertical deflection was accomplished by a pair of deflection coils, while high speed horizontal deflection was obtained by a pair of shaped plates.

Later, improvements in deflection circuits made possible a simpler design, in which both horizontal and vertical deflection is obtained by the use of deflection coils.

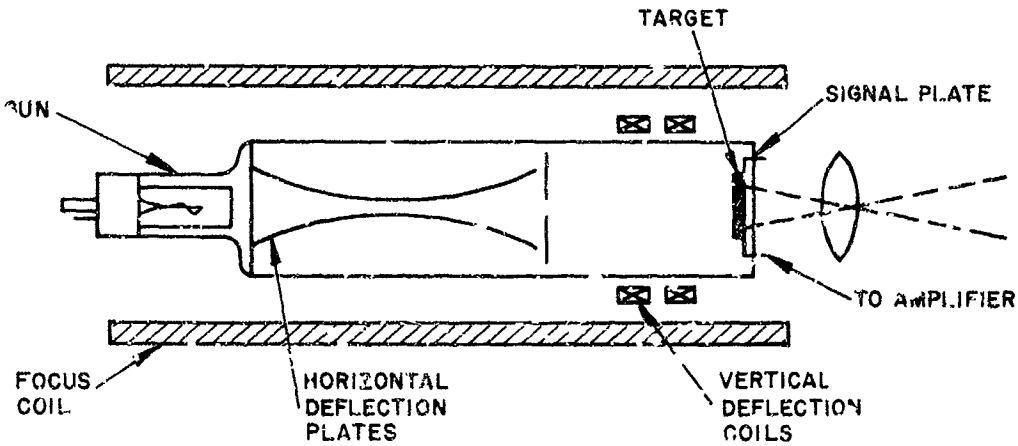

Figure 3-6. The Orthicon

In operation, the scene is imaged on a photoemissive, insulating target, allowing a positive charge pattern to be established. The scanning beam approaches the target with very low velocity. Where a positive charge exists, some electrons in the beam land on the target, neutralizing this charge. The signal plate on the opposite side of the target senses the fraction of beam current which lands on the target, and transmits this signal to the amplifier.

The output is proportional to incident light intensity over a wide range. Low light level operation is limited primarily by TV amplifier noise; at very high light levels, the scanning beam is easily defocused and deflected by potential differences on the target.

Performance linearity and freedom from spurious shading resulted in wide use of this tube in this country and abroad for commercial broadcasting in the 1940's. On the other hand, the limited signal range of the tube caused problems in reproducing scenes having a wide contrast range. Furthermore, since the cathode potential of the target is metastable, a sudden bright flash of light can charge the target to the point where it is locked by the scanning beam to the relatively stable potential of the anode. A substantial period of time is then required to return the target to cathode potential. Due to these limitations, and the existence of superior tubes of other types, the Orthicon is not considered further in this report. An improved design, the CPS-Emitron, is discussed below.

e. The CPS-Emitron

The Orthicon was introduced in this country commercially in 1940, and superseded a few years later by the Image Orthicon. Further work was done on the Orthicon in England, however, where it is called the CPS-Emitron. A diagram of an improved CPS-Emitron is given in Figure 3-7.

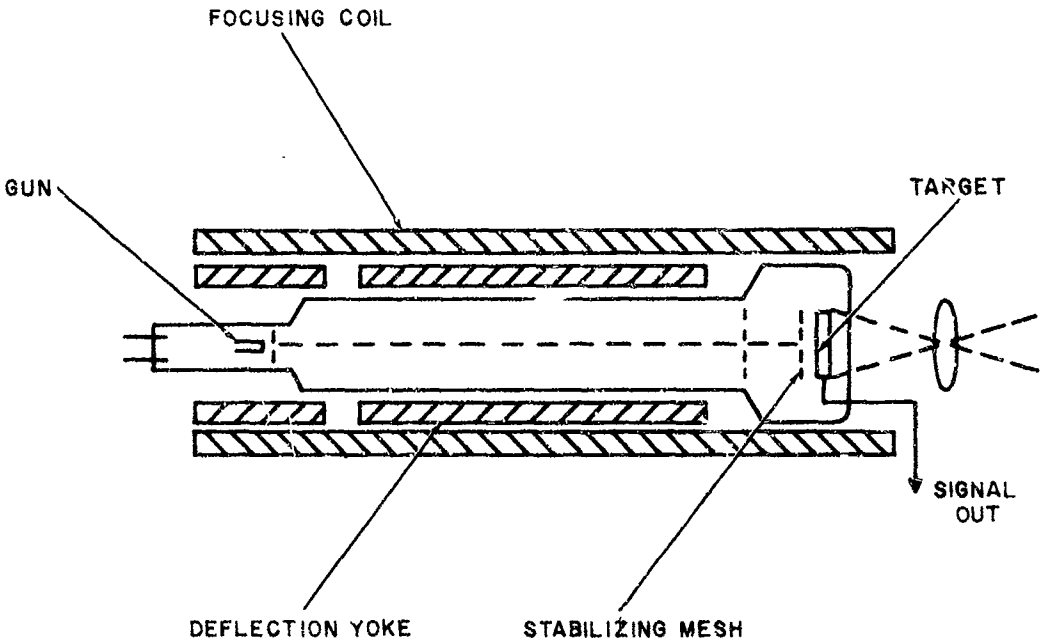

Figure 3-7. The CPS-Emitron

This tube produces high quality pictures and is used in some commercial broadcasting. Recent improvements include the incorporation of a high sensitivity tri-alkali (S-20) photosurface in the target, and the use of a fine screen, closely spaced from the target, on the scanned side. The S-20 photosurface improves sensitivity by a factor of three over earlier versions of the tube, while the screen prevents the abovementioned unstable target operation characteristic of the Orthicon.

Detailed operation of the CPS-Emitron will not be considered here, since it is essentially the same as that of the Orthicon. In its present form, this tube represents a significant advance over earlier versions of the Orthicon, and some performance data is presented in subsection C. 5. However, because

other tube types of comparable or superior performance are more readily available in this country, no further serious consideration is given to the use of this tube in the SMS sensor system.

f. The Image Orthicon

The TV tube most often used in commercial broadcasting today is the Image Orthicon. Developed nearly 20 years ago, the Image Orthicon and tubes developed from it provide the highest sensitivities yet attained for most advanced applications. The tube owes its high sensitivity to the use of an electron image section and a signal multiplier.

A cross sectional diagram of the Image [illegible] presented in Figure 3-8. The scene is imaged on a semitransparent photocathode which is deposited on the inside face of the tube. Emitted [illegible] are focused by the coil, and accelerated to form an electron image [illegible]

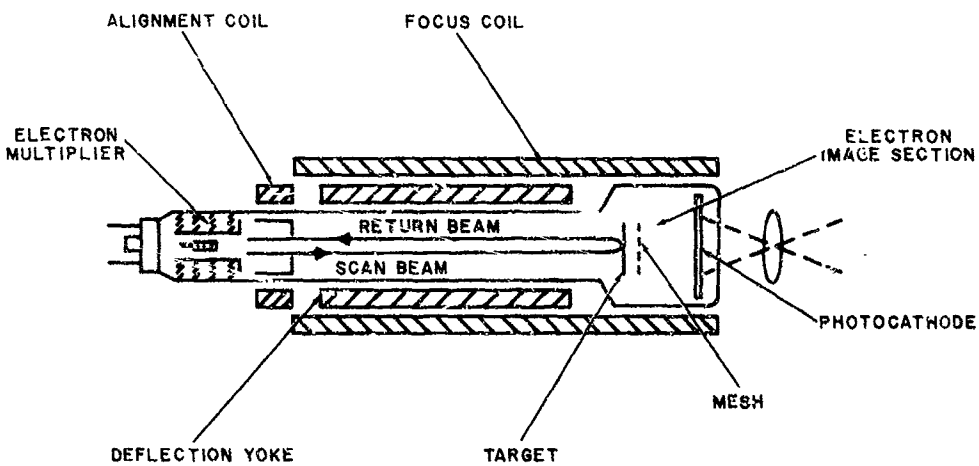

Figure 3-8. The Image Orthicon

surface of the target may be processed to give it a secondary emission ratio (γ) substantially larger than unity. The charge stored on the target can thus be greater than that of the emitted electrons by a factor (γ - 1), since γ electrons are emitted from the target per incoming (trapped) primary photoelectron. A fine mesh target screen collects secondary electrons and serves as a signal plate in determining target capacitance. Target potential becomes a few volts more positive in the lighter areas than in the darker regions, giving the same polarity charge pattern which would appear if the target itself were photoemissive.

A low velocity electron beam scans the reverse side of the target, depositing electrons in correspondence to scene brightness. The resistivity and thickness of the target film are chosen so that lateral leakage does not degrade resolution, while transverse leakage through the film is still adequate for electrons deposited by the beam to neutralize the picture charge in one scan period.

While a video output signal could be derived from the target mesh, operation is actually achieved by passing the modulated portion of the scanning beam which fails to be deposited on the target back into an electron multiplier which is located in the gun region. This modulated beam is referred to as the return beam.

Return beam signal modulation is generally less than 35% and provides maximum current in dark areas of the scene. Although beam noise is present in the output signal and limits sensitivity at very low light levels, the multiplier permits operation at signal levels considerably below the noise levels set by the camera amplifier. At higher signal levels, the useful multiplier gain rapidly decreases.

Before 1958, Image Orthicon targets generally consisted of a thin sheet of semiconducting glass accurately placed close to the target screen. Such targets often show irreversible changes after many hours of operation, due to ionic conduction. These changes result in image fading, afterimages, and general performance deterioration. When prolonged exposure and charge storage are required, as in the present instance, it is advantageous to have a target whose lateral resistivity is considerably greater than its transverse resistivity. Since 1958, tubes have been constructed in which the glass target is replaced by a much thinner film of magnesium oxide, about 500 angstroms thick, but of much higher resistivity; in addition, tri-alkali photocathodes (S-20 response surfaces) have been incorporated in these tubes. The magnesium oxide film target meets the necessary requirements of higher resistivity parallel to, rather than normal to, its surface. Transverse resistivity is sufficiently low to ensure a short discharge time-constant for TV operation, while lateral resistivity is high enough to reduce charge spreading over the surface. The result is an improved image resolution in normal TV operation, coupled with an improvement in integration capability. Since magnesium oxide is highly efficient as a secondary electron emitter, multiplication of primary photoelectrons at the target surface is appreciably greater than for glass. Further, ionic conduction deterioration effects are not found in such targets, resulting in improved tube aging characteristics.

Considerable data is available on the performance of Image Orthicons, including tubes containing glass and magnesium oxide targets. General manufacturers' data are presented in subsection C.6. Curves comparing Image Orthicons with other tube types may be found in subsections C.5 and F.

g. The Image Intensifier Orthicon

The Image Intensifier Orthicon represents the closest approach yet achieved to the theoretical performance of an ideal pickup tube at low light levels. Figure 3-9 shows a cross-sectional drawing of such a tube. Primary electrons are electrostatically focused onto the first intensifier screen. This

screen is a glass membrane coated on the image side with an aluminum-backed layer of fluorescent material; the other side is coated with a photocathode whose spectral response matches that of the phosphor. Photoelectrons penetrate the film, producing fluorescence in the phosphor. In turn, the fluorescence excites photoemission from the sensitized surface.

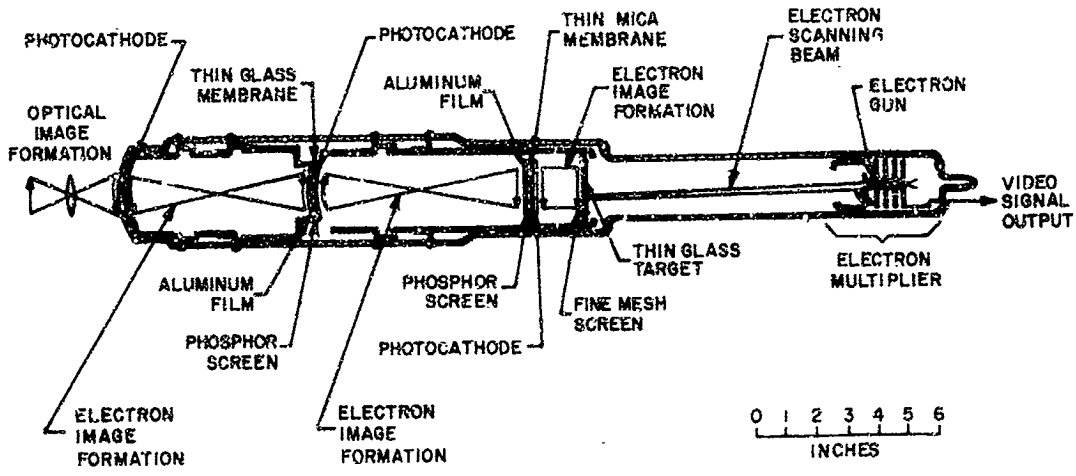

Figure 3-9. The Image Intensifier Orthicon

With several thousand volts between cathode and intensifier screen, each primary electron can cause 10 to 20 emitted electrons. The entire process may be repeated in a second intensifier section, with similar gain. (Figure 3-9 shows such a two-stage device.) Additional stages may be added, but there is little advantage in going beyond two or three stages, as will be made clear shortly.

For a two-stage intensifier, then, each electron leaving the first photocathode will cause about 100 to leave the last cathode and impinge on the target; each of these will produce about 5 secondary electrons from the target. The target can thus be fully charged and peak white produced with a primary optical image intensity 1/100th of that required by the conventional Image Orthicon. Each primary photoelectron could produce about 500 electron storage charges on the target, if all its daughter electrons were to reach the target. In practice, about 40% of these electrons are intercepted by the target mesh, so that only 60 electrons reach the target surface, to produce about 300 electron charges on the target by secondary emission.

After deposition on the target, stored charges are read out by means of the usual low velocity Image Orthicon beam, and the modulated return

beam signal is passed into an electron multiplier as in the Image Orthicon. A total gain of several hundred prior to scanning is sufficient to raise the stored signal level to a point where fundamental noise from the primary photocathode exceeds the scanning beam noise. Since this gain is reached in a two or three stage intensifier, there is little purpose in adding additional stages. Although a picture obtained at very low light levels is inherently noisy and limited in resolution, the Image Intensifier Orthicon approaches the ultimate in performance under these conditions. At higher light levels the signal to noise ratio is comparable to an Image Orthicon having the same target capacitance, but resolution deteriorates through the successive imaging processes.

Actual performance data, comparing Image Intensifier Orthicons both with one another and with other tube types, are given in subsections C.6 and F, respectively.

h. The Image Isocon

The Image Orthicon suffers from two serious disadvantages in obtaining optimum signal to noise performance under low light level conditions: the beam modulation is comparatively low (approximately 35%) and the signal polarity is inverted (i.e., peak return beam current corresponds to black in the imaged scene). Since both faults arise from the beam scanning mode, some other mode of operation appears to be desirable.

The Image Isocon's operation is based on the scattering of low velocity electrons by the target. Although a low velocity Image Orthicon-type beam is used, only the fraction of the return beam which has been scattered by the target is admitted into the multiplier. Since most of the electrons are scattered by the most positive areas of the target, and none from the dark areas, the scattered beam has the desired polarity, and, theoretically, close to 100% modulation can be achieved. Signal polarity inversion is achieved here without interfering with the charge pattern polarity on the target. (Other ways of obtaining the desired polarity in the video output signal of Orthicon-type tubes have been proposed from time to time, but these have generally involved tampering with the target's stored charge polarity and distribution, which is undesirable.) An additional advantage of the Image Isocon is that the target surface can be made to have a reflection coefficient greater than 0.5, resulting in an actual signal gain.

Image Isocon scan offers an attractive alternative to Orthicon return beam scan. (Indeed, as shall be seen presently, it is possible to combine both scan modes in a single tube type, and operate in either mode, as desired.) The advantages of the Image Isocon mode are high signal modulation, high signal to noise ratio, capability of handling an extremely wide dynamic range in a single scene, and a signal polarity which gives a minimum output signal for minimum photon input.

The cost of these improved characteristics is increased electron optical complexity, since the electron optical conditions for separating diffusely scattered electrons from those which are specularly reflected from the target are rather critical. In the Image Isocon illustrated in Figure 3-10, separation is carried out at the rim of an aperture placed at an antinode position in the

return beam. A screen on the scanned side of the target is used to provide a uniform decelerating field, since loss of resolution and spurious signal generation may result from beam bending near the target.

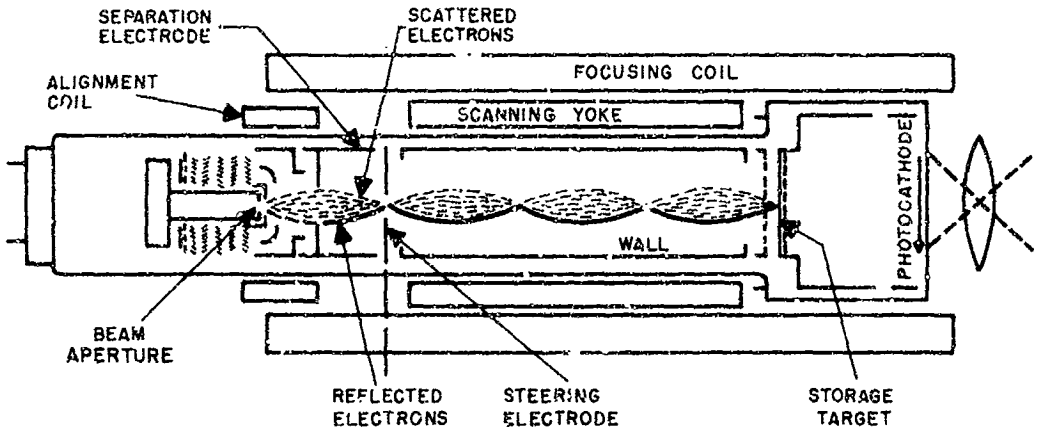

Figure 3-10. Dual Operating Mode Image Isocon

The tube shown is operable in an Orthicon scan mode when an axially-aligned scanning beam is used. The separation aperture is sufficiently large for both scanning and return beam to pass unhindered. Isocon operation is achieved by perturbing the magnetic field with the alignment coil to produce a fixed transverse velocity component in the beam. Steering fields force the return beam to straddle the edge of the separation aperture at a point where the bulk of the scattered electrons is closer to the tube axis than the return beam reflected electrons. Flexibility in selecting the point along the aperture edge where separation is to occur permits establishment of optimum operating conditions. Since the steering field cannot easily be made uniform over large cross sections of the tube, steering is applied at a nodal point, where deflection is small.

Orthicon mode operation for the tube illustrated is said to be no more difficult to adjust than in the regular Image Orthicon. Transition from the Orthicon to the Isocon scan mode may be made without interrupting the output signal, making this mode easier to establish in the combined tube than in single-purpose Image Isocons. The large opening of the electron multiplier is a potential drawback, since spurious signals may find their way back into the multiplier section. Tubes designed only for Image Isocon operation do not suffer from this drawback.

Although 100% modulation is theoretically possible, spurious scattering of electrons from surfaces within the tube limits beam modulation to about 85%. Even in its present state of development, the Image Isocon has improved the signal to noise ratio 2 to 3 times over a wide range of light levels below the full target charge region. In addition, the Image Isocon has provided at least an order of magnitude reduction in low light level threshold; an order of magnitude greater dynamic range in a single scene; and highlight resolution which is comparable to that of an ordinary Image Orthicon. Comparative performance data are presented in later sections of the report, but it is clear from the foregoing discussion that further development of this device seems a desirable step in the effort to achieve the ultimate performance with pickup tubes.

3. Photoconductive Devices

When considering devices other than those discussed above, the distinction between photoemission as an imaging medium and other techniques becomes somewhat obscure and arbitrary. Consequently, attention will now be given to techniques which are clearly photoconductive. Combined or special sensors are discussed in subsection C.4.

a. The Vidicon

The potential advantages of sensitivity and reduced complexity of a photoconductive camera tube were recognized years ago. Photoconductive and photovoltaic tubes were investigated extensively during the 1930's, but none of these even began to compete in sensitivity with the Iconoscope, which was then available. (This, even though the latter tube type is quite inferior by current image standards.) Photoconductive surfaces for pickup tubes were discarded until the advent of semiconductor devices in the late 1940's.

The Vidicon, resulting from this recent development, has gone far to meeting its promise of reduced size and operational simplicity. While Vidicons have not yet equalled the sensitivity of the best photoemissive tubes described in subsection C.2, some recent Vidicon-type devices are beginning to show considerable promise even in this direction.

The most common form of Vidicon, shown in Figure 3-11, is a tube 1 in. in diameter by 6 in. long, magnetically deflected and focused, consisting primarily of a gun and a target. More recent tubes, which are discussed in subsection C.6, have included 1/2 and 1-1/2 in. diameter versions, as well as electrostatic models.

In operation, the gun projects a beam of electrons along the tube axis. This beam is focused, aligned, and deflected by the magnetic coils shown in the illustration. The beam travels in a field-free space as far as the mesh. The end wall (Figure 3-12) of the tube is a flat glass plate which has a conducting transparent coating, the signal plate, on its inner surface. This coating is connected conductively through the ring to the signal resistance, and through a capacitor to the grid of the first tube in the preamplifier.

There is a thin layer of photoconductive material on the conducting signal plate; amorphous selenium or antimony trisulfide is often used. This

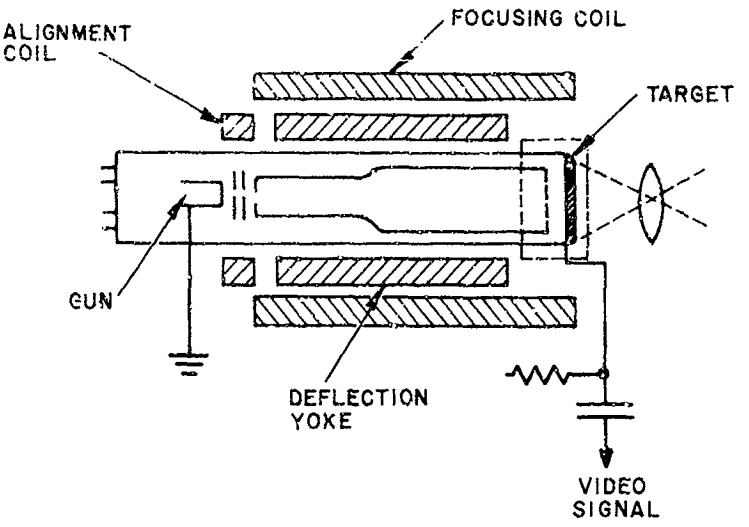

Figure 3-11. The Vidicon

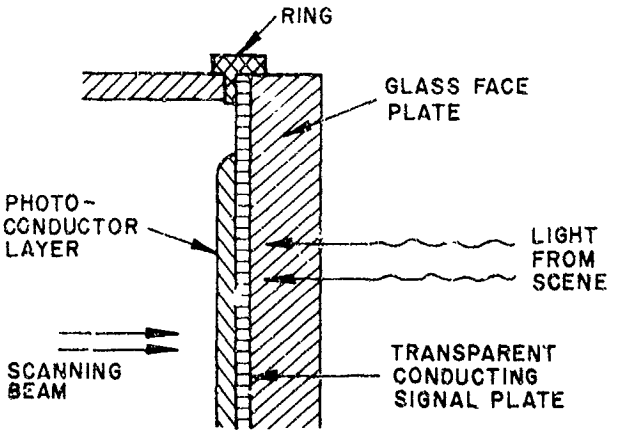

Figure 3-12. Vidicon End Wall Detail

layer is about 1 micron thick, so that light from the image formed on it by the lens penetrates substantially through it, and lowers its resistance. When no light falls on the photoconductive layer, its resistance is high, and its front surface will be maintained at cathode potential by the continuous scanning action of the beam. However, since a constant positive potential (of somewhere between 10 and 40 volts) is maintained on the other side of the photoconductive layer by the signal plate, a small positive current flows through the photoconductive layer, driven by the continuous scanning action of the beam across the free surface of the layer. This steady dark current depends on the potential difference maintained across the photoconductive layer. It must be small compared with the signal current, and uniform from place to place on the photoconductive surface, otherwise it will contribute noise and shading to the video output signal.

When a scene is focused on the target, its conductivity increases in the bright areas, causing the scanned surface to rise positively a few volts during the interval between scans. The beam deposits sufficient electrons to return the scanned surface to ground potential, and in doing so generates a video signal in the signal plate lead. The target is sensitive to light during the entire frame time, permitting full charge storage.

The best photoconductive material available at present has a response time that is appreciably greater than the frame time used in standard TV operation. Thus, there is some lag from one picture frame to the next, and this constitutes the main limitation in tube sensitivity. This lag can become objectionable in normal televising of moving scenes, if more than 5% of the signal properly belonging to one scene is carried over to the next frame. This may be due to two different causes: 1) the scanning beam may be unable to discharge all the charges built up on the mosaic, either because of lack of beam current or because the target has too high a capacity; 2) the photoconductivity excited in the dielectric layer may persist, and hence allow charging current to flow for more than one frame period. In the Vidicon, the latter is the main cause of lag. The greater the average illumination on the dielectric, the greater the percentage decay in induced conductivity in a given period of time. Thus the lag effect is lessened for brighter images, and becomes more serious as the scene illumination is reduced. In present Vidicons, it is the incidence of unacceptable lag which sets a practical limit to tube sensitivity, since this becomes objectionable for moving targets before the signal to noise ratio becomes excessively low. For general TV purposes, a target illumination of 1 lumen/square foot is required; but if the object is not moving, and lag is unimportant, the light level can be reduced by an order of magnitude below this figure before amplifier noise begins to be objectionable.

Currently, the Vidicon is used in applications where its smaller size and weight, lower cost, and simplicity of operation make it more desirable than Image Orthicons. Such applications range from industrial surveillance and process control to commercial broadcasting and scientific satellites. For remote operation its size and simplicity are advantages, but under poor lighting conditions picture quality is inferior to that produced by an Image Orthicon because of noise and lag.

Smaller experimental Vidicons using the electrostatic principle are under development; these tubes promise to advance the sensitivity and performance of Vidicons considerably within the next few years. Data on performance of existing tubes, as well as comments on the newest experimental devices, are presented in subsection C. 6.

4. Special and Combined Devices

Devices discussed in this subsection either represent combinations of sensor elements previously considered in subsections C. 2 and C. 3, or use techniques which thus far have not been described. An example of the latter is the use of materials which become conductive upon bombardment by primary electrons, or upon emission of secondary electrons. In some instances, little more than the basic design parameters have been set forth, since most of these devices are in experimental or early developmental phases. Consequently, it is not possible to represent many of these tubes in diagrammatic form, and data is sketchy at best. Where sufficient information is available, and the sensor appears to hold promise for the SMS application, a generalized discussion is presented here, and performance data are included in subsection C. 6. Where information is inadequate, or where the device does not appear applicable in its present form for use in the cloud cover sensor package, all available information is presented in this subsection.

a. The Permachon

The Permachon is an optical input-electrical output storage tube built by Westinghouse, which uses a special photoconductive storage material. When exposed to light, local longitudinal resistivity varies with incident light intensity. When scanned by an electron beam, the original values of longitudinal resistance due to exposure are regenerated or maintained for a considerable length of time. In normal photoconductors, resistivity becomes stabilized over the entire surface of the material after several passages of the scanning beam.

The Permachon photoconductive surface can thus store an optical image for substantial periods of time, and then permit the image to be electrically read out, with what is claimed to be little or no loss of image fidelity. New information may be stored only after erasure of the old image, a process which takes anywhere from a few milliseconds to several seconds to accomplish, depending on the erasure method. Rapid erasure requires that light from a flat field source impinge on the Permachon faceplate; a minimum illumination of 20 foot-candle-seconds is required. A second method involves switching off the beam for a period up to 10 seconds. Note that even in a slow readout system the beam would have to scan the sensitive surface continually, to prevent erasure between readout scans.

Two basic tube types have been developed thus far: the WL-7383, which is similar to a 1 in. Vidicon in structure and operation; and the WX-4025, which is a 3 in. tube using Image Orthicon focus and deflection coils, a return beam mode of operation, and an electron multiplier.

Sensitivity of the semiconductor surface is relatively poor; a minimum of between 0.2 and 0.8 foot-candle second illumination is required on the faceplate for adequate performance. Maximum limiting resolution is claimed to be 1200 TV lines for the 3 in. tube; the 1 in. tube will resolve 600 TV lines after 5 minutes of storage, and 450 TV lines after 10 minutes. Due to its low sensitivity, the Permachon is not considered to be particularly useful for SMS application.

b. The Ebicon

The Ebicon, developed by Westinghouse, might be described as a Vidicon with an image storage section. The storage target is a thin insulator whose conductivity changes when bombarded by high energy electrons; such a material is referred to as an EBIC (electron bombardment-induced conductivity) surface.

A diagram of an early version of such a tube is shown in Figure 3-13. Electrons from the photocathode are focused on the EBIC target, which consists essentially of a thin insulating layer backed by a conducting film which is thin enough to be easily penetrated by electrons. A low velocity beam from the Vidicon section scans the surface of the insulator, producing a high field across the layer, and extracting a video signal from the conducting film.

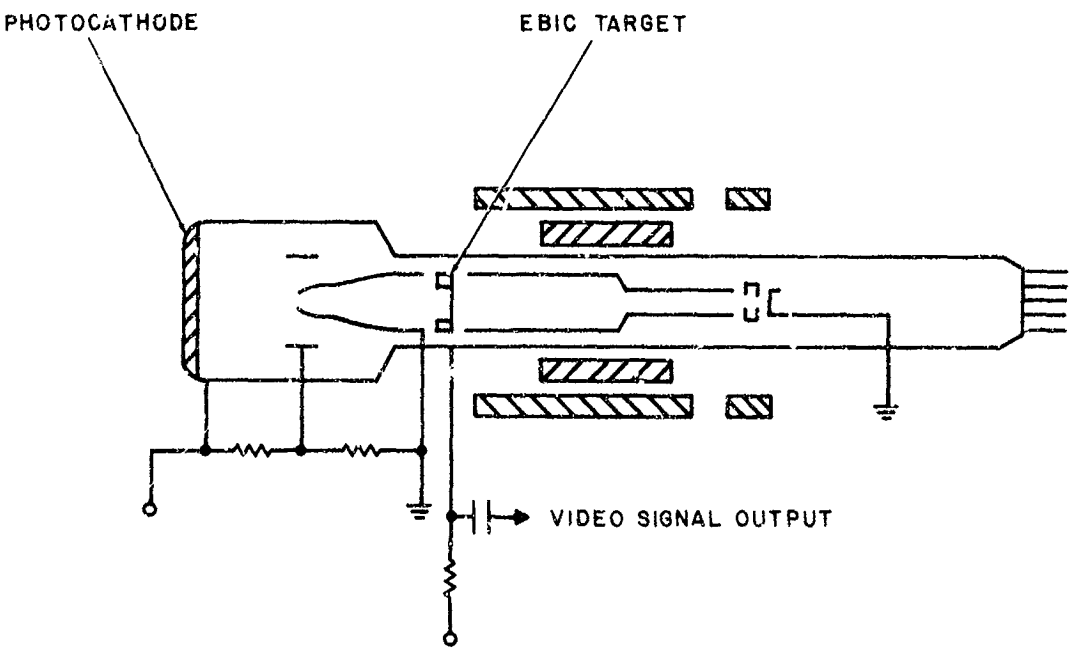

Figure 3-13. An Early Version of the Ebicon

The additional energy produced by the image section yields a tube which is intermediate between the Vidicon and the Image Orthicon in sensitivity. A storage time of 60 seconds or more should be possible, with a comparable readout rate, but target uniformity and structural support problems must be solved before this tube type can be seriously considered for space applications.

With a higher gain target and a return beam-electron multiplier readout, the sensitivity of this tube could probably be improved to approach the limits imposed by the photocathode; however, these modifications have not yet been made. The relatively high target capacity permits a high signal to noise ratio at large signal levels, but may cause poor modulation and capacitive lag at very low levels. Target thickness cannot be made arbitrarily large, since the bombardment electrons must penetrate the layer to yield maximum gain.

Westinghouse currently manufactures an Ebicon which is optimized for the visible spectral region. This tube, the WX-4772, is slightly shorter than the usual 3 in. Image Orthicon, and has a 3-1/2 in. diameter imaging section. The tube is electrostatically imaged, focused, and deflected, and has a field flattener built into the faceplate. Electron optics and target size tend to limit resolution, which is currently about 400 TV lines at 10^{-2} foot-candle photocathode illumination; the operating threshold is about 10^{-5} foot-candle. Two other tubes, the WX-4532 and WX-4791, are also available. Both possess ultraviolet-sensitive photocathodes, and are called Uvicons, the former is identical in design to the WX-4772, while the latter has a magnetically focused and deflected scanning section which provides superior resolution. Presumably, the experience gained in developing these tubes would enable Westinghouse to design an Ebicon with a magnetically focused and deflected scanning section, resulting in improved performance over that of the WX-4772. Based on Image Orthicon experience, the same comments would apply to the development of an Ebicon with return beam-electron multiplier readout. Since the results of such a program would be a tube which, at best, might approach the performance of current Image Orthicons, this tube type appears to offer no real advantage over Image Orthicons for the SMS application.

c. Solid State Imaging

At least two devices using sold state imaging are currently in early stages of development. The first, which is more properly an image intensification device, uses alternate layers of photoconductive and electroluminescent materials. If the target of an "Intensifier Vidicon" were to be so constructed, light imaged on the first photoconductive layer would be amplified and possibly shifted in spectral content within the electroluminescent material, and would excite conductivity in the second photoconductive layer. This layer could then be read out by a standard Vidicon beam section. While attractive in principle, materials presently available would not yield a significant improvement in sensitivity over current image tubes.

The second imaging system, currently under development by Electro Radiation, Inc. (under contract to Jet Propulsion Laboratories) sandwiches ferroelectric and photoconductive layers between thin film transparent conductors, in an imaging matrix system. A pulse is applied during optical imaging, which changes the polarization of the ferroelectric layer in accordance

with incident light intensity. While readout is presently accomplished by a flying spot scanner, later developments will include an electroluminescent layer to complete the imaging.

Readout mechanization is complex, and the device suffers from sensitivity limitations since it uses photoconductivity as the imaging mechanism. The device is several years away from realization as a practical image tube, and is unusable in the SMS program in its present state.

d. The Intensifier Photoconductor Tube

In principle, it should be possible to construct a device which combines an intensifier front end with Vidicon readout. Optics Technology, Inc. is reported to be developing such a system by coupling an image intensifier, through fiber optics, to what is apparently a Vidicon-type pickup tube. In practice, such an intensifier Vidicon should have performance comparable to that of the Ebicon, although fiber optics coupling losses may tend to degrade it somewhat. Even with a front end gain of 100, Intensifier Vidicon-type devices could not equal the sensitivity of current Image Orthicons, and would possess the additional disadvantages, for space applications, of requiring high voltage for operation.

e. The Panicon

During Republic's SMS study program, the Itek Corporation proposed the development of a new image tube, which they designated the Panicon (for Panoramic Image Converter). The tube would be a Vidicon-type image converter with a built-in rotating storage drum. The purpose of the drum is threefold: 1) it isolates the imaging section from the scanning section, preventing field interactions between these regions; 2) it permits readout to be made from the same side of the surface on which the information is written; and 3) it permits image motion compensation in a spinning satellite, by suitably synchronizing the rotation of the drum with the rotation of the vehicle. Two separate drive motors are provided for drum rotation, so that exposure and readout times may be independently selected and controlled.

Two different sensor designs have been formulated; one would operate in the visible spectral region, while the other would function in the infrared. The basic tube is shown in Figure 3-14. In the visible light sensor, the imaging surface is photoemissive. This surface converts the optical image to an equivalent electrical image which is impressed on the storage drum and read off by a scanning electron beam. The imaging surface for the infrared system is a bolometric, mosaic-type drum, having a comparatively short storage time. Bolometric detectors are available, with time constants of 0.01 second, which could be built into such a sensor drum. The visible region Panicon drum would be constructed from an insulator which is either secondary electron emissive, as in the Image Orthicon, or an EBIC material, as in the Ebicon.

Readout could be accomplished either with a direct beam Vidicon-type gun, or with a return beam-electron multiplier Image Orthicon gun. To some extent, the readout mode depends upon the charge storage mechanism employed. The usual type of secondary emission storage surface could not properly be read

out by a Vidicon-type scan. The EBIC surface, or a coplanar grid, secondary emission surface, would be compatible with the Vidicon readout.

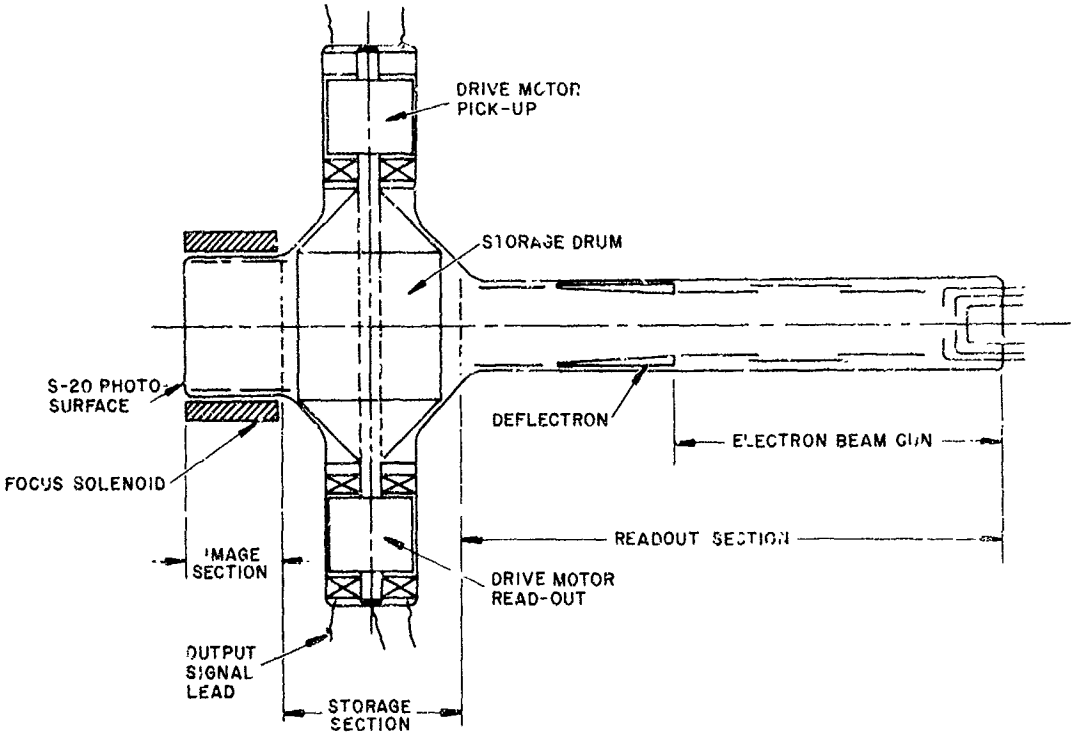

Figure 3-14. The Panicon

It is estimated that the Vidicon-type scan, with magnetic focus and deflection, would consume less than 2 watts. Scans of this type are available in either electrostatic or magnetic modes of operation. The electrostatic mode which is estimated to require less than 1/2 watt, is a far simpler, inherently more stable system. An Image Orthicon scan, magnetically focused and deflected, would require several times the power. Regardless of the scan mode, the image section would probably be magnetically focused.

Photocathode pulsing would be used to compensate for variations in scene illumination over a range of three orders of magnitude. Itek estimates that the Panicon would fall somewhere between the Image Orthicon and the Vidicon in sensitivity.

In spite of its many attractive features, the Panicon is only in the conceptual stage and many formidable problems await solution before serious consideration may be given to its application in the SMS system.

f. The Astracon

A family of image intensifier tubes, named "Astracons" by Westinghouse, is included as being generally representative of intensifier tubes which are currently available. All these devices may be considered light input-light output transducers.

Typically, the Astracon consists of an input photoemissive surface, four or five stages of transmission-secondary-emission electron multiplication in a dynode section, and an output phosphor screen. The tube is magnetically focused. Neither electron beam scanning nor charge storage takes place within the device; it can only act as a photon multiplier. Many Astracons have sufficient gain to be capable of registering single photoelectrons as visible scintillations on the output phosphor.

The WX-4826A tube has a cesium-antimony S-9 photocathode and a P-11 output phosphor screen. The tube has a brightness gain of 20,000 and is capable of resolving 1300 TV lines per picture diameter, on a 1 in. diameter screen, at a highlight illumination of 10^{-4} foot-candle on the photocathode. The WX-4826 tube is similar in design and construction, but has a lower brightness gain (4000) and lower resolution (1100 TV lines per picture diameter).

The WX-4342 and WX-4701 tubes have cesium-antimony S-11 photocathodes and a P-11 output phosphor screen, matching the spectral response of other photosensitive devices and photographic plates. The WX-4701 tube has a brightness gain of about 2000, while the WX-4342 tube has a gain of 400, since it has only four electron multiplier stages. Each tube gives 600 TV lines per picture diameter resolution at low photocathode illumination.

While useful for many Earth-based applications, a light output signal is undesirable in the case of the SMS, since this signal would then have to be viewed by a video camera for data transmission. Additional light loss between the intensifier and the video sensor would tend to degrade resolution performance. Finally, the high voltage (typically, 30 to 36 KV) and high magnetic fields (400 to 600 gauss) required for operation make the tubes undesirable for any satellite application. Adequate image intensification would normally be available in the imaging section of Image Orthicon or Image Isocon type tubes to meet the requirements of the SMS program.

g. Dielectric Tape Camera

RCA's Astro-Electronics Division is developing several electrostatic tape cameras which are capable of electrically storing an optical image for long periods of time. The tape can be stored for future readout or can be read-out immediately. Readout can be made nondestructive (which might reduce resolution) or partially destructive. The tape is erasable in less than 1/2 second and can be reused many times.

RCA is developing a 35 mm tape camera system for NASA to be used in the Nimbus program. Also under development is a 70 mm tape camera for the Air Force (which is also sponsoring developments in improved tapes). Information was obtained only in those areas where no security classification was involved,

which restricted data gathering to the NASA sponsored program.

The electrostatic tape consists of four functionally separate layers:

A transparent cronar (Mylar) supporting layer

A transparent conducting backing layer of gold

A high quantum efficiency photoconductive layer (such as antimony selenide)

A layer of pure polystyrene, in which is stored

The gold backing electrode is brought out along the edges of the tape, which simplifies making contact with the backing electrode and also spaces adjacent layers to prevent physical contact when the tape is rolled up for storage. The optical image passes through the transparent supporting and backing layers, and is focused on the photoconductor. The polystyrene layer faces an electron gun.

Prior to using the dielectric tape, it must be prepared by scanning the insulating layer with the electron gun while simultaneously illuminating the tape with uniform light, approximately two to three times greater than the expected highlight illumination of the scene. The electron gun used can be either the readout gun (which is a finely focused beam) or a separate flood gun. In this "prepare" mode, the potential to which the dielectric layer is to be charged is established. The energy of the flood gun is sufficient to liberate secondary electrons from the target (which are gathered by a collecting mesh). The photoconductive layer is maintained conductive by the uniform illumination, and therefore the dielectric layer is uniformly charged. All previously stored information is removed and the tape is ready for optical exposure.

To record on the prepared tape, an optical image is focused upon the photoconductor while the flood gun simultaneously illuminates the dielectric layer. The potential stored in the polystyrene layer can now discharge toward zero under the combined influence of the flood gun and the photoconductive layer. The time constant of the discharge is determined by the resistance of the photoconductive layer, which in turn is determined by illumination variations in the scene. At the end of the exposure period, the discharge process is arrested and an electrostatic charge pattern corresponding to the optical image is fixed on the tape.

In the readout operation, the stored charge image is scanned by a finely focused electron beam. As the high energy electron beam scans the target, secondary emission occurs in the dielectric layer. (The secondary emission ratio is directly related to the stored charge.) The output video signal is taken from a signal resistor connected to the backing layer. Readout can also be accomplished by using standard Vidicon techniques, or by using return beam modulation and electron multiplication as in the Image Orthicon.

Present requirements for NASA are a peak-signal to rms-noise ratio of at least 100:1 in a 700 KC bandwidth. The primary source of noise at this time is in the amplifier, as in the Vidicon. Ten gray steps related by $\sqrt{2}$ are anticipated. The dynamic range goal is 32:1 in one exposure, with a total range of up to 64:1. Measurements of limiting resolution (about 10% response) indicate 90 TV lines per mm, which, on a 25 mm active width (35 mm tape) corresponds to 2250 TV lines. The primary resolution limiting device is the electron readout beam. Figure 3-15 depicts the general configuration of the prototype NASA Dielectric Tape Camera system. The sensitivity of the present Dielectric Tape Camera is comparable to that of the Vidicon, approximately 0.01 foot-candle-second. Improvements in sensitivity can be made by adding an imaging section, and using return beam modulation with electron multiplication. This would, of course, also increase the complexity of the device.

In addition to using continuous tape in reel form, RCA has successfully constructed and tested a Vidicon-type electrostatic charge storage tube, in which the Vidicon target is replaced with a dielectric tape target.

h. The SEC Vidicon

A new type of tube(called the "SEC Vidicon") based on conduction by secondary electrons which are liberated by primary electron bombardment, is under development by Westinghouse. Experimental tubes of this type have been built in both electrostatic and electromagnetic versions, using direct beam readout. The tube consists basically of a photoemissive cathode in an image section, the SEC (secondary electron conduction) target, and a direct beam readout Vidicon gun. Photoelectrons are accelerated and focused onto the target at a primary voltage of approximately 10 KV. Secondary electrons produced by the primary electrons in the dielectric layer of the target result in a multiplication of the photoelectron image current. An electron beam reads and erases the resulting charge pattern at the target, generating the video signal.

Under the impact of a primary electron, a large number of free electrons are created within the layer. A fraction of these electrons escapes from the exit surface of the target and is collected by the wall screen. The remaining electrons liberated within the target are normally not observed, since they are absorbed after a number of collisions within the target material. However, if an electric field is applied across the target, these electrons can be transported through the layer.

The electrons released in this fashion are the free electrons traveling in the interparticle volume of the layer, and should not be confused with these electrons in the conduction band of the material. This statement is based on response time measurements which show that the response of such a layer is very much faster than that for solid state conduction. In addition to free electrons created within the layer, electrons are probably also excited into the conduction band. However, their contribution to conduction across the layer is insignificant at normal target voltages, which correspond to a field of only about 1 KV/cm, due to interparticle barriers.

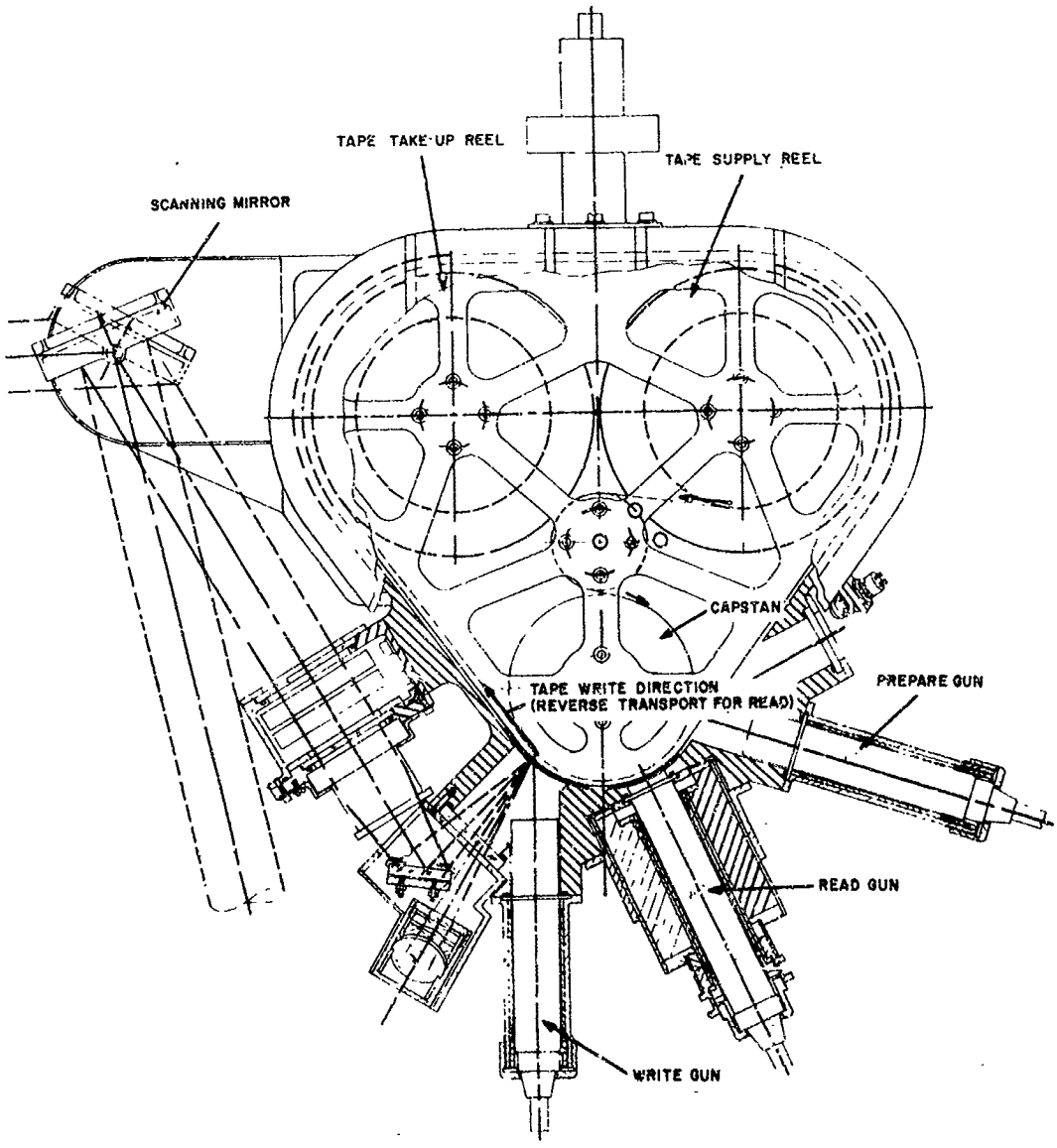

Figure 3-15. Dielectric Tape Camera

Typical SEC targets developed at Westinghouse are reported to provide noiseless charge gains of 200 or more, together with fast response. Limiting resolution of tubes constructed with such targets approaches 1000 TV lines per inch. With charge integration, performance exceeding that of typical Image Orthicons (operated at normal TV frame rates) is reported, and signal to noise ratios of more than 100:1 have been observed.

While the SEC Vidicon must still be considered a laboratory device, on the basis of its performance thus far it shows great promise of competing successfully with both Image Orthicons and Vidicons in time to come. Some additional experimental performance data is available on the SEC Vidicon, and is included in subsection C.6.

5. Theoretical Performance of an Ideal Imaging Device

When a scene is imaged upon the photocathode of a pickup tube, the illumination pattern consists of a stream of light photons or quanta. The photocathode responds to this illumination by emitting photoelectrons. On an average, more photons arrive at, and photoelectrons are emitted from, that part of the photocathode corresponding to a bright part of the scene. However, both the arrival of photons and the emission of photoelectrons are random processes; while the average numbers will be constant for a stationary scene if the average is taken over a sufficiently long time, the number arriving or leaving in a short interval may radically depart from the average. By determining how the eye responds to pictures of random, discrete flashes of light, and by computing statistical fluctuations in the photons comprising the image, a prediction can be made of the performance of an ideal pickup device. Several such investigations have been performed; they are listed in the bibliography at the end of this section.

Reasoning that fluctuations in both light and dark areas must interfere with the ability of the eye to resolve a pattern, and using data obtained from a number of observers, Coltman described his results by the equation

$$Pmin = 1000\left(\frac{2-C}{C^2}\right) \qquad (3-1)$$

where

Pmin = minimum number of flashes per second required to recognize a 20 TV line bar pattern at a contrast C

C = contrast, defined as $\frac{P\ white - P\ dark}{P\ white}$

For an ideal black and white pattern, the population in the dark area, P dark, in terms of flashes per second, is zero and the contrast is unity. Pmin is the population in the highlights (light bars), referred to the entire area of the test pattern.

To translate this into TV terminology, assume an aspect ratio of 4:3 and a resolution N measured in TV lines per picture height. Coltman's equation becomes

$$Pmin = \frac{4}{3}\left(\frac{N}{20}\right)^2(1000)\left(\frac{2-C}{C^2}\right) = 3.33\left(\frac{2-C}{C^2}\right)N^2 \qquad (3-2)$$

This is the minimum number of scintillations per second required to resolve a dark and light bar pattern of N TV lines per picture height with a contrast C between the light and dark bars.

This equation gives the maximum sensitivity performance limit for any ideal image amplifying device, in which each electron leaving the photocathode results in a flash of light at the output, assuming the eye is the final element in the system and the number of flashes used by the eye to perceive the picture sensation is based only on the memory time of the eye. The memory time of the eye has been experimentally determined to be about 0.2 second.

There is now sufficient information to predict ideal imaging performance. All that remains is to determine the number of flashes per second that can be realized from a scene of given illumination. To determine the number of photoelectrons available from the photocathode per second, the following equations are used:

$$I = SEA \tag{3-3}$$

$$P = \frac{SEA}{e} \tag{3-4}$$

where

I = photocathode current in amperes, or coulombs per second

S = sensitivity of the photocathode per unit area, in amperes per lumen

E = highlight illumination on the photocathode (assuming the entire photocathode is illuminated at highlight intensity) in lumens per square foot (foot-candles)

A = area of the photocathode in square feet

e = charge of the electron = 1.6×10^{-19} coulombs

P = number of photoelectrons leaving the photocathode per second.

A typical value of sensitivity for recently developed multi-alkali photocathodes (S-20 spectral response) is 150 microamperes per lumen. Using a 3 in. image tube with a 3 x 4 aspect ratio and maximum useful diameter of 1.6 in., the area is 8.5×10^{-3} square feet. Substituting in Eq 3-4,

$$P = \frac{1.5 \times 10^{-4} \frac{\text{coul/sec}}{\text{lumen}} \times 8.5 \times 10^{-3} \text{ sq. ft.} \times E \frac{\text{lumen}}{\text{sq. ft.}}}{1.6 \times 10^{-19} \text{ coul/electron}}$$

$$P = 8 \times 10^{12} E$$

Substituting this result into Eq 3-2,

$$N^2 = \frac{C^2}{2-C} (2.4) \, 10^{12} E \tag{3-5}$$

A plot of this equation is shown in Figure 3-16. It can be seen that an ideal device cannot resolve better than 150 lines at 10^{-8} foot-candle on the photocathode for a 100% contrast scene. For a reduced contrast of 50%, the required illumination must increase to 5.5×10^{-8} (5.5 times), while if the scene contrast is only 10%, the illumination must be increased 180 times.

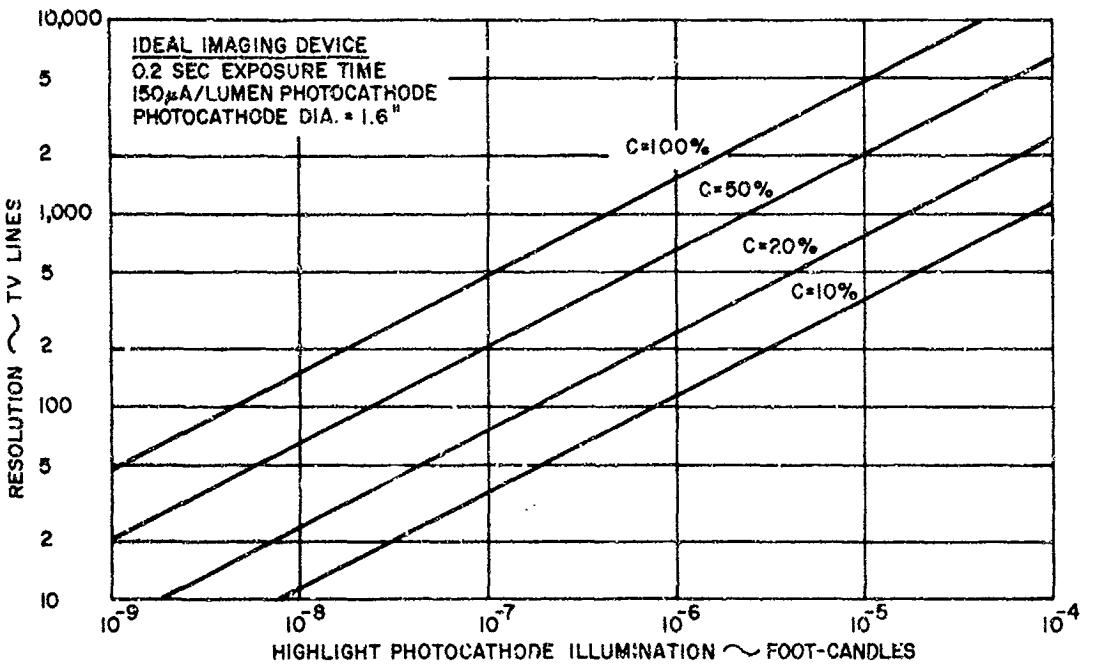

Figure 3-16. Effect of Contrast on Resolution

A word of caution is necessary concerning sensitivity and spectral response. Photocathodes are generally rated by exposing them to radiation from a tungsten filament operating at a color temperature of 2870°K. This source is set to produce a visible light flux of one lumen on the photocathode, as measured by a photometer having a spectral response approximating that of the "average" observer. The measured photocurrent is the response in microamperes per lumen. This definition ignores the fact that the tungsten light source radiates more strongly in the infrared region than it does in the visible, and the photocathode may respond to the infrared as well as the visible. Thus, in theory, it is possible for a surface to have no visible response and yet, because of its infrared sensitivity, exhibit a sensitivity of 50 microamperes per lumen. The definition and measurements must be properly interpreted, since the lumen is a measurement only of visible radiation.

A measurement of the response to 2870°K light is completely useful only when the light reaching the photocathode from the scene has the same spectral distribution as a tungsten light at 2870°K. For all other sources, whenever accurate predictions are required, the product SE in Eqs 3-3 to 3-5 must be determined from:

$$SE = \int S(\lambda)\, E(\lambda)\, d\lambda$$

over the wavelength region where neither S nor E is zero. $S(\lambda)$ is the spectral response of the photocathode in amperes per watt per unit wavelength, $E(\lambda)$ is the spectral distribution of the incident radiation in watts per unit wavelength, and λ is the wavelength.

In Figure 3-17 the performance of ideal imaging devices is plotted as derived independently by Hall and Weimer. There is close agreement between the performance curves of the ideal devices, although different assumptions were made in the derivations. Image Intensifier Orthicon curves are also plotted. It is interesting (and surprising) to note that the measured performance exceeds that of the ideal device over a considerable range of illumination. This apparent discrepancy is probably due in part to spectral response in the infrared, as mentioned in previous paragraphs. Additionally, when operating at low illumination levels (and therefore low beam currents) target lag increases. It would appear that if the lag exceeds the 0.2 second integration time of the eye, the integrated light flux actually seen by the tube will exceed that for the ideal device, and the tube will therefore exhibit higher resolution.

An additional plot of some interest is due to an analysis by Weimer (Figure 3-18) which shows the calculated signal to noise ratios for various types of camera tubes, assuming in each case the most sensitive photosurface currently in wide use. The scanning period is taken to be 1/30 second; utilizing the 0.2 second integration time of the human eye would increase the effective ratios to some extent at any given value of photosurface light flux. The Image Intensifier Orthicon, wide- and close-spaced Image Orthicons, and Image Dissector all assume photocathode sensitivities of 150 microamperes/lumen; the CPS-Emitron and Iconoscope assume sensitivities of 75 microamperes/lumen; the RCA C74008 has a nonporous photoconductive target, while the experimental Vidicon uses a porous photoconductor.

The extremely poor sensitivity of the Image Dissector, due to its lack of storage capability, is clearly shown. As stated earlier, this tube requires five orders of magnitude more photosurface illumination than an ideal device to achieve corresponding signal to noise performance. The Iconoscope is also shown to be decidedly inferior to other tube types which are currently available. These curves are based partly on measurement, and partly on the use of Weimer's equation:

$$R = (C/\ell)\ \sqrt{EAt\,\theta}\ \ 1.01 \times 10^{6} \qquad (3\text{-}6)$$

where
- R = ratio of the peak to peak signal to RMS noise
- (EAt) = integrated light flux (lumen-seconds) falling on the photocathode during exposure time t
- ℓ = the TV line number corresponding to the resolution of the picture to be transmitted

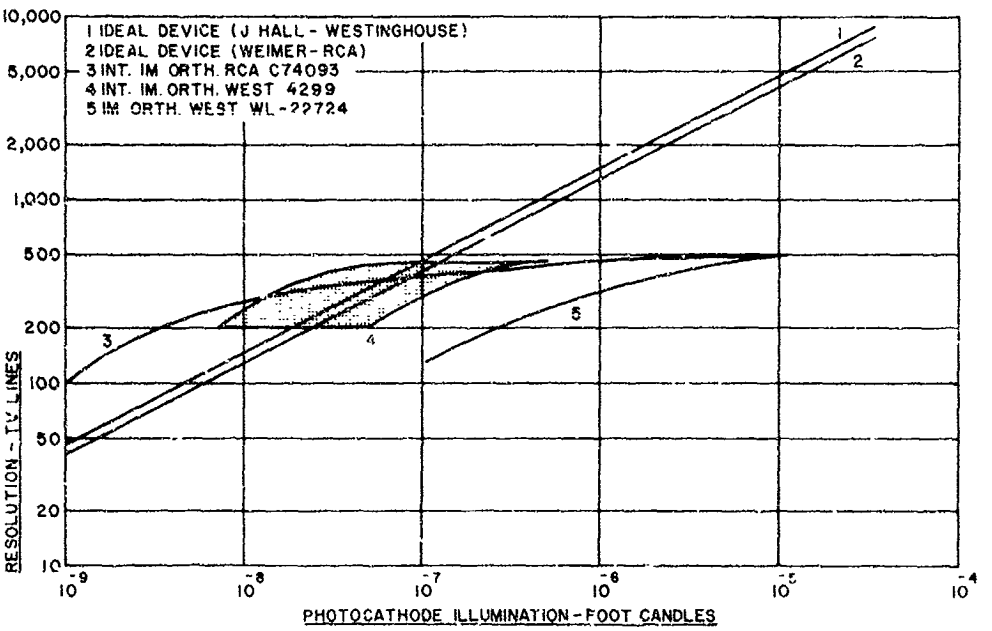

Figure 3-17. Resolution Versus Illumination for Imaging Devices

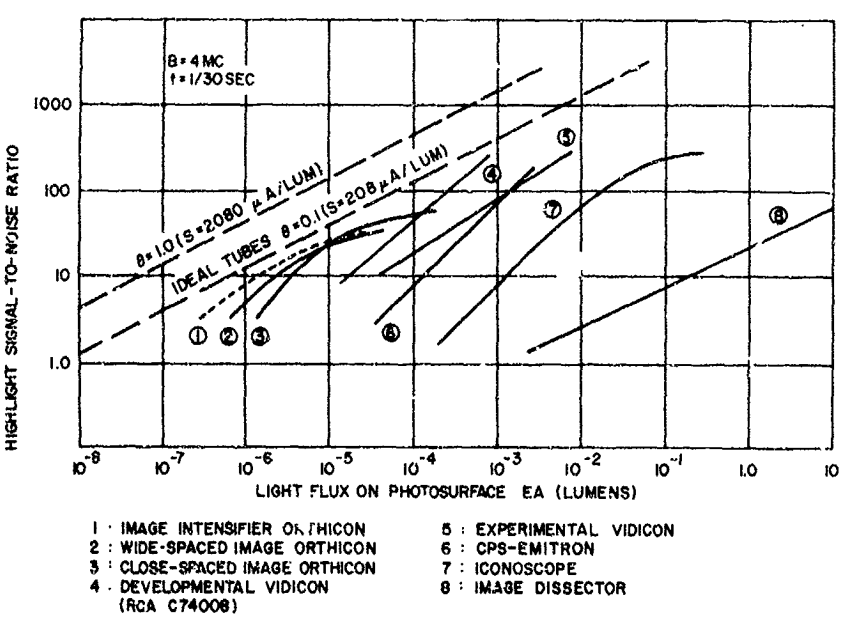

Figure 3-18. Signal to Noise Performance for Various Imaging Devices

θ = the quantum yield of the photocathode
c = contrast, as defined in Eq 3-1

a. Effects of Slow Scan Operation

Under conditions of low incident illumination, some increased performance can be obtained by a technique comparable to time exposure in photography. In this case the frame rate is decreased, corresponding to a longer interval between readout scans. If the pickup tube is capable of integrating the light flux in this interval, an increase in sensitivity can be realized.

Shelton and Stewart have shown that the light level required to achieve a fixed signal to noise ratio decreases directly with frame rate for the Image Orthicon, and decreases with the 3/2 power of the frame rate for the Vidicon. Experimental data were taken for two Image Orthicons (5820 and 6474) and two Vidicons (both 6326). Figure 3-19 shows the increased sensitivity for both tube types. The significance of these curves lies in the trends they represent, rather than in their absolute values. The Image Orthicons used were both of the glass target variety, whereas the most sensitive tubes presently used incorporate metal oxide thin film targets. To obtain useful data at low frame rates, it was necessary to reduce the tube temperature to obtain increased resistivity (and hence integration time). In the case of the Vidicon, performance at long frame times is a compromise between target voltage, resolution and dark current. Several additional reasons are presented in the article for considering trends rather than absolute magnitudes.

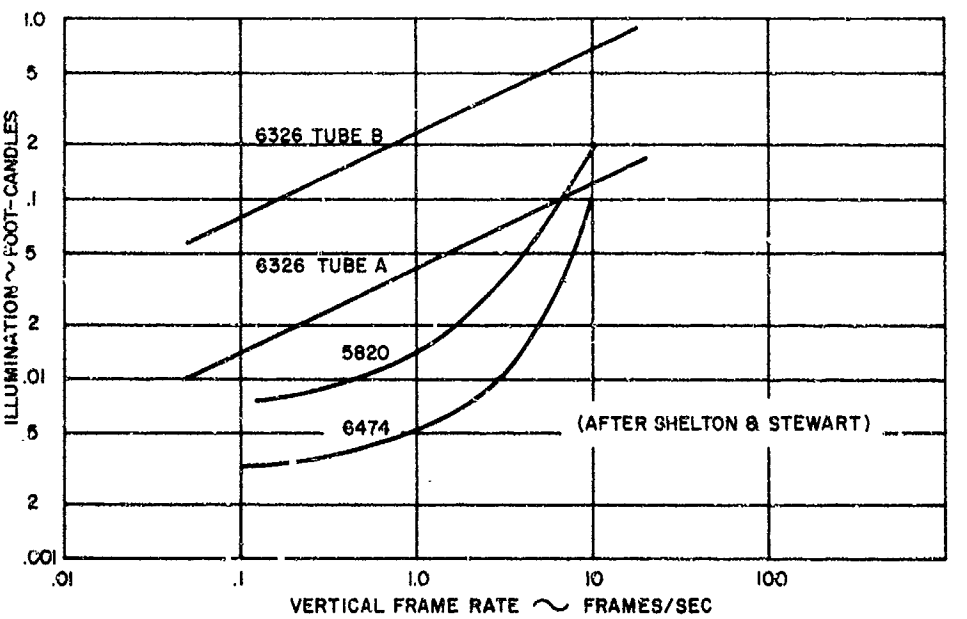

Figure 3-19. Vidicon and Image Orthicon Illumination for Signal to Noise Ratio of 10

Although the data referenced above were taken 6 years ago, experimentation at astronomical observatories using the new high sensitivity tubes also indicates improved performance at longer frame times. While quantitative data are not complete, storage times of greater than 5 minutes have been observed with no perceptible degradation. (See subsection C.6 for more information on these phenomena.)

Slow-scan techniques are useful only when the scene being viewed has no motion during the scan frame time. It is not anticipated that the scene viewed from the SMS will have motion during a few-second interval. However it is possible that the vehicle may have angular rates which can result in image motion during frame time. Figure 3-20 shows the angular rate control required to restrict image smear (measured in feet on the ground) to allowable limits as a function of exposure or frame time. For example, if a 1 mile ground smear is tolerable, and a frame time of 10 seconds is used, the vehicle's angular rates must be controlled better than 2.5×10^{-4} degree per second.

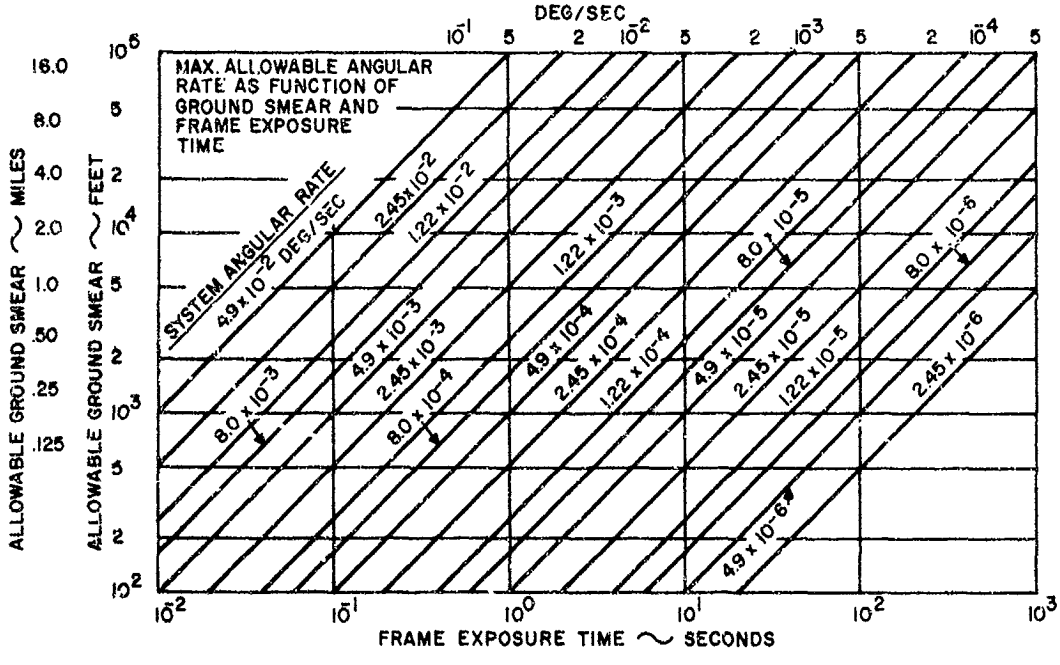

Figure 3-20. Maximum Allowable Angular Rate as Function of Ground Smear and Frame Exposure Time

6. Sensor Tube Performance Data

Many sensor tube types have been considered in subsections C.2 through C.5; until now, the treatment has been largely theoretical and general in nature (with the exception of subsections C.4 and C.5, which presented some performance data). Based on the results obtained thus far, the sensors listed in Table 3-1 are not considered applicable to the SMS cloud cover system, for the reasons indicated.

TABLE 3-1
SENSORS UNFIT FOR THE CLOUD COVER MISSION

Sensor	Reason
Image Dissector	Poor sensitivity; no storage capability
Iconoscope; Image Iconoscope	Poor performance; no longer manufactured
Orthicon	No longer manufactured; performance is exceeded by other available sensors
CPS-Emitron	Not manufactured in the United States; performance is equalled or exceeded by other existing tubes
Permacon	Poor sensitivity; performance characteristics do not match SMS operational requirements
Panicon	Too highly conceptual in nature at present time
Astracon	No storage capability; very high voltage (over 30 KV) required for operation
Solid-State Imaging Devices	Too early in development stage to predict performance with confidence
Intensifier Photoconductor	Requires very high voltage (15 to 20 KV) for operation; probable performance is equalled or exceeded by existing sensors

With the exception of the Image Dissector, no additional information will be presented here on any of the sensors listed in Table 3-1.

A number of tube types discussed in subsections C.2 through C.5 appear to offer some promise of meeting the SMS cloud cover imaging requirements. These include Image Orthicons, Image Intensifier Orthicons, Image Isocons, Vidicons, the SEC Vidicon, the Dielectric Tape Camera, and the Ebicon. The Dielectric Tape Camera and the Ebicon have already been described in as much detail as available in subsection C.4. More complete performance information, including actual tube data, is presented on the remaining sensors in the following paragraphs.

a. Image Dissector Performance

The ITT Laboratories of Fort Wayne, Indiana, is the primary manufacturer of Image Dissector tubes. They list four models (FW-110, FW-122,

FW-125, and FW-146) as being representative of this device. Specific information is currently available only on the FW-122 and FW-146, and this data is tentative. These tubes are 4 1/2 in. in diameter and 13-3/8 in. long, without magnetic deflection or focus coils for the image section; typical coils for the FW-146 are 7 in. in outside diameter by 14-3/4 in. long, and weigh 16 lb. The FW-146 tube is normally supplied with an S-1 photocathode; the FW-122 and FW-125, which are mechanically similar to the FW-146, are available with S-11 or S-20 photocathodes, as desired. The FW-110 is a smaller tube, packaged by ITT Laboratories in a camera head 3 in. in diameter by 11 in. long.

The resolution of Image Dissectors is claimed to be as high as 3000 TV lines, which exceeds the capability of other photoemissive tubes by a substantial margin. The transfer characteristic of Image Dissectors is nearly unity γ over wide ranges of illumination.

Since the multiplier gain per stage averages 3.1 at 150 volts, overall gain of these tubes (which contain 11 secondary emitting dynodes and an anode in cascade) is 3.1^{11} or 250,000. While this gain is some 500 times greater than that available in the multiplier section of a typical Image Orthicon, the Orthicon's storage capability and image section gain result in far superior performance under all but the very highest illumination conditions. The equivalent electron gain of the Image Orthicon, from photocathode to load resistor, is typically 1000 times greater than that of the Image Dissector.

CBS has developed an image tube, the CI-1147 Reconotron, which is an electrostatically deflected and focused Image Dissector. The tube is 1-1/2 in. in diameter and 6-7/8 in. long, with a multiplier section designed like a 12-stage photomultiplier tube. With a gain of 10^7, this tube lies between the standard Image Dissector and the Image Orthicon in sensitivity, and has a limiting resolution of 1000 TV lines per in. over a 0.6 in. diameter area. The Reconotron does not contain a storage target, and hence suffers from the same disadvantages as standard Image Dissector tubes.

b. Vidicon Performance

A detailed discussion of the design and construction of Vidicons is presented in subsection C.3, and will not be repeated here. The original Vidicon design used magnetic focus and deflection. Recently, electrostatically focused and, finally, fully electrostatic tubes have been developed. As with other scanning beam imaging tubes, the Vidicon beam must land on the storage surface at close to normal incidence to preserve shading uniformity in the picture and yield maximum edge resolution. This requirement is met in magnetically deflected tubes by accurate alignment of the beam with the center of deflection. Electron optics problems complicate beam control in the electrostatic case if conventional deflection plates are used, so most successful tubes of this type use the "deflectron" principle; i.e., an electrostatic deflection system having one center of deflection.

Magnetically deflected Vidicons are available in 1/2, 1, and 1-1/2 in. diameters; electrostatic Vidicons are presently constructed in 1 and 1-1/2 in. sizes. Larger tubes are manufactured by some European companies, but only tube types fabricated and currently available in the United States have been included in this sensor survey.

Before reviewing some collated tube data, it is of interest to consider the form in which this information was made available. Most tube manufacturers tend to present comparatively little data in their standard data sheets; this is particularly true of sheets which carry designations such as "tentative data,""developmental device," or some equivalent qualifying statement. On sheets describing existing tube types, more information is available, but even here different companies tend to emphasize different performance data as being significant. In summarizing the tube performance data which Republic obtained during the study, it was decided that the most significant information which should be graphically presented in the case of Vidicons would be transfer characteristics, signal to dark current ratios, decay characteristics, and square-wave response curves. These data are summarized in Figures 3-21 through 3-24, for all tubes on which such information is available. Most Vidicons are small, lightweight devices; the major size and weight contributions in a complete camera assembly come from synchronization and drive circuitry (and from focus and deflection coils in the case of a magnetic tube). Consequently, tube size and weight are not included as primary data in this section; instead, size, weight, and power requirements for the various proposed satellite equipment configurations (i.e., complete camera chains) are given in subsection F.

Figure 3-21 shows typical Vidicon transfer characteristics for a variety of tubes manufactured by RCA, Westinghouse, and Machlett. Several tubes have curves for more than one dark current value; for a given tube, dark current generally varies directly as target voltage. The Machlett ML 7351A, RCA 8051 and 8134, and the Westinghouse WX-4915 are examples of tubes displaying relatively high signal output (0.02 microampere or more) at low faceplate illumination (0.01 foot-candle). All curves are plotted for 1/30 second frame time; data on performance at longer integration times is not generally available, except for the Westinghouse tubes, which are slow scan Vidicons.

Figure 3-22 shows signal to dark current characteristics for the same tubes analyzed in the preceding figure. The high values for the Westinghouse WX-4915 and WX-7290 slow scan tubes result from their extremely low dark currents, which the manufacturer claims is due to the exceptionally high dark resistivity of the target. Again, since nonstandard frame rate data is not available for any but the slow scan tubes, the figure is plotted for 1/30 second frame rates only.

Figure 3-23 shows typical persistence data for a number of RCA tubes. In each instance the output signal current, as a percentage of its initial value, is plotted as a function of the time after initial illumination is removed. The C-73496 and C-74078 tubes, which are, respectively, a magnetic 1/2 in. Vidicon and a ruggedized 1 in. electrostatic tube, each have a somewhat higher photo-conductor lag than the other tubes. This lag would be objectionable for normal TV use, but is relatively independent of light level on the faceplate.

Figure 3-24 shows typical uncompensated horizontal square-wave response for a number of tubes. The RCA 8051 is a 1-1/2 in. high-resolution magnetically focused and deflected tube designed primarily for broadcast film pickup and data transmission purposes. The design features precision construction, a mesh electrode, and an extremely uniform photoconductive surface. Resolution is about 1200 TV lines at 8 foot-candles faceplate illumination.

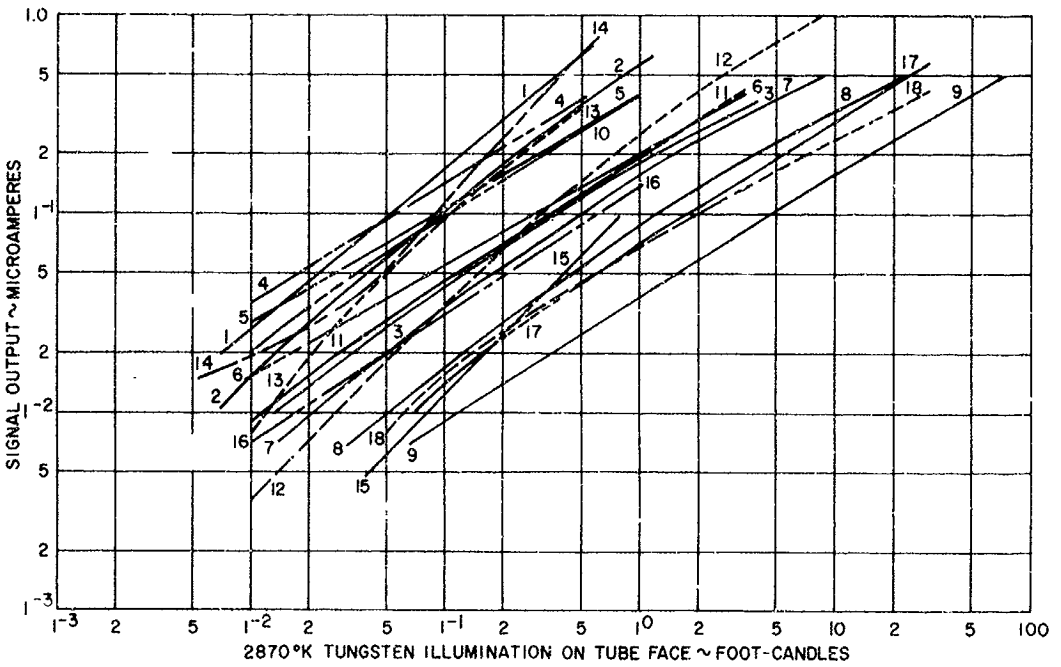

			DARK CURRENT (MICROAMPERES) =
1	THE MACHLETT LAB INC	ML 7351A	0.08
2	"	"	0.02
3	"	"	0.008
4	RCA	7735A	0 20
5	"	"	0 10
6	"	"	0.02
7	"	8051	0.05
8	"	"	0.02
9	"	"	0.005
10	"	8134	0.10
11	"	2084A, 7262A, 7263A, 8134 & 7697	0.02
12	"	DEV TYPE C-73496	0.02
13	"	" " C-74078	0.02
14	WESTINGHOUSE	WX 4915	0.002
15	"	7290	0.0002
16	RCA	4427	0.05
17	"	7038	0.02
18	"	6326	0.02

Figure 3-21. Vidicon Transfer Characteristics

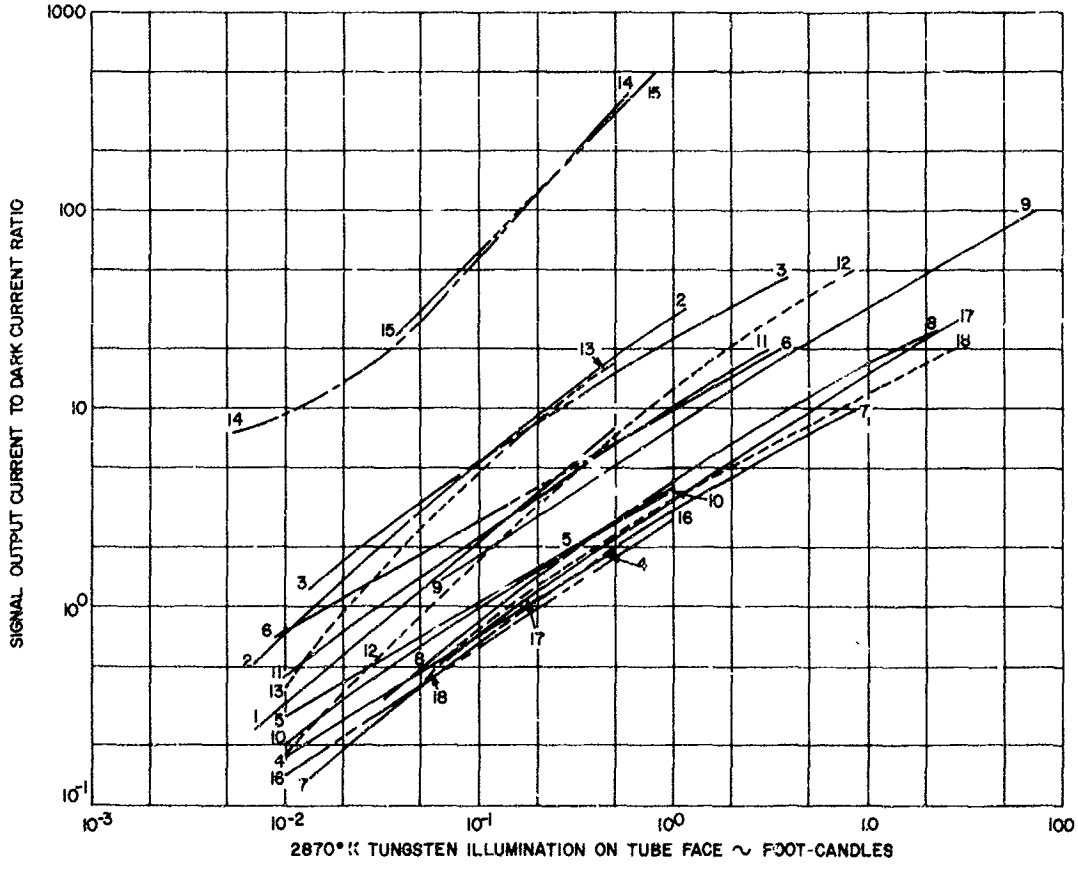

			DARK CURRENT (MICROAMPERES) =
1	THE MACHLETT LAB, INC.	ML 7351A	0.08
2	"	"	0.02
3	"	"	0.08
4	RCA	7735A	0.02
5	"	"	0.10
6	"	"	0.02
7	"	8051	0.05
8	"	"	0.02
9	"	"	0.005
10	"	8134	0.10
11	"	2084A, 7262A, 7263A, 8134 & 7697	0.02
12	"	DEV TYPE C-73496	0.02
13	"	" " C-74078	0.02
14	WESTINGHOUSE	WX 4915	0.002
15	"	7290	0.0002
16	RCA	4427	0.05
17	"	7038	0.02
18	"	6326	0.02

Figure 3-22. Vidicon Signal to Dark Current Characteristics

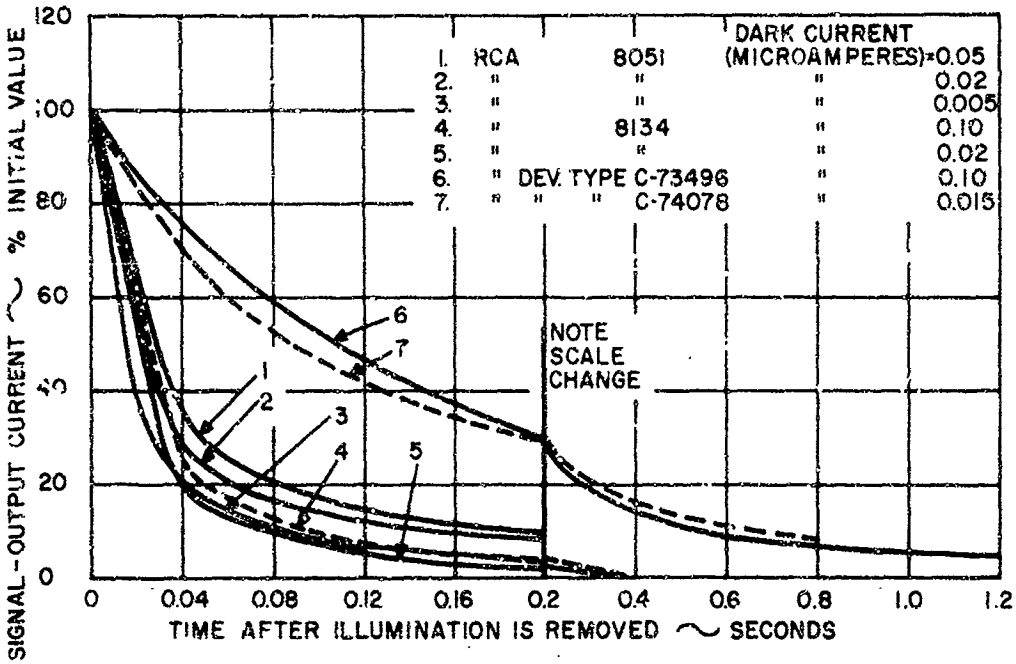

Figure 3-23. Decay Characteristics

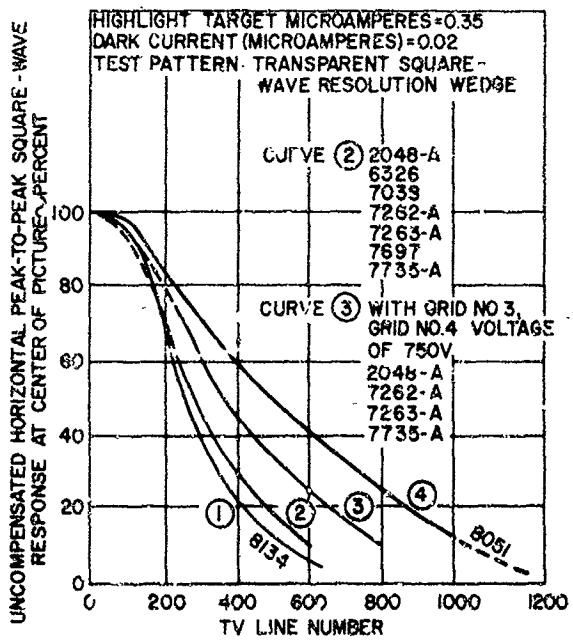

Figure 3-24. Typical Amplitude Response, RCA Vidicons

In addition to the plotted data, some further comments on resolution and tube design are in order. The RCA C74053 is an example of a typical 1/2 in. magnetic Vidicon; resolution is limited to about 400 TV lines, with sensitivity extending to 0.2 foot-candle. The RCA 7038 is a 1 in. magnetic tube, with 600 TV lines resolution at 2 foot-candles. These resolutions are specified at normal field strengths, and without video compensation. Increasing the focus field strength and beam accelerating potential improves resolution at the cost of increased deflection power. A 7038 may be raised above 1000 TV lines by this method plus aperture compensation in the video.

The RCA 7263A is an example of a severe environment magnetic tube designed to meet MIL-E-5272B and MIL-E-5400 specifications. Figures 3-21 and 3-24 indicate that its electrical performance is comparable with that of more conventionally constructed tubes.

The RCA 8134 is a 1 in. hybrid tube, which is electrostatically focused and magnetically deflected. Elimination of the focus coil removes 70% of the magnetic component weight, and reduces deflection power requirements by a factor of 8. Resolution is as high as 700 TV lines, with basic 1 in. Vidicon sensitivity.

As an example of electrostatic tube performance, the Westinghouse WX-4306 is a conventional deflection plate design 1 in. Vidicon with a stated center resolution of 350 TV lines, while the General Electric ZL-7815 is a 1-1/2 in. Vidicon with deflectron optics plus a focus reflex modulation gun structure; this tube has a resolution of 800 TV lines with a 1000 volt accelerating field. The Westinghouse WX-4915 is a long-lag integrating photoconductor Vidicon, fully electrostatic, with a resolution of 200 TV lines at 10^{-3} foot-candle, and 500 TV lines at 10^{-1} foot-candle.

From information presented in this section it is clear that Vidicons, particularly of electrostatic design, show considerable promise of meeting cloud cover sensor requirements for the SMS system, when scene illumination levels exceed a few tenths of a foot-candle; this situation corresponds to daylight viewing. A more detailed discussion of the performance and configuration of such equipment may be found in subsection F.

c. SEC Vidicon Performance

Data has been received from Westinghouse on time lag, integration and storage, resolution, and overall tube performance of the SEC Vidicon. While this information is experimental and highly tentative in nature, it is nonetheless valuable in illustrating the current developmental status of this tube.

Time-lag measurements have been performed, and no lag has been observed at normal operating voltages. This tends to substantiate the theory that the signal generating mechanism is largely due to free electrons created by the primary electrons and collected either by the backplate or wall screen. If the target voltage is increased beyond normal operation values, a time-lag becomes noticeable. This can be explained by the fact that the electric field within the layer is now high enough to permit significant solid-state conduction. Generally, it is found that photoconductive targets or EBIC targets which exhibit high gain show

an excessive time-lag. The onset of conductive lag is associated with an increase in gain. Therefore, an SEC target may be operated at relatively low voltages in the fast mode with a gain of about 200, or at higher voltages, thereby sacrificing speed of response in favor of higher gain.

It is important to make resistivity as high as possible to achieve long integration times. Extensive tests have been performed to gauge tube integration performance under a variety of operating conditions. Small input signals have been successfully integrated for periods up to 1-1/2 hours. These experiments demonstrate that it is possible to integrate extremely weak signals for periods up to hours without background contribution due to target leakage current.

In measuring resolution, it is necessary to distinguish between the resolution capabilities of the target, the maximum resolution of a tube incorporating such a target, and the resolution limitations set by the associated equipment. No attempts were made to measure the intrinsic resolution capabilities of the SEC target directly. Based on the thickness of the target, however, it seem reasonable to assume that up to 1800 TV lines per in. should be resolvable on the target before scattering of primary electrons significantly degrades resolution.

Resolution measurements have been made with sealed-off tubes using electrostratic focusing in the image section and with demountable tubes employing all-magnetic focusing. In the first case, maximum resolution was found to be 300 TV lines per in. referred to the photocathode, or 600 TV lines per in. on the target, since these tubes employ a linear minification of 2:1 in the image section. Tubes with magnetic focusing of the image section clearly resolve 1000 TV lines per in. on the photocathode, indicating that in the electrostatically focused tubes the upper limit to resolution is set by the electron optics. Resolution obtained with magnetically focused tubes is limited by the bandwidth of the video amplifier.

The performance of a sealed-off tube was evaluated by measuring limiting resolution as a function of photocathode highlight illumination, using a 100% contrast test pattern. The tube employed electromagnetic focusing for both image and scanning sections; the photocathode was of the flip-over type with a useful diameter of 5/8 in. Sensitivity after tip-off was 25 microamperes per lumen measured against a 2870°K light source. The results of this test are shown in Figure 3-25 where limiting resolution is plotted against photocathode illumination.

Curve 1 was taken with 10 volts target voltage and curve 2 with 40 volts target voltage. In both cases, the target was scanned continuously (30 frames per second), and limiting resolution was determined by visual observation of the monitor screen. For comparison, the equivalent data are given for an Image Orthicon (taken from Morton and Ruedy, Advances in Electronics). For both target voltages, no picture "sticking" was observed. The maximum resolution under optimum illumination was found to be 1000 TV-lines per in.

Curve 3 was taken with 10-second integration, and Curve 4 for 30-second integration. The target voltage was 30 volts in both cases. Since the integrated charge is read out and displayed essentially within one frame time (1/30 second), it is difficult to observe limiting resolution directly. Therefore, limiting resolution for Curves 3 and 4 was determined from Polaroid photographs taken of the monitor.

Another version of this tube type(Figure 3-26)is similar to an Image Orthicon but uses direct beam readout. It employs electromagnetic focusing and deflection and contains a high sensitivity S-20 photocathode and a 1 in. diameter SEC target. Resolution has thus far been limited by the equipment employed in making these measurements to about 15 line pairs per mm. Readout speed is fast, i.e., the signal is erased to less than 10% of its initial value after 1/60 second. Another feature of importance is the large dynamic range over which these targets operate satisfactorily. Signal to noise ratios of more than 100 have been obtained. Integration of input signals is superior to that in conventional Image Orthicons with thin film targets.

Although still in a relatively early stage of development, the SEC Vidicon appears to offer significant advantages in television camera tube performance. The high charge gain, fast response, large storage capacity, and high resistivity should make it adaptable to a wide range of operating conditions.

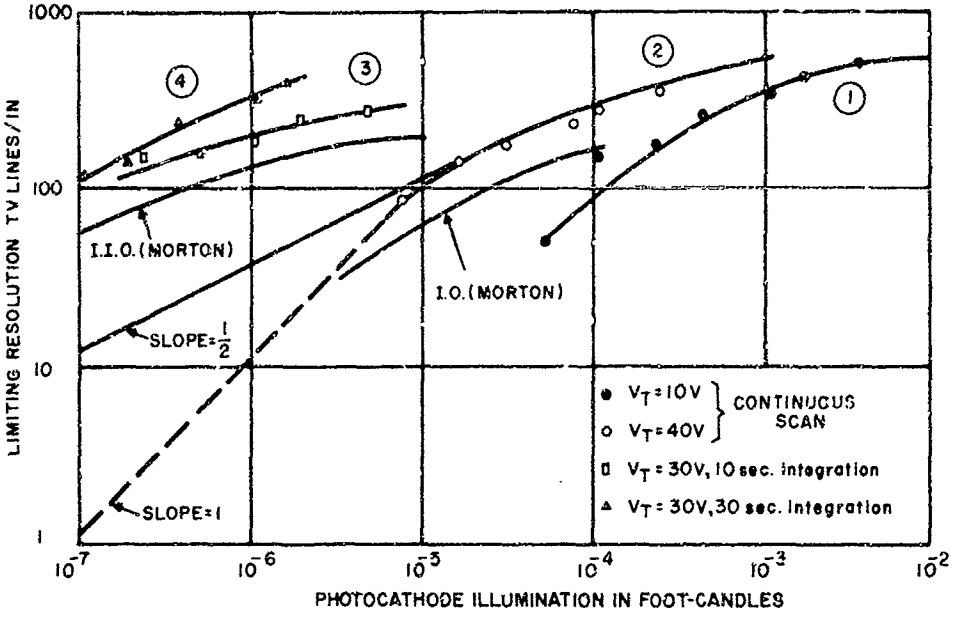

Figure 3-25. Performance of Experimental SEC Vidicon

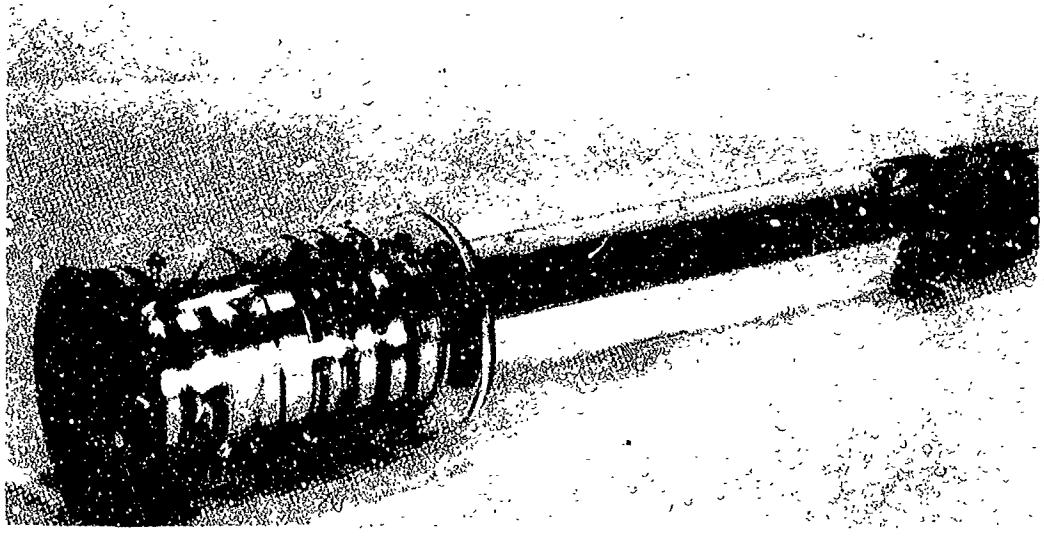

Figure 3-26. Electromagnetic SEC Vidicon

d. Image Orthicon Performance

The theory and operation of the Image Orthicon were described in considerable detail in subsection C.2. Basically, the device consists of an image section, a storage target section, a scanning section, and a dynode electron multiplier. An optical image, focused on the photoemissive surface in the image section, produces an electrical image which is accelerated and focused on the target. Secondary electrons escape the target and land on a collector mesh, leaving a charge pattern stored on the target. The collector-mesh assembly forms a capacitor; wide-spaced assemblies have a smaller capacitance, and thus produce a larger voltage for a given quantity of charge, resulting in higher sensitivity. Unfortunately, the smaller total charge produces a poorer signal to noise ratio.

The charge pattern stored on the target is scanned by an electron beam, which neutralizes the stored charge. The beam is made to land on the target surface at near normal incidence, and at close to zero velocity. Some tubes employ a second mesh, called the field mesh, on the scanned side of the target to produce more uniform landing. The return beam enters the secondary emission electron multiplier where the weak current is amplified, producing a signal current of 10 microamperes or less in the load resistor.

The original Image Orthicon has a 3 in. diameter image section and a 2 in. diameter scanning section. Focusing of both sections was by magnetic and electrostatic fields, with magnetic deflection of the scanning beam. The storage target may either be a glass disk or a thin magnesium oxide film, depending upon tube application and performance requirements. If a glass target is used, its volumetric resistance is selected in accordance with standard TV broadcast frame rates; if such a target is used at slower scan rates, the stored charge tends to redistribute, reducing resolution and contrast. The anisotropic resistance properties of thin film targets virtually eliminate lateral leakage, permitting much longer readout periods. The effective capacitance of the thin film target is less than that of the glass target, resulting in a reduced maximum signal to noise ratio where all other parameters remain fixed.

Virtually all Image Orthicons produced in this country are manufactured by Westinghouse, General Electric, or RCA. A representative selection of these tubes has been chosen, and their performance data summarized in Figures 3-27 through 3-29. Since it is anticipated that the cloud cover sensor will find maximum utility if it images a square format on the Earth, resolution data has been normalized to a square raster pattern, rather than the more usual 4:3 pattern; maintaining the usual TV convention, resolution is cited in terms of TV lines per target height.

Figure 3-27 is a plot of limiting resolution versus photocathode illumination for a number of different tubes. Resolution of the RCA C74034 exceeds 800 TV lines per target height (square raster) at 10^{-5} foot-candle photocathode illumination; the Westinghouse WL-22722, WL-22724, and WL-22730 yield 150 TV lines per target height (square raster), limiting resolution at 10^{-7} foot-candle photocathode illumination, but are inferior to the RCA tube in resolution at photocathode illumination levels above 6×10^{-7} foot-candle. Data on the RCA C74081 is estimated on the basis of highly preliminary information given at two

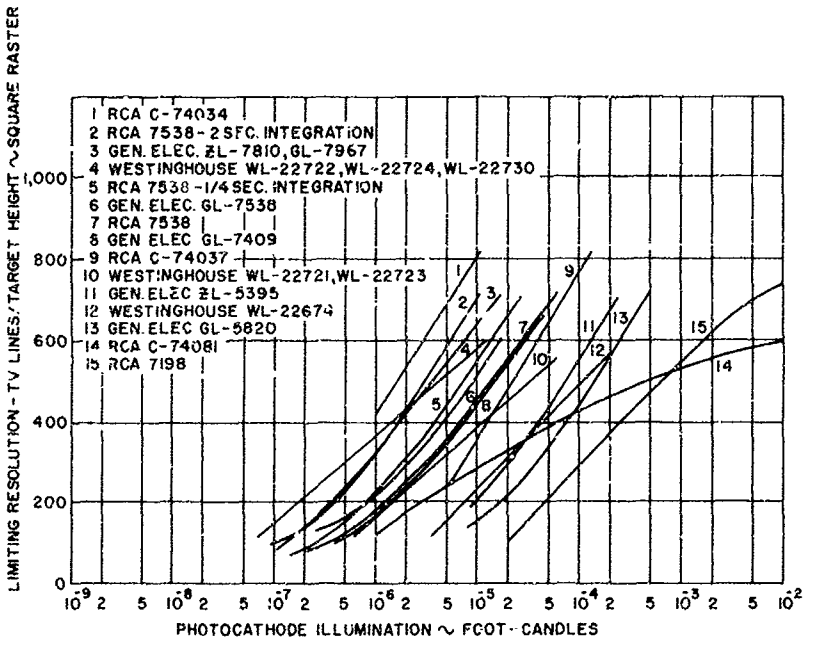

Figure 3-27. Typical Resolution - Sensitivity Characteristics of Image Orthicons

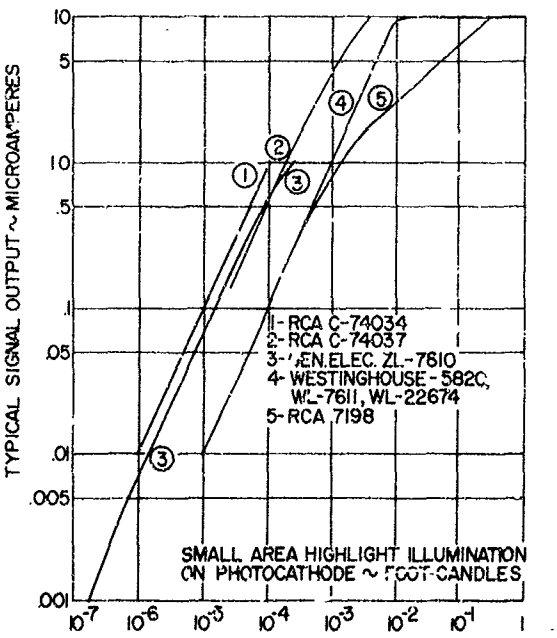

Figure 3-28. Signal Response of Image Orthicons as a Function of Photocathode Illumination

illumination values. All curves plotted in the figure are for standard TV broadcast (1/30 second) frame rates.

Figure 3-28 shows the light transfer characteristics of seven different tubes. The Westinghouse 5820, WL-7611, and WL-22674 all display the same characteristic curve, with a pronounced knee at 10^{-2} foot-candle small area highlight photocathode illumination. Below the knee, signal response increases with illumination; above the knee, electron redistribution tends to delineate highlight areas, permitting imaging to take place, though with some loss in contrast. These tubes all have glass targets, which accounts for the presence of the knee. The RCA C74034 and C74037 show greater signal response at the same photocathode illumination levels; both these tubes utilize thin film, high gain targets.

Figure 3-29 shown the relative center square-wave amplitude response of the Westinghouse 5820 and WL-7611, and the RCA 7198. The Westinghouse curves are identical, corresponding to 10^{-2} and 2×10^{-2} foot-candle highlight illumination on the photocathode; the 7198 data is taken at 3×10^{-2} and 3×10^{-3} foot-candle photocathode highlight illumination. These tubes all employ glass targets. Amplitude response data was not available on magnesium oxide target tubes.

In addition to the performance curves presented, some further comment is in order on tube size and construction. Image Orthicons may be classed as miniature (2 in.), 3 in., and 4-1/2 in. tubes, according to the approximate diameter of the image end. Each classification will be considered separately.

1) Miniature Image Orthicons. There are presently two miniature Image Orthicons both under development for the US Signal Corps. The RCA C74081, which is under development for ERDL, Fort Belvoir, on contract DA44-009-ENG-4575, is a magnetically focused and deflected tube with a 2.1 in. diameter image section and a 1-3/8 in. diameter scanning section. A photograph of the tube, which is 9-1/4 in. long, is presented in Figure 3-30. The tube is a miniaturized version of a standard 3 in. Image Orthicon, except for its 6.3 volt, 95 milliampere filament; standard Image Orthicon heaters draw 600 milliamperes at 6.3 volts. The tube uses an S-20 photocathode with a thin film magnesium oxide target and a field mesh. Expected limiting resolution is 100 TV lines (4:3 raster) at 10^{-6} foot-candle photocathode illumination, with a center resolution of 500 TV lines (4:3 raster) and a signal to noise ratio of about 20:1 at 10^{-2} foot-candle.

The other miniaturized Image Orthicon is the General Electric ZL-7804, which is a fully electrostatic tube 2 in. in diameter at the image end and 12-1/2 in. long. A diagram of the tube is shown in Figure 3-31, while a photograph of an experimental model is presented in Figure 3-32. The photocathode faceplate is curved, as a result of the conventional electrostatic focus image section design. Unfortunately, this design is expected to produce electron images which are distorted, badly shaded, and of poor off-axis resolution, even with curved end plates. General Electric is currently developing a new type of electrostatic focus image tube with a flat optical faceplate and a curved mesh behind the photocathode for electrostatic focus capability. This design, when incorporated into the image end of the electrostatic Image Orthicon, should be capable of results approaching that of the magnetically focused converter. Furthermore, this plane-to-plane image converter may be electronically zoomed since the output image size

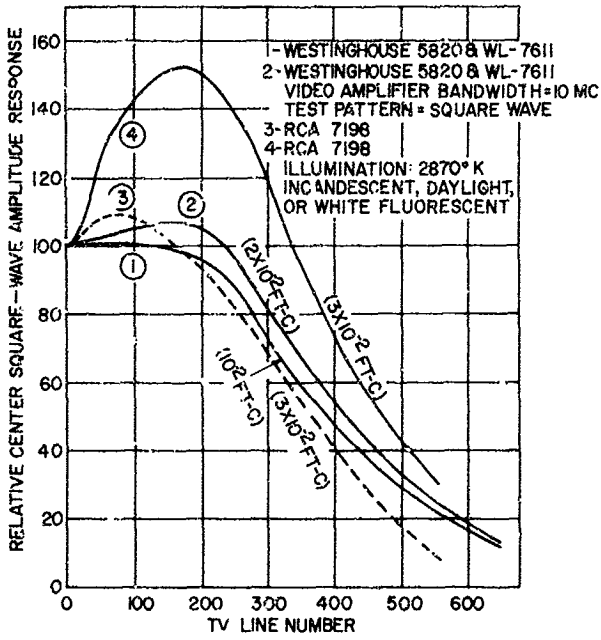

Figure 3-29. Amplitude Response of Image Orthicons

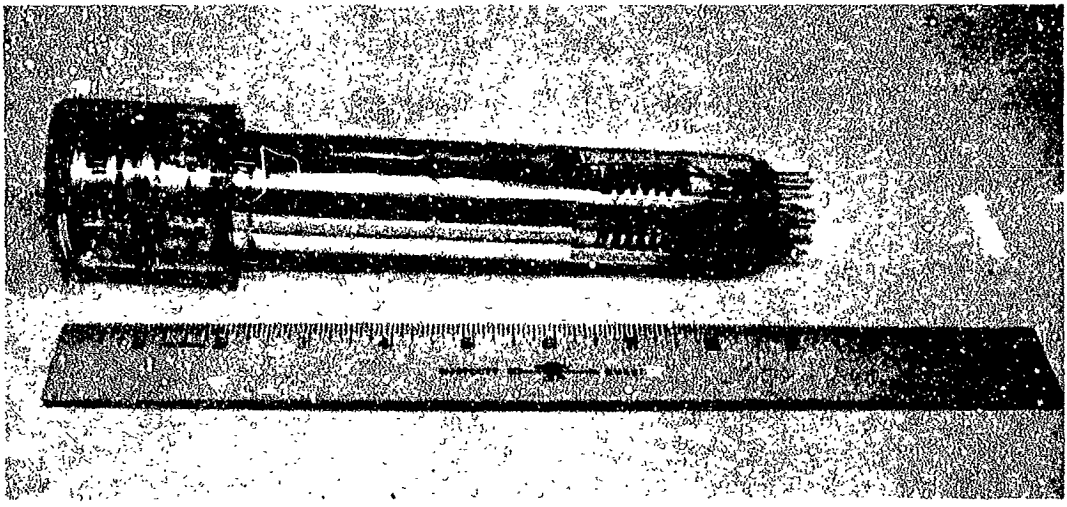

Figure 3-30. The RCA C74081 2-Inch Magnetic Image Orthicon

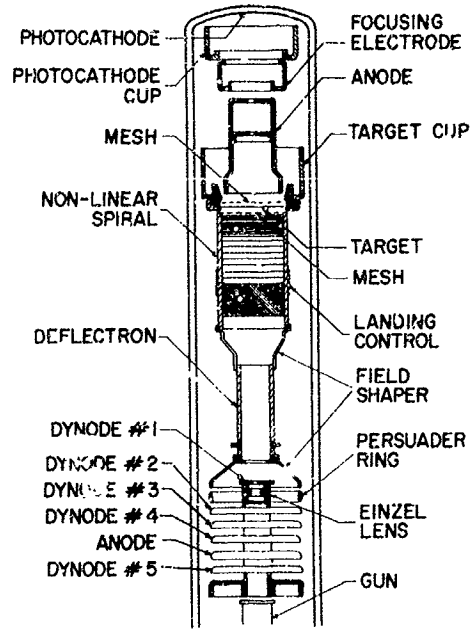

Figure 3-31. Electrostatic Image Orthicon, Cross Section

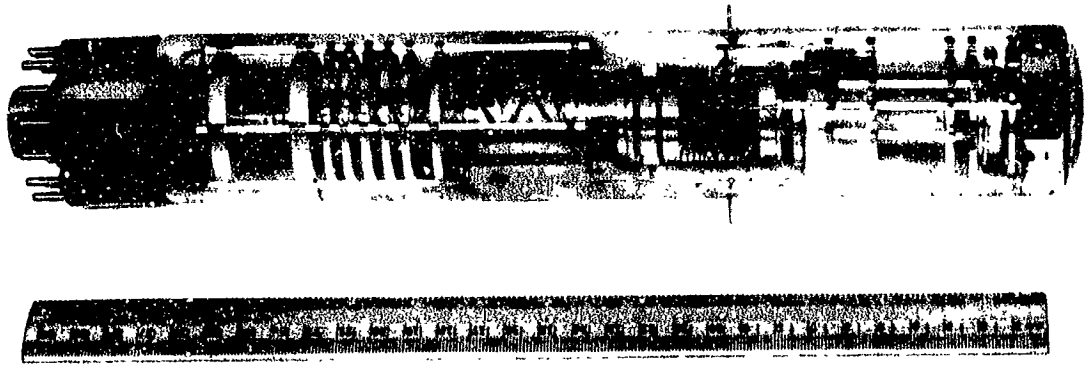

Figure 3-32. Electrostatic Image Orthicon

is a prime function of the tube operating voltages supplied. The final configuration of the ZL-7804 image section has not yet been determined. This is the major remaining developmental problem in this tube. The nonlinear spiral accelerator permits maximum deflection sensitivity. Tubes developed to date use a conventional Image Orthicon gun structure, but it is anticipated that the final design will incorporate a focus reflex modulation gun structure for maximum resolution and minimum change in beam focus with beam current.

2) Three-Inch Image Orthicons. The most popular Image Orthicon in production today is the 3 in. design. The standard of reference for Image Orthicon development is the 5820 tube, which is a closely spaced collector mesh tube having a glass target but no field mesh. Resolution data for this tube, and for most of the others discussed in this section may be found in Figure 3-27. It is of interest to note that most of the tubes cited exceed the 5820 "standard" in resolution performance. The light transfer curve for this tube (Figure 3-28) shows a knee which is typical of glass target tubes. Limiting resolution is 625 TV lines (4:3 raster) at 2 x 10^{-2} foot-candle photocathode illumination, and a signal to noise ratio of 40:1 at 525 lines and 1/30 second frame time with a video bandwidth of 4.5 MC.

The 7513 is also a glass target tube, but it has the advantages of much closer mesh spacing (0.0007 in.) and the addition of a field mesh. Its performance is superior to the 5820, having a limiting resolution of 675 TV lines (4:3 raster) and a signal to noise ratio of 55/1 with its knee at 3 x 10^{-2} foot-candle photocathode illumination.

The RCA 7538 and General Electric ZL-7810 are examples of magnesium oxide target tubes which do not exhibit knees in their transfer characteristics; the former uses an S-10 photocathode, while the latter has an S-20 surface. Figure 3-33 presents typical resolution-sensitivity characteristics of these tubes, showing the effect of image integration time. Using an S-20 photocathode in place of the S-10 would improve the sensitivity of the 7538 by a factor of 3. It should be noted that these curves indicate target saturation effects; all things being equal, and increase in integration time from 1/4 second to 2 seconds should result in a decrease in illumination by the factor of 8 required to achieve the same limiting resolution. Interpretation of these curves must include the property of the observer's eye to integrate for approximately 0.2 seconds when viewing a monitor repetitively scanned at 1/30 second. For increased integration times, the camera tube was being scanned at a 30 cycle rate, but the target charge was not being replenished; consequently, the eye's importance in determining resolution is less effective.

Figure 3-34 shows the effects of contrast on tube resolution sensitivity characteristics. These curves show the range of values which would be encountered with an RCA 7538-type tube, at 1/30 second frame times.

The Westinghouse WL-22724 is an example of a magnesium oxide target, S-20 photocathode Image Orthicon which is designed to meet MIL-E-5272 environmental specifications. Its electrical performance is similar to the General Electric ZL-7810. Center horizontal resolution at 3 x 10^{2} foot-candles photocathode illumination is a minimum of 350 TV lines (4:3 raster) with 5g applied acceleration in the frequency range from 50 to 500 cps.

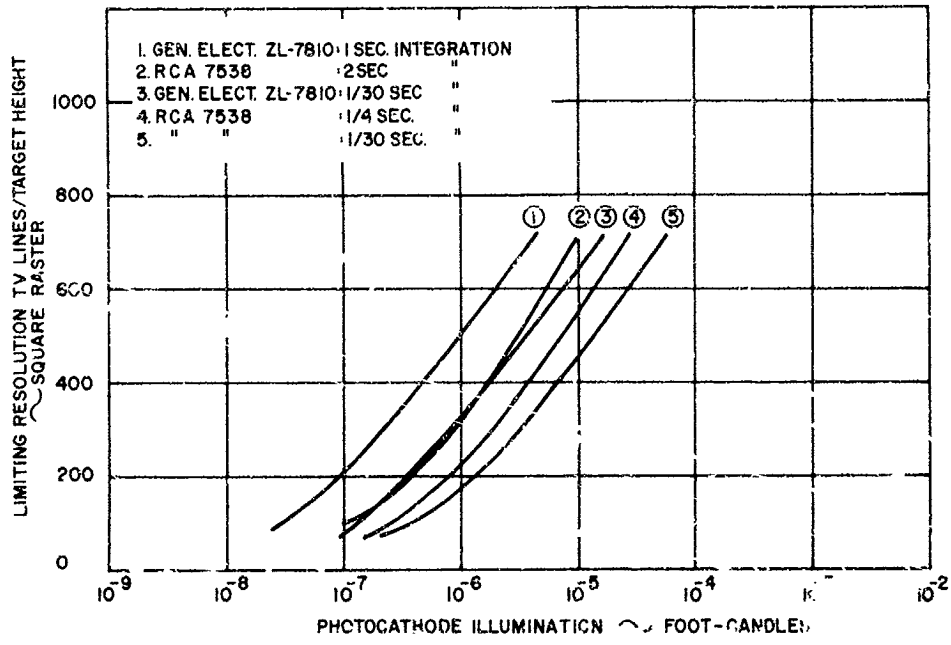

Figure 3-33. Typical Resolution - Sensitivity Characteristics of Image Orthicons (for Various Integration Times)

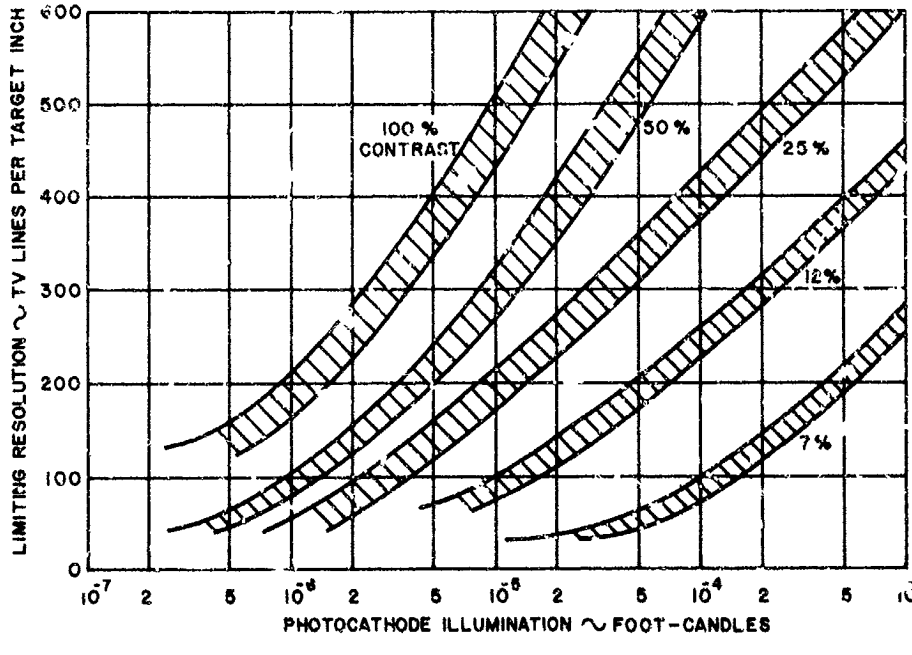

Figure 3-34. Image Orthicon Tube Resolution - Sensitivity Characteristics as a Function of Contrast

3) Four and One-Half Inch Image Orthicons. The primary objective of larger diameter Image Orthicons is to improve resolution and signal to noise ratio by tripling the target area. This results in increased resolution for a given scanning beam size, and increased target to mesh capacitance for a given mesh spacing. Increasing the total target capacity without decreasing the spacing maintains reasonable sensitivity (9×10^{-2} foot-candles at the knee for a 4-1/2 inch version of the RCA 7293A) while increasing the signal to noise ratio of the tube to 90:1 with a 4.5 MC video bandwidth at 1/30 second frame time and 525 TV lines (4:3 raster) resolution.

Electrical performance improvements are not without penalty, however, since the size, weight, and power requirements of the 4-1/2 in. Image Orthicon are about triple those of the 3 in. version. In addition, the ruggedization of these devices required for military and space applications has not progressed nearly as far as with the smaller tubes.

4) Slow Scan Performance. Since the SMS cloud sensor requirements will most likely necessitate use of slow scan rates and image integration to optimize system performance, it is appropriate to consider what data is available on such techniques before leaving the subject of Image Orthicons.

In slow scan applications, the Image Orthicon has the advantage of separating photocathode and target characteristics for optimization of each parameter. Measurements of uncontaminated magnesium oxide targets by themselves indicate a storage capability of up to 4-1/2 hours without loss or redistribution of charge. When such targets are actually incorporated into imaging tubes, contamination by metals from the photosurface ensues; the S-20 photosurface contains cesium, potassium, sodium, and antimony, with cesium being the primary target contaminant. During operation, especially at elevated temperatures, the target tends to become further contaminated.

Tests have been made on 3 in. Image Orthicons for integration and storage characteristics of magnesium oxide and glass target tubes. At Kitt Peak Observatory, tests indicate a noticeable reduction in resolution at integration times of 1 minute. Westinghouse, Elmira, has conducted experiments under two Air Force contracts on the interaction of photoemissors on storage targets. As a result of these tests, Westinghouse specifies a minimum resolution of 600 TV lines after 10 seconds of storage on many of their new magnesium oxide target Image Orthicons. Westinghouse has also developed a bi-alkali photocathode which does not contain cesium; its characteristics are similar to the S-10 surface in sensitivity and to the S-11 in spectral response. Image Orthicons using this photocathode have shown integration and storage for 4-1/2 minutes without loss in resolution. They are also developing a new photocathode designed for 15 minute storage, and estimate that a storage time of 1 hour may be possible with this material.

General Electric, Syracuse, has conducted tests for the Frankfort Arsenal on storage as a function of temperature for magnesium oxide target Image Orthicons. The tests consisted of short optical exposures (0.1 to 1.0 second) followed by 3 to 9 seconds storage and readout with a 1/30 second frame

rate; temperatures ranged between -50°C and +50°C. The picture did not change qualitatively over the temperature range, and was equivalent to what would be obtained under normal operation without storage.

RCA has conducted tests on the effects of slow scan readout, but their tests were conducted on glass target tubes. The basic conclusion reached was that for a given target charge, the signal to noise ratio remains constant as the scan rate is changed from 1/30 second to 3 seconds, but the illumination required varies directly with the frame rate. Theoretically a slower scanning rate merely means that the same number of electrons must be deposited on a given target element over a longer period of time. Hence, while current and bandwidth are reduced, the same primary to secondary electron emission ratio, and the same secondary electron redistribution should be found as in the normal scan period. The effect of time on redistribution of secondary electrons is not known; in addition, since the scanning beam current cannot be reduced in direct proportion to the scanning rate in a practical tube, the magnitude of this effect is also not known.

Most Image Orthicon tube engineers do not feel that slow scan readout will noticeably affect the signal to noise ratio and resolution on a magnesium oxide target tube at readout times of 10 seconds or less. Hazeltine, which is currently developing a slow scan camera for NASA's Nimbus program (based on the General Electric 2 in. electrostatic Image Orthicon), intends to test slow scan readout characteristics of this system in considerable depth as part of their development program.

e. Image Isocon Performance

Details of Image Isocon design and construction were presented in subsection C.2. The basic difference between the Image Orthicon and the Image Isocon is that the former extracts a video signal by passing the reflected scanning beam into an electron multiplier in the gun section, while the latter passes the beam which is scattered from the target back into the multiplier. The Image Isocon signal current is reversed in polarity from that of the Image Orthicon, with a saturated white signal resulting in a maximum signal output current.

The Image Isocon has been under development for several years at RCA, under Air Force contracts AF33(600)-7696, AF33(616)-5728, and AF33(616)-6497. While the most recent tube information was not available to Republic during the study, sufficient data was found to indicate trends and demonstrate tube capability.

Figure 3-35 is a plot of signal to noise ratio as a function of incident photocathode illumination for Orthicon and Isocon scan modes, comparing dual mode tubes (i.e., tubes which are capable of operating in either scan mode). One tube has a low capacitance target (0.030 in spacing between target and collector mesh) while the other has a standard 5820 Image Orthicon spacing (0.0025 in.). In each case the beam current was retained at the level required for the highlight condition. The signal to noise ratio decreases rapidly in the low illumination range; the threshold occurs at a higher illumination level for Orthicon scan than for Isocon scan. The signal to noise ratio for Isocon scan of a particular target charge is seen to be at least three times greater than for Orthicon scan in dual mode tubes. The signal to noise performance of standard Image Orthicon tubes lies between that of the two modes of operation for laboratory constructed dual mode tubes; at full target charge, differences are minimum.

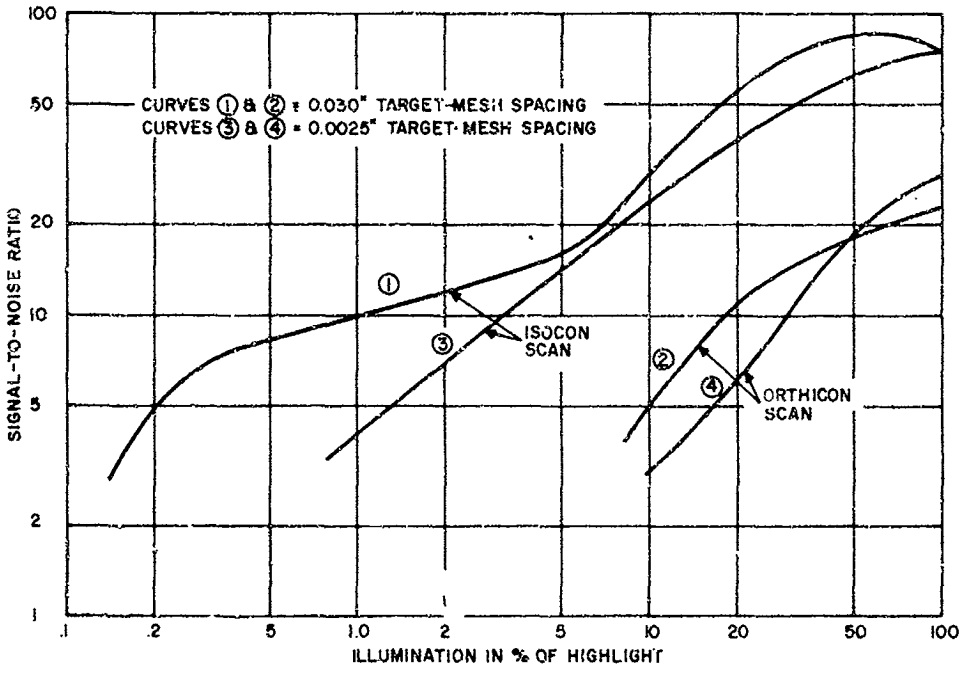

Figure 3-35. Signal to Noise Ratio as a Function of Illumination for Dual Mode Isocon Tubes

Figure 3-36 is a plot of signal modulation (i.e., the ratio of signal current to total output current) while Figure 3-37 gives output current as a function of illumination; each plot compares Orthicon and Isocon operation for both dual mode tubes. It is interesting to note that modulation remains almost constant when the beam current is optimum in the closely spaced tube. At some low value of illumination, modulation drops and decreases rapidly with further reduction in illumination. Despite signal loss at the target, the Isocon mode output signal is invariably larger than the Orthicon mode signal in each tube. This results from gain achieved in the scattering process, since on the average three incident electrons are scattered for each electron which is retained at the target to neutralize a stored charge. Tube dynamic range may be obtained by examining these curves; this is simply the range of variation in light level which lies between the full target charge highlight and that low light level associated with minimum tolerable signal to noise ratio. Isocon scan represents an order of magnitude improvement over Orthicon scan in this respect.

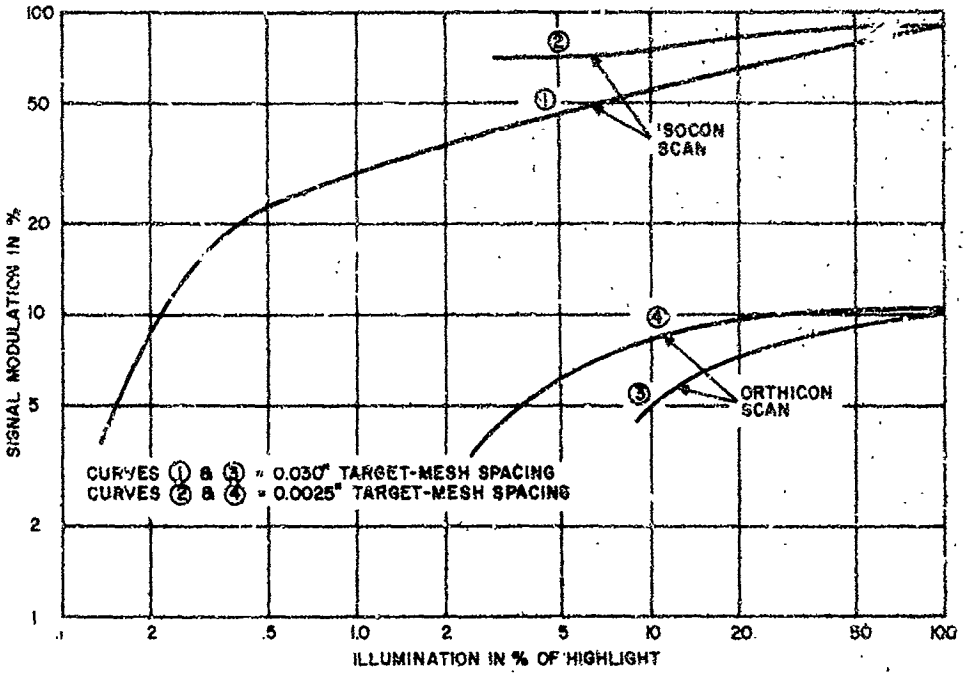

Figure 3-36. Signal Modulation as a Function of Illumination for Dual Mode Isocon Tubes

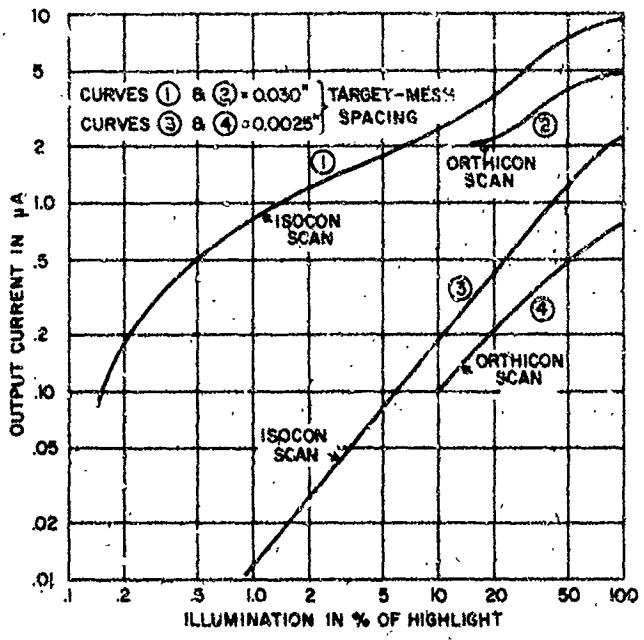

Figure 3-37. Output Signal as a Function of Illumination for Dual Mode Isocon Tubes

Aperture response (Figure 3-38) for Isocon scan with no beam deflection effects is inferior to that of Orthicon scan; when beam deflection at the target is permitted, the Isocon mode response is enhanced. Sine wave response for Orthicon scan of a dual mode tube is equivalent to a standard 5820 Image Orthicon. Near threshold illumination, a difference of 50 to 100 TV lines in favor of Isocon scan can be expected.

As mentioned previously, the most significant features of the Image Isocon are its improved signal to noise ratio and its very wide dynamic range. The additional electron optical elements required complicate the setup of the Isocon, and reduce the probability of successful unattended operation for prolonged periods. The tube is still under development; when it becomes completely operational, it should compete rather successfully with the Image Orthicon for such applications as the SMS cloud sensor system.

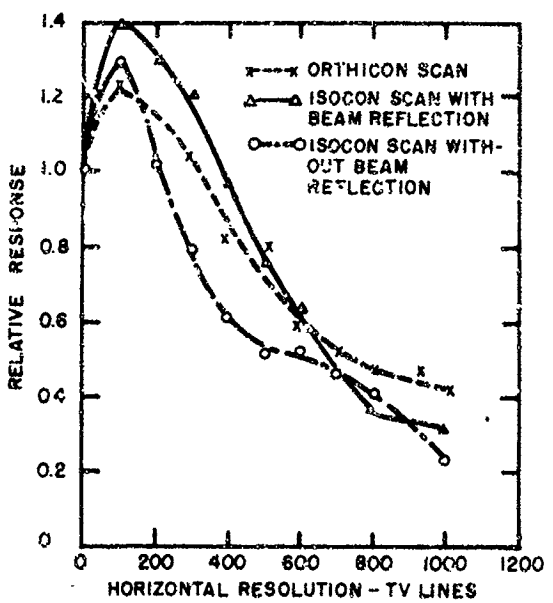

Figure 3-38. Sine Wave Aperture Response Curves - Image Isocon

f. Image Intensifier Orthicon Performance

The Image Intensifier Orthicon was described in subsection C.3 in considerable detail. Basically, this tube can be characterized as a cascading of an intensifier section between an optical image and an Image Orthicon image section. The result is an increase in low light level sensitivity of the Orthicon by an amount roughly equal to the gain in the intensifier section. At higher light levels, the signal to noise ratio is comparable to that of an Image Orthicon having similar target capacitance, but resolution degrades as a result of the successive imaging process.

Data is available on three current Image Intensifier Orthicons; these are the RCA C74036 and C74093, and the Westinghouse WX-4299. Resolution sensitivity characteristics are presented for these tubes in Figure 3-39. The WX-4299 is represented by two curves, one for best performance and the other for nominal performance within its operating range. Note that here again, as with the Image Orthicon curves, resolution is stated in terms of lines per target height, for a square raster (subsection C.6.d). In addition, curves of output signal and peak signal to RMS noise ratio versus light level are presented in Figure 3-40 for the RCA tubes; this data was not available on the WX-4299.

The C74036 uses a tetrode image converter section, a high gain oxide target, and an S-20 second photocathode. The tube is 4.2 in. in diamter at the image end, 2 in. in diameter in the magnetic scanning section, and 25 in. long. Stated resolution, for a 4:3 raster, is 370 TV lines at 10^{-6} foot-candle photocathode illumination, and 100 TV lines at 10^{-9} foot-candle. The C74093 was developed to provide improved highlight resolution capability. This tube uses a triode image converter section; it is 4.15 in. in diameter at the image end, 2 in. in diameter at the magnetic scanning section, and has an overall length of 22.4 in. Stated resolution is 450 TV lines for a 4:3 raster at 10^{-6} foot-candle photocathode illumination, and 100 TV lines at 10^{-9} foot-candle. Both tubes employ electrostatic focusing in the intensifier section; the primary limitation in resolution lies in the thin film coupling between intensifier phosphor and image section photocathode.

The WX-4299 differs from the RCA tubes in that it has a sixth dynode in the multiplier, and utilized a magnetically focused image intensifier section. The tube has a thin film storage target with very low lateral leakage, permitting signal integration for up to 10 seconds to improve sensitivity. Stated resolution is 450 TV lines at 8×10^{-8} foot-candle (4:3 raster) and 200 TV lines at 7×10^{-9} foot-candle. The data cited are for 100% contrast, at 30 frames per second, with continuous imaging.

Major drawbacks to the use of such tubes in space applications are the complexity of tube adjustment for optimum performance, and the problems of unattended operation for long periods of time. In addition, the intensifier section requires very high voltage; first photocathode voltage ranges from 20,500 volts in the RCA tubes to 13,000 volts in the Westinghouse design. Finally, while these devices are unequalled in performance at very low light levels, their resolution above 10^{-6} foot-candle photocathode illumination is distinctly inferior to that of current Image Orthicons. Unless absolutely required by scene illumination conditions, Image Orthicons would be preferable for use in the SMS cloud sensor package. This point is discussed further in subsection F.

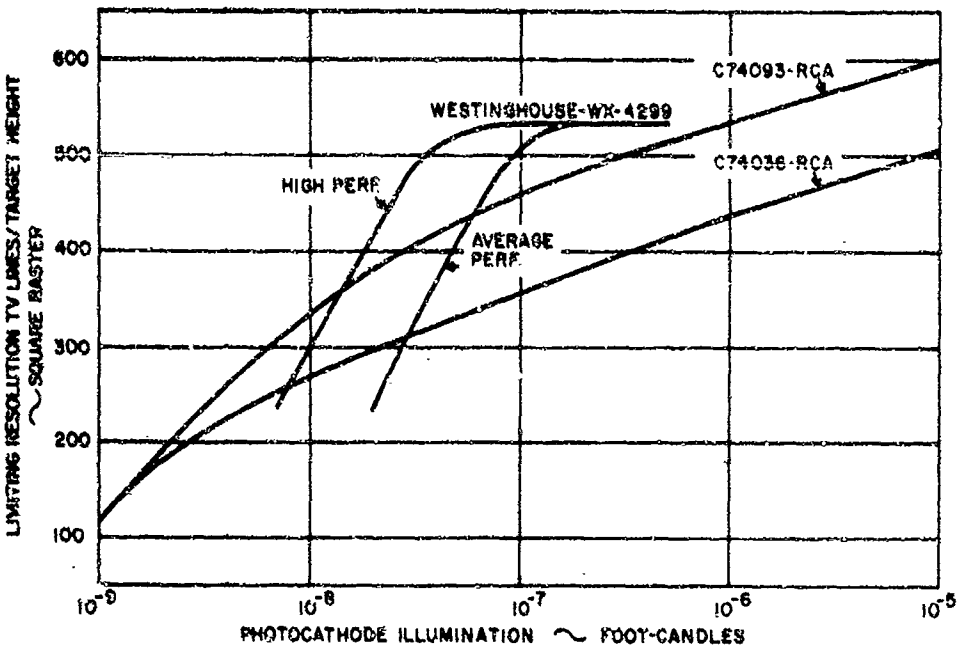

Figure 3-39. Typical Resolution - Sensitivity Characteristics of Image Intensifier Orthicons

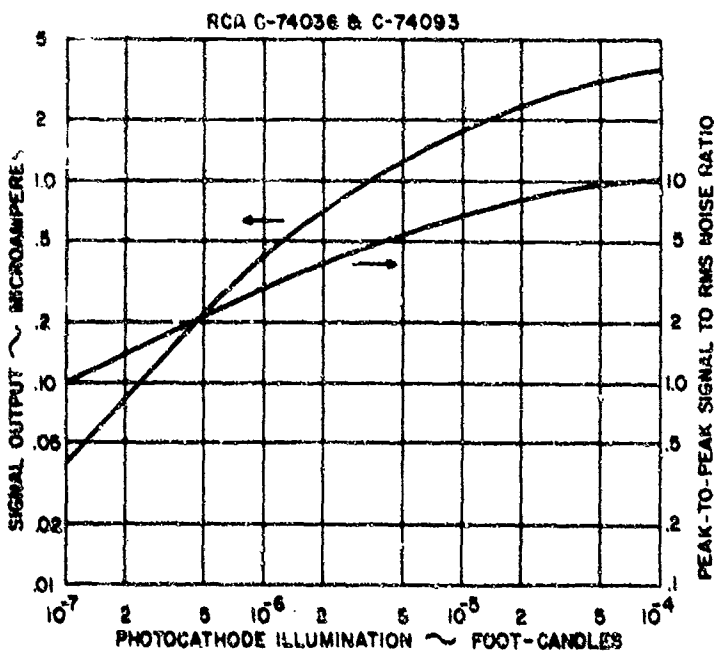

Figure 3-40. Electrical Characteristics of Image Intensifier Orthicons (RCA C74036 and C74093)

In 1961, RCA was reported to be working on an Image Intensifier Isocon, the C74060. This tube was based on the C74056, and used a dual mode Isocon structure. A feasibility study was being carried out with Air Force support on contract AF33(616)-7696 to determine whether gains in signal to noise ratio and dynamic range due to using the Isocon scan mode would lead to a significant improvement in an Intensifier Isocon design. The outcome of this program is not known.

D. OPTICAL CONSIDERATIONS

The extreme altitude of the satellite presents formidable optical problems, especially when the design objective is to view the Earth's cloud cover under both day and night conditions at high resolution. The present state of the optical art offers both refractive and reflective optical systems in numerous designs and variations that possess inherent resolving powers in excess of presently available or even future sensor tube resolution capabilities. The optical considerations which determine use of a particular lens design or type are dependent upon such factors as sensor tube characteristics, desired area coverage, format size, satellite weight, and spatial limitations.

In considering the optical requirements for visible light sensors, no attempt was made to define, in detail, the exact characteristics of an optical system. Lens design begins with the designer's goal of perfection and is followed by a series of compromises resulting from the materials available, manufacturing difficulties, and other practical limitations. Finally, the lens represents the best compromise in resolution, distortion, size, and weight that will provide acceptable performance for the intended application. This subsection will, however, consider major optical system characteristics and interrelated functions which would influence the selection of a particular optical system for various resolutions and coverages.

1. Optical Parameters

The SMS optical requirements have been considered for full Earth disc coverage and for various smaller coverage areas. The basic optical relationships are straightforward, as is shown below:

$$\frac{\text{Object Size}}{\text{Image Size}} = \frac{\text{Distance}}{\text{Focal Length}} = \frac{\text{Scale Factor}}{1}$$

Since the sensor platform is at a constant (synchronous) distance above the nadir, the three remaining parameters can be varied to obtain the best combination for performance, size, and weight. If image size is reduced, the focal length of the optical system is reduced proportionally, and accordingly, the ground coverage is inversely proportional to image size. Therefore, the interrelation of the three parameters must be carefully considered and viewed broadly to properly establish the optimum configuration.

A nomograph (Figure 3-41) has been developed to illustrate comprehensively how the optical and sensor parameters are related, and indicate the effect of parameter variation. The nomograph relates sensor tube picture height, focal length, and ground coverage as one set of parameters and TV lines per picture height, ground resolution at the nadir, and ground coverage as another set of parameters. Datum points on the picture height scale are indicated for convenience for various sensor tubes. This scale is based on a square format; subsection C.6.d. discusses the use of such a format for SMS applications.

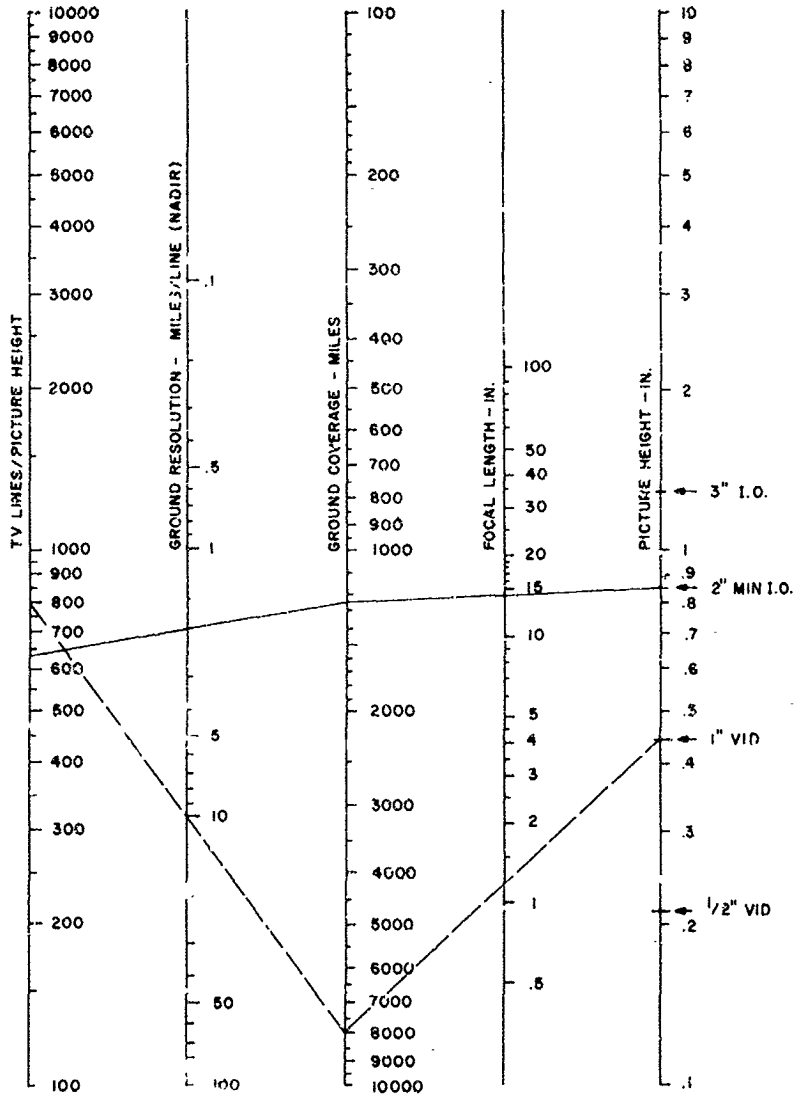

Figure 3-41. Optical Sensor Parameters - Single Frame Coverage

Two sample problems are depicted on the nomograph. The first is for a full Earth disc. Using a typical 1 in. Vidicon as a starting point and 8000 miles coverage as the end point, it is seen immediately that a 1.25 in. focal length lens is required for this format and coverage. To obtain a 10 mile resolution under these conditions, a sensor resolution of 800 TV lines per picture height is required. Reference to tube capabilities shows that this is feasible; indeed, better resolution is possible with certain tubes.

For the narrow angle sensor system, a 2 in. minature magnetic Image Orthicon was selected as the second example. In this system, some consideration must be given to picture overlap and side lap for mosaicing. Using a 10% overlap in each direction, a 1250 mile square picture would yield a 1000 mile square nonredundant coverage in each frame. Under these conditions a 14

in. focal length optical system is required. For a 2 mile ground resolution over a 1250 mile picture, a sensor resolution of 625 TV lines per picture height is required. Since the 2 in. magnetic Image Orthicon currently possesses a limiting resolution of about 600 TV lines per picture height (square raster), the optical system parameters determined above appear reasonable, assuming a modest improvement in tube performance.

2. Optical Resolution

The maximum possible resolving power of an ideal lens is a function of the wavelength of light being resolved and the aperture of the lens. The Rayleigh limiting angle of resolution θ is defined in radians as

$$\theta = \frac{1.2\,\lambda}{d}$$

where λ = the wavelength of light, in millimeters
d = the diameter of the lens aperture, in millimeters

For visible light recording, the linear resolving power at the image plane is expressed by

$$\frac{1}{R} = 0.6\,\lambda\,(\text{f/number})$$

where R = linear resolving power, in line pairs per millimeter
λ = the wavelength of light, in millimeters
f/number = the focal ratio of the lens

The lens resolving power will vary over different areas of the image plane with the highest resolution at the optical axis and slightly reduced resolution at the format diagonals.

In considering the visible light sensor optics, the maximum resolving capabilities of a perfect lens (Table 3-2) should be taken into account.

TABLE 3-2
IDEAL LENS - MAXIMUM RESOLUTION

Focal Ratio	On Optical Axis (L.P./mm)	Radial 10° Off Optical Axis (L.P./mm)	Equivalent TV Lines At Lowest Resolution
f/1.0	745	740	1480 L/mm or 37,600 L/in.
f/2.0	373	368	736 L/mm or 18,700 L/in.
f/2.8	266	262	524 L/mm or 13,300 L/in.
f/4.0	187	184	368 L/mm or 9,350 L/in.
f/5.6	133	131	262 L/mm or 6,650 L/in.
f/8.0	93	92	184 L/mm or 4,675 L/in.
f/11.0	66	65	130 L/mm or 3,300 L/in.

From a comparison of equivalent TV line resolutions, it is evident that a high quality optical system can image more TV lines onto the 10 mm target of a 1 in. Vidicon than the tube can ever reproduce. Indeed, the optical system resolution exceeds that of the Vidicon tube by more than an order of magnitude.

In practice, optical designs such as reflecting mirror systems that cover a very narrow field of view can be made substantially free from detrimental distortions such as coma and spherical aberration, and will be capable of resolution performance approaching theoretical limits. With but modest effort, optical designers will be able to modify existing refracting lenses for optimum SMS performance to produce a twofold increase in resolution. Such capability has been indicated by Goerz Optical Company, Inwood, New York, and Pacific Optical Company of Los Angeles.

The very nature of cloud cover imaging requires that relatively low f/number optical systems be employed to provide sufficient illumination at the sensor photosurface. This requirement provides further assurance that the optics will not limit overall sensor system performance.

3. Optical Systems

The two basic types of optical systems considered are categorized as refracting and reflecting. The number of variations possible within each category is perhaps limited only by the optical designer's ingenuity because of the wide selection of materials available today for optical technology. In general, refracting lenses are employed for wider angular coverage and smaller aperture diameters, as compared to the narrower angle, larger aperture reflecting sustems. Since the limiting lens resolution is a function of lens aperture, reflecting systems inherently provide higher performance. Where longer focal lengths are required, reflecting systems also provide superior performance, since folded optical path designs yield improvement in overall length to focal length ratios by as much as 5 to 1.

Because of the known difficulties that exist in the design and manufacture of large diameter refractive optics, as well as inherent size and weight considerations, the narrow coverage requirements can best be satisfied by several existing designs of modified Cassegrain systems. Such systems are catadioptric designs that eliminate aberrations by the use of correcting glass elements. Notable designs employing variations of this technique are the Maksutov, Bouwers, Dahl-Kirkham, Schwarzchild, Baker and Schmidt systems. Differences between these systems are primarily in the thickness and location of correcting lens elements. No attempt has been made to evaluate performance differences or recommend a particular system.

For the wide coverage where focal lengths are short, a Petzval lens design offers distinct advantages because of its inherent resolution uniformity at high f/number over the entire image field. Such a lens, with a field flattener element added, would provide additional assurance of maximum definition. The Petzval design produces a flat field up to about 25° total angular coverage, which is more than adequate for the full Earth disc sensor.

A hybrid refractive design which was considered is the Vari-Focus lens, i.e., the Zoomar lens. Such a lens attempts to provide a means of continuously varying the focal length or magnification while keeping the image in precise focus

over the focal range and maintaining a constant aperture. Hence, such a system seems to provide an ideal replacement for separate wide angle and narrow angle lenses by a single lens. A closer examination discloses serious problems, however, as discussed in the following paragraphs.

Vari-Focus lenses have enjoyed wide application in amateur home movie cameras and a studio television equipment, where the image is viewed subjectively, and where the central area of the picture is the prime area of interest. For these applications, magnification ratios are generally small. A Vari-Focus lens for meterological satellite applications would require highly corrected optics as well as uniform field resolution and illumination, together with a large aperture and a magnification range of 12 to 1. Such a lens does not exist at present, and there is considerable doubt that it can be designed at all. In addition, the resolution fall-off within 3° off-axis of present day Vari-Focus lenses is so drastic that lens manufacturers prefer to avoid publishing such data.

It is admittedly difficult to design a fixed focus lens containing from four to six elements, but the problems of designing and fabricating a Vari-Focus lens containing the 15 or more elements needed to satisfy the previously defined requirements would be virtually insurmountable. On the basis of judgments obtained from optical designers, as well as conclusions reached during the investigation, it is recommended that Vari-Focus lenses be eliminated from consideration for SMS optical system applications.

4. Optical Coatings

Anti-reflection coatings for refractive elements of the visible light sensor are essential if the lens is to function at maximum efficiency. The advantages of lens coatings are two fold. First, lens coatings eliminate ghost images and flare spots; secondly, they increase the illumination that the lens can transmit. In practice, multi-element lenses having an uncoated efficiency of about 65% have shown improvements in speed of nearly 1/2 f-stop after coating.

For the SMS application, the advantage of anti-reflection optical coatings would be clearly evident for low contrast imaging. Undesirable reflections caused by optical surfaces tend to lower the contrast of a scene, and since the expected contrast ratio of cloud types is small, every effort should be made to minimize contrast degradation. Anti-reflection, thin films, such as calcuim and magnesium floride, would provide excellent protection from intra lens reflections.

5. Vignetting

The design of the visible light sensor optical systems for both day and night coverage should consider the reduction in illumination resulting from lens vignetting. The relationship of the lens barrel length to the front and rear apertures causes oblique rays to be cut off, with the result that illumination decreases to the point of extinction, depending upon the angle of obliquity. In general this should not be a problem area in the SMS program, particularly if Vari-Focus lenses are eliminated from consideration.

Investigation of a typical Vari-Focus lens shows that an illumination fall-off due to vignetting, over a range of focal lengths, can exceed 50%. Such a reduction of illumination would seriously compromise sensor low light level capabilities. It should be noted that this reduction of illumination over the field of the lens is in addition to that resulting from the $\cos^4$ law which functions whether or not vignetting exists in a lens design so that when both effects are present image illumination is seriously reduced off the central format area.

6. Interior Lens Reflections

The second largest contribution of unwanted illumination can be attributed to the interior lens design. Non-image-forming light entering the lens aperature finds its way to the focal plane, where its effect on image contrast is readily apparent. The primary cause of this stray light reaching the image plane is lack of sufficient interception means within the lens housing. Interior lens reflections can be either totally eliminated or drastically reduced, depending upon the lens design, by proper placement of baffles and use of matte, nonreflecting housing surface treatments. A sketch of a typical catadioptric lens (Figure 3-4[illegible] illustrates the type of construction which should be employed to eliminate unwanted reflected and scattered interior light. For the SMS system, where lightweight construction is of paramount importance, the lens housing lightening voids must be made light-tight by such means as a matte/foil shroud.

7. Filters

Filtering of two types warrants consideration for the visible light sensor. The first is spectral filtering to reduce the contrast-degrading effects of scattering in the intervening atmosphere between the satellite and the scene viewed. Sensor tube photocathode response characteristics in the 0.3 to 0.4 micron region where atmospheric scattering is highest, would indicate the need for some filtering. A sensor employing an S-20 photocathode could usefully employ a filter because of its high response in the 3000 to 4000 angstrom band. Since the filter absorbs some image-forming light, an increase in exposure time would be required to compensate for this absorption. Applicable filters, such as Wratten numbers 12 and 15G should be considered.

The second type of filtering to be considered is non-spectral and involves the use of graduated neutral density filters for exposure control. The percent of highlight illumination transmitted through neutral filters can be adjusted by selecting appropriate values of optical density.

Standard neutral density filters are available to provide illumination attenuation covering a range of four orders of magnitude in descrete steps. When used in combination, as in a dual filter wheel system, intermediate values of transmission are obtainable.

Deposition of the neutral density filter on a thin base, such as Cronar, will introduce negligible focus shift when the filter is inserted into the optical path.

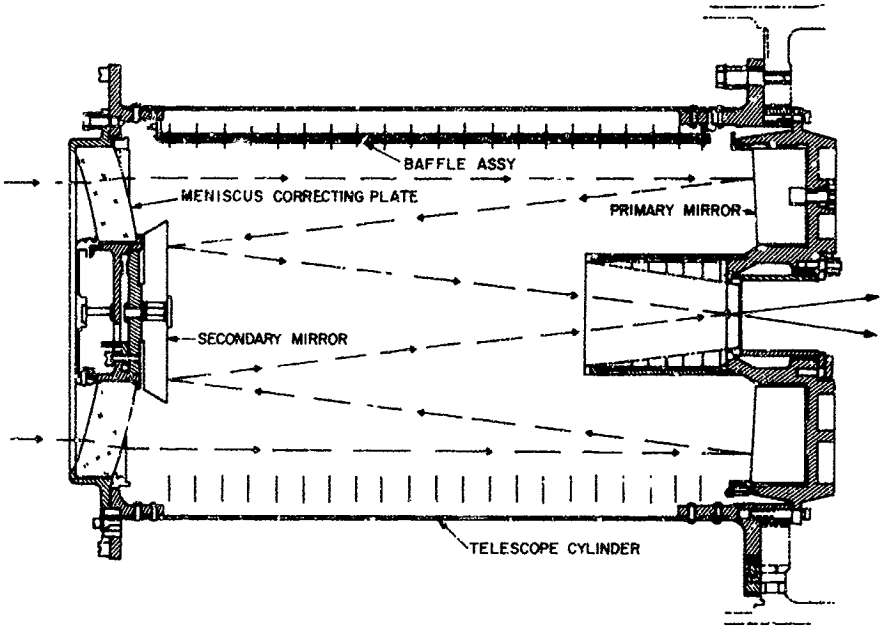

Figure 3-42. Typical Catadioptric Lens System

8. Image Motion Compensation

For synchronous satellites the problem of image motion compensation is greatly reduced by the elimination of forward vehicle motion. However, image motion will be caused by vehicle perturbations due to inaccuracies in the attitude control system. The penalty for image motion is loss of resolution, which manifests itself as ground smear.

Image compensation for different types of satellite stabilization systems presents different problems. In the case of a spin-stabilized satellite where the vehicle rate is 10 RPM, the total allowable exposure time would be 1/4000 second to reduce ground smear to a 5-mile equivalent resolution element, as shown by Figure 3-43. This exposure time can be accomplished by means of either rotary or curtain type focal plane shutters comparable in design to military reconnaissance shutters. Wieldable mirrors were investigated as a possible means of producing image motion compensation for the spin stabilized satellite. However, based on control system problems of accurately providing mirror de-spining rates, together with the complexities associated with precision servo control of the mirror such an approach appears to be marginal, if at all feasible.

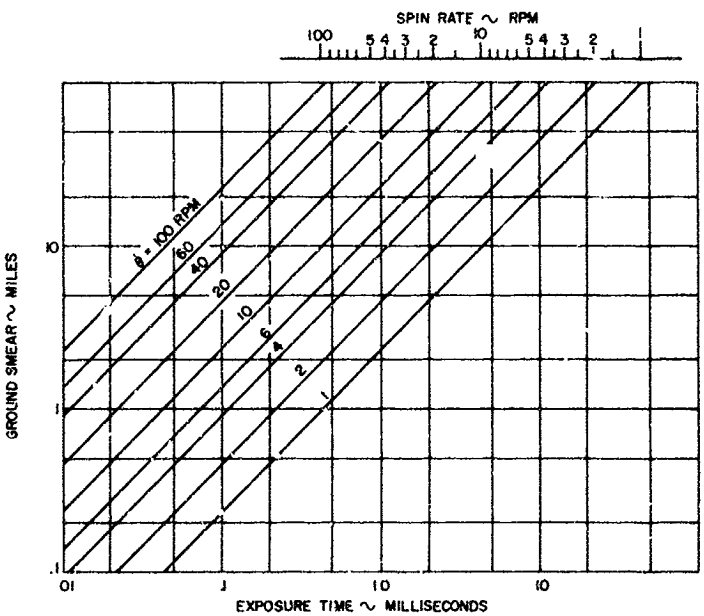

Figure 3-43. Exposure Time for Spin-Stabilized Vehicle

The 3-axis and gravity gradient attitude control systems provide stabilization which enables the visible light sensors to operate over an extremely wide range of exposure times. Figure 3-20 presents, in graphical form, the relation of exposure time to the visible light sensor to the allowable ground image smear, and to the angular stabilization rates required for a particular exposure and smear combination. From Figure 3-20 an exposure of 0.5 second for an allowable 1.0 mile ground image smear would require a SMS stabilization rate of about 5×10^{-3} degree per second. Similarly, for the same exposure but a 5.0 mile ground image smear, the stabilization requirements would be reduced to about 2.5×10^{-2} degree per second.

9. Wielding Mirror

The narrow coverage cloud sensor will require a wielding mirror to direct the sensor optical system to the desired area of surveillance.

The wielding mirror is essentially a precision optical flat, accurate to fractions of a wavelength, mounted in a gimbaling fixture which is accurately aligned to the optical system central axis. Mirror positioning is accomplished by a servo drive on the x and y axes of the gimbaling fixture. Direct ground command, preprogrammed positioning, or both, may be employed to direct the optical axis to a desired area of interest. Shaft angle transducers attached to each axis could be employed to provide pointing accuracy data.

If a programmed mode of operation were employed, the sequence of picture taking could be planned to eliminate mirror translation in one axis for an exposure sequence before indexing to a new position in the other axis. In this manner, wide variations in scene brightness would be avioded by remaining in an area of relatively uniform illumination, and disturbing torques could also be minimized.

Image rotation due to the 2-axis translating mirror will be present. This should not be detrimental, however, since the degree of rotation will be predictable, and image de-rotation can readily be accomplished at the ground receiver station.

10. Shutters

Protection of the visible light sensors from direct sunlight is mandatory. Image Orthicon tube imaging sections would be destroyed and Vidicons would be particlly disabled or destroyed by exposure to the Sun's image. To prevent such catastrophic sensor failure, a capping-type shutter would be required to occlude the Sun's image. During those periods when such accidental exposure is possible, as in the cases of the spin-stabilized vehicle sensor and the full Earth disc sensor of the larger vehicles, occultation could be provided by a dual-purpose, electromagnetic shutter of a design developed by Systems Associates Inc. of Haiesite N. Y. This design serves as a high speed, controlled exposure time as well as a capping shutter.

The present designs cover about a 1 in. aperture, and provide speeds up to 1/1500 second; they could be developed for speeds better than 1/2000 second, which is adequate for the Image Orthicon sensor. For a 1 in. Vidicon having a format of 0.62 in. in diameter, the same design shows promise of meeting the necessary 1/4000 second speed to also satisfy the spin-stabilized vehicle image motion requirement.

The System Associates shutter has been developed for special purpose aerial photography and is presently used in military mapping cameras. The shutter principle is applicable to either between-the-lens or focal-plane type devices. For the intended application, a high speed focal plane type appears to be preferable. The shutter consists of A and B sets of blades that are cocked and latched with one set open and the other closed. A small reset motor is energized only for the cocking function and then shut down. Electromagnetic latches hold the blade pairs and are released upon command. Delay time between the release of the blade sets establishes the shutter exposure time desired.

Similar shutter designs have been accomplished by Optomechanisms, Inc., Plainview, N. Y. and 1/4000 second speeds are promised for small format sizes.

Rotary focal plane shutters were considered for the controlled time exposure function and could provide slightly nigher speeds than the electromagnetic shutter. However, they are not as readily adaptable for capping functions and therefore are not considered as preferable for dual purpose operation.

For reliability the Sun protection shutter function would require a command pulse from a Sun sensor or similar device to initiate closure before the Sun is within dangerous proximity to the optical field of view.

11. Aperture Control

The wide dynamic range of illumination inherent in day and night cloud cover imaging necessitates the use of aperture control in addition to filter attenuation and shutter speed variation for proper adjustment of exposure. Aperture variation can be accomplished with either iris or Waterhouse type diaphragms. Present day aerial reconnaissance cameras employ both types of diaphragms, with more recent designs showing a preference for a two bladed, scissors type, Waterhouse diaphragm. Where reliability is important, as in the SMS system, this type has marked advantages over a mulitblade iris type by virtue of substantially fewer moving parts. In addition, the Waterhouse diaphragm can provide a backup capping function for Sun occultation.

Changes in aperature opening would be accomplished by a small servo system that sets the relative aperature to the required position. For additional reliability, the diaphragm should be designed so that the system would automatically return to the maximum aperture in the event of malfunction. This feature would enable continued system operation through variation of shutter speed or filter attenuation, to provide the same incident illumination of the tube photocathode over a substantial range of scene brightness levels. Figure 3-44 shows the relation of aperture to exposure time and the equivalent f/number for various exposure fractions. For example, if a predetermined time exposure were halved, and the scene brightness held constant an equivalent f/number could be selected to mainatin constant photocathode illumination. As an example, if a basic relative aperture of f/4.0 were used, and the exposure were reduced by one-half, the aperture would have to be increased to f/2.8 to provide the same exposure.

A further consideration in aperture control would be to permit ground override of the automatic exposure system based on scene conditions and the meteorological significance of the cloud image.

12. Materials and Weight

The problem of satellite weight limitations requires that the optical systems employ the lightest weight materials commensurate with resolution and structural considerations. Materials for optical systems are limited, and the weight ratios between materials may be as high as 5 to 1. Optical first surface mirrors can be produced from glass (quartz/pyrex), aluminum, or beryllium having densities of 0.10 lb/cu.in, 0.11 lb/cu.in. and 0.06 lb/cu.in., respectively. From this comparison it is apparent that beryllium affords the lowest weight potential. In addition, utilization of the mirror proper for structural tie-in would further improve weight savings which can be accomplished with nonglass materials.

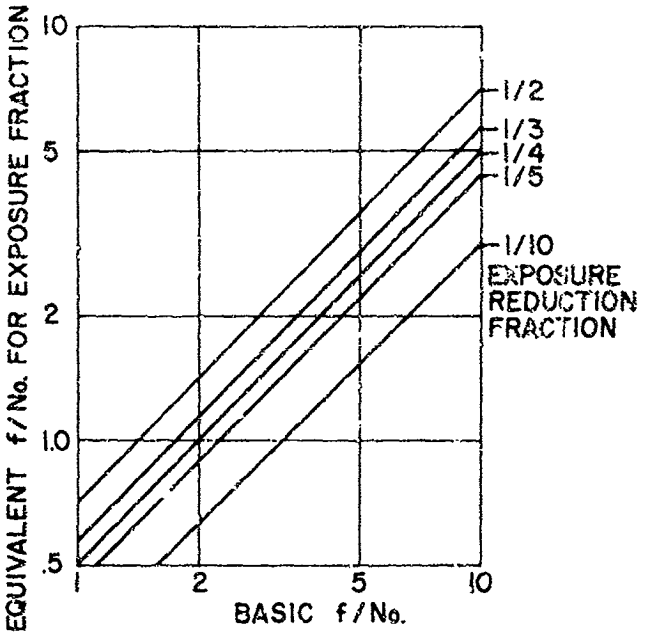

Figure 3-44. Exposure - Aperture Relationships

The reflective system structural design would necessitate careful consideration for maintenance of optical relationships while minimizing weight. Thermal considerations are of importance and are reflected in the lens housing design. For example, Perkin-Elmer of Norwalk, Conn., has produced space probe prototype optical systems employing all-Invar designs to maintain optical integrity. Conversely, Itek Corp. of Lexington, Mass., has built all-aluminum housings and mirrors that are designed to maintain focus with thermal expansion by compensating for variations in focal length. Weight ratios between such systems may be 3 or 4 to 1. Thermal gradients within the optical system have been minimized, according to Perkin-Elmer, by covering the lens housing with a black matte backed aluminum foil. It is not anticipated that automatic focus compensation of the SMS sensor optical systems would be required due to the comparatively small range of vehicle temperature variation expected (± 10° C about a nominal temperature of 25°C).

A survey of optical systems was made to determine, if possible, relationships between optical parameters and system weight. In conducting such a survey it is important to recognize that optical systems of the same relative aperture and focal

length can vary considerably, depending upon overall design. A catadioptric system employing a large corrector plate would weigh more than a purely reflective system; similarly, refractive lenses of comparable focal length and aperture would vary, depending upon the number of glass elements in the lens design.

With these potential variations in mind, a graphical presentation (Figure 3-45) was prepared to illustrate the relative weights of refractive and reflective optical systems as a function of aperture diameter. The refracting lens data is based on typical lenses designed for aerial reconnaissance by the Pacific Optical Division of Chicago Aerial Industries. It will be noted that, with the exception of one lens, a straight line can be drawn with a fair degree of confidence. The reflecting systems weight-to-aperture relations are based upon both actual and estimated data obtained from Perkin-Elmer, Itek, Electro-Mechanical Research, the Westinghouse Air Arm Division, and Republic Aviation Corporation.

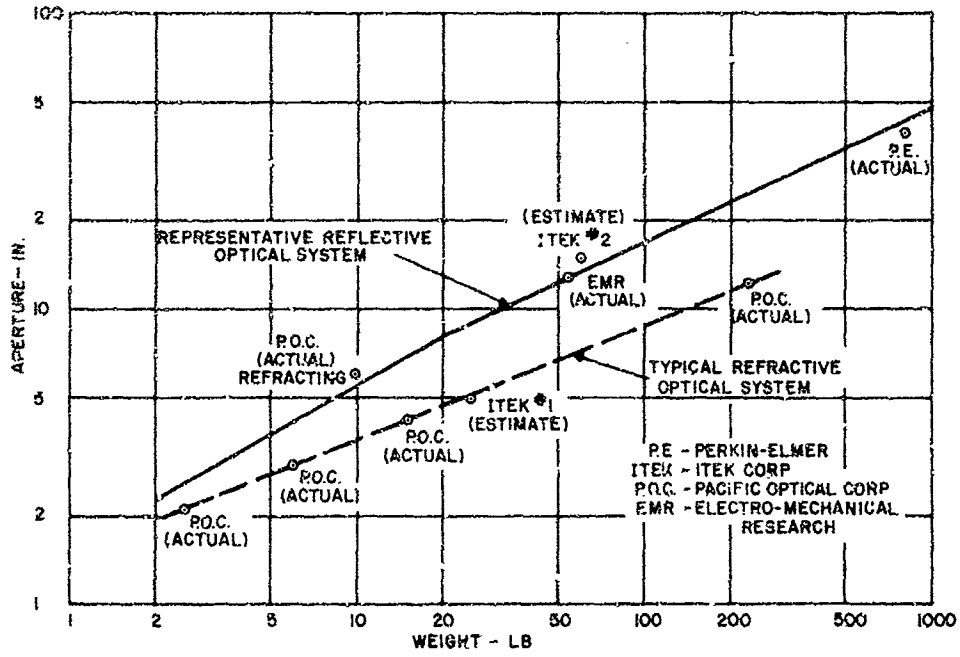

Figure 3-45. Optical System Weight Versus Aperture

E. SPECIAL TECHNIQUES FOR DAY-NIGHT EXPOSURE CONTROL

It has previously been shown that the range of illumination levels expected at the sensor photocathode varies at least eight decades for a day-night visual sensor. Successful use of any known sensor dictates frequent adjustment of the optical and camera control settings to obtain optimum performance. It is difficult to make these adjustments through the command link without potentially subjecting the sensor to a condition resulting in permanent damage. Therefore, it is essential to automate as many operational parameters as possible, while recognizing the penalties involved in additional weight, size, and complexity. It should also be realized that the net system reliability may be increased through this automation process. The following paragraphs describe techniques for adjusting the camera system to obtain an unattended TV system with optimum performance throughout the entire day-night environment.

1. Neutral Density Filters

Neutral density filters are commonly used to reduce light intensity in accurate steps. There is a precise relationship between density (D) and transmittance through the filter; thus, 10^{-D} = transmittance. Filters are available in a wide variety of density values from 0.1 through 4.0 from Eastman Kodak Co.; densities of 0.1 and 4.0 correspond to transmittances of 80% and 0.01%, respectively.

One practical method of incorporating neutral density filters is to insert two filter wheels arranged in cascade in the light path. By locating them at a nodal point in the optical system, their sizes can be reduced. One filter wheel contains four different density filters; the other wheel contains eight filters and is geared to rotate four times as fast as the first wheel. Thus, for each filter in the first wheel, the high speed wheel acts as a vernier with eight steps. Norden Ketay is utilizing such a system in an Image Orthicon camera chain presently under development, and expects to obtain approximately six orders of magnitude control of illumination.

There are several ways in which an error signal can be derived to operate the filter wheel drive motor. The video signal can be sampled, compared to a reference level, and the resulting error signal made to control the motor rotation for constant video amplitude. A separate photoconductive or photovoltaic cell could also be used to sense changes in illumination. These could be used in either an open-loop or closed-loop system. Similarly, a photomultiplier can be used. An additional method which has been successfully employed is to use the photocathode current to indicate average photocathode illumination.

In an existing camera chain, Bendix uses a three-sector filter wheel with interpolation between sectors accomplished with iris control for a total density variation of 6.3. This system is completely automated.

2. Automatic Iris Control

In this method of light control, error signals can be derived as described in the preceding paragraphs. By physically stopping a lens from f/2.0 to f/128, a 4000:1 reduction in photocathode illumination is achieved. It should be recognized that diffraction limitation effects exist as a lens aperture is reduced, and suitable precaution must be taken to insure that the lens does not become the limiting element in system resolution.

3. Photocathode Pulsing

This technique is based on the principles underlying the operation of the imaging section of an Image Orthicon. The photocathode emits photoelectrons instantaneously when light quanta are imaged upon it. These photoelectrons are electronically imaged upon a target that stores its accumulated charge in the interval between successive beam scans. The target integrates the photoelectrons from the photocathode. Photocathode pulsing is a technique for periodically interrupting this stream of photoelectrons to achieve target buildup control. It is implemented by pulsing the accelerating voltage between the photocathode and the target. By varying the duty cycle or the repetition rate (or a combination of both) of the pulsed accelerator voltage, a range in excess of 1000:1 in effective light intensity can be achieved.

The photocathode pulsing method of electronic shuttering is not achieved without observing precautions. The waveshape of the pulsed voltage must be accurately controlled to achieve short rise and fall times while the top of the waveshape (corresponding to the "on" time of the photoelectron stream) must not only be extremely flat but also reach the same absolute potential if defocusing is to be avoided. The photocathode is continuously being exposed, so care must be taken to prevent it from overheating. Additionally, since the photocathode is transparent, light will fall upon the target. The target consists of materials with high secondary emission characteristics, and correspondingly low work functions, resulting in some photoelectric properties. Although the target is not in the optical focal plane, some light will reach it. Suitable precautions must be taken to prevent deleterious effects on picture quality.

4. Target Feedback Control

If the foregoing methods are employed to maintain illumination at approximately 10^{-4} to 10^{-3} foot-candle, excellent quality pictures can be obtained. As the illumination on the photocathode is decreased, the scanning beam current required to discharge the target is decreased approximately in direct proportion. If, under these conditions, a bright object appears in the field of view, the beam will be insufficient to discharge the highlights. This will result in image "blooming" and can in some instances result in complete deterioration of the picture.

To alleviate this possibility, a technique has been utilized, by Dr. W. Livingston of Kitt Peak National Observatory. It consists of sampling the video signal, amplifying it, and feeding it back to the target mesh. The video variations are coupled to the target by means of the target-mesh capacitance. In effect, the beam sees a constant potential field. During the scan, each picture element receives approximately the same quantity of charge from the beam. The video signal becomes the voltage variations on the target mesh.

This method results mainly in improvement of dynamic range by extending the capability for discharging the target at levels of illumination above that for which the beam current is set.

5. Target Voltage Switching

This is a technique for extending the dynamic range of illumination over which an Image Orthicon operates. It can extend the range of illumination from approximately 60:1 to 600:1 within one exposure.

In operation, the target mesh potential is increased to a positive value (10 to 20 volts) and the target scanned by the reading beam with the lens capped. This establishes the scanned side of the target at cathode potential. The beam is then cut off and the lens uncapped. With the termination of the desired exposure, the lens is again capped. The target is now charged in correspondence to the scene illumination. This may extend from 0, to 10 or 20 volts. The tube is limited in its ability to faithfully reproduce this dynamic range because the target is unable to modulate the return beam fully, and also because the low level illumination signals are masked by beam noise.

If the target potential is reduced to 1/3 the initial voltage, some areas of the target will be below cathode potential. In these areas, the scanning beam is repelled and no modulation occurs. However, in other areas modulation does occur and video signals are generated. These correspond to high scene illumination areas where the target has been charged close to the full initial target voltage. When these areas are scanned, electrons from the beam are accepted, discharging these highlights. The target potential is next switched to about 2/3 the initial target voltage in the interval between frame scans. Now, areas of the target that previously were at less than cathode potential are raised in voltage and are capable of modulating the beam. After completion of this frame, the target is sequenced to the original voltage and again scanned out.

The above description was written for three-step target switching. Excellent results have also been obtained in a two-level system. It should be recognized that the normal frame interval is increased by the number of steps used. A target with excellent storage capabilities is required. General Electric has reported that the magnesium oxide target is capable of storing a 500 line picture for 5 minutes in an uncooled tube with no visible degradation in resolution.

6. Video AGC and Beam Control

The technique described here was developed by the Admiral Corporation and incorporated in an underwater low light level Image Orthicon camera for the United States Navy.

In an optimally designed camera system, the low light level performance is limited essentially by the scanning beam noise of the Image Orthicon tube. The signal to noise ratio of the Image Orthicon output signal is approximately proportional to the square root of the highlight illumination in the scene. This can be seen from the following argument. Optimum beam current adjustment occurs when there is just sufficient current to discharge the scene highlights. Thus the beam current (and therefore the signal current) is approximately proportional to the illumination. The noise, however, is proportional to the square root of the beam current. Hence, the signal to noise ratio is proportional to the square root of the illumination.

The basic design of automatic video gain and scanning beam current control for the Image Orthicon is based on satisfying two inverse transfer functions. These are best exemplified by the fact that, in operation under high highlight illumination, the scanning beam current is at a maximum while the video gain is at a minimum. The converse is true when operating near the sensitivity threshold of the Image Orthicon tube. Fortunately, these inverse functions are reasonably linear over the operating range of the tube. A sensing method is used to detect the peak whites or highlights in the picture and generate the error signal for control purposes.

Video gain is varied by adjusting the amount of negative feedback applied to three different amplifier stages. Negative feedback is adjusted by a potentiometer connected in series between the emitter and ground, the emitter side being bypassed down to frame frequency. The three potentiometers are driven by a common shaft connected to the drive motor.

The scanning beam current is adjusted by varying the control grid potential of the scanning gun. This is accomplished by a potentiometer on the same shaft as the video gain potentiometers. Three other controls are associated with the beam control to adjust its range and starting level, and to provide proper tracking with the video gain controls. These controls are adjusted to match the characteristics of the individual Image Orthicon.

The video signal is fed to a detector which produces a DC signal proportional to the peak white level. A comparator circuit compares the detected signal with a reference potential and generates an error signal in a chopper circuit. The amplitude of the chopper output is proportional to the magnitude of the error, and its phase corresponds to the polarity of error. The chopper output is amplified and used to drive a control motor on whose shaft are the three video gain controls and the beam potentiometer. The motor turns in the proper direction to maintain a constant video output level.

The system has been operated with the Westinghouse WX 4323, General Electric GL-7538, RCA C-74034 and 5820 Image Orthicons. A dynamic range of light control of four orders of magnitude is claimed. Response time of the loop is 1.5 seconds for full excursion of the shaft.

7. Bandwidth Rolloff

The low light level Image Orthicon exhibits fall-off in resolution as the illumination at the photocathode is reduced. Typical tubes can resolve about 700 lines at 10^{-4} foot-candle and 100 lines at about 3×10^{-7} foot-candle. As the light level reduces, resolution and signal fall to the point where beam noise establishes the tube threshold.

Improvement of signal to noise ratio can be achieved if the reduced available resolution of the Orthicon is used. By reducing video bandwidth until it is just adequate for the available resolution, high frequency beam noise is reduced, resulting in a better signal to noise ratio and ultimately in an improved displayed picture.

From the discussion in the previous paragraphs, video gain was seen to increase with decreasing light level. It is now seen that bandwidth must decrease with decreasing light level. Both conditions can be satisfied almost simultaneously if bandwidth rolloff is made a function of video gain. This can be accomplished by using emitter degeneration. Care must be taken in this sytem to preserve adequate bandwidth for the available resolution; otherwise, unnecessary degradation will be introduced.

Bandwidth rolloff has been used by the Admiral Corporation with what is reported to be a significant improvement in system signal to noise performance and picture quality.

F. SYSTEM ANALYSIS

This subsection discusses the major factors considered in determining the parameters of a visible sensor system for observing clouds from synchronous altitude. Many considerations are involved, and the interrelationships between them are presented in parametric form by the use of tables, nomographs, and graphs. The range of parametric variation should fulfill the requirements of presently available configurations as well as any that may become practicable in the foreseeable future.

1. Design Considerations

a. Resolution Degradation Off the Nadir

An imaging system in which the Earth is focused on a plane sensor can be regarded as having the flat-faced sensor projected upon the curved Earth. Equally spaced scan lines on the sensor project on the Earth as unequally spaced lines; the spacing increasing as the distance from the nadir increases. Figure 3-46 shows the increase in resolution element size as a function of the angle subtended at the center of the Earth. It can be seen that at 50° off the nadir, the resolution element is twice as large as at the nadir; at about 75°, it increases by a factor of 10.

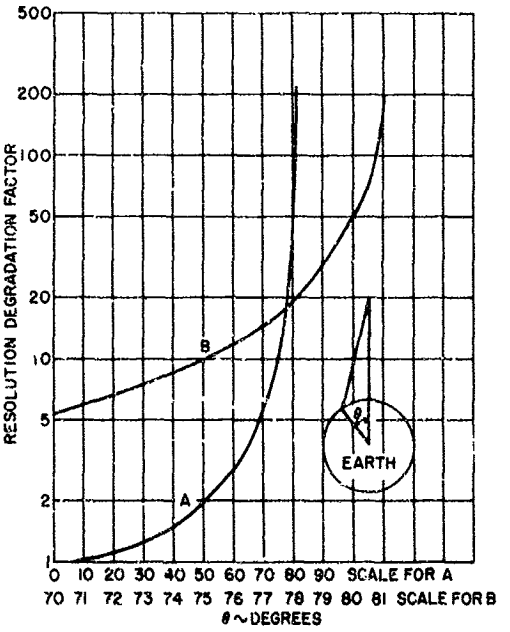

Figure 3-46. Resolution Degradation Versus Angle Off Nadir Normalized to Nadir

b. Exposure Time

The allowable exposure time of the sensor is limited by the requirement of image immobilization during exposure. In the case of a spin-stabilized vehicle, exposure time is a function of the spin rate. For a 3-axis stabilized vehicle, the ability of the attitude control system to reduce vehicle motion determines the exposure time. Figure 3-43 shows the exposure time required for a spinning synchronous satellite to reduce ground smear to specified values. It is seen that for a spin rate of 10 rpm and an allowable ground smear of 1 mile, an exposure time no greater than 0.043 millisecond must be used. Figure 3-20 is a similar plot for a 3-axis stabilized vehicle, which enables the control system rates to be specified. For example, if it is desired to have a 10 second exposure time and a 1 mile ground smear, the vehicle angular rates must be less than 2.5×10^{-4} degree per second.

c. Illumination Variation

Section 2 contains a detailed examination of the illumination levels expected at the sensor sensitive surface. From the vantage point of the synchronous satellite, extremely wide variations of illumination are encountered. Daytime viewing conditions result in approximately 5×10^3 foot-candles at the sensor from the tops of cumulonimbus clouds (albedo = 0.7) at 46,000 feet altitude. During nighttime viewing, the sensor illumination can be lower than 10^{-6} foot-candle. While this range of illumination is greater than nine orders of magnitude, it can be accommodated by techniques described in Section 3, subsection E, provided it does not occur in a single exposure.

No sensor yet devised has the ability to accommodate this range of illumination in one scene. Typical sensors (Vidicons, Image Orthicons, etc.) have a maximum dynamic range of between 35 and 100 to 1. (Certain special types, such as the SEC Vidicon and Image Isocon, may range as high as 200 or 250 to 1.) Because a synchronous satellite is essentially stationary over a point on the equator, its field of view covers nearly half the Earth's surface. When it is noon at the satellite subpoint, the entire disc of the Earth is illuminated by direct sunlight. Even under this condition, which occurs for a short period of time every 24 hours, the range of illumination at the sensor corresponds to sunrise at the west edge of the disc, sunset at the east edge of the disc and high noon at the satellite meridian. In general, some portion of the Earth's disc will be in sunlight for greater than 90% of the time, and the terminator (line of demarcation between day and night on the Earth) will be within the field of view.

Since the range of illumination levels is likely to be greater than the dynamic range capability of the sensor, the only practical method of obtaining complete Earth cloud cover is to use a mosaic of pictures with the illumination range in any one picture restricted to about two orders of magnitude. If a single picture of the full disc of the Earth is desired, the best obtainable would be one in which only the sunlit portion of the Earth is correctly exposed.

d. Sensor Selection

Section 3, subsection C presents the results of an extensive survey of existing and planned visual sensors. Although many devices are described, the choice narrows to two (Vidicon and Image Orthicon) which are sufficiently advanced to accommodate the SMS. The Vidicon can, within the limits of

present technology, be used for daytime viewing. The Image Orthicon is suitable for both day and night viewing, but not without penalties in size, weight, power, complexity, and reliability. Another device, intermediate between the Vidicon and Image Orthicon with respect to resolution, sensitivity, and complexity, is the SEC Vidicon. It may fill in the gap between the other two in the next few years.

A fourth device, the Image Isocon, promises a substantial improvement in signal to noise ratio and dynamic range performance over the Image Orthicon, at the cost of increased operating complexity. If further development is carried out over the next few years, and this tube becomes fully operational, it may well supplant the Image Orthicon in such applications as the SMS program.

Finally, while no tube available today approaches the low light level capability of the Intensifier Image Orthicon, its drastic fall-off in resolution at higher light levels, together with its large size and high voltage, renders this sensor unacceptable for the cloud cover system. Image Orthicons with even average sensitivity provide adequate resolution, with 1 second exposure periods, under near starlight scene illumination conditions.

In the paragraphs that follow, an attempt is made not only to select a sensor but also to predict its performance. In any such attempt, it is most desirable to be armed with experimental data closely related to the intended application. It is expected that in an SMS system the method of using the sensor will be different enough from conventional TV that judicious use of existing data will be mandatory. This is not to say that existing data is of no use; rather, it should be treated as a foundation upon which extensions can be built. Strong emphasis must also be placed on the techniques by which existing data were obtained, to assess with confidence its applicability to situations for which the original measurements were not intended.

There are many differences between conventional TV systems and those for use in the SMS. The most important are that conventional TV uses a multiple scan, high frame rate presentation and displays the information on a monitor. Continuous imaging upon the sensor is used, as is simultaneous readout. In the SMS application, a single scan will be used, the scan rate will be drastically reduced, and sequential exposure and readout is contemplated. In conventional multiple frame systems, integration of signal and noise takes place in both the monitor phosphor and the observer's eye, resulting in adequate visual pictures obtained with electrical signal to noise ratios of the order of 0.1. Comparable performance in a single frame exposure requires a signal to noise ratio of about 20, or 200 times greater. Some compensation is provided however, since slow scan operation results in higher signal to noise ratios than conventional scan rates. In addition, other benefits accrue from low frame rates. Longer photocathode exposure times are available, permitting image integration to occur and thus build up a given charge pattern with lower light levels. Because readout beam velocity is lower, the beam current required to discharge a given target charge is reduced. This results in a potentially increased resolution because of reduced beam cross section and refined electron beam optics, as well as less beam noise (since beam noise is directly related to beam current). By using a slow scan, the video bandwidth is reduced, and techniques such as Target Feedback control can be applied that are extremely difficult to use under standard rates (Section 3, subsection E.4). Reduced video bandwidth, of itself, permits higher signal to noise ratios by filtering the noise spectrum, and also allowing higher input impedances to develop larger signals.

While the above describes the trends taken by various effects, the quantitative results of their combined effect has not been measured, and there is no substitute for experimental verification. Experiments in slow scan operation of Image Orthicons have been made at several astronomical observatories, but caution must be used in applying the results. Here, point sources of light (stars) are being viewed. The signal to noise ratio required for threshold detection of point sources is lower than for extended sources (such as clouds). The sensors used were cooled to temperatures not anticipated in the SMS. The camera systems were not designed for automatic, unattended operation. Finally, many results were obtained by a combination of target integration and photographic film integration.

From the above discussion and judicial use of existing data, it is postulated that sensor performance be estimated as follows. Resolution versus illumination for conventional TV systems is used to determine resolution for a specific photocathode illumination. For a slow scan system with 10 second frame time and simultaneous exposure and scan, the illumination required by the SMS sensor is reduced by a factor of ten, and the resolution increased by 50%. A further modification of illumination can be made if scene contrast is less than 100%. The illumination increase required for a particular scene contrast is obtained from Figure 3-16, which is based on the performance of an ideal imaging device. These modifying factors are judged to be obtainable, and are probably on the conservative side.

Considering the Vidicon and the Image Orthicon as potential sensors, the choice between them is not a difficult one to make, if the mission objectives and constraints are defined. For night viewing, only the Image Orthicon can be used. Figure 3-27 is a plot of limiting resolution versus photocathode illumination for typical Image Orthicons operated in a conventional manner. From this figure, a selection can be made on the basis of resolution and light level. Other factors, of course, are involved. The spectral characteristics of the photocathode should match those of the scene to be viewed. For night viewing, it is desirable to have a high efficiency photocathode with infrared response, such as the S-20. Also, if high sensitivity is to be achieved by target integration, it is necessary to use thin film metal oxide targets.

The Vidicon signal to dark current ratios for several tubes are plotted in Figure 3-22. The limiting source of noise in well designed Vidicon camera systems is in the video amplifier. However, there is another source of noise in the tube itself, the dark current, which can exceed the video amplifier noise current in some tubes. If slow scan is used, or long exposure times are contemplated, a tube should be selected that exhibits good storage and low dark current. It should be recognized that dark current of itself is not a noise contribution, but rather noise stems from the variations of dark current. Dark current is indicative of these variations and is therefore used as a measure of noise for the purposes of Figure 3-22.

Another factor of prime importance to the meteorologist is the gray scale rendition in a picture. Figure 3-47 is a plot of the signal to noise ratio required to resolve a given number of gray steps, each step related to the next by a factor of 1.414. Present thin film Image Orthicons can reproduce eight or nine gray steps. Vidicons are capable of about nine or ten gray steps. Estimates for improved tubes run as high as thirteen or fourteen steps.

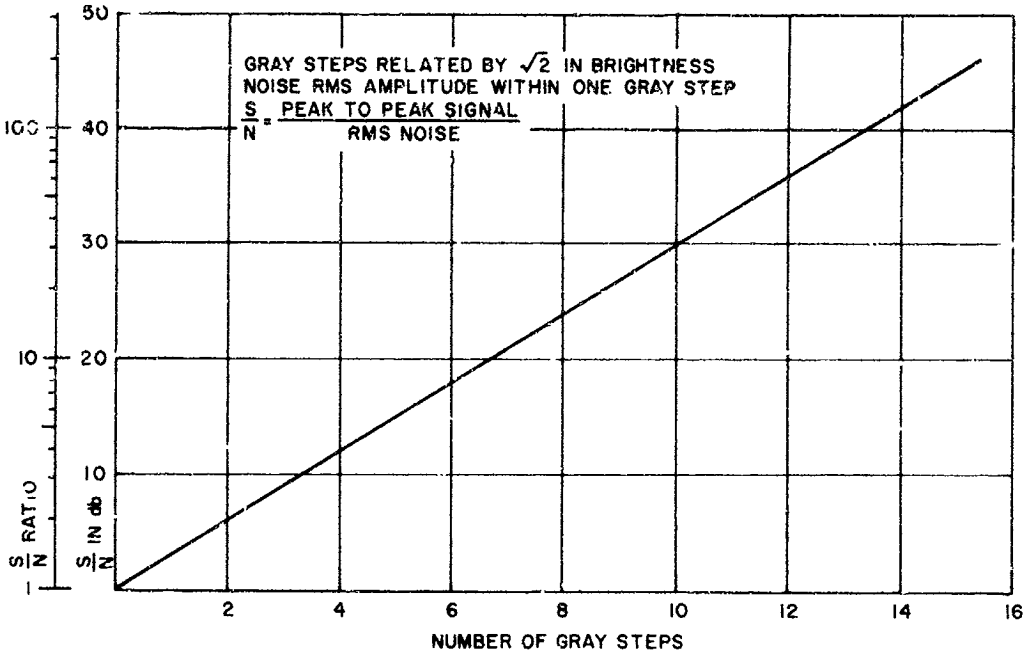

Figure 3-47. Gray Scale Versus Signal to Noise Ratio

e. Optical-Sensor-Illumination Interrelationships

Figure 3-48 is a combined presentation of the relationships between scene illumination, scene reflectivity, lens efficiency, photocathode illumination, and typical sensor resolution. Perhaps the best method of describing its utility is to illustrate its use in a typical example. Consider that for a specific condition it is determined that the illumination on the scene is expected to be 1 millifoot-candle (corresponding roughly to quarter Moon conditions), and that at least 500 lines resolution is desired. Inspection of the sensor characteristics shows that if the photocathode illumination is 5×10^{-5} foot-candle, the following Image Orthicons can be used: WL-22724, GL-7967, and C-74034. The intersection of 5×10^{-5} photocathode foot-candle, and 10^{-3} scene foot-candle occurs at a multiplier constant of 0.005. This multiplier constant is achieved for an f/4.5 lens and scene reflectivity of 0.4, or an f/5.3 lens and scene reflectivity of 0.6, which is typical of stratos and nimbus type clouds. The tube data plotted has been modified by increasing resolution by 50%.

f. Earth Coverage and Resolution

Figure 3-41 is a nomograph that relates sensor resolution, sensor size, ground resolution at the nadir, Earth coverage, and lens focal length. It is designed to be used with the central scale (ground coverage) as a pivot point for a straightedge. Typical examples will be used to describe its use. Suppose that a 1 in. Vidicon is to be used to cover the full Earth disc in one picture. A straightedge placed between 0.44 in. picture height and 8000 miles ground coverage shows

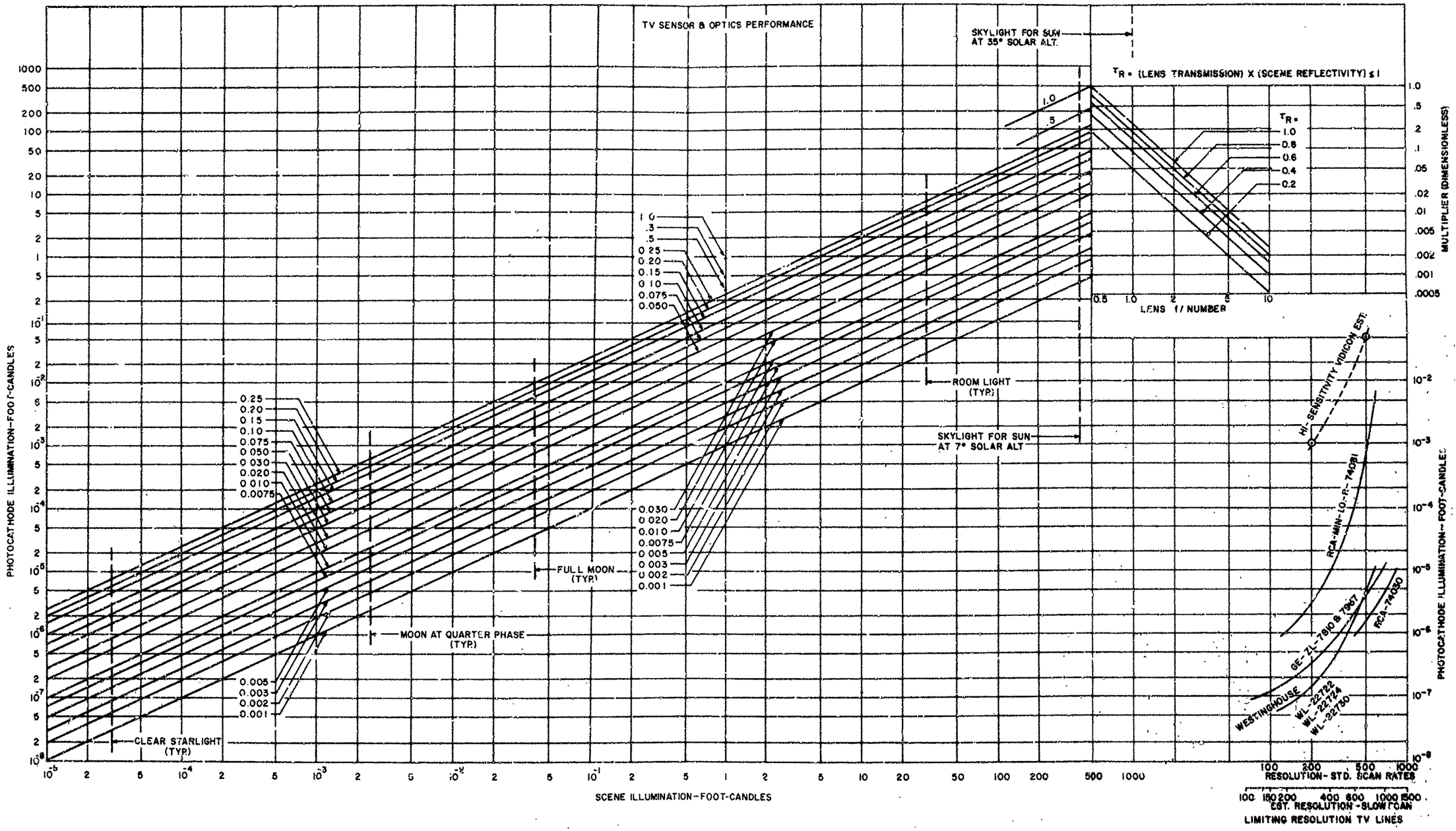

Figure 3-48. Combined Relationship of Sensor-Illumination-Optical Factors

that a 1.2 in. focal length lens is required. Pivoting the straightedge about 8000 miles indicates that 10 mile ground resolution can be achieved with 800 TV lines resolution per picture height. Another example that can be worked out on this nomograph is that 3000 line resolution is required to achieve 1 mile ground resolution with a coverage of 3000 miles. If a 3 in. Image Orthicon were available for this, it would require the use of a 9 in. focal length lens.

g. Optical System Weight

Subsection 3.D is concerned with the optical considerations involved in the SMS. Figure 3-45 of that section depicts the weight of an optical system as a function of the aperture diameter. The aperture can be obtained by using the relationship:

$$D = \frac{\text{focal length}}{\text{f/number}}$$

The weight of the optical system can now be approximated with the aid of Figure 3-45.

h. Readout Time and Transmission Rate

After a determination of ground resolution and coverage has been made, the trade-off of readout time and transmission rate can be obtained by using Figure 3-49. This figure is a nomograph that has been designed with the center scale as a pivot point. A straightedge placed between known values of ground resolution and ground coverage will intersect the center scale. Pivoting the straightedge about this point enables one to determine the transmission rate (in picture elements per second) corresponding to a given readout time. In an analog communication system, the baseband frequency bandwidth required is approximately half the transmission rate, since one frequency cycle corresponds to two picture elements. For example, the disc of the Earth can be covered with 1 mile nadir resolution in a system transmitting 6.4×10^6 picture elements per second and using a readout time of 10 seconds. Figure 3-41 can be used to determine that accomplishing this in one frame requires a sensor resolution of 8000 lines per picture height, assuming a square raster.

If a mosaic of pictures is to be used for large area coverage, several additional considerations are involved. If the maximum capability of the sensor is most efficiently used, a square raster is required. To cover an area that lies in a square inscribed within the disc of the Earth, suitable overlap of individual pictures must be allowed to ensure complete coverage. The percentage of overlap will vary with the system and is influenced by vehicle stability and pointing accuracy of the sensor system. If coverage of the disc of the Earth with resolution greater than that allowed by one picture is required, a mosaic can be used. Here, also, overlap should be considered.

There is another factor in this situation. One might be tempted to increase ground resolution by covering the Earth with two pictures. However, nothing is gained in this situation, since the size of each frame is identical to that in the one-frame case. The same situation applies for three-picture coverage of the Earth. With four pictures, it is possible to increase ground resolution by a

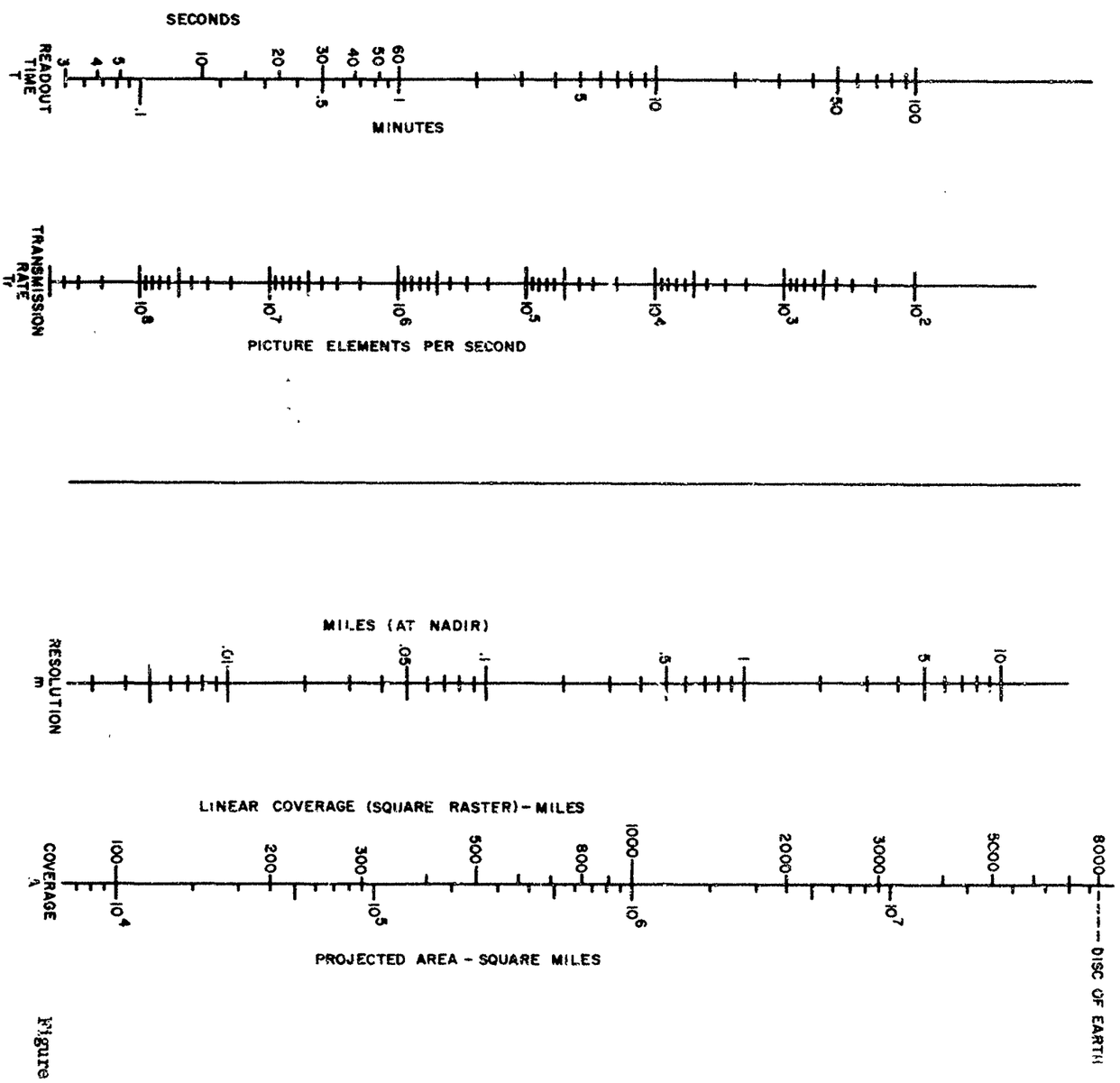

Figure 3-49. Data Transmission Factors

factor of two (linear dimension). But again, five-picture coverage is no better than four-picture coverage. It can be seen that improvement is achieved only when the number of frames is a perfect numerical square, i.e., 1, 4, 16, 25, 36, etc. When this series reaches 49 pictures, another factor arises. With 49 frames, four will be in the corners of the Earth disc circumscribed square and can be eliminated since they contain no useful information. Therefore, the above series continues as: 45, 60, 77. All intermediate numbers offer no improvement over the next lowest allowable ones from the series.

i. Size, Power, and Weight

It is well recognized that size, power, and weight are of prime importance in satellite systems. It is likewise axiomatic that increased performance is accompanied by increased penalties in these parameters. Trade-offs are necessitated in the face of conflicting requirements of maximum performance and reliability on the one hand, and minimum complexity, size, weight, and power on the other. While consideration was given to these parameters during the course of the SMS study program, there was insufficient time and available data to fully explore them. Another complication is the current unavailability of an Image Orthicon camera system for satellite use. Presently available Image Orthicon camera systems would require modifications to be compatible with long term unattended operation. It is possible to add remote control through telemetry to existing Image Orthicon systems, but this would not result in an optimum package. On the other hand, Vidicon camera systems are used in Tiros, and are in an advanced state of development for Nimbus. It is quite likely that even these cameras can be miniaturized, perhaps using thin film techniques and integrated modules.

There are several sizes and types of Vidicons and Image Orthicons, and while specific size, weight, and power are difficult to ascertain with a fair degree of accuracy, it is possible to assess their positions on a relative scale. In the Vidicon category, the 1/2 in. type (as used in Tiros) is most compact and least complex. The 1 in. and 1-1/2 in. tubes rank next. A considerable savings in power, weight, and size can be achieved in the electrostatic versions of these tubes. Even in the electrostatic types, there are further subclasses of electrostatic focus, magnetic deflection and the all-electrostatic version.

Image Orthicons are available in 2 in., 3 in., and 4-1/2 in. diameters, with both electrostatic and magnetic versions in some classes. The potentially most compact Image Orthicon camera is one built around the GE 2 in. electrostatic tube. Both Hazeltine and GE are building camera systems using this tube. The next most compact, low power camera would use the RCA 2 in. magnetic Image Orthicon. A camera system using this tube is under development by Raytronics. The Hazeltine and Raytronics cameras are intended for use in Nimbus, and will therefore contain control circuits for unattended operation. GE's camera is a general purpose engineering model. Company plans are to modify the camera for unattended operation by late 1964. The 3 in. and 4-1/2 in. Image Orthicons are available only in the full magnetic type, are larger and need more power. However, their performance exceeds that of the smaller tubes.

Table 3-3 contains data on cameras which are either operational or under development. All figures exclude the optical systems except where noted.

TABLE 3-3
SUMMARY CHARACTERISTICS OF TYPICAL CAMERA SYSTEMS

Manufacturer	Camera Tube Type	Camera Tube Number	Total Weight (lb)	Average Power Watts	Volume cu. in.
General Electric	2 in. E.S. I.O.	ZL-7804 (GE)	14	25	367
Hazeltine	2 in. E.S. I.O.	ZL-7804 (GE)	15	30	320
Raytronics	2 in. Mag. I.O.	C-74081 (RCA)	18	36	450
RCA (Tiros)	1/2 in. Mag. Vid.	C-73496 (RCA)	9.7 (Includes Lens)	9	184
RCA (Nimbus-APTS)	1 in. Mag. Vid.	-	20.6	19	482
RCA (Ranger)	1 in. Mag. Vid.	-	14 (Includes Lens)	19	300

2. Typical Examples

This subsection applies the considerations described above to implement typical camera systems. Two examples are presented which are believed to be typical of expected performance, although no formal optimization or error analysis is executed. The performance guide lines within which each system is constrained are as follows:

(1) Minimum Capability Vehicle

- Full Earth disc coverage
- Spin-stabilized vehicle, 10 RPM spin rate
- Minimum size, weight, power

(2) Medium Capability Vehicle

- Full Earth disc coverage, low resolution
- Selected area, high resolution pictures, 25 frames maximum
- Cycle time, once every 30 minutes
- Vehicle stabilization 0.003 degree per second, 3-axis stabilized
- Moderate size, weight, power

a. Minimum Capability Vehicle

The requirements of minimum size, weight, and power dictate the use of a Vidicon camera system. Although ground resolution is not specified, a reasonable figure of not less than one scan line per 10 miles at the nadir will be assumed. D. S. Johnson, in an article in the Journal of the SMPTE, January 1960, used a photograph of a simulated satellite picture which shows that many major cloud features are retained at this resolution. For a permissible smear of 1/2 TV line (5 miles) at the 10 RPM spin rate, Figure 3-43 indicates an exposure time of 0.2 millisecond.

Having selected a Vidicon suitable for slow scan operation and an exposure time, we can predict the illumination levels over which the system will operate. A typical high sensitivity Vidicon (Machlett 7351A) produces 500 line resolution at 5×10^{-2} foot-candle on the photocathode. Another high sensitivity Vidicon (Westinghouse WX-5915) is capable of 200 lines at 10^{-3} foot-candle. With increased accelerating potentials and magnetic fields, the resolution increases by about 60%, corresponding to 800 lines and 300 lines, respectively. These figures are for normal scan rates. Following the procedure outlined in subsection F.1.d the illumination required is reduced by 10, and resolution is increased by 50% when a 10 second slow scan system is used. Thus 1200 lines should be obtained at 5×10^{-3} foot-candle, and 450 lines at 1×10^{-4} foot-candle for slow scan operation with continuous imaging. For shuttered operation, the target is assumed to be an excellent integrator, and the product foot-candle-seconds remains constant. With a 10 second readout time, the photocathode illumination for 0.2 millisecond exposure is 250 foot-candles for 1200 lines resolution, and 5 foot-candles for 450 lines resolution. These illuminations correspond to highlight levels, and

because of the dynamic range of the tube, det ils will be observed at much lower scene illumination. With the aid of Figure 3-41, it can be determined that 1200 lines, using a 1 in. Vidicon, will require a 1.25 in. focal length lens to cover the disc of the Earth with less than 7 miles nadir resolution. From Figure 3-48 assuming an f/1.5 lens and 60% scene reflectivity, it can be determined that the scene illumination is about 3750 foot-candles for 250 foot-candles on the photocathode, and 75 foot-candles for 5 foot-candles on the photocathode. These values correspond to 1200 and 450 line resolution, respectively. The maximum illumination incident upon the photocathode during daylight hours is about 1000 foot-candles. To operate the Vidicon at its optimum illumination level (about 250 foot-candles), light control over a range of 4:1 is required. However, if no light control is employed, the maximum illumination will be equivalent to two f-stops above the knee of the transfer characteristic. This is tolerable because the knee is not well defined and also because typical commercial operation is one f-stop above the knee.

The optical exposure is achieved with either a curtain type focal plane shutter or a rotary focal plane shutter. By using a slow scan Vidicon, long frame readout times can be employed with a concomitant reduction in video bandwidth and transmitter power. Figure 3-49 shows that a transmission rate of 140,000 picture elements per second corresponds to a 10 second readout. The resulting video bandwidth is about 70 KC. Because of the slow readout time, it may be necessary to use a digital sweep generator to obtain good linearity. The shutter exposure initiation time can be obtained from a horizon sensor, which indicates when the Earth comes into the field of view.

b. Medium Capability Vehicle

This system requires both full Earth coverage (assumed low resolution) in one frame, and multiple-frame pictures at high resolution. With a 3-axis stabilized vehicle whose stabilization rate is 0.063 degree per second, Figure 3-20 shows that an exposure time of 1 second will produce a 1 mile ground smear. A 2 in. Image Orthicon presently capable of 625 line resolution (square raster) should resolve about 1000 lines at slow scan rates. From Figure 3-41 it can be determined that a 14 in. lens permits 1280 mile coverage at 1.3 mile nadir resolution. Maximum ground smear is about 3/4 of a resolution element. At standard scan rates, the RCA 2 in. Image Orthicon C-74081 produces 200 lines resolution at 3×10^{-6} foot-candle and 625 lines at 10^{-2} foot-candle on the photocathode. Under slow scan operation, at a 10 second frame time, the tube should be capable of 1,000 lines at 10^{-3} foot-candle and 320 lines at 3×10^{-7} foot-candle, assuming continuous imaging and readout. For 1 second exposure and 10 second readout, the illumination requirements become 10^{-2} foot-candle for 1,000 lines, and 3×10^{-6} foot-candle for 320 lines. Using Figure 3-48, assuming an f/4 lens and 60% scene reflectivity, it can be determined that 1,000 lines resolution occurs at 1 foot-candle on the scene and 320 lines resolution occurs at 3×10^{-4} foot-candle. This latter illumination corresponds to that obtained on the Earth under conditions between clear starlight and quarter Moon. These values are for highlight illumination, so that details within the scene at lower light levels will be seen at reduced resolution, although the tube's dynamic range decreases with reduced illumination. To achieve optimum performance under high illumination levels, it is necessary to attenuate the illumination so that the photocathode level is maintained at 10^{-2} foot-candle. Table 2-14 shows

that 8080 foot-candles would be incident upon the sensor photocathode for a high altitude (40,000 ft), high reflectivity (0.7) cloud, when the Sun is over the nadir. The calculations were made using an f/0.5 lens. Assuming that the worst conditions resulted in 10,000 foot-candles with an f/0.5 lens, the photocathode illumination with an f/4 lens would be approximately 160 foot-candles. The range of light control required is then 1.6×10^4:1. This is well within the range obtainable with neutral density filter wheels. (See subsection 3.E.) For illumination levels below the control range, the optical system is operating at maximum efficiency, and tube parameters should be adjusted to accomodate varying illuminations. The methods of paragraphs 3.E.6 and 3.E.7 can be used to obtain maximum performance within the restrictions of limited light levels.

With the aid of Figure 3-49, it can be determined that a readout time of 10 seconds requires a transmission rate of 100,000 picture elements per second. A frame time of 10 seconds is judged to be a good compromise between transmission rate (and therefore transmitter power), circuit complexity, number of pictures in a sequence, and conservative design with reasonable expansion capability.

To obtain full Earth disc coverage in one picture, a Vidicon system can be used that is identical to the one described for the minimum capability vehicle. Although a longer exposure time can be used (because of 3-axis stabilization instead of spin stabilization), it is difficult to take advantage of this to increase sensitivity. This is because correct exposure occurs for the picture highlights, and for more than 90% of the time some portion of the Earth disc is in sunlight. If the sensitivity were increased to permit observation at full Moon conditions, it could be used for less than 10% of the total observation time. Greater utility could be made of this capability if occulting of the sunlit portion of the Earth is used, but it is Republic's opinion that the additional equipment complexity is not justified by a corresponding increase in performance.

In operation, the wide angle Vidicon camera system will present a coarse (7 mile), overall view of the cloud cover. The high resolution system gives usable pictures at close to starlight illumination. At least 25 such pictures can be transmitted in a 30 minute period. Assuming an overlap of 10% in the linear direction of each picture, high resolution (1.3 miles at the nadir and at daylight) pictures are obtained for that area of the Earth within its inscribed square. More overlap would, of course, reduce the area coverage. A fixed program of sequenced pictures can be used with ground override capability through the telemetry link. This feature is useful when continued observation of a specific area is of interest.

During the 10 second frame time interval, the lenses of both camera systems are capped. The wielding mirror can be repositioned during this time. There is adequate time allotted to the light control systems to stabilize and thus ensure 25 optimum pictures within a 30 minute interval.

Reference to Figure 3-45 shows that the high resolution lens system (14 in. focal length, f/4 lens) will weigh between 5 and 10 lb.

G. BIBLIOGRAPHY

Coltman, J.W., "Scintillation Limitations to Resolving Power," Journal of the Optical Society, March, 1954

Hall, J.H., "Ultimate Performance of Sensitive Image Amplifiers," Westinghouse Report, ET 95-1262-19

Johnson, D.S., Journal SMPTE, Jan. 1960

Morton, G.A., and Ruedy, J.E., Advances in Electronics, Vol. XII, 1960

Rose, A., "Television Pickup Tubes and the Problem of Vision," Advances in Electronics, Vol. I, 1948

Shelton, and Stewart, "Pickup Tube Performance With Slow Scanning Rates," Journal SMPTE, July, 1958

Weimer, P.K., "Television Camera Tubes: A Research Review," Advances in Electronics and Electron Physics, Vol. XIII, 1960

Advances in Electronics and Electron Physics, Vol. XII, 1960

Advances in Electronics and Electron Physics, Vol. XVI, 1962

SECTION 4 - HEAT BUDGET MEASUREMENT

A. GENERAL

To gain knowledge of the heat budget of the Earth, measurements are desired relating the quantity of energy entering and leaving the Earth as viewed from the SMS.

The quantity of energy entering can be precisely determined as a function of time of day, time of year, position of the Moon, and phase of the Moon. The quantity of energy leaving can be measured to a fairly accurate degree within defined spectral regions.

The energy leaves the Earth through two fundamental methods: reflection and emission. The difference between the energy falling on the Earth and that lost by reflection, heats the various portions of the Earth (land, sea, and clouds). These portions then reradiate (emit) the energy. The energy reradiated by each portion can be trapped by one of the other portions (i.e., land and sea to clouds) but eventually it will be reradiated (Figure 4-1).

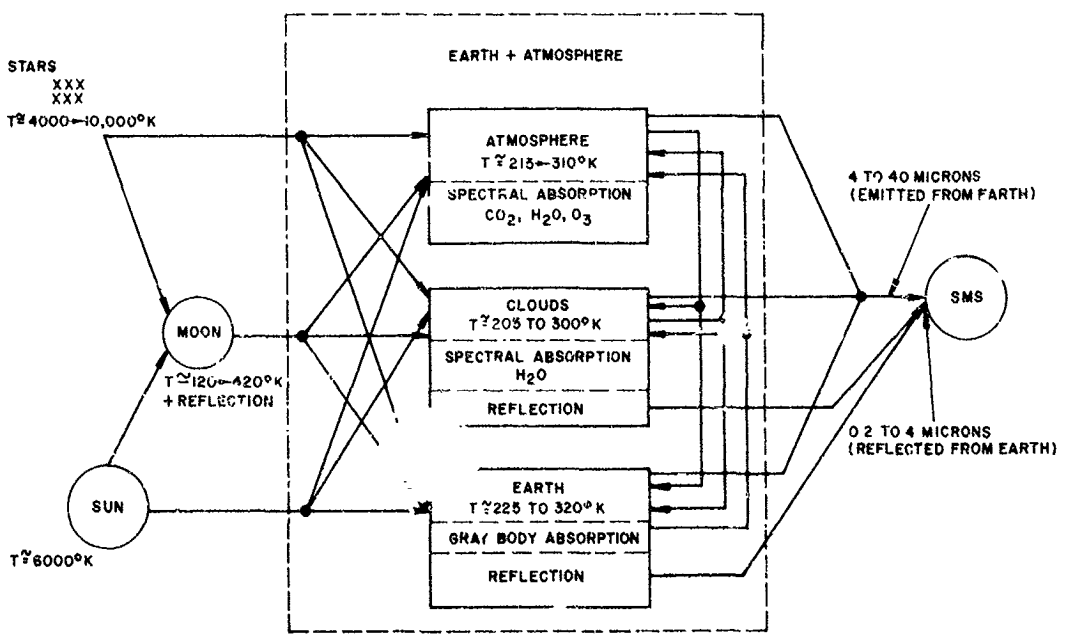

Figure 4-1. Energy Interchange Diagram

It has been found that the major portion of energy lost by reflection occurs at short wavelengths while the major portion of that lost by emission occurs at longer wavelengths. It is desirable to utilize some of the natural atmospheric phenomena to separate the two methods of energy loss. In the original choice for the Nimbus spectrum coverage, five bands were recorded. These bands are as follows:

(1) 6.5 to 7.0 μ (water vapor absorption)

(2) 10 to 11 μ (atmospheric window for Earth radiation)

(3) 0.55 to 0.75 μ (visible reference and daytime cloud cover)

(4) 7 to 30 μ (thermal radiation)

(5) 0.2 to 4 μ (reflected solar radiation)

The Nimbus resolution element size was 30 miles at the nadir with a coverage of approximately 1500 miles across the frame. The instantaneous field of view of the scanner was 50 milliradians with scanning in only one direction being required, since the satellite's orbit provided the second scan dimension.

For the Tiros, in addition to the same type of five-channel radiometer used in the Nimbus, a two-channel wide field radiometer was incorporated. This radiometer had an instantaneous field of view of 50° and therefore had a ground resolution of 370 miles. The spin of the vehicle provided the means of scan when the tilt of the vehicle with respect to the nadir was considered. The two-channel radiometer provided data in accordance with Suomi's Explorer VII experiment, wherein the heat balance data obtained was for total radiation and infrared radiation.

B. REQUIREMENTS

The Earth's heat budget requirements, as defined by the NASA work statement and subsequent redirection, are to be limited to the measurement of the quantity of energy leaving the Earth. To accomplish this objective, the spectral bandwidth was defined to encompass a maximum range of from 0.2 to 40 microns. The resolution of the heat budget measurements in terms of area coverage and temperature has been defined as from 100 to 300 miles, 1°C or better for a high resolution system, and a single data point full Earth coverage for a minimal capability system.

A sensor survey was conducted to provide information on infrared sensing devices. Since thermal imaging tubes and quantum detectors are limited in the spectral bandwidth coverage as defined above, their inclusion as part of the survey is primarily for completeness of possible sensors.

C. SENSOR SURVEY

1. General

The instrumentation for the measurements of the Earth's heat budget requires the employment of radiation detectors that are sensitive over the spectral

region extending from 0.2 to 40 microns. The current state of the art offers a wide selection of detector types and characteristics, few of which meet this wide requirement. A trade-off in method of measurement (wherein the spectral region is divided and therefore a detector need only operate over a smaller spectral increment) greatly increases the types of detectors which can be used. Not all of the apparently suitable detectors are usable for long-term measurements from a vehicle in a space environment. Some of the factors which immediately rule out many detectors and relegate others to a state of extreme doubt are responsivity, time constant, noise level, operating temperature, and reliability.

Infrared detectors may be classified into two principal groups:

(1) Point detectors, in which the sensitive surface integrates the total incident radiant energy and provides a single electrical output signal

(2) Area detectors, in which the two-dimensional distribution of radiant energy incident on the sensitive surface produces a corresponding variation in a parameter of the surface. Information at every point in the field of view is provided by an appropriate electrical signal readout.

Point detectors in general require an external method of varying the specific area under investigation. These methods usually consist of varying the axial angle of the optical system or shifting the detector over the focal plane. The materials used as the sensitive surfaces for area detectors are the same types that are used for point detectors, except that they are deposited over a large extent of surface, or arranged in an extended mosaic of small elements. The most promising approach to area detectors is an imaging tube, sensitive to infrared radiation. In this type of tube, the sensitive surface is deposited on the face plate, which is also the infrared window, and is scanned by an electron beam to provide the electrical signal readout. These "thermal imaging tubes" and their characteristics are indicated in Section 5 of this volume.

From a functional point of view, there are two important classes of infrared detectors for each of the above groups.

(1) Thermal detectors, in which the energy of the incident photons is converted to lattice vibration in the sensitive material. This effect causes a local increase in temperature, producing a measurable change of properties in the material.

(2) Quantum detectors, in which absorption of the impinging photons produces a change in state of the electron distribution within the sensitive material.

The principal advantages of the thermal detectors are their broad range of spectral response, and their ability to operate at higher temperatures than the quantum noise temperature. Quantum detectors, by contrast, have extremely limited spectral operating ranges and, in general, must be cooled to cryogenic temperatures for realization of their optimal detection efficiency. The principal disadvantage of the thermal detectors is their inherently slower speed of response to radiation signals, as compared with the quantum detectors. The best thermal

detectors have response time capabilities only as short as 0.5 to 1.0 millisecond, where the quantum detectors exhibit performance with time constants as low as 0.1 microsecond. The quantum detectors exhibit superior detection capabilities in the infrared spectral region; however, this superior detection capability only exists over limited wavelengths. The limits of operation of each quantum detector are dependent upon the material from which it is constructed.

2. Thermal Detectors

A thermal detector is one which measures incident radiation through a change in some physical property caused by an increase in the temperature of the sensitive material. Thermal detectors have been widely used in the fields of laboratory spectroscopy and radiometry, and a number of different types have been developed for various applications. The more commonly used detectors include:

- Thermocouples
- Thermopiles
- Golay pneumatic detectors
- Metal bolometers
- Thermistor bolometers

The thermocouple and thermopile indicate the presence of radiant power by generation of a voltage at the junction of two dissimilar metals. The thermopile consists of a series arrangement of a number of thermocouples resulting in a greater detection sensitivity, but longer response time.

The Golay pneumatic detector employs, as its sensing element, a volume of xenon gas which expands when heated by radiation incident on an absorbing film. The increased gas pressure causes flexure of a small membrane on which is evaporated an antimony mirror. The resulting optical deflection produces modulation of a light beam, which is sensed by a photocell and converted to an electrical output signal.

Both the metal bolometer and the thermistor bolometer respond to incident radiation by a change in their electrical resistance. By placing the bolometer in a balanced bridge circuit and applying a suitable DC bias voltage, the resistance change is converted to an electrical output signal which may be used to indicate the intensity of the incident radiant power. Metal bolometers are commonly fabricated of platinum, gold, and nickel in the form of thin films or wires. Higher response units have been developed by various sophisticated techniques such as electroplating, vacuum deposition, and sputtering of thin films. Thermistor bolometers are composed of sintered oxides of manganese, cobalt, and nickel formed into flakes about 10 microns thick. These flakes are mounted on substrates of glass, quartz, or other suitable heat sinks to obtain fast response. Thermistor bolometers are readily available in either of two material formulations known as Type 1 and Type 2, the principal difference being the range of electrical resistance. Although the ultimate limit of detection of the thermistor and metal bolometers is identical, the thermistor has wider

application because of its faster response and its superior responsivity (due to higher temperature coefficient of resistance), which may be as much as 1000 times greater than for a metal bolometer.

A special type of metal bolometer is based on the phenomenon of superconductivity. Certain materials such as lead, tin, tantalum, niobium nitride, and niobium stannide exhibit a sharp change in resistivity at temperatures near absolute zero. Each of these materials has a critical temperature below which its electrical resistance falls to essentially zero, and the material is said to be superconducting. By maintaining the material at the critical temperature, an extremely sensitive response to incident radiant power can be obtained as the heating effect causes variation of resistance in the transition region. Unfortunately, the transition takes place within only a few tenths or hundredths of a degree, posing the difficult problem of extremely precise control of the temperature. Although the superconducting bolometer is superior in performance to the metal and thermistor bolometers (because of reduced thermal noise and heat capacity due to the low temperature) the problems of low temperatur operation and precise control prevent its being a practical device at the present time.

Of the thermal detectors described, all but the thermistor bolometer must be eliminated as practical devices for the SMS mission after consideration of significant performance characteristics such as response time, responsivity, and structural reliability. The thermistor has consistently been selected as the most efficient thermal detector for airborne and spaceborne infrared detection devices, particularly in systems requiring moderately fast data gathering capability.

The considerations that define the specific performance requirements and selection of a suitable thermistor bolometer detector are discussed elsewhere in this section.

3. Quantum Detectors

This class of detectors encompasses a number of different materials which exhibit changes in their electron distribution in response to incident photons, or quanta. Ideally, quantum detectors measure the rate at which quanta are absorbed; their response at any wavelength being proportional to the rate at which the incident photons arrive at the surface. Because the number of photons per second per unit of radiant power is proportional to wavelength, the response of a quantum detector should increase with wavelength. However, various factors such as spectral dependence of absorptivity and quantum efficiency contribute to limit the effective utilization of energy to relatively narrow regions of the infrared spectrum.

The following four different types of quantum responses are currently recognized in photon detector materials.

a. Photoemissive Effect

The photoemissive effect is produced by the emission of free electrons from the surface of the material in response to incident photons. This phenomenon is well known, and detectors of this type have been in common use

for many years. For the SMS heat budget measurements, photoemissive detectors have virtually no application because their response is limited to an extremely narrow region of the infrared spectrum.

b. Photoconductive Effect

The photoconductive effect comes about through the production of added carriers by the incident photons. The energy levels are not sufficient to free electrons from the surface of the material, but they become available for additional conduction within the material. The result is an effective decrease in electrical conductivity during exposure to incident photons. Materials exhibiting this effect compose the great majority of infrared quantum detectors.

c. Photovoltaic Effect

The photovoltaic effect is produced by the generation of free electron-hole pairs in the detector material at a point where a potential barrier exists. The diffusion of the free carriers is influenced by the electric field, resulting in the production of an output voltage. Materials demonstrating this effect have been investigated, but few have shown applicability to infrared detection. The only materials of this type in wide current use are indium antimonide (InSb), indium arsenide (InAs), and gallium arsenide (GaAs).

d. Photoelectromagnetic Effect

The photoelectromagnetic effect depends on the production of free charges in the presence of a magnetic field. The diffusion of these carriers is influenced by the magnetic field, and an output voltage is generated which is indicative of the incident photon rate. The only useful infrared detecting materials of this type are indium antimonide (InSb) and indium arsenide (InAs).

A considerable amount of development of photoconductive detectors has been accomplished and is still in progress. Continued efforts are being made to improve the sensitivity and extend the spectral response of these detectors. At present, due to their restricted spectral response characteristics, most of the photoconductors find their widest application in the intermediate infrared region to approximately 9 or 10 microns. A few detectors have shown capabilities at wavelengths up to 20 microns, and work is currently being performed on materials which extend as high as 40 microns. A tabulation of the more significant quantum detectors and their characteristics, some of which have security classification, is presented in Volume 7 of this report, which is classified.

The utility of quantum detectors is affected not only by their spectral response characteristics, but also by the requirement that many must be operated at cryogenic temperatures, particularly those that exhibit good sensitivity at the longer wavelengths. The earlier photoconductors, such as lead sulphide (PbS) and lead selenide (PbSe) can be operated at room ambient temperature, but their spectral capabilities are limited to 2.5 microns and 4.2 microns, respectively. Indium antimonide can also be operated at room temperature up to 7 microns, but its sensitivity is inferior to the others by almost two orders of magnitude. The spectral cutoffs of PbS and PbSe can be extended to 3.0 microns and 5.4 microns,

respectively, with an order of magnitude increase in sensitivity, by cooling them to an operating temperature of 195°K. This is within the capability of available thermoelectric cooling devices, and the resulting sensitivities compare favorably with those of the more exotic detectors. The difficulty, of course, is that the spectral coverage is still inadequate for long wavelength heat budget measurements. Under the same temperature condition, InSb response is reduced to 6 microns, and even with the accompanying sensitivity increase it is still an order of magnitude below the lead salts.

By cooling to 77°K, further significant improvement in sensitivity is obtained for PbS, PbSe, and InSb, but the gains in spectral bandwidth are modest. At this point, the impurity type photoconductors become important. For example, 77°K, gold-doped germanium (Ge:Au) will provide good sensitivity up to 7.1 microns.

To extend the spectral bandwidth beyond 7 microns, detector materials must be cooled below 77°K by using gaseous or liquid helium cryogenerators. At 50°K, zinc-antimony-doped germanium (Ge:Zn, Sb) performs up to 15 microns; zinc-antimony-doped germanium-silicon alloy (Ge-Si:Zn, Sb) performs up to 13 microns, and gold-doped germanium-silicon alloy (Ge-Si:Au) performs up to 10 microns. Below 25°K, cadmium-doped germanium (Ge:Cd) is useful to 21 microns; and below 20°K, copper-doped germanium (Ge:Cu) performs to 27 microns. The material yielding the best far-infrared response is zinc-doped germanium (Ge:Zn) which extends to 39 microns, but requires an operating temperature of 4.2°K.

Although some of the more recent quantum detector developments appear to be approaching the performance that is required for long wavelength heat budget measurements, there are fundamental considerations that make their application to the SMS vehicle problematical at the present time. Two of the most outstanding of these problems follow:

(1) A practical cryogenic cooling system to operate in a space environment for extended periods of time has not yet been developed.

(2) Long wavelength quantum detectors are still being investigated and are not readily available as practical, reliable components.

Although these considerations appear to present formidable obstacles to the immediate use of quantum detectors, there is a considerable level of effort being expended towards further development and improvement of detectors and coolers. It is not unrealistic to anticipate that practical operational components might be available for use in the near future.

D. SYSTEM CONSIDERATIONS

1. Optical

To obtain data for any heat budget measurement, it is desirable to include all wavelengths from 0.2 to 40 microns. If refractive optics are used for optical gain, only several materials can be used for the optics. The materials which can be used include cesium bromide, cesium iodide, and diamond. The

refractive index of these materials is also essentially constant over the desired spectral range. Unfortunately, the cesium compounds are extremely soluble in water and are hygroscopic. Diamond has yet to be manufactured in the size required for lenses. Another possibility for refractive optics is to divide up the spectrum into the two regions (0.2 to 4 and 4 to 40 microns) and use separate optimum refractive optics for each region. Implementation of data calibration becomes difficult, and should a scanning system be employed, the data correlation problem is made even more difficult.

A second method of obtaining optical gain is to use reflective optics. If front surface reflection is used, all wavelengths are reflected in the same manner and the system is essentially independent of wavelength of the impinging radiation. In this instance, only one optical system is required for scanning or nonscanning systems. Some form of spectral division and filtering will be required to separate the desired information into spectral regions due to the detector limitations indicated in subsection C. A pure polished germanium flat located 45° to the focal axis could readily perform this function. Its reflection characteristics would cause all wavelengths less than 4 microns to be totally reflected. Wavelengths longer than 4 microns will be transmitted 50% or more, depending on the characteristics of the anti-reflection coating used. Additional filters of different materials can be employed to further define the spectral irradiance impinging on the detector. The weight of optics used to obtain heat budget data would be comparable to that described for a cloud cover sensor which utilizes reflective optics, wherein the diameter of the optics is the weight determining factor. A weight saving can be realized by utilizing an "egg-crate" or "honeycomb" structure for supporting the mirror surface, and by employing lightweight structural members.

2. Temperature

When detectors require cooling to temperatures below ambient, a means of removing heat from the detectors must be incorporated in the system. Several methods can accomplish this to varying degrees. Among the methods which are applicable to a vehicle in space are:

- Sublimation cooling systems
- Space heat-sink cooling systems
- Open cycle cryogenic systems
- Closed cycle cryogenic systems
- Thermoelectric cooling systems
- Joule-Thompson effect

The last four of the above methods are considered standard methods for infrared systems and further explanation of the techniques involved can be found in Volume 5, Section 4 on infrared cooling. The first two methods are described here:

a. Sublimation Cooling

Sublimation cooling systems use the vacuum property of the space in which the vehicle is expected to operate. As defined by the following equation:

$$G = \left(\frac{5.8p}{100}\right)\left(\sqrt{\frac{M}{T}}\right) \quad \frac{\text{gram}}{\text{sec cm}^2}$$

where G = rate of vaporization per unit surface area

p = vapor pressure at temperature T in Torr (mm of Hg)

T = temperature in degrees Kelvin

M = molecular weight of the material

The amount of heat removed from the bulk material is equal to the sum of the heat of fusion and the heat of vaporization (solid to liquid + liquid to gas). A typical example using hydrogen (13 calories per gram and 108 calories per gram heat of fusion and vaporization) indicates a system weight of approximately 65 lb for a cooling system operating at 13° Kelvin for one year when the heat load is in the order of 100 milliwatts.

b. Radiative Cooling

Space can be used for a heat sink. Unfortunately the cryogenic temperatures which must be obtained indicate that a large radiator must be used. The area of the radiator can be determined from the equation

$$A = \frac{1.92 \times 10^3 W}{\epsilon T^4}$$

where A = the area in square feet

W = the heat load in watts

ϵ = the emissivity of the radiator surface

T = the temperature of the radiator in degrees Kelvin

when it is assumed that no heat is impinging on the radiator (radiator is not pointing toward the Sun).

In actuality, the radiator heat sink (space) is not absolute zero but some small temperature above, due to all contributing sources. If it is assumed that this temperature is 4°K, then for all absolute radiator temperatures above 12.6°K the radiator area will be affected less than 1%. For a 1 watt heat load at a temperature of 30°K, the area required would be 265 sq. ft when the emissivity of the radiator is 0.9ϵ.

3. Sensor Protection

When thermally sensitive devices are used to determine temperature, they are restricted in their regions of normal operation. A sensor which uses the Sun as its signal source will not be able to "see" the Earth, and inversely, a sensor which used the Earth as its signal source should not be permitted to look at the Sun.

Sensor protection from direct Sun or specularly reflected sunlight from cirrus clouds will be required. It is suggested that a solenoid operated shutter be inserted in the light path to prevent all radiation from falling on the detector when the energy in a defined field of view exceeds a specified value. Two items which should independently cause the shutter to operate to the close position are the sensor being off, and an excessive signal.

The Sun can impinge 100,000 times the normal expected energy on the detector. Considering the maximum orientation rate of change of the vehicle, the shutter must operate within 1 millisecond when the instantaneous field of view is 4.5 milliradians (100 mile resolution element). With an assumed Sun temperature of 6000° K, the maximum shutter time can be calculated from the formula

$$t = 1.17 \times 10^{-14} \alpha [(1 + k)\, T]^4 \beta'$$

where t = the shutter operation time in seconds

T = the detected temperature at which a shutter operation signal is initiated

k = the maximum allowable normalized increase over T

α = the instanteous field of view in milliradians for a square detector

β' = the transmission factor for the Sun path

$(1+k)T$ = the maximum temperature that the detector can view without being damaged

For larger fields of view (above 5 milliradians) the limited angular coverage from the Sun (round Sun effect) tends to increase the actual value of t. For a round detector, t will also tend to increase.

E. SYSTEM ANALYSIS

For the SMS, the radiometer can assume several configurations.

The first configuration to be considered would be a nonscanning radiometer looking at the entire Earth. The basic philosophy of the sensor would be in accordance with Suomi's experiment, wherein the radiation is impinged on separate black and white painted thermistors each located at the apex of a cone. As in Suomi's experiment, the black painted thermistor is sensitive to all radiation wavelengths and the white only to the infrared. To maximize the differential

response, the conical angle subtended by the detector's field of view should be equal to or less than the conical angle subtended by the Earth as viewed from the satellite. Since this angle is approximately 17.2° (0.3 radians), the total capture angle is 0.0715 steradians. The gain introduced by a cone is now a function of the detector area and the areas of both ends of the cone, provided that the ends of the cone are greatly different in area. The temperature of the walls of the cone influences the data and therefore must be taken into account. A simple chopping wheel in front of the large end of the cone causes the cone to become a black body chamber when the end is closed by the chopper. If the temperatures of the chopper and cone walls are known, the signal can be calibrated. If spectral filtering is desired, the signal should be chopped prior to and after filtering (at different rates) to provide accuracy of measurement. A temperature sensitivity of better than 0.02° can be obtained with a system of this type.

A second configuration utilizing the same basic philosophy as the first could be considered for a high resolution Earth scanning system. The scanning mirrors would be external to the detection system. Constant diameter tubes could be used instead of cones, to restrict the field of view of the black and white thermistors. The length of a tube would determine the instantaneous field of view for any finite diameter tube. With a thermistor detector of approximately 1/2 in. diameter at the window surface, the length of the tubes becomes fairly large for any reasonable ground resolution (i.e., approximately 37 inches for a ground resolution of 300 miles). The emissivity and temperature gradient along the tube will have an effect, causing a reduction in sensitivity. It is therefore considered impractical to use the Suomi philosophy for a high resolution system (high resolution is defined for this case as any instantaneous field of view below 2°).

A third configuration utilizes reflective type collection optics for gain. In a nonscanning system for the whole Earth heat budget, the diameter and focal length of these optics are extremely short. The short optics produce problems in physical implementation of the theoretical parameters. As such, it is felt that the Suomi type system yields more practical performance values.

A fourth configuration would also utilize optics for gain. These optics would have a scanning capability. The instantaneous field of view would be restricted to a small portion of the total field of view. The optical system would be all-reflective so that all wavelengths could be received. The total energy content from the instantaneous area received by the optics would be divided by a pure polished germanium flat (beam splitter). The reflected beam from the flat contains the majority of the reflected solar data which is impinged on one detector, while the transmitted beam through the flat (which contains the infrared emitted data) is impinged on a second detector.

Choppers (reticles) permit the use of high gain AC amplifiers. When known references are used to establish the gain of the amplifier, absolute temperature can be determined very accurately.

Based on the present requirement for heat budget measurement, it is felt that only the fourth type of configuration, which utilizes a scanning optical system, has the required capability. This type of configuration also has the greatest potential in terms of resolution (spatial) improvement.

The optical scanning heat budget system was further analyzed. The signal output from the system is in analog form and is related to the absolute temperature of the average target in the field of view. The signal is converted to digital form prior to transmission.

For the analyzed system, it was found desirable to "overscan" the the Earth so that the uncertainty in the local vertical would not cause any loss of data. A total scan angle of 20° was therefore assumed.

For this configuration, it is assumed that a thermistor bolometer is used to detect the infrared energy passing through the germanium flat, and a photomultiplier or second thermistor detector is used to detect the energy reflected from the germanium flat.

The equation which affects the selection of infrared equipment parameters follows

$$NET = \frac{49.3\sqrt{A_{tot}}\ h C \sqrt{f}\ \ell^2 f\ell}{T^3\ \epsilon\beta A D^2 \sqrt{t}}$$

for an equipment in a synchronous orbit which must view the full Earth the $\sqrt{A_{tot}}$ h can be assumed to be 175 x 10^6 then

$$NET = \frac{8.63 \times 10^9\ C\sqrt{f}\ \ell^2 f\ell}{T^3\ \epsilon\beta A D^2 \sqrt{t}}$$

where
- NET = noise equivalent temperature in degrees C
- $f\ell$ = focal length
- ℓ = optical efficiency
- f = amplifier bandpass in CPS
- C = reticle chopping factor
- ϵ = emissivity of target
- β = atmospheric transmission over the spectral region
- T = target temperature in degrees K
- A = target area in square miles
- D = diameter of optics in inches
- t = total time to scan the full raster

The above equation has been set up in the nomograph in Figure 4-2. A typical system can be selected parametrically as follows:

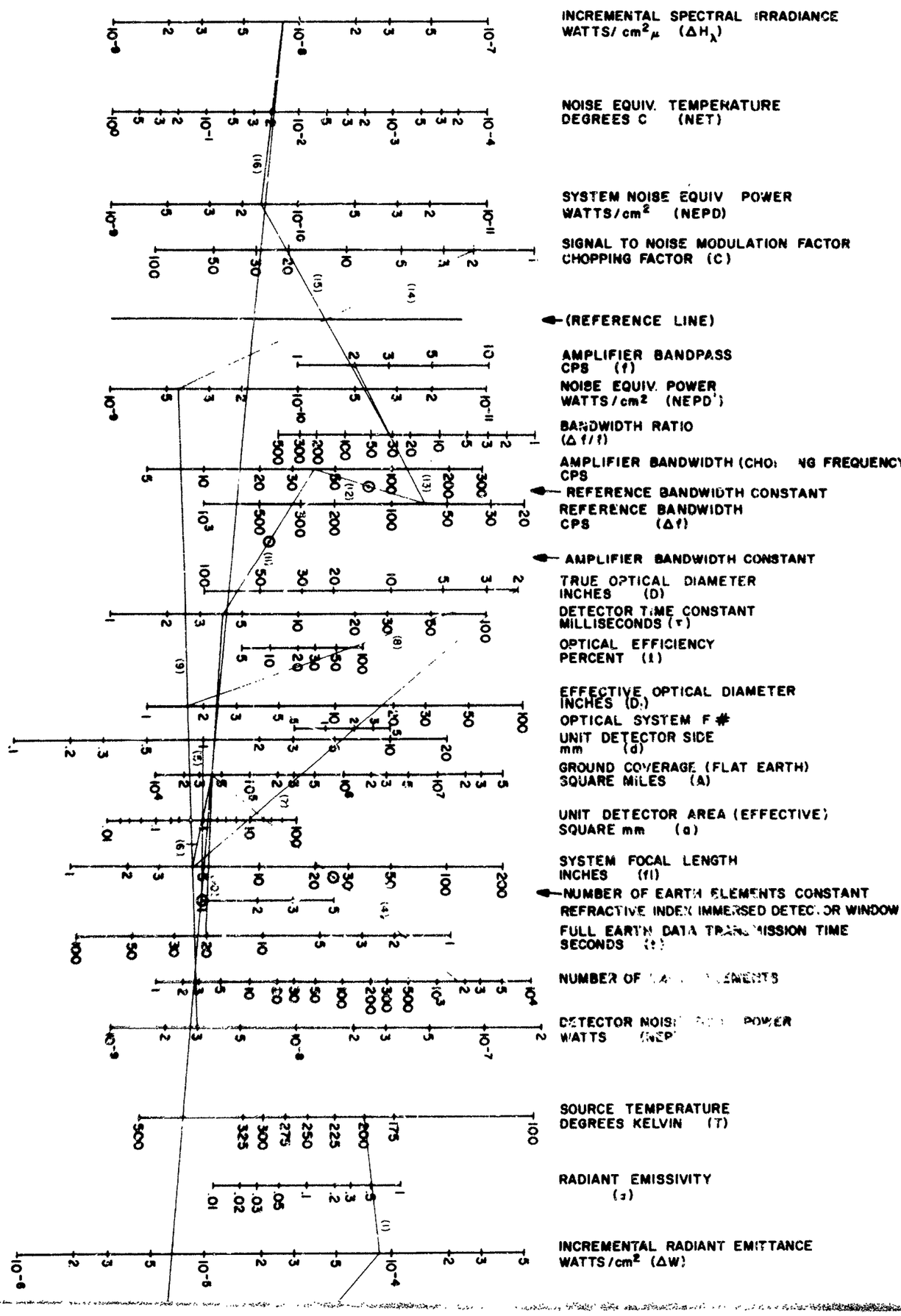
INCREMENTAL SPECTRAL IRRADIANCE WATTS/ cm² μ (ΔH_λ)
NOISE EQUIV. TEMPERATURE DEGREES C (NET)
SYSTEM NOISE EQUIV POWER WATTS/cm² (NEPD)
SIGNAL TO NOISE MODULATION FACTOR CHOPPING FACTOR (C)
(REFERENCE LINE)
AMPLIFIER BANDPASS CPS (f)
NOISE EQUIV. POWER WATTS/cm² (NEPD')
BANDWIDTH RATIO (Δf/f)
AMPLIFIER BANDWIDTH (CHOPPING FREQUENCY), CPS
REFERENCE BANDWIDTH CONSTANT
REFERENCE BANDWIDTH CPS (Δf)
AMPLIFIER BANDWIDTH CONSTANT
TRUE OPTICAL DIAMETER INCHES (D)
DETECTOR TIME CONSTANT MILLISECONDS (τ)
OPTICAL EFFICIENCY PERCENT (t)
EFFECTIVE OPTICAL DIAMETER INCHES (D_e)
OPTICAL SYSTEM F #
UNIT DETECTOR SIDE mm (d)
GROUND COVERAGE (FLAT EARTH) SQUARE MILES (A)
UNIT DETECTOR AREA (EFFECTIVE) SQUARE mm (a)
SYSTEM FOCAL LENGTH INCHES (fl)
NUMBER OF EARTH ELEMENTS CONSTANT
REFRACTIVE INDEX IMMERSED DETECTOR WINDOW
FULL EARTH DATA TRANSMISSION TIME SECONDS (t)
NUMBER OF EARTH ELEMENTS
DETECTOR NOISE EQUIV POWER WATTS (NEP)
SOURCE TEMPERATURE DEGREES KELVIN (T)
RADIANT EMISSIVITY (ε)
INCREMENTAL RADIANT EMITTANCE WATTS/cm² (ΔW)

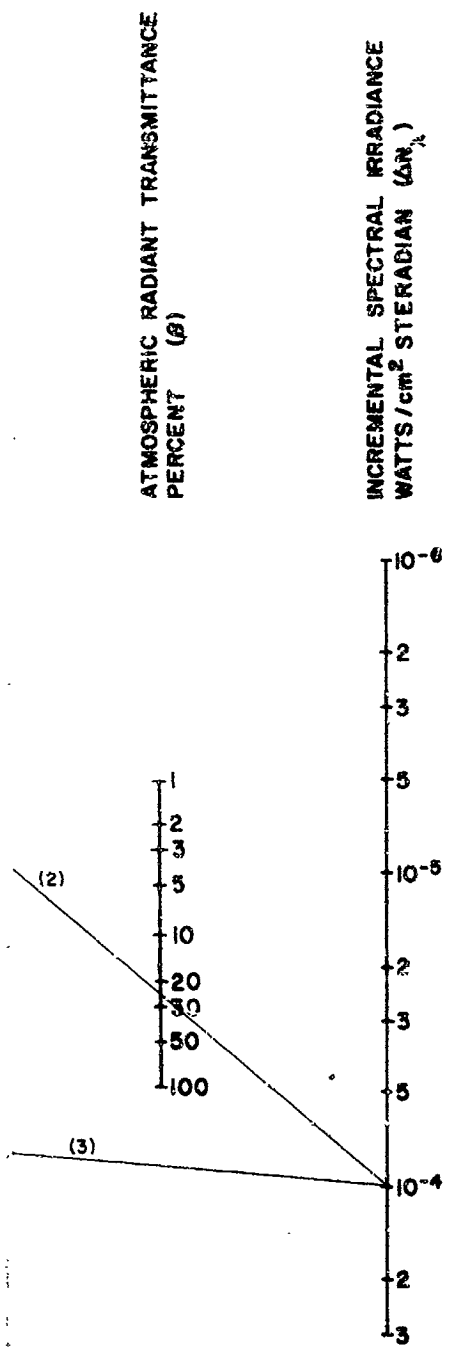

RESTRICTIONS: a) THERMISTOR TYPE BOLOMETER

b) WAVE LENGTH – 4 TO 40 MICRONS

c) SPATIAL SCANNING SYSTEM

d) REFERENCE RETICLE FOR s/n IMPROVEMENT

$$NET = \frac{k l^2 C f l \sqrt{f}}{T^5 \epsilon \beta D^2 A \sqrt{t}}$$

$k = 8.63 \times 10^9$ FOR 20° SQUARE RASTER AT 22,240 MILES

Figure 4-2. Parametric Relationship Nomograph

(1) Select the lowest expected target temperature (T) and the lowest expected emissivity of the target (ϵ) and draw line 1: for T = 200°K and $\epsilon = 0.5$, $\Delta W = 8.5 \times 10^{-5}$.

(2) Determine the approximate percentage of atmospheric transmission (β) for the selected target temperature from Figure 2-17, Section 2, and draw line 2; $\Delta W = 8.5 \times 10^{-5}$ and $\beta = 25\%$ (from Equation 2-17), $\Delta H_\lambda = 10^{-4}$.

(3) Select the instantaneous resolution area (A) to be scanned and draw line 3; for $\Delta N_\lambda = 10^{-4}$ and A = 200 x 200 miles, $\Delta H_\lambda = 8 \times 10^{-9}$.

(4) Using the same area (A) selected in step (3), draw line 4 to obtain the number of these elements in a square raster: for A = 200 x 200 number of elements = 1600.

(5) A typical thermister detector such as the Servotherm (Servo Corp.) Model No. S133140D has a data sheet which indicates an NEP of 3×10^{-9} watts and a time constant of 4 milliseconds when the size of the detector flake is 1 mm x 1 mm. A silver chloride window is used on this detector. The NEP, τ, and d are entered on the nomograph.

(6) Since a flat window is used on this detector, the net refractive index is 1 and line 5 can be drawn to determine the effective area of the detector: for d = 1 mm and flat window, a = 1 mm^2.

(7) Using the same ground area (A) selected in step (3) and the effective area (a) from step (6), draw line 6 to determine the system focal length: for A = 2×10^4 $miles^2$ and a = 1 mm^2 $f\ell \cong 4$ inches.

(8) By assuming an F number for the optical system, a true optical diameter (d) can be determined by drawing line 7 from the focal length determined in step (7): for $f\ell = 4.0$ in. and F = 2.0, D = 2.0 in.

(9) An effective optical diameter (D_1) is obtained by assuming an optical efficiency (ℓ) and drawing line 8 from the true diameter obtained in step (8): for D = 2.0 in. and $\ell = 0.75$, $D_1 = 1.6$

(10) The NEPD of a bridge system (system capable of DC amplification) can be determined by drawing line 9 from the NEP entered in step (5) through the effective optical diameter (D_1) determined in step (9): for NEP of 3×10^{-9} with $D_1 = 1.6$ in., NEPD = 4×10^{-10} watts/cm^2.

(11) Using the time constant τ entered in step (5) and the area of step (3), the total transmission time for full Earth coverage with an unchopped system can be found by drawing line 10: for τ = 4 milliseconds and A = 4×10^4 $miles^2$, t = 20 seconds.

(12) The required amplifier bandwidth can be obtained from the detector time constant entered in step (5) by drawing line 11: for τ = 4 milliseconds, amplifier bandwidth = 40 CPS.

(13) The amplifier bandwidth determined in step (12) is also the chopping frequency when a reticle is used. An information reference bandwidth (Δf) can be obtained by drawing line 12 from the amplifier bandwidth (chopping frequency): for chopping frequency 40 CPS, Δf = 65 CPS.

(14) When a reticle and chopping frequency are system parameters, a bandpass (f) has to be assumed for the amplifier. By drawing line 13 from the Δf obtained in step (13) to this assumed bandpass, a bandwidth ratio can be obtained: for Δf = 65 and f = 2, $\Delta f/f$ = 32. The transmission time t is now 1600/2f = 400 seconds.

(15) A reticle also tends to reduce the average amount of energy available to the detector. If the reticle has the 50% average transmission factor (energy totally obscured 50% of the time) a chopping factor (C) of 2 is said to exist. From the NEPD' from step (10), draw line 14 to the assumed chopping factor.

(16) The system NEPD is determined by the crossed intersection of line 14 and the reference line by drawing line 15 through the same point from the bandwidth ratio found in step (14): for C = 2, NEPD' = 4×10^{-10} and $\Delta f/f$ = 32, NEPD = 1.6×10^{-10}.

(17) The system NET is determined by the ratio of the NEPD found in step (16) and the ΔH_λ obtained from step (3). This ratio is determined when line 16 is constructed: for $\Delta H_\lambda = 8 \times 10^{-9}$ and NEPD = 1.6×10^{-10}, NET = 0.2°C.

In the example shown in the nomograph, the following items were assumed:

T = 200°

ϵ = 0.5

A = 4×10^4

F = 2

ℓ = 75%

C = 2

f = 2 CPS

The β of 25% was obtained from Figure 2-17 based on the T of 200°K. Detector parameters were considered fixed at NEP = 3×10^{-9} watts; d x d = 1 mm^2; τ = 4 milliseconds; and a flat window.

Design parameters obtained were $f\ell$ = 4 in.; D = 2 in.; and t = 400 seconds.

Amplifier bandwidth center established at 40 CPS and NET = 0.02°C.

When the same types of detector restrictions are used for the second configuration as were utilized in Suomi's experiment (detector size selectable and not mounted in a standard shell) it is feasible to obtain data with a limited

angular resolution and usable NET. The nomograph of Figure 4-2 can still be used in the same manner as before except that the focal length obtained is half the length of a constant diameter tube whose true aperture is equal to the detector area. At tube lengths greater than four times the detector diameter, a conical configuration can be used with the included angle equal to the instantaneous field of view. The true aperture is degraded to an effective aperture by including the losses due to the cone walls and usable area of the detector in relation to the area of base of the cone, and other heat losses.

The order of magnitude of a system can be estimated from the nomographs (assuming a 50% reduction from the true aperture). Assuming a detector flake of 1 mm^2 effective area, the optical diameter for a cone whose approximate length is 17-1/2 in. is found to be 0.156 in. plus 1 mm or 0.16 in. total. The effective diameter is therefore 0.08 in. From the nomograph, a NET of better than 10° C can be obtained for this system.

A medium resolution (angular) Suomi type sensor can be postulated. This sensor would require scanning optics. For a NET of 0.2°C, the angular field of view (using the nomograph) would be of the order of 43 milliradians, or a ground coverage diameter of 950 miles (assuming no system losses). When system losses are included, the coverage must be increased to compensate for the losses. The system can be assumed to be of the form α^2 x NET = k, where α is the instantaneous field of view in milliradians, NET is noise equivalent temperature in degrees centigrade, and k is a constant. A NET of 2° is obtainable in the lossless system when the ground resolution is 300 miles in diameter. This type of performance trade-off is indicated in Figure 4-3.

For purposes of this report, three different vehicles are being considered. In order of size they are 100 lb, 500 lb, and 1000 lb. The 100 lb vehicle would be spin-stabilized, while the 500 and 1000 lb vehicles would be stabilized in such a fashion that they would constantly face the Earth.

The high resolution system, to have a reasonable temperature sensitivity, must use an optical system for gain. A typical system of this type is indicated in the nomograph in Figure 4-2. The previously described α^2 x NET = k relationship is still applicable, except that the constant is dependent upon the size of the optical system. The constant is smaller for this type of system as indicated in Figure 4-3. Some losses must still be included (i.e., germanium flat, etc.). The weight, power, and volume requirements of this type of system are the maximum of the three usable types described in subsection E. The reliability is the lowest.

A whole earth Suomi type sensor is reliable, consumes very little power, and does not cost much in weight and vehicle space. It is felt that this experiment can be carried on all vehicles.

A medium angular resolution Suomi type system has some advantages (i.e., very little power is required for the sensor). The majority of the power will be required for the scanning mirror. The reliability of the system is degraded due to the incorporation of this mirror and its driving mechanism.

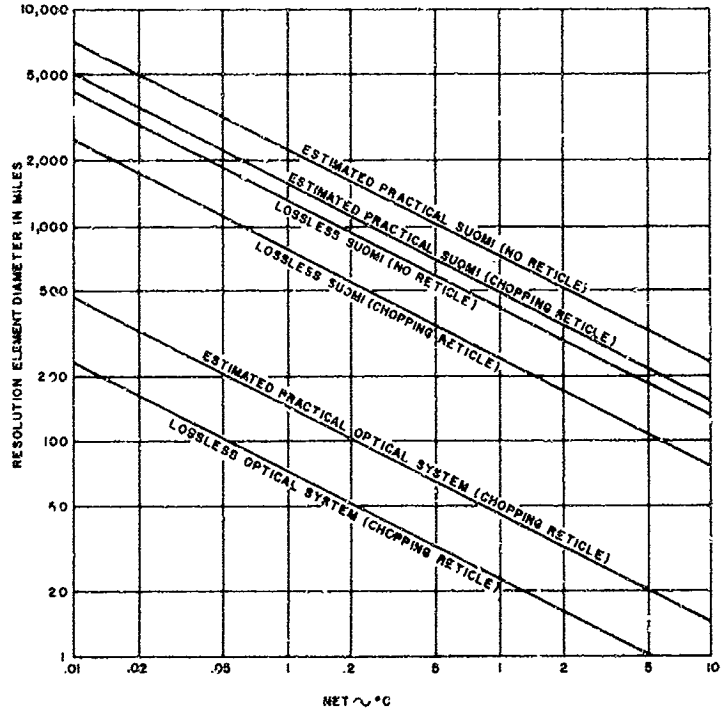

Figure 4-3. Spatial Resolution Versus Temperature Resolution Trade-Off

When a chopper is used, the NET would improve by some factor dependent upon the chop factor, detector time constant, and amplifier bandpass. The reliability would tend to decrease, while the weight, power, and volume of such a system would increase.

Cone efficiency at the large and small ends, thermistor mounting tolerance, wall absorption and conduction, detector emissivity, lead conduction, and several other factors all contribute to losses which exist in the system. An approximation of the effect of these factors is indicated in Figure 4-3. The normal method of construction of this device would be to include some roughly calculated gross safety factor and then to calibrate the instrument upon completion of construction. These medium resolution systems could find use in all three vehicle configurations.

If weighting factors can be given to the function of angular resolution, temperature resolution, weight, power, volume, reliability and any other function deemed relevant, then the optimum type of system for any vehicle can be determined. The weight to be given to each factor must be determined by the user in accordance with the end result desired for a particular application.

F. BIBLIOGRAPHY

DeWaard, R., "Plastic Technology in Satellite Optics," Barnes Engineering Company, Product Design and Engineering, 1961

Hanel, R. A., "A Low-Resolution Unchopped Radiometer for Satellites," Goddard Space Flight Center, NASA Technical Note, 1961

Holter, M. R., Nudelman, S., Suits, G. H., Wolfe, W. L., and Zissis, G. J., Fundamentals of Infrared Technology, MacMillan, 1962

Hummer, R. F., and Malinowski, F. R., "Nimbus Five-Channel Scanning Radiometer," Santa Barbara Research Center, IRIS Paper, 1963

Weinstein, A. I., Friedman, A. S., and Gross, U. E., "Cooling to Cryogenic Temperature by Sublimation," Aerojet-General Astrionics Division, IRIS Paper, 1962

State-of-the-Art Report - Infrared Quantum Detectors, Institute of Science and Technology, The University of Michigan, IRIA Report MAVEXOS-P-2329, 1961

State-of-the-Art Report - Optical Materials for Infrared Instrumentation, University of Michigan, Willow Run Laboratory, IRIA Report 2389-11-S, 1959

SECTION 5 - INFRARED SYSTEMS FOR CLOUD COVER IMAGING

A. GENERAL

The requirements for obtaining low and high resolution pictures of the Earth's cloud cover are outlined in subsection 3.B. The cloud imaging systems described therein use sensors that are sensitive to radiation only in the visible region of the electromagnetic spectrum. The requirement for cloud cover pictures during night conditions, with the attendant low level of reflected visible illumination, suggests the possibility of exploiting the longer wavelength infrared radiative characteristics of clouds as an energy source for the imaging of night cloud cover. The principal advantage in using the infrared spectrum is that the cloud masses, which behave characteristically almost as black body thermal radiators, provide a higher level of self-radiant power over this much broader spectral region than is available in reflected visible light originating from night illumination sources.

B. INFRARED TRANSMISSION

The capability of an infrared device to provide a usable image of clouds against Earth background depends almost entirely on detecting differences in radiant power between the clouds and the Earth background, that is, temperature contrast. If the clouds and background were the only factors to be considered, then the problem of designing an infrared device would be fairly conventional because the contrast under those conditions is a fairly well understood function of temperatures and emissivities. However, analysis of the case in which the infrared device is to be at a remote location in space is considerably more complex, because the radiations must pass through the Earth's atmosphere where deterioration of contrast takes place as a result of molecular absorption, particulate scattering, temperature inversion, and other processes. Although the mechanics and qualitative effects of these various phenomena are reasonably well understood, there does not yet exist a means for quantitative expression of results to be expected under these conditions. Analysis of infrared data from Tiros and other satellites might improve this situation.

The transmission of infrared radiation through the atmosphere is subject to selective attenuation as a result of absorption by molecules present in the Earth's atmosphere. Figure 5-1 indicates the absorption spectra of molecules present in the atmosphere, with the composite atmospheric absorption characteristic shown at the bottom of the figure. Observation of the composite solar-absorption spectrum shows that there are two principal spectral regions (atmospheric "windows") that are transparent with respect to infrared energy. The first transparent region, which is from 1 micron to 5 microns, will transmit roughly 50% of the radiant energy there. There is an opaque region from 5 microns to 8 microns. A second window, from 8 microns to 14 microns, will pass about 80% of the radiant energy there. Other windows exist in the longer wavelength regions of the spectrum, but effective use can not be made of them in space applications of infrared devices, because infrared detector technology is not sufficiently advanced.

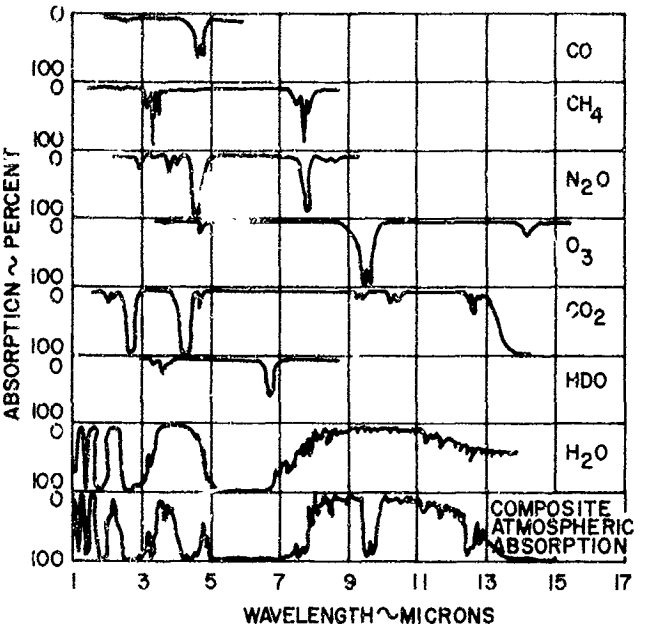

Figure 5-1. Near Infrared Solar Radiation and the Absorptivity of Various Compounds in the Atmosphere

The infrared windows are shown in relation to the Earth's radiant energy distribution in Figure 5-2. The total radiant energy present in the windows is represented by the shaded areas under the curve. The 8 to 14 micron region contains approximately 32% of the total radiant energy, and the 1 to 5 micron region contains only 0.33%. In designing an infrared device, it would be extremely desirable to use the 8 to 14 micron region, because the available energy is vastly greater than in the 1 to 5 micron window. At the present time, long wavelength infrared detectors of quantum types are not adequate for sustained use in a space environment. The application of thermal detectors, which have the required long wavelength capability, is severely limited by virtue of the other performance factors discussed in Section 4.

1. Imaging Systems

The two basic types of infrared systems that might be used for cloud cover imaging are the object plane scanner, and the image plane scanner.

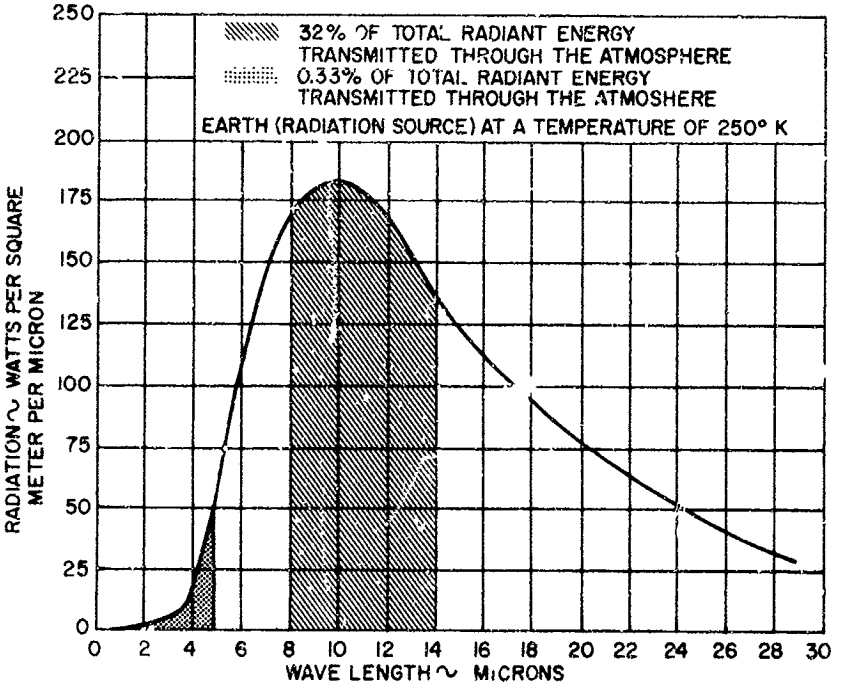

Figure 5-2. Earth Radiation and Atmospheric Windows

In the object plane scanner, the detector, which is located at the focus of the optical system, receives energy from a small element of the total field of view. The optical system is moved so that it will cause the detector to look sequentially at contiguous elements of the field until the entire area is covered. In the simplest case of a spinning satellite, the scanning motion of the optics is imparted by the spinning and orbital velocities of the vehicle. The instantaneous field of view of the system is adjusted so that each rotation of the vehicle sweeps out a transverse strip equal in width to the orbital distance traversed during that time, which results in a continuous map of contiguously scanned strips. When the satellite is vertically stabilized, without spin, the transverse scan must be provided by the imaging system, in which case a deflecting element, such as a mirror or a prism interposed in the incident energy path, is rotated at a rate commensurate with the orbital rate and the system resolution to provide contiguous scan lines. In the most advanced situation, where the satellite is vertically stabilized and in synchronous orbit (no motion relative to the surface of the Earth), scanning in both dimensions must be provided by the imaging system. When object plane scanning is used, the two dimensional scan must be achieved by a mechanical method. Of the many methods available for instrumenting the required type of scan, most can be eliminated on the bases of:

(1) Mechanical complexity

(2) Excessive mass of moving components

(3) Excessive changes in momentum

(4) Structural problems arising from high translational and rotational velocities.

For satellite application, the most desirable type of system is one in which mechanical motion occurs at a constant, moderate speed and involves low mass elements in a simple mechanical configuration. One device that fulfills these requirements is a diasporameter scan system, in which two optical wedges are rotated relative to one another to cause the axis of an otherwise fixed optical system to be deflected in predictable fashion. A system of this type is analyzed later in this section.

In the image plane scanner, the entire area of interest is imaged on an extended detecting surface. The distribution of thermal energy in the viewed scene is reproduced on the sensitive surface at the image plane, which produces corresponding variations in a parameter of the sensitive surface. The information obtained by this imaging process is removed and converted to electrical signals by scanning the surface with an electron beam. The image plane scanner has the desirable characteristic of requiring no moving parts (the scanning process being accomplished entirely by electronic techniques). The difficulties in implementing this type of system so that it can operate in the infrared spectral region arise from problems of manufacturing detector surfaces having the requisite sensitivity, uniformity, and resolution.

2. Detectors

The object plane scanner makes use of a detector which fills the instantaneous field of view of the scanner. Since the instantaneous field establishes the finest angular resolution capability of the system, the detector surface is usually quite small in systems with optics of practical size. The class of infrared detectors known as "point detectors" would be employed for this type of imaging system. A detailed description of thermal and quantum point detectors is given in Section 4, and Volume 7, Table 7-2 and Figure 7-1. While many of the available infrared detectors have excellent sensitivity, there are basic obstacles to their extended use in a space vehicle.

In the case of quantum detectors, the major problem is that of maintaining the required operating temperatures of 77°K or lower. Cooling systems having this capability have not yet been developed for extended operation in space. Even if present developmental systems could be made usable, there is serious doubt whether the large electrical power and volume requirements could be readily supplied in a space vehicle, particularly if reliability considerations dictated a need for redundancy.

Perhaps the most important problem in using thermal point detectors (thermistor bolometers) is that the response time (time constant) of a bolometer is very long compared with quantum detectors. The better bolometers have time constants no shorter than 1 millisecond, which restricts the information-acquisition rate to 500 CPS. In systems where higher data rates are required, bolometers can be arranged in arrays with a separate electronic channel

required for each array element. The separate channels must eventually be reduced to a single information channel; therefore, electronic commutators with very stable DC characteristics and extremely low switching-noise levels are required. The information rate required for application in a synchronous satellite, under near optimum conditions, is a minimum 5000 CPS and probably will be higher (at least 10,000 CPS). If bolometers were to be used, 10 to 20 channels would be required, resulting in complexity and unreliability considered excessive for long term satellite use. Furthermore a large DC bias voltage (several hundred volts) of extremely low noise level is required for bolometer operation. Attempts to provide electronic supplies for this purpose have been unsuccessful; the only alternative is the use of high voltage batteries. Because rechargeable, high voltage storage batteries are not readily available, dry cells or mercury batteries must be used.

The image plane scanner uses an area detector, of which the only practical configuration is the infrared image tube. Two types of infrared image tubes are currently available:

(1) The infrared Vidicon, which operates like a conventional Vidicon, except for its region of spectral sensitivity.

(2) The thermal image tube, in which an absorbing layer conducts incident thermal energy to a layer of thermistor material. The impinging infrared image produces corresponding variations in the electrical resistance of the sensitive surface.

The infrared Vidicon uses a photoconductive sensitive surface which must be cooled in order to attain useful sensitivity. Current developmental infrared Vidicons require cooling to temperatures of 77°K or lower, and their spectral responses are restricted to a few microns. Recent developments have produced a tube which has acceptable sensitivity at 150°K, but the frame storage characteristics are inadequate. Other work is being done to achieve spectral response extending to 13 microns, but operating temperatures of 4.2°K are required.

The thermal image tube, although it operates at room ambient temperatures and has a spectral response to 20 microns or more, presents other problems, principally, sensitivity, response time, and resolution. To date, temperature sensitivity of approximately 12°C is the best obtained, although 4°C sensitivity has been achieved in the laboratory with cooling applied to the tube. The response time of thermal tubes is characteristically much longer than photoconductors, presenting the problem of long data acquisition times and image smearing due to vehicle attitude uncertainty. Also, the best resolution obtainable is 250 to 300 TV lines (estimated) which can provide ground resolution of 30 miles at best, with a full Earth field of view. Some independent work is being done to develop thermal image tubes further, but it is doubtful if significant breakthroughs can be expected in the near future.

3. Resolution

The state of the art in object plane scanning devices is such that no finer angular resolution than approximately 1 milliradian can be achieved under controlled conditions with useful sensitivity. In a practical system, when various parameters, such as aperture effects, extraneous noise sources, and target recognition and interpretation are considered, the limiting resolution appears to more nearly approach 2 milliradians. For the SMS system, 2 milliradians corresponds to a ground resolution of approximately 45 miles. In an object plane scanner this figure is invariant, regardless of the total field of view angle.

In the image tube scanner, the considerations are somewhat different. Here the resolution is determined by the number of elements (lines) that can be resolved on the sensitive surface, and has a complex dependence on surface granularity, uniformity, and thermal diffusion as well as on electron beam characteristics and electron optics parameters. The best available infrared thermal image tubes provide resolution of approximately 250 to 300 lines, or about 30 miles ground resolution with full Earth coverage. With the image plane scanning system, the ground resolution can be improved by narrowing the total field of view, since the number of resolution lines remains constant. If the field is reduced from full Earth coverage to 1200 mile coverage, then the ground resolution becomes approximately 4.5 miles.

The resolution considerations for the optics of an infrared system also have some influence on the physical size of the optics. The Rayleigh limit criterion can restrict the minimum diameter of the optics. This effect occurs much sooner for the longer wavelengths. The equation for the Rayleigh limit can be written in the form

$$\alpha = \frac{47.25 \times 10^{-6} \mu}{D} \qquad (5\text{-}1)$$

where α = instantaneous field of view in radians
μ = wavelength of the radiation in microns
D = diameter of the optics in inches

The instantaneous field of view and its relation to the ground resolution at the nadir obeys the equation

$$L = \alpha h \qquad (5\text{-}2)$$

where L = resolution in miles
α = instantaneous field of view in radians
h = altitude in miles

The above equations have been constructed in Figure 5-3. In the example given, a 2 mile resolution element would require a minimum optical diameter of 5 in. when the wavelength is 10 microns. For operation in the 8 to 14 micron window, the minimum diameter would be 7 in. The resolution in miles at the nadir is stated in Eq (5-2).

The spot size of the focal plane along the focal axis can be stated in the equation

$$d = \alpha \, fl \qquad (5\text{-}3)$$

where d = spot size in inches
α = instantaneous field of view in radians
fl = focal length in inches

The above equations have been constructed in Figure 5-4. In the example given, a 2 mile resolution element would require an 11 in. focal length for a detector spot size of 0.001 in. The instantaneous field of view is 0.9×10^{-4} radian.

The combined use of Figures 5-3 and 5-4 reveals that for a 2 mile ground resolution, an infrared system operating in the 8 to 14 micron region must have a focal length of 11 in. for a 0.001 in. spot size, and the diameter of the system must be greater than 7 in. The f/number of the system is therefore 1.57.

C. CLOUD IMAGING SYSTEM DESIGN FACTORS

1. Scope

This subsection presents the development of relationships significant to the design of an infrared imaging system, and to the equation defining its detecting capability. The system is presumed to be borne in a synchronous satellite at an orbit altitude of 22,240 miles. The physical characteristics of the system are taken as follows:

(1) Optics

- Collector type, parabolic mirror
- Field of view, 20° (0.35 radian)
- Focal ratio N = f/D = 1

(2) Detector

- Type, PbSe, thermoelectric cooling to 200°K
- Detectivity, $D^* = 5 \times 10^7$ cm-cps$^{1/2}$ watt^{-1}

(3) Vehicle attitude rate, 0.01° per second (1.75×10^{-4} radian per second).

The focal ratio, N, is the quotient of effective aperture diameter, D, into the focal length, fl. Hence, it has the same meaning as the f/number used in photography as a measure of speed or light-gathering power. The normalized detectivity, D*, is a figure of merit for the weakest signal detectible under the indicated test conditions.

A diasporameter type of scanner is used to cover the conical field of view. This type of scanner uses two optical wedges rotating at different speeds to deflect the optical axis progressively in such a way as to generate a spiral scan pattern. This spiral scan results in a circular frame, more efficient than a square one for viewing a round object such as the Earth.

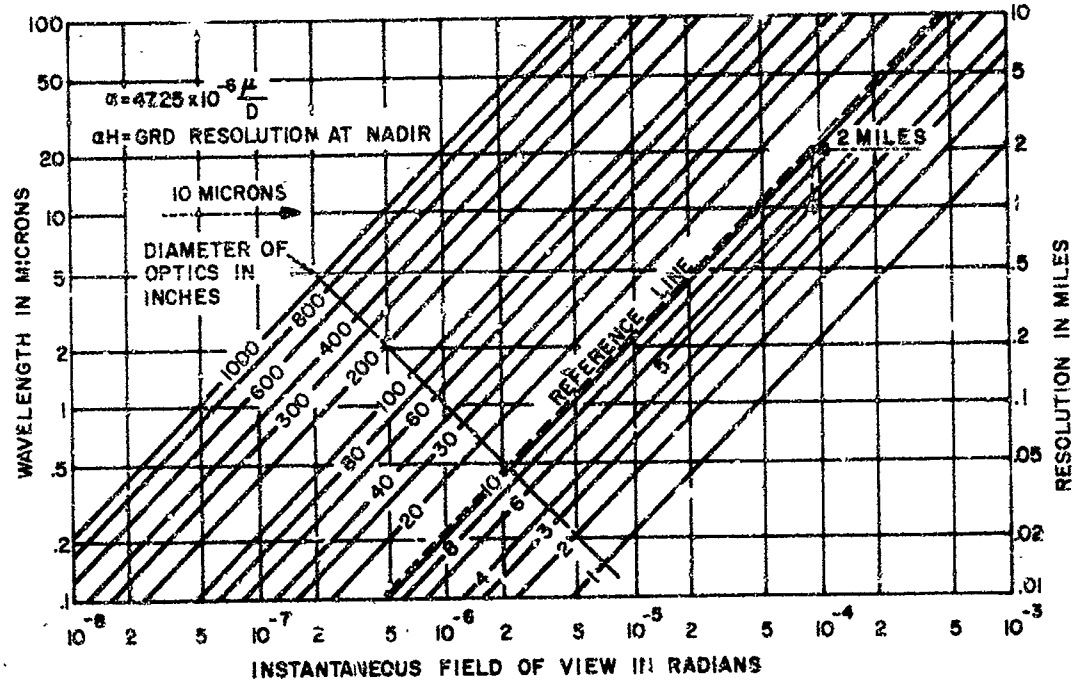

Figure 5-3. Rayleigh Limit Criterion

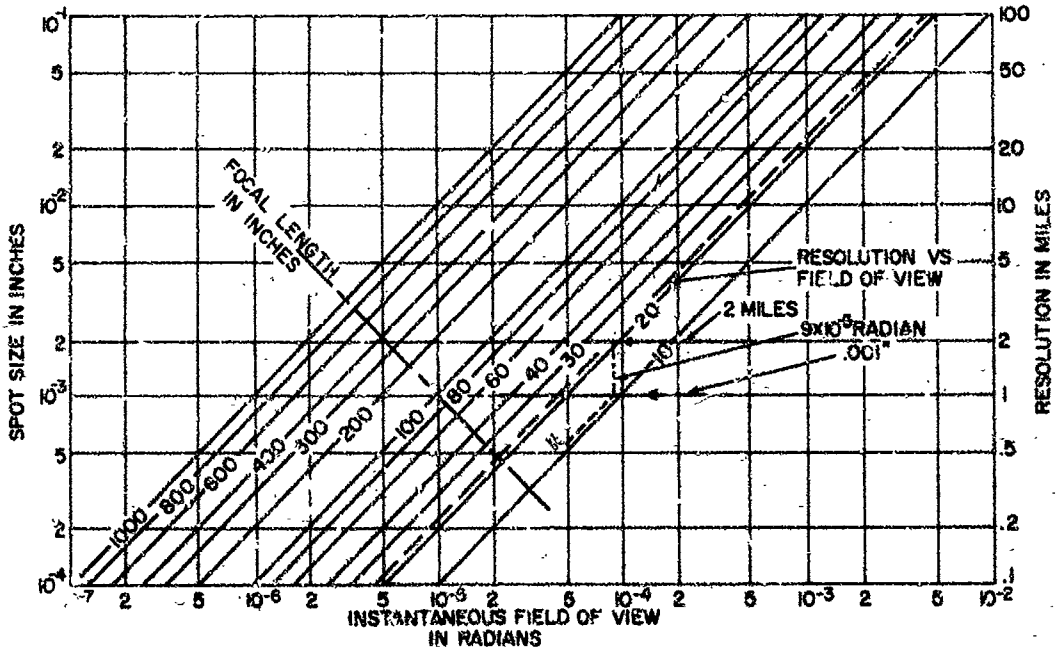

Figure 5-4. Instantaneous Field of View Versus Resolution

2. Resolution Elements, E

In the interest of simplicity, the number of resolution elements in the scan frame is determined approximately. The approximation used will result in a somewhat conservative figure for overall system sensitivity, but adjustments can be made if desired. The scan field is assumed to be generated by a number of spirals C, and to have angular resolution of element size α. The field is approximated by C concentric circles, each composed of the same number of resolution elements. The total number of resolution elements, E, in the field is then:

$$E = \frac{\pi F}{\alpha \cdot 10^{-3}} \cdot \frac{F}{2} \cdot \frac{1}{\alpha \cdot 10^{-3}} = \frac{\pi F^2 \cdot 10^6}{2 \alpha^2} \qquad (5\text{-}4)$$

where F = field of view, radians
α = angular resolution milliradians

The scan time per element is short enough so that vehicle motion introduces negligible blur.

3. Scan Frame Time, S

The scan frame time is a function of the permissible geometric distortion in the picture that arises as a result of vehicle angular motion. The distortion, d, is considered as the angular motion of the vehicle equivalent to 1/4 of a resolution element during a scan frame. The time required to scan a frame is then:

$$S = \frac{d}{\omega_v} \cdot 10^{-3} = \frac{\alpha}{4 \omega_v} \cdot 10^{-3} \qquad (5\text{-}5)$$

where S = frame time, seconds
d = distortion
ω_v = vehicle angular rate, radians per second

4. Data Rate, DR

The scan field is assumed to be composed of a number E alternate black and white resolution elements, representing two discrete levels of radiation intensity. The rate at which data bits are scanned is

$$DR = \frac{E}{S} \qquad (5\text{-}6)$$

where DR = data rate, bits per second

5. Electronic Bandwidth, BW

For the alternate black and white pattern, the fundamental sinusoidal frequency is 1/2 of the data rate, which will be the maximum frequency generated by the scan.

$$BW = \frac{1}{2} DR \tag{5-7}$$

where BW = electronic bandwidth in CPS

Substituting Eqs (5-4), (5-5), and (5-6), Eq (5-7) becomes:

$$BW = \frac{\pi F^2 \omega_v}{\alpha^3} \cdot 10^9 \tag{5-8}$$

6. Spirals per Scan Frame, C

For complete coverage of the scan field, a spiral is required for each resolution element along the radius of the field, F.

$$C = \frac{F}{2} \cdot \frac{1}{\alpha \cdot 10^{-3}} = \frac{F}{2\alpha} \cdot 10^3 \tag{5-9}$$

where C = number of spirals per frame

7. Scan Rotational Rate, ω_S

To complete a scan frame, the total number of spirals per frame must be generated during the frame time. The scan rotational rate is:

$$\omega_S = \frac{C}{S} \tag{5-10}$$

where ω_S = scan rotational rate in RPS

Substituting Eqs (5-5) and (5-9), Eq. (5-10) becomes:

$$\omega_S = \frac{F}{2\alpha} \cdot 10^3 \cdot \frac{4\omega_v}{\alpha} \cdot 10^3 = \frac{2F\omega_v}{\alpha^2} \cdot 10^6 \tag{5-11}$$

Equation (5-11) defines the angular rate of the prism that determines the basic scan rate. The second prism, which generates the spiral pattern, must spin at an angular rate of:

$$\omega'_S = \omega_S \left(1 + \frac{1}{2C}\right) \tag{5-12}$$

8. Optical Relationships

A square detector element is considered here. For angular resolution, α, and optical focal length, f, the dimension of a detector located at the focal point of the optics is:

$$a = f\alpha \cdot 10^{-3} \tag{5-13}$$

where a = detector side in centimeters
f = focal length in centimeters
α = resolution in milliradians

The detector area, A_d, is then

$$A_d = a^2 \tag{5-14}$$

The area of the collecting mirror is:

$$A_o = \frac{\pi D_o^2}{4}$$

and the focal ratio, N, of the optics is:

$$N = \frac{f}{D_o}$$

Therefore:

$$A_o = \frac{\pi f^2}{4 N^2} \tag{5-15}$$

From the geometry of the optics and the solid angle of the instantaneous field of view,

$$\frac{A}{R^2} = \frac{A_d}{f^2} \tag{5-16}$$

where A = area of instantaneous field of view

9. System Sensitivity Relationships

One measure of the sensitivity of a detecting system is its capability to distinguish between two adjacent sources of different radiant powers. As a general approach, consider two sources at absolute temperatures T_1 and T_2. The difference in radiant power (ΔW) from the two sources is:

$$\Delta W = A_1 E_1 \sigma T_1^4 - A_2 E_2 \sigma T_2^4 \tag{5-17}$$

where A_1 and A_2 = source areas
E_1 and E_2 = source emissivities
T_1 and T_2 = source temperatures
σ = Stephan-Boltzmann constant

In an imaging system, $A_1 = A_2 = A$ = angular resolution field. It will be assumed that the sources are black bodies where $E_1 = E_2 = 1$. Then Eq (5-17) becomes:

$$\frac{\Delta W}{A} = \sigma \left(T_1^4 - T_2^4 \right) \qquad (5\text{-}18)$$

If the temperatures T_1 and T_2 are very close to one another, Eq (5-18) can be expressed in an approximate form more convenient for manipulation. Because

$$\frac{W}{A} = \sigma T_1^4$$

by differentiating:

$$\frac{d W}{A} = 4 \sigma T_1^3 \, d t$$

and

$$\frac{\Delta W}{A} = 4 \sigma T_1^3 \, \Delta T_1$$

Because the sources are extended area sources, the radiation flux density per unit source area, according to Lambert's Law, is:

$$\Delta P = \frac{1}{\pi} \cdot \frac{\Delta W}{A} = \frac{4 \sigma T_1^3 \Delta T_1}{\pi}$$

where P = flux density, watts per steradian per square centimeter

The solid angle subtended by the collecting mirror is A_o/R^2, where R is the distance to the source. The total power available at the detector is then:

$$P = (\Delta P) \frac{(A_o)}{R^2} \, (A)$$

or

$$P = \frac{4 \sigma T_1^3 \Delta T_1}{\pi} \cdot \frac{(A_o)}{R^2} \cdot (A) \qquad (5\text{-}19)$$

If a value of minimum detectable power is defined for which P = NEP (noise equivalent power), then ΔT_1 becomes, by definition, the minimum detectable temperature difference, NET (noise equivalent temperature), and:

$$NEP = (NET) \frac{4 \sigma T_i^3 A_o A}{\pi R^2}$$

or

$$NET = (NEP) \frac{\pi R^2}{4 A_o A \sigma T_i^3} \qquad (5\text{-}20)$$

The detector figure of merit D* is defined as:

$$D^* = \frac{\sqrt{A_d \, \Delta f}}{NEP}$$

where $\Delta f = BW$

Substituting in Eq (5-20) gives:

$$NET = \frac{\sqrt{A_d \, BW}}{D^*} \cdot \frac{\pi R^2}{4 A_o A \sigma T_1^3} \qquad (5\text{-}21)$$

By making substitutions from Eqs (5-8), (5-13), (5-14), (5-15), and (5-16), and introducing an optical transmission efficiency factor, η, then:

$$NET = \frac{1.96 \, N^2 \sqrt{\omega_v \cdot 10^7}}{D^* f \alpha^2 \sigma T_1^3 \eta \sqrt{\alpha}}$$

Further substitution of $D^* = 5 \times 10^7$ (cm-cps$^{1/2}$ - watt^{-1}) and $\sigma = 5.67 \times 10^{-12}$ (watt-cm^{-2} - degree^{-4}) yields:

$$NET = \frac{69.2 \, N^2}{f \alpha^2 T_1^3 \eta} \frac{\sqrt{\omega_v}}{\sqrt{\alpha}} \cdot 10^9 \qquad (5\text{-}22)$$

for this specific application it will be considered that ω_v, N, and T_1 are invariant and:

$\eta = 0.5$
$\omega_v = 1.75 \times 10^{-4}$ radian per second
$N = 1$
$T_1 = 250°K$

Therefore:

$$NET = \frac{117}{f \alpha^2 \sqrt{\alpha}} \qquad (5\text{-}23)$$

To express this relationship as a function of linear resolution at the Earth's surface, the substitution $r = 22.24 \, \alpha$ is made:

r = ground resolution in miles
α = angular resolution in milliradians

$$NET = \frac{273}{f r^2 \sqrt{r}} \qquad (5\text{-}24)$$

10. System Performance

Equation (5-23) expresses the dependence of system sensitivity on factors that are generally a function of the mission and the characteristics of the vehicle. Imaging systems characteristically require fine resolution and low distortion, both of which influence NET in an adverse direction. In general, the requirement for fine resolution is of greater importance because a mildly distorted image could be interpreted, whereas one with insufficient detail is of no value. (For which reason considerable caution must be exercised when specifying the resolution requirement of a system.) Variation of the focal length presents a means of partial compensation for sensitivity reduction due to improvement of resolution. In the system under consideration, an increase in focal length causes a corresponding increase in the diameter of the collecting optics because of the fixed focal ratio. If increased size of the optics is no problem, then this alternative could be used within the limits of attendant secondary effects, such as optical fabrication problems and structural effects in rotating members. In cases where a larger optical diameter is impractical, focal length cannot be increased because the focal ratio, N, will increase, resulting in disproportionately lower optical gain and a net loss in sensitivity, as shown in Eq 5-22.

Figures 5-5 and 5-6 show the effect on NET of varying the parameters of Eq (5-24). Figure 5-7 shows how the scanning prism rotational speed is affected by choice of system resolution. (Also refer to Eq (5-11).) This factor should not be ignored in a system design because the rotational rates could be severely limited by structural problems, mechanical wear, and vibration.

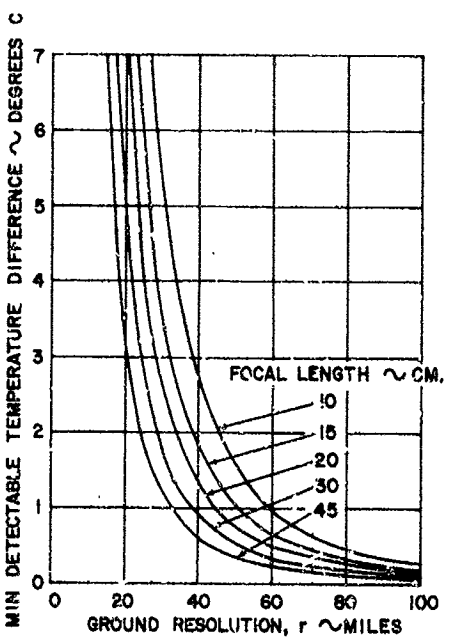

Figure 5-5. Temperature Difference Versus Resolution, Focal Length as a Parameter

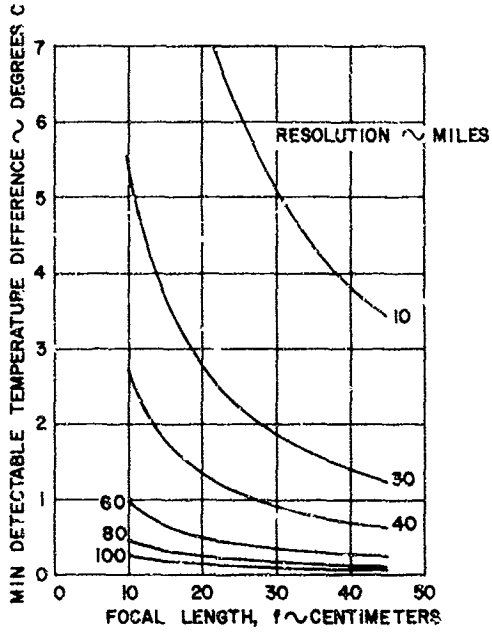

Figure 5-6. Temperature Difference Versus Focal Length, Resolution as a Parameter

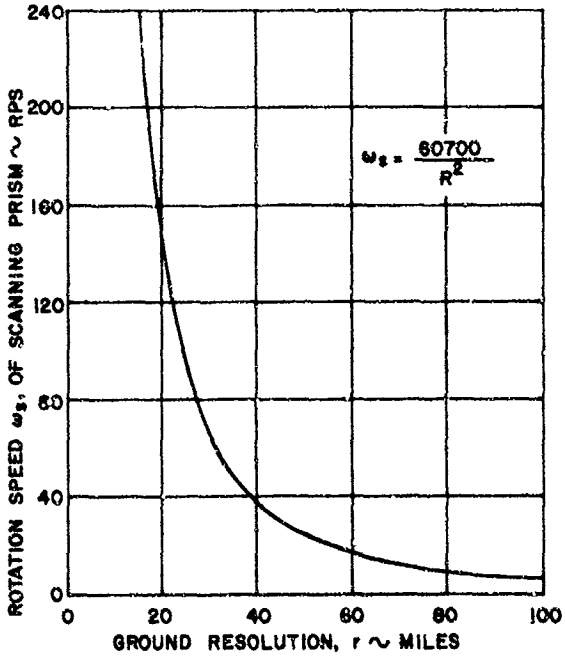

Figure 5-7. Required Scanning Speed

D. CONTRAST AND ATMOSPHERIC EFFECTS

The required NET for an imaging system is determined principally by the contrast characteristics of the object field. For example, in a reconnaissance or mapping system, the average contrast between adjacent terrain features is low, requiring a system NET of considerably less than 1°C for useful data. In a cloud against Earth imaging system, however, higher contrast generally exists between subject and background, permitting a less stringent requirement on NET. Clouds vary in temperature from as low as 210°K to 290°K, and the occurrence of cloud to Earth contrast of less than 1 or 2° would be rare. This means that a system having a NET of approximately 2°C would see the cloud patterns most of the time, with occasional lapses into blindness when low contrast occurs.

Another aspect of the contrast problem arises as a result of atmospheric absorption and scattering of the radiant energy, an area in which little data are available with reference to transmission through vertical paths into space. Certainly, some degree of contrast loss is to be expected, but most clouds generally exist at altitudes sufficiently high to avoid the most significant portion of absorption in the low altitude, higher density region of the atmosphere. The phenomenon of particulate scattering exhibits dependence both on particle size and on particle density. Again, there is a rapid decrease in scattering with height above the Earth's surface, due to the decreasing particle size and density. The distribution of particle size is usually such that there is less scattering at the longer wavelengths, and scattering attenuation is less pronounced in the middle and far infrared regions than it is in the near infrared, where again it is less than in the visible wavelengths. Another factor that works to advantage is that in many cases the cloud tops are associated with, but physically above, a temperature inversion which tends to limit the majority of the particulate matter to the atmosphere below the inversion.

Scattering is not the only type of atmospheric attenuation. In addition, there are selective absorption effects involved. These effects depend on, and vary with, the constituents of the atmosphere. The water content of the atmosphere introduces large variations.

Considering all of these factors, it is to be expected that the atmosphere will reduce the apparent contrast among objects at the surface of the Earth, but that it will enhance the contrast of clouds against Earth background because of the altitude difference and associated discrimination against radiations from the Earth's surface, in particular against the shorter wavelengths that go with higher temperatures.

The atmospheric filtering effects for the SMS can be expected to be substantially the same as those for any other satellite. Hence, it will be useful to review the experience and data available from Tiros, Nimbus, and other satellite programs.

Positive quantitative conclusions cannot be made now concerning the extent of atmospheric attenuation. In an imaging system design, some factor must be included to account for attenuation, but, at the present time, it can only be estimated on the basis of comprehensive studies of the phenomena involved. In the system sensitivity analysis presented here, a transmission efficiency factor, η,

of 50% was used for calculation purposes. This factor was not intended to include atmospheric attenuation, but was meant rather to portray a conservative estimate of optical efficiency. In a firm system design, the estimated atmospheric attenuation factor must be incorporated as a separate factor.

E. OPTICAL MATERIALS

The optical transmission factor, η, which was arbitrarily set at 50%, is primarily a function of the materials used for the rotating prisms and the detector window. A commonly used infrared-transmitting material, which is available in sizes to 18 in. diameter and which has good stable mechanical characteristics, is arsenic trisulphide, As_2S_3. The spectral transmission of arsenic trisulphide extends from 1 micron to 12.5 microns, which is more than adequate for a PbSe detector. A disadvantage of this material is its attenuation, which permits only 80% of the energy to pass (in typical thicknesses), causing a net attenuation to 64% when two prism elements are cascaded. A further optical loss is sustained through the detector window, where sapphire, which has a transmission efficiency of 90%, but a spectral range extending only to 5 microns, should be used. With a sapphire detector window, the net optical attenuation, including 4% for primary mirror reflection loss, would reduce the transmission to 53%. A definite improvement in this figure could be achieved by using sapphire throughout, if it were available in the required configuration. In this event, the net transmission would be about 70%.

In either case, a further loss would be sustained if a protective window were required in front of the optics. It is felt, however, that after consideration of the environment of the system, a design could be evolved that would eliminate the need for such a window.

F. DYNAMIC RANGE

An important design consideration for an imaging system is the dynamic range of the signal to which the detector is exposed. During most of its operation in the SMS, the equipment will view areas of darkness, daylight, and sometimes the Sun itself. This requires particular design consideration to prevent overloading the detector and/or electronic system. Also, immediately before and after the short period of total darkness, during which time the equipment has its greatest utility, it could be exposed to direct radiation from the Sun, which could damage the detecting element permanently. Protection of the detector against direct solar incidence can be solved by automatically (or permanently) interposing a germanium shutter; this will attenuate about 92% of the solar-spectrum energy while passing about 40% of the infrared energy. The problem of the large range of signals resulting from the Earth's brightness range must be studied carefully before a solution can be postulated. If overloading of the system occurs as a result of insufficient range in the electronics, measures such as signal limiting and signal compression could be taken. If the overloading occurs in the detector, the problem is more serious, requiring further study in the areas of detector materials and the possible use of variable optical filters.

G. BIBLIOGRAPHY

Statement of Work for Studies of Synchronous Meterorological Satellite Systems Problems, National Aeronautics and Space Administration, Goddard Space Flight Center Document X-653-62-2, 7 June 1962.

A Meteorological Evaluation of Aeros, Glaser, A.H., Allied Research Associates Document No. ARA-M-7582, prepared for Republic Aviation Corporation, 4 May 1962.

A Review of Visible Light Imaging Techniques as Applied to Aeros Satellite, Republic Aviation Corporation Report 719, 17 April 1962.

Infrared Sensor Considerations, Republic Aviation Corporation Report MSD 517-320, 10 April 1962.

SECTION 6- PROBLEM AREAS

A. GENERAL

During the course of the study, it was possible to isolate a number of significant problem areas relating to the meteorological sensors. Many of these are considered in this section. Wherever possible, recommendations and suggestions for possible solutions are included.

B. STANDARDIZATION OF NOMENCLATURE AND MEASUREMENTS

During the sensor survey portion of the program, a number of potential cloud cover and heat budget measuring devices were studied, and a substantial amount of measured data was accumulated on the performance of these sensors. It soon became clear that considerable variation exists in defining performance parameters, and in measuring such quantities. In the visual cloud cover-TV imaging device area, for example, tube resolution is often expressed in TV lines per picture height, TV lines per target diagonal, TV lines per horizontal picture width, as well as the ambiguous term, "TV lines." Other examples of ambiguity exist, both in the visual and infrared areas.

In addition to the problem of nomenclature, a very real difficulty arises in attempting to compare data on similar sensors. In TV imaging systems, for example, data on resolution performance under conditions of varying integration times and scan rates is scanty at best (as described below in subsection C) and thoroughly nonstandard in content. Thus, some experimenters have determined integration and slow scan effects by, displaying the video information on the screen of a monitor, utilizing the observer's eye with its inherent 0.2 second effective integration time, to determine resolution. Other experimenters, in an attempt to circumvent the screen-eye combination, have resorted to photographing the monitor screen. Often, where the scene is stationary, several exposures are made and the integration property of the film is utilized. The net result of these efforts has been to accumulate data which is not necessarily comparable; however in many instances these experimental procedures were aimed at understanding the mechanisms involved, rather than gathering data. Even under standard commercial operation, measurement procedures have not been completely standardized. While wide use is made of the RETMA square-wave response resolution charts in determining tube performance, a number of companies are now utilizing sine-wave response charts in their measurements.

It appears that there are both short and long range solutions to these problems. The immediate solution is for each system engineer, working with published data, to exercise great caution in using these data in system design and analysis. Where data units are not clearly indicated (as in the case of resolution stated in "TV lines") or where required information is not readily available (as, for example, in the case of resolution data on Vidicons) the sensor manufacturer should be contacted and questioned at length on these matters before such data are used.

As a long range effort, the appropriate technical group (RETMA, or perhaps the IEEE in the case of TV imaging systems, and IRIS in the infrared field) should

attempt to standardize both nomenclature and measurement procedures, and bring pressure to bear for the adoption of these standards throughout the industry. While some success has already been achieved in this area, considerably more work remains to be done.

C. UNAVAILABLE TUBE DATA

While substantial amounts of data exist on the performance of TV imaging sensors operated at standard commercial TV rates (where frame integration and scanning times each equal 1/30 second) virtually no data exist on longer integration times and slow scan systems. Much of the data that does exist on Image Orthicons operated under these slow scan conditions appear in Section 3. subsection C. 6. About the only commercially available data on Vidicons operated in this fashion appear in data sheets on slow scan tubes.

The above problems are emphasized in Section 3, subsection F, where a system analysis is presented of the visual spectral region cloud cover sensor systems. Based on Republic's estimates and evaluation of what little data exist, it was assumed that increasing frame (scan) time from 1/30 second to 10 seconds would improve sensitivity by a factor of ten for a continuously imaged system; i. e., only 1/10 as much illumination would be required for the same resolution. In addition, the slow scan readout would result in a resolution improvement of approximately 50%. Since the stabilization requirements of the 3-axis stabilized satellite yielded a maximum tolerable scene exposure time of 1 second, an increase of perhaps ten times in illumination is required over that needed for a 10 second exposure. Thus, the net effect of going to a 1 second exposure and 10 seconds frame time, as compared to the 1/30 second frame time continuous exposure case, is identical sensitivity with a 50% improvement in resolution. These data are presented in Figure 3-48.

The basic need however, is for detailed data on the effects described above. Estimates, such as the ones made in the preceding paragraphs, as well as theoretical treatments, such as those given in Section 3, subsection C. 5, are satisfactory for establishing general trends, but certainly they do not provide a substantial basis on which to design and predict the performance of specific systems. The lack of definitive data on nonstandard operation of these tubes is understandable. Until recently, there was little interest in, or need to operate such devices in modes other than those required for normal commercial broadcasting. Recent requirements, arising from astronomical, military, and satellite needs, have changed the situation somewhat in the past few years. Even today, with tube manufacturers emphasizing the commercial aspects of TV imaging systems, there is comparatively little impetus for these companies to gather such data. In general, the problem has been placed with the camera chain developers to obtain such information for their own particular applications, and they, along with the sensor manufacturers and the ultimate users of such systems, are beginning to generate the required information.

Performance data on Image Orthicons and Vidicons is especially needed with regard to resolution, signal to noise ratio, aperture response as a function of slow multiple and single scan operation, and integration in the storage section. Data on other tubes (Ebicons, Isocons, SEC Vidicons, etc.) are also critically needed.

It is recognized that obtaining data as a function of variation in tube operating parameters is sometimes a difficult process. For this reason, the development of specific equipment to accomplish these ends is a vital necessity. The most advanced equipment of this nature was recently described in a requirement established by the NASA Aeronomy and Meteorology Division at Goddard. Basically, the instrument is a universal tube tester, capable of exercising a variety of TV imaging tubes through a range of illumination levels, exposure (integration) times, and readout times. With this device, it will be possible to generate data needed to predict the actual performance of potential systems under a wide range of operating conditions. Also, this data will be standardized, fully comparable (from tube to tube) and obtainable in a much shorter time than has previously been possible. Republic considers it vital that this type of program be encouraged. It appears to offer the most feasible and direct means yet proposed for bringing order out of chaos in the tube data field, and removing one of the most serious impediments currently existing in the development of special purpose TV imaging systems. Also, the availability of such a device will most certainly stimulate independent researchers, as well as sensor manufacturers, to a more complete understanding of the mechanisms involved in tube operation; and for this reason alone, the development of this equipment is more than justified.

D. IMAGE ORTHICONS FOR SPACE APPLICATIONS

The use of Image Orthicons in the cloud cover sensor system for the SMS program introduces two types of problems which warrant consideration. The first problem relates to optimizing the use of such sensors in a feasible, operational system, and points to the unique advantages which accrue to a stationary satellite system, when a ground based observer is incorporated into the control loop. The second problem stems from the general requirement of operating a sensitive electronic device in a space environment, and involves the potential problems which arise therefrom, and the degree of automation needed to assure adequate system performance with high reliability during an orbital lifetime of one year. These problem areas are discussed in greater detail in the following paragraphs.

In analyzing sensor systems for the SMS, it is comparatively simple to indicate the problems generated by the satellite parameters. The formidable stabilization requirements and relatively large optical system both arise primarily from the necessity for achieving adequate resolution for meaningful meteorological observation from an extreme altitude. One point sometimes missed is that the very characteristics which render adequate resolution difficult to obtain also serve to yield unique benefits which are not to be found in other meteorological satellites. Since the SMS always remains essentially fixed over an equatorial ground point, and is always in sight of the command and control station in North America, a good opportunity exists to factor a ground based observer into the picture taking sequence. This presents a distinct advantage over the Tiros and Nimbus satellites, which remain within sight of their command stations for a comparatively short portion of any given orbit. The near-real time transmission of sensor data from the SMS should enable an observer at the command station to examine each frame of cloud cover photography, determine the quality of the resulting picture, decide on which camera chain parameters to vary to improve and optimize the photograph, and transmit the appropriate commands to the satellite sensor system. The requirement, then, is that the necessary adjustment capability be built into the satellite camera system.

Since some parameter adjustment capacity must be provided, it is of interest to determine which parameters are involved. The Image Orthicon represents an excellent sensor to consider, since its range, sensitivity, and complexity of adjustment far exceed that of the Vidicon. Nevertheless, the basic concept of ground-controlled adjustment also applies equally well to the Vidicon sensor.

In the case of an Image Orthicon camera chain, it would appear that beam current, illumination on the photocathode, focus and deflection fields (either electrostatic or magnetic), electronic zoom (in the case of the GE 2 in. electrostatic Orthicon), target voltage, image section accelerating voltage, video AGC, and bandwidth rolloff adjustment, as well as numerous other parameters could profitably be adjusted to optimize system performance. Also, perhaps integration (exposure) time and readout (scan) time could be varied. If many or all of these adjustments are to be made from the ground, the means for varying these parameters must be built into the camera chain itself; i.e., potentiometers, switches, variable voltage supplies, etc., must all be incorporated into the satellite-borne system. If this is the case, the addition of appropriate diagnostic sensors and control circuits would enable automatic, internal adjustment of these parameters without the need for the ground link. The extent to which the system should be self-adjusting, as opposed to adjusting upon ground command, is rather difficult to determine at this point, and requires additional study. It seems clear that the degree of automated self-adjustment needed would be less than in a Nimbus-type camera, because of the near-real time data transmission and the presence of the observer in the control loop. On the other hand, a number of these functions could quite probably be better handled if internally adjusted, particularly those relating to automatic occultation and Sun protection.

In summary, it appears that many functions should be made self-adjusting, with virtually all of them capable of command adjustment, with ground override where required. Such a system would provide maximum flexibility with improved reliability, and is apt to be less complex than a fully automated internally adjustable system, which would have to carry additional parameter variation sensors and more complicated servo and drive circuits.

An additional advantage of incorporating the man into the control loop is that problems of tube aging should be simplified. Tube aging would tend to produce performance degradation which would be virtually impossible to compensate for in an internally-adjusted system. Aging processes are not fully understood, and hence are not easily predictable. Raytronics, which is developing a camera for the Nimbus program utilizing the RCA 2 in. magnetic Image Orthicon, has the intention of investigating this phenomenon in considerable detail during a later phase of their program. It seems quite reasonable to assume that a ground based observer could override internal adjustment controls, and extract optimum performance from an aging tube with considerable success.

For diagnostic purposes, it seems desirable to include a resolution test pattern of some sort in the camera system. Referenced periodically, such an internal calibration system would be capable of determining camera chain performance, and would provide some separate means for determining the performance of the optical system. In addition, this calibration source would enable the ground observer to better assess camera system performance, and optimize the system parameters more rapidly and efficiently. Finally, such a source might well provide the only definitive means for determining tube aging effects. It is recommended that such a system be seriously considered for inclusion in the final camera system.

While there is some basis for doubt that a 1 year operational lifetime will be successfully achieved with a fully automated camera system incorporating an Image Orthicon, it seems clear that the chance of realizing this goal will be materially improved in the SMS system through the use of a human observer and a command adjustment capability. Therefore, it is concluded that the use of a man in the control loop will materially enhance the flexibility and reliability of the cloud cover sensor system. To the extent to which the man is utilized, the resulting SMS system should be an improvement over the day-night Nimbus-type camera system.

E. LIGHTWEIGHT OPTICS

Investigations of optical areas have indicated a significant variation in optical system weights, depending upon the type of materials employed for the housing and mirror systems. The weight penalty for indiscriminate selection of optical systems is readily apparant for the low and medium capability satellites. Discussions with optical designers and organizations show divergent views in materials selection based in great part upon manufacturing skills. The resulting optical system weights consequently evidence a weight variation between comparable systems.

Optical manufacturing techniques for beryllium mirrors are presently being investigated by industry and should be expanded to cover using beryllium for structures as well. Admittedly, this material is toxic and requires that special precautions be taken during processing for the protection of the optician. Beryllium affords the promise of substantial reduction of optical system weight because of its light weight, as compared to quartz or aluminum in mirror construction, and aluminum and Invar for structural components. In overall considerations the thermal stability of beryllium does not compare unfavorably with that of heavier optical materials.

F. VARIABLE OCCULTATION

Scene brightness variations within the field of view of the visible light sensors will in most instances exceed the dynamic range capabilities of the sensor tubes. Attenuation of the ground scene illumination incident on the sensor photocathode to within the inherent capabilities of the sensor tube can be accomplished (as previously described in Section 3, subsection E) through the use of filter wheels and other special techniques. These techniques are effective in that the sensor tube is optimized for a given photocathode high light illumination level within the dynamic range of the sensor. Consequently, low light level regions within a particular scene are compromised if the ratio between high and low illumination levels exceeds the sensor's capabilities. This ratio may range from 30:1 to perhaps 100:1, (at the very best it may approach 200: 1) depending upon the sensor tube. This means that for a wide range of illumination within a scene a decision must be made as to the brightness level at which to optimize the sensor.

Two sensor characteristics must be considered: inherent dynamic range and absolute sensitivity. For a full Earth disc sensor such as the Vidicon, which may view extremes of illumination within a single picture, the problems of obtaining maximum data are more severe than with a narrow coverage I.O. sensor which only experiences excessive scene variation in a frame encompassing the day-night terminator. Proper programming of a narrow coverage sensor could possibly minimize or even eliminate this problem.

An approach, as yet unimplemented, has been considered whereby a sensor's dynamic range and sensitivity may be utilized to the fullest extent. This approach would employ a variable occulting mask which would permit a series of optimum exposures over discrete portions of the sensor's field of view within the limits of attainable tube sensitivity and resolution. The occulting mask would be positioned so that the high light portions of the scene are in effect removed from the sensor's field of view, thereby allowing an exposure to be made (at optimum conditions) of the remaining portions of the picture. Through a series of such dissecting exposures, governed by sensor characteristics, the maximum capabilities of the sensor could be realized. The resulting composite of maximized scene sections could be reconstructed by the ground station recording equipment (if the sensor is capable of storing a series of exposures) without adjacent area blooming, and a single composite picture could also be transmitted to Earth.

Admittedly, such a device would require development for reliable operation in space as well as ground or pre-programmed control for mask positioning. The benefits derived, however, appear to warrant further investigation and possible development for application to the SMS program.

G. AUTOMATIC SUN PROTECTION

Protection of all of the meteorological sensors from direct exposure to the Sun is mandatory if a reliable one year orbital lifetime is to be attained.

Sensitive devices such as the Image Orthicon are almost instantaneously destroyed by direct Sun exposure. Vidicons, infrared sensors, and photomultiplier tubes may suffer damage ranging from partial disability to total destruction depending on the length of exposure.

Protection can be provided in the form of occluding shutters or variable field stops, triggered by a signal from a Sun proximity sensor. Additionally, since the Sun position in relation to the satellite can be predetermined, the field of view could be restricted by limit stops on sensor aiming mirror excursions, as well as shutdown of sensors during those periods when interception of the Sun image is possible.

Although practical Sun protection can be attained through the use of various auxiliary devices and sensor programming, there are associated penalties of additional complexity, weight, and operational restrictions. Such penalties could be eliminated if an automatic, self-attenuating, Sun protector were available. An automatic system must possess the inherent capability of instantaneously altering its light transmission characteristics from 100% to some value near 0.01% (neutral density 4.0), together with a rapid recovery to 100% once the Sun's stimulus is removed.

Photochromic dyes offer excellent possibilities for automatic occultation of the Sun's image. Since these dyes are activated by the Sun's ultraviolet component, and react in proportion to the intensity, the only addition to a sensor system would be the dye coating and a possible substrate. Significant programs are currently underway for protecting human eyes and Vidicon tubes from damage by atomic explosion flashes. Near instantaneous reaction and high densities are also required for this application.

Organizations such as National Cash Register of Dayton Ohio; Polacoat of Cincinnati, Ohio; and Marx Polarizer Corp. of Queens, New York are engaged in the development of photochromic dyes of various types and characteristics.

Both study program time constraints and security restrictions have prevented a detailed investigation of photochromic dyes for automatic Sun protection. However, based on the limited data available to Republic, reaction times of 20 to 30 microseconds with densities of 4.0 or better, and recovery or reversal times of milliseconds appear to be feasible. A recommendation is therefore made that this area be investigated for possible application to the SMS.

In addition to the efforts discussed above, some consideration has also been given to the extent to which operational restrictions might arise if Sun protection via sensor shutdown were instituted.

The following paragraphs apply to wide field sensors which are designed to produce cloud pictures or heat budget data covering, in one frame, the full disk of the Earth, to and beyond the horizon.

For sensors of this type, the problems of Sun protection arise only on certain days before and after each equinox, and on these days for only brief periods before and after local midnight at the satellite subpoint. Within these same time periods, there appear also the related problems of loss of solar power because of passage of the SMS through the shadow of the Earth. For larger types of SMS vehicles, (700 to 1000 lb weight class) it is feasible to store enough energy for operation of sensors during periods of eclipse. For lighter satellites the penalties become more serious. For all weight classes, additional storage of energy deserves consideration only to the extent that available sensors can produce useful and needed data under midnight illumination conditions.

The simplest answer for the power problem is to lock the meteorological sensors and data transmitters in an "off" or "standby" condition during passage through the shadow. The simplest answer to the Sun protection problem is to keep the sensor optics closed whenever their fields of view would include the Sun.

A brief investigation was conducted to determine how much and what fractions of observation time would be lost by these operating procedures. The principal results are shown in Figure 6-1.

The inner curve for umbra only, is the same as Figure 4-1 in Volume 5. The curve for umbra plus penumbra was derived by addition of the two curves of that figure. The outer curve was constructed by adding the time just before and just after the shadow period, during which the Sun would be in view of sensors with a field of view defined by a cone of 20° total angle. This value was chosen to provide a 1.5° margin on each side of the 17° subtended by the Earth's disk from the SMS. Such a margin might be required by errors in attitude sensors. The outside rectangular "curve" of Figure 6-1 shows the corresponding loss of observation time for a square field of view of 20°.

The principal conclusions regarding the power problem and the Sun protection problem are as follows:

(1) Both problems occur only in association with the equinoxes, and only close to local midnight.

(2) For 253 days, or 70% of the days of the year, neither problem arises.

(3) For the remaining 112 days, or 30% of the year, the daily loss of observation time never exceeds 87 minutes or 6% of each day.

(4) For a 20° square field, the daily loss remains constant over the 112 days. This corresponds to a loss of less than 2% of the possible observation time over one year.

(5) With a circular 20° field, losses due to both problems exceed 60 minutes per day, or 4% on only 80 days (22%) of the year.

(6) The relatively small losses of observation time do not seem to justify acceptance of substantial weight or complexity penalties to provide power for meteorological sensors and data transmitters during the shadow period, or to mask out the Sun just before and after these periods.

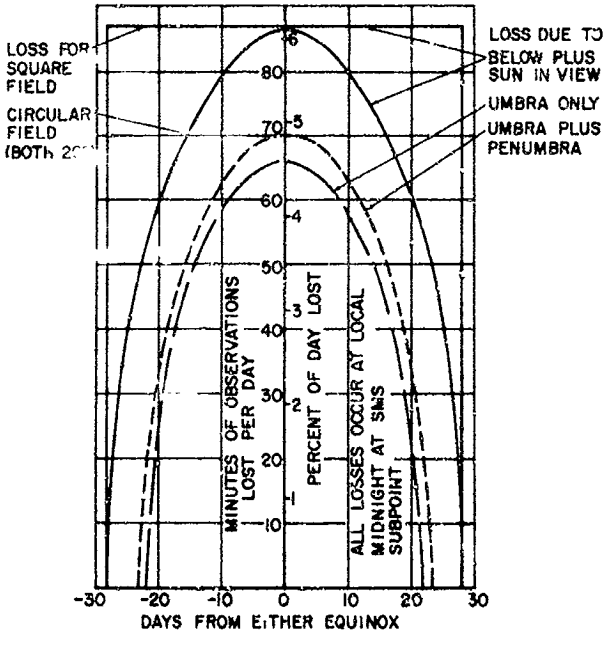

Figure 6-1. Losses of SMS Observation Time Due to Sun and Shadow

H. IMAGE DISSECTORS FOR SPACE APPLICATIONS

The problem of achieving full Earth disc coverage in one picture could be solved if a sensor were available that was capable of high resolution, wide dynamic range, and high sensitivity. Although such a sensor doesn't exist, the Image Dissector meets the requirements of wide dynamic range (three to six orders of magnitude) and high resolution (3000 lines). Unfortunately, this tube has no storage capability, and therefore, its sensitivity is much lower than the Image Orthicon and the Vidicon. Two potential solutions exist: one is to employ long exposure times, the other is to incorporate a storage capability in the tube.

The first solution imposes hardships on the attitude stabilization control system. This manifests itself not as image smear (as would be the case for a sensor incorporating storage) but as displacements of large areas, corresponding to geometric distortion. The second approach, that of incorporating storage capability into the Image Dissector, could enable the SMS to obtain high resolution cloud images simultaneously for day and night illumination conditions. Because of the potential advantages, it seems reasonable that future efforts in the meteorological sensor subsystem include investigations of these possibilities.